ESTUDIO DE LOS CAMBIOS INDUCIDOS POR LA DEFICIENCIA DE HIERRO EN EL PROTEOMA DE PLANTAS

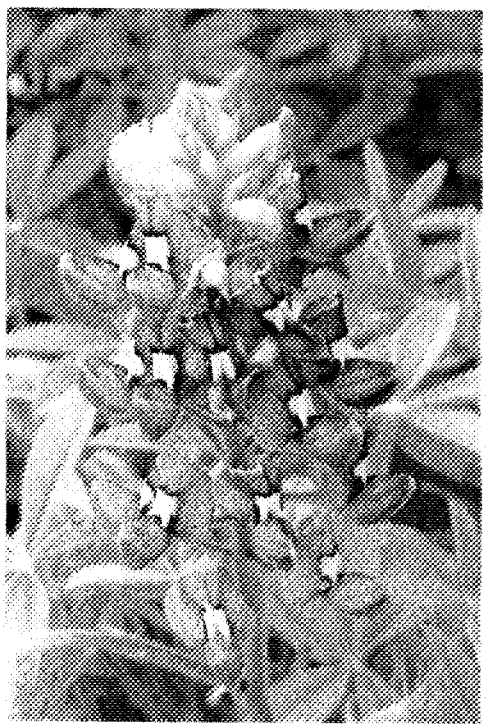

TESIS DOCTORAL

Sofía Andaluz Gil

CSIC

5-1

Estación Experimental de Aula Dei
Consejo Superior de Investigaciones Científicas (CSIC)
Zaragoza
Departamento de Nutrición Vegetal

TESIS DOCTORAL

ESTUDIO DE LOS CAMBIOS INDUCIDOS POR LA DEFICIENCIA DE HIERRO EN EL PROTEOMA DE PLANTAS

Memoria presentada por Dña. Sofía Andaluz Gil, Licenciada en Bioquímica y en Ciencias Químicas, para optar al grado de Doctor en Ciencias.

Zaragoza, Julio de 2005

Dña. ANUNCIACIÓN ABADÍA BAYONA, Investigador Científico del Consejo Superior de Investigaciones Científicas y D. JAVIER ABADÍA BAYONA, Profesor de Investigación del mismo Organismo

CERTIFICAN

Que la Tesis Doctoral titulada **"Estudio de los cambios inducidos por la deficiencia de hierro en el proteoma de plantas"**, ha sido realizada por la Licenciada en Bioquímica y en Ciencias Químicas Dña. SOFÍA ANDALUZ GIL, en el Departamento de Nutrición Vegetal de la Estación Experimental de Aula Dei del Consejo Superior de Investigaciones Científicas bajo su dirección y reúne, a su juicio, las condiciones requeridas para optar al Grado de Doctor en Ciencias

Zaragoza, Julio de 2005

Fdo. Anunciación Abadía Bayona

Fdo. Javier Abadía Bayona

Dña. MARÍA F. FILLAT CASTEJÓN, Profesora Titular del Departamento de Bioquímica y Biología Molecular y Celular de la Facultad de Ciencias de la Universidad de Zaragoza

CERTIFICA

Que la Tesis Doctoral titulada **"Estudio de los cambios inducidos por la deficiencia de hierro en el proteoma de plantas"**, ha sido realizada por la Licenciada en Bioquímica y en Ciencias Químicas Dña. SOFÍA ANDALUZ GIL, bajo su tutela como ponente en el Departamento de Bioquímica y Biología Molecular y Celular de la Facultad de Ciencias de la Universidad de Zaragoza y, a su juicio, reúne las condiciones requeridas para optar al Grado de Doctor en Ciencias

Zaragoza, Julio de 2005

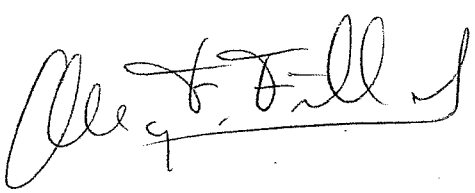

Fdo. María F. Fillat Castejón

En este trabajo que ahora finaliza han participado, de una u otra forma muchas personas, y desde estas primeras líneas quisiera mostrarles a todas ellas mi más sincero agradecimiento.

En primer lugar, a mis directores de Tesis, la Dra. Anunciación Abadía y el Prof. Javier Abadía, por darme la oportunidad de trabajar en su laboratorio y realizar estar Tesis, por su confianza, su ayuda y la formación brindada.

A la Dra. Ana Flor López Millán, por su apoyo en todo momento, su ayuda con los experimentos, el análisis de los resultados y la redacción de este trabajo, por sus consejos y su amistad. Gracias también a Tim por el tiempo robado.

A la Dra. María F Fillat, mi tutora en la Universidad de Zaragoza, por su disposición y su ayuda.

A la Dra. M Luisa Peleato, por sus clases de Fisiología Vegetal, sus consejos al acabar la carrera y su ayuda en estos años de Tesis.

A los Prof. Lello Zolla de la Universidad de la Tuscia (Italia) y Eva Mari Aro de la Universidad de Turku (Finlandia) por permitirme trabajar en sus laboratorios y aprender nuevas técnicas.

A las Dras. Cristina Echevarría y Rosario Álvarez de la Universidad de Sevilla por su ayuda en el trabajo de la PEPC y proporcionarnos los anticuerpos necesarios para su estudio.

Al Dr. Javier de las Rivas del Centro de Investigación del Cancer, por su ayuda y consejo en los primeros análisis de MALDI.

Al Ministerio de Educación y Ciencia, por la beca predoctoral que me ha permitido realizar este trabajo.

A todas las personas que trabajan en la Estación Experimental de Aula Dei y, en especial, en el Departamento de Nutrición Vegetal, por facilitarme el trabajo de cada día.

A mis compañeros de laboratorio durante todos estos años, Yolanda Gogorcena, Tatiana, Y-Chieh Chang, Roberto, Alejandro, Rebeca, Cristina, Paula, Ana, Victoria, Fermín, Ajmi, Aurora, Piluca, María, Irene, Ruth, Rubén, Iñaki, Nacho, Ade y Vitor, por sus consejos y críticas, por su apoyo y

ayuda independientemente del problema, por sus conversaciones y buenos momentos dentro y fuera de Aula Dei. Gracias por vuestro compañerismo y amistad.

A mis compañeros de Aula Dei, Conchita, Tere, Concha, Carmen, Jesús, David, María Angeles, Yoli, Marta, Estrella, Ana, Azahara, Mariví Ramiro, Raquel, María Bernal, Mariam, Sara, Vanesa, Miguel, Mariví, MC, Jorge Loscos, Manu, Fernando, Curra, María Clemente, Loreto, Javier, Carmen Pérez, David Moret, Jorge Álvaro, Manuel, Pepa, María Muñoz, Merche, Meriam, Olfa, Sawsen, Sergio y Nadhem, por los desayunos, comidas y cafés, sus charlas y discusiones, el buen humor y las risas, gracias a esos momentos las horas se hacen cortas y los problemas pequeños.

A mis amigos de siempre, César, Mari, Tomás, Dani, Maribel, Eva, Alberto, Ana, Jano, Javi, Bea, Jesús, Elena Hdz., Miriam, Elena Santacruz, Carlos, Roser, Silvano, Ale, Martín, Melinda y Daniel, por su amistad, por cada fin de semana de charlas y risas, por las excursiones y escapadas. Gracias porque, aunque algunos no estéis cerca fisicamente, sé que puedo contar con vosotros siempre.

A Marta, por su amistad y cariño, por sus buenos consejos y las conversaciones sin reloj.

A mis padres, Rebeca, mi abuela Emilia, Manuel y toda la familia, por su amor y cariño, por animarme siempre a seguir adelante y enseñarme que no hay nada que no se pueda superar. A Rafael y a los abuelos Miguela, Antonio y Reinaldo, sé lo que les hubiese gustado verme acabar este trabajo, y de alguna forma lo estarán haciendo.

A Armando, por su amor, por hacerme reir, por estar ahí cada día, por no dejarme caer en los momentos malos y compartir los buenos, por enseñarme que todo es relativo y porque todo este esfuerzo también es suyo.

A Armando

A mi familia

Abreviaturas

AP_5A	Adenosina-5'pentafosfato-5'adenosina
APS-IgG	Anticuepos específicos frente al sitio de fosforilación de la PEPC C_4 de sorgo
ATPasa	adenosina 5'-trifosfato sintasa
BN PAGE	Blue Native Polyacrilamide Gel Electrophoresis
BPDS	ácido 4,7-difenil-1,10-batofenantrolin-disulfónico
Chl	clorofila
CS	citrato sintasa
DGDG	digalactosil diglicérido
DMRLs	6,7-dimetil-8-ribitil lumazina sintasa
EDTA	ácido etilen-diamino-tetraacético
EGTA	ácido etilen-glico-tetraacético
ESI	electrospray
F6P	fructosa-6-fosfato
FAD	dinucleótido de riboflavina y adenina
FC-R	reductasa férrica
FMN	riboflavina 3-monofosfato
FW	peso fresco
G3PDH	gliceraldehido 3-fosfato deshidrogenasa
G6PDH	glucosa 6-fosfato deshidrogenasa
GTP	guanosina trifosfato
HPLC	cromatografía líquida de alta resolución
IC_{50}	concentración requerida para producir una inhibición del 50% de la actividad
IDH	isocitrato deshidrogenasa
IEF	isoelectroenfoque
IPG	Isoelectric Focusing Gel

ITP	proteína transportatora de Fe
LHC	complejo antena
LIFT	Lasser Induced Dissociation
MALDI	Matrix-Assisted Lasser Desorption Ionization
MDH	malato deshidrogenasa
MGDG	monogalactosil diglicérido
MS	espectrometría de masas
MW	masa molecular
m/z	relación masa/carga
NA	nicotianamina
NADH	dinucleótido de nicotianamida y adenina reducido
NADPH	2'-fosfonucleótido de nicotianamida y adenina reducido
NAS	nicotianamina sintasa
NAAT	nicotianamina aminotransferasa
OEC	complejo productor de oxígeno
PAGE	electroforesis en gel de poliacrilamida
PAR	radiación fotosintética activa
PEPC	fosfoenolpiruvato carboxilasa
PFK	fosfofructoquinasa
p*I*	punto isoeléctrico
PK	piruvato quinasa
PMSF	fluoruro de fenil metil sulfónico
PS	fitosideróforo
PSI	fotosistema I
PSII	fotosistema II
PVDF	fluoruro de polivinilideno
PVP	polivinil pirrolidona
Rubisco	ribulosa 1,5-bisfosfato carboxilasa/oxigenasa
RuBP	ribulosa 1,5-bisfosfato
TCA	ácido tricloroacético
TOF	Time of Flight
U	unidades de actividad
Vh	voltio hora
WZ	zona blanca de las puntas deficientes en Fe
YZ	zona amarilla de las puntas deficientes en Fe

Índice

Capítulo 1

INTRODUCCIÓN

ÍNDICE

1. EL HIERRO EN LA PLANTA

El hierro es un micronutriente esencial para las plantas, animales y otros organismos, ya que es un constituyente indispensable de un gran número de enzimas y agentes redox que intervienen en algunas de las principales funciones del metabolismo de los seres vivos. La gran versatilidad del Fe en sus funciones biológicas es debida al potencial del par redox Fe(III)/Fe(II), que varía dependiendo del ligando al que se encuentre unido, permitiendo así su uso en forma, por ejemplo, de grupo hemo o centros Fe-S. En plantas, el Fe interviene en la síntesis de clorofila y es esencial para la fotosíntesis y el mantenimiento de la estructura del cloroplasto (Terry y Abadía, 1986; Abadía, 1992). Además, interviene en procesos como la respiración, la fijación de nitrógeno (Clark, 1983) y en la síntesis de ADN y hormonas (Briat y Lobréaux, 1997). Sin embargo, a pesar de ser un elemento esencial, el hierro libre en la célula puede reaccionar con el oxígeno, mediante la reacción de Fenton (Guerinot y Yi, 1994) y generar especies de oxígeno reactivas, como el peróxido de hidrógeno, que conducen a una situación de estrés oxidativo. Por este motivo, la homeostasis del hierro en la planta a nivel de órgano, tejido y célula, está altamente regulada, con el fin de mantener un aporte suficiente de hierro para el metabolismo, evitando al mismo tiempo niveles excesivos que pueden ser tóxicos para la planta.

Para prevenir el daño oxidativo, el hierro se encuentra habitualmente acomplejado con compuestos de bajo peso molecular o unido a proteínas. En las plantas, aproximadamente el 63% del hierro de la hoja está asociado a proteínas, y el 80% del total está localizado en los cloroplastos (Young y Terry, 1982). Las proteínas más comunes a las que está unido el hierro son:

- Proteínas con grupo hemo. Este grupo está formado por las enzimas que tienen un grupo prostético hemo Fe-porfirina. Ejemplos de estas enzimas son los citocromos, catalasas y peroxidasas.
- Proteínas con centros Fe-azufre. En este grupo de proteínas, el Fe está coordinado bien con un sulfuro inorgánico, bien con un grupo tiol de la cisteína, o con ambos. Ejemplos de este tipo de proteínas son ferredoxina, superóxido dismutasa, aconitasa y xantina oxidasa.
- Fitoferritina. Es un proteína de reserva de hierro y representa aproximadamente un 35% del Fe en la hoja, llegando a contener hasta el 80% del hierro de los cloroplastos (Marschner, 1995).

2. BIODISPONIBILIDAD DE HIERRO

La biodisponibilidad del hierro afecta a la distribución natural de las especies vegetales (Grime y Hutchinson, 1967; Snowden y Wheeler, 1993; Gries y Runge, 1995; Tyler y Falkengren-Grerup, 1998) y puede limitar el crecimiento de especies consideradas de gran importancia económica (Chen y Barak, 1982; Vose, 1982).

El hierro es el cuarto elemento más abundante de la corteza terrestre después del oxígeno, el silicio y el aluminio. Su abundancia en el suelo es aproximadamente de un 5%, y la mayor parte se encuentra en forma de silicatos de hierro y magnesio. Sin embargo, en suelos alcalinos y calcáreos, que constituyen un 30% de la superficie terrestre (Chen y Barak, 1982), el hierro se encuentra en forma de óxidos e hidróxidos de muy baja solubilidad, por lo que su disponibilidad para la planta es baja. La concentración de hierro disponible en estos suelos es de aproximadamente 10^{-10} M, mientras que los niveles necesarios para la planta son mucho mayores, cercanos a 10^{-7} M (Loeppert, 1986). Por este motivo, el hierro es frecuentemente un elemento deficitario para la planta.

Los principales factores que pueden provocar deficiencia de hierro en la planta son:

- Factores que afecten a la solubilidad y movilidad del hierro en el suelo, tales como elevado pH, tamaño de partícula de suelo grande, estructura muy cristalina de los minerales de Fe, suelos aireados, baja cantidad de agentes quelantes (Loeppert, 1986), alta salinidad (Awad *et al.*, 1988) y altas cantidades de fosfatos (Lindsay y Schwab, 1982). Todas estas condiciones causan una baja solubilidad del Fe en el suelo y, por tanto, producen una disminución en la disponibilidad del Fe en el mismo.
- Factores que afecten a la absorción y metabolismo del Fe en la planta (Romera y de la Guardia, 1991). Entre éstos destacan: i) los factores de tipo genético; ii) los que inhiben el crecimiento de las raíces, tales como la compactación del suelo y el encharcamiento (Chen y Bark, 1982; Chaney, 1984), las bajas temperaturas, los herbicidas (Chaney, 1984), y iii) los que inhiben la absorción del Fe, como la presencia de fosfatos y metales pesados.
- Factores que afecten a la actividad del Fe dentro de la planta. Se ha descrito (Römheld, 1997; Morales *et al.*, 1998) que en frutales crecidos en el campo el contenido en Fe de hojas de plantas deficientes en Fe puede ser similar o incluso algo superior al de las hojas verdes, y, sin embargo, las hojas presentan un amarilleamiento en la zona internerval, conocido como clorosis férrica y que es síntoma de deficiencia de Fe. Estas altas concentraciones de Fe en hojas deficientes parecen indicar que el Fe podría estar acumulado en alguna zona de la hoja en una forma

no utilizable por la planta. Se ha propuesto que los fosfatos y un elevado pH del apoplasto podría provocar la precipitación del Fe en el exterior de las células impidiendo su utilización (Mengel y Geurtzen, 1986). Sin embargo, la explicación de este fenómeno, conocido como la "paradoja de la clorosis férrica", está todavía por elucidar.

- El bicarbonato merece una mención especial, ya que afecta tanto a la absorción del Fe como a la actividad del Fe dentro de la planta. Los factores que favorecen la formación de bicarbonato, como la humedad alta del suelo, la compactación y el aporte de materia orgánica fresca, también son inductores de clorosis (Chaney, 1984). Todavía no se conocen con certeza las bases fisiológicas de la deficiencia de Fe en plantas inducida por una concentración alta de bicarbonato (Loeppert y Hallmark, 1985; Mengel, 1994), pero no parecen deberse ni al alto pH *per se* (Alhendawi *et al.*, 1997) ni a la disminución en la disponibilidad fisiológica del Fe por precipitación en las hojas debido a la alcalinización del apoplasto y citoplasma (Romera *et al.*, 1992; Mengel, 1994). El bicarbonato absorbido a través de las raíces podría utilizarse en la síntesis de ácidos orgánicos, siendo fijado *in situ* por la fosfoenolpiruvato carboxilasa (PEPC), para dar oxalacetato, que es reducido a continuación para dar malato (Cramer *et al.*, 1993). Este proceso permitiría también la asimilación de CO_2 por las raíces. Por otro lado, la presencia de bicarbonato en la solución nutritiva durante el crecimiento de las plantas moderaría el aumento inducido por la deficiencia de Fe en la actividad de la reductasa férrica (Susín *et al.*, 1996), causando así una disminución en la eficiencia de la planta ante esta deficiencia nutricional.

3. SÍNTOMAS DE LA DEFICIENCIA DE HIERRO

La deficiencia de hierro es un estrés abiótico que se caracteriza principalmente por un amarilleamiento de la zona internerval de las hojas jóvenes. Este fenómeno recibe el nombre de clorosis férrica y, en casos extremos, la hoja puede adquirir prácticamente un color blanco, pueden aparecer manchas necróticas e incluso se puede producir la muerte de la planta (Chaney, 1984). Este amarilleamiento está provocado por un cambio en la composición pigmentaria de los cloroplastos de las hojas (Morales *et al.*, 1990, 1994; Abadía y Abadía, 1993). En la Figura 1-1 se pueden apreciar estos síntomas en remolacha.

Figura 1-1. Síntomas de la deficiencia de Fe en remolacha.

La deficiencia de Fe tiene mucho menos efecto en el crecimiento de la hoja, el número de células por área o el número de cloroplastos que en el tamaño de los cloroplastos y su contenido proteico (Terry, 1980). De hecho, sólo en el caso de una deficiencia severa de Fe se produce una disminución en el crecimiento de la hoja (Abbott, 1967).

La deficiencia de Fe afecta a un alto porcentaje de las plantaciones de frutales en toda el área mediterránea (Sanz *et al.*, 1992; Tagliavini *et al.*, 2000). La clorosis férrica es el problema de explotación más importante desde el punto de vista técnico y económico en muchos frutales cultivados en esta zona ya que, si la deficiencia no se corrige, el crecimiento de los árboles se ve afectado, la floración es más escasa y los frutos son menos numerosos y más pequeños, pudiéndose llegar en casos extremos a la muerte prematura del árbol. Sólo en la cuenca del Ebro se ha estimado en más de 13 millones de euros por año el gasto que suponen los tratamientos correctores de la clorosis férrica (Sanz *et al.*, 1992).

4. ADQUISICIÓN DE HIERRO POR LA RAÍZ EN CONDICIONES DE DEFICIENCIA DE HIERRO.

Para mantener la homeostasis del Fe, las plantas deben adaptar los mecanismos de adquisición de este elemento a las condiciones externas. Ante la deficiencia de Fe, las plantas pueden permanecer indiferentes (plantas no eficientes) o desarrollar mecanismos de adaptación para aumentar su capacidad de adquirir Fe del suelo (plantas eficientes). Dependiendo de la forma de adquisición del Fe, las plantas se dividen en dos grupos distintos: plantas de Estrategia II, formado por gramíneas; y plantas

de Estrategia I, formado por dicotiledóneas y monocotiledóneas no gramíneas.

4.1 Estrategia II

Las plantas gramíneas utilizan una estrategia basada en la quelación del Fe(III) para adquirir las cantidades necesarias de este microelemento.

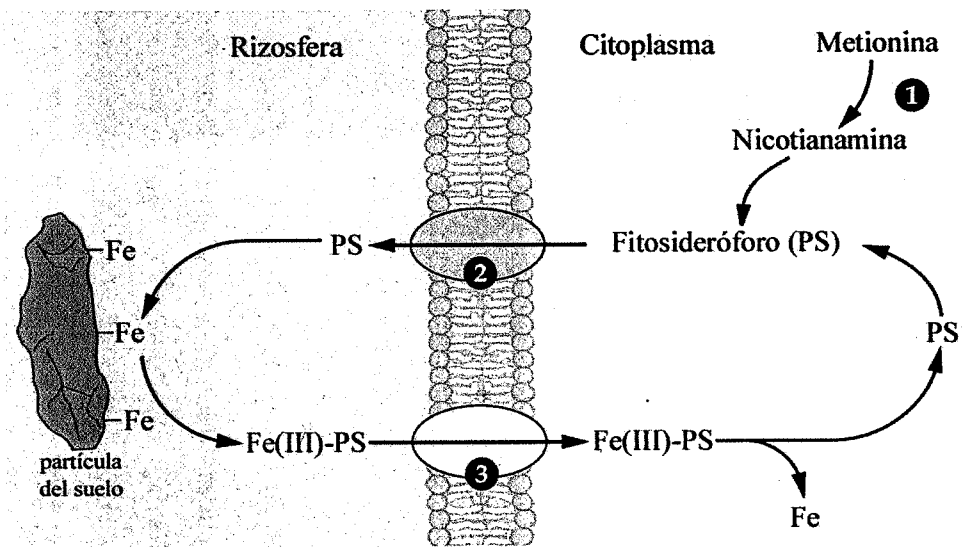

Figura 1-2. Estrategia II (Buchanan *et al.* 2000).

Las gramíneas producen y secretan a la rizosfera compuestos de bajo peso molecular llamados fitosideróforos. Debido a su alta afinidad por el Fe, los fitosideróforos solubilizan de forma muy eficaz el Fe (III) por quelación, produciendo complejos Fe(III)-fitosideróforo (Fe-PS) que son introducidos en la raíz a través de un transportador específico situado en la membrana plasmática (Fig. 1-2).

La producción y excreción de fitosideróforos aumenta en condiciones de deficiencia de Fe y la tolerancia a la deficiencia de este elemento se relaciona con la cantidad y clase de fitosideróforo secretado. Los fitosideróforos son derivados del ácido muginéico (Takagi, 1976). El paso inicial de su síntesis (Fig. 1-3), catalizado por la nicotianamina sintasa (NAS), consiste en la condensación de tres moléculas de S-adenosil metionina para producir una molécula de nicotianamina (NA). Aunque la síntesis de NA se produce tanto en plantas de estrategia I como II, los pasos siguientes hasta la obtención de los distintos ácidos mugénicos son específicos para las plantas de estrategia II (Curie y Briat, 2003). La actividad de las enzimas nicotianamina sintasa (NAS) y nicotianamina aminotransferasa (NAAT), primera y segunda enzimas de la ruta biosintética, aumenta en raíces de cebada deficientes en Fe (Mori, 1999);

igualmente, aumenta la expresión de los genes de cebada que codifican los enzimas de la ruta biosintética de los ácidos mugénicos: *Hvnas1-7, naatA, naatB, Ids2* e *Ids3* (Higuchi *et al.*, 1999; Nakanishi *et al.*, 1993; Okumura *et al.*, 1994; Takahashi *et al.*, 1999).

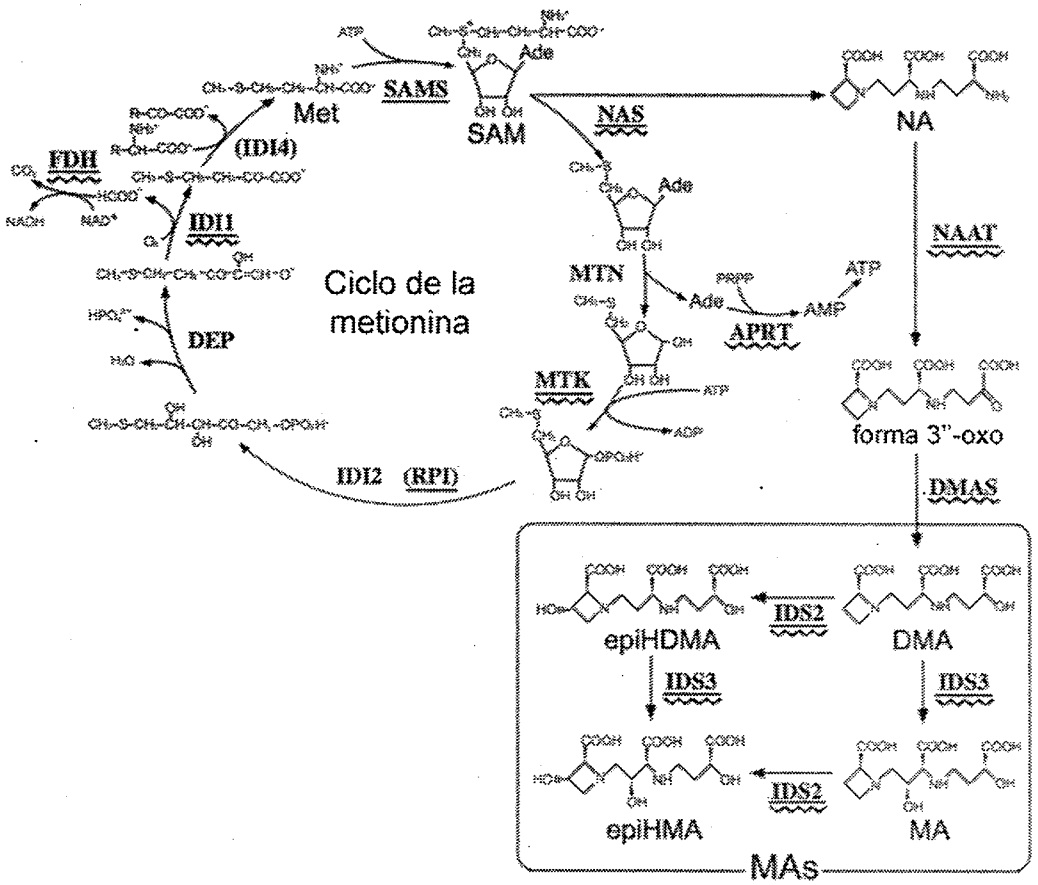

Figura 1-3. Ruta de síntesis de los fitosideróforos (Negishi *et al.*, 2002).

Al contrario de lo que ocurre con la ruta biosintética de los ácidos mugénicos, los mecanismos moleculares de la excreción de éstos todavía no han sido totalmente esclarecidos, aunque Sakaguchi *et al.* (1999) mostraron que los fitosideróforos son secretados como aniones monovalentes, probablemente a través de canales aniónicos. Negishi *et al.* (2002) han sugerido que en la liberación de los fitosideróforos podría estar implicado el transporte vesicular ya que en células de raíces de cebada deficientes en Fe aparecen gran cantidad de vesículas engrosadas.

Una vez formado el complejo Fe-PS, éste debe ser transportado al interior de la raíz. La existencia de un transportador específico de Fe-PS fue demostrada por primera vez por von Wirén *et al.* (1994), gracias a la existencia de un mutante de maíz *yellow–stripe 1 (ys1)* que tiene un defecto en el sistema de transporte del complejo Fe-PS a través de la membrana de la raíz. Posteriormente, Curie *et al.* (2001) identificaron y clonaron el gen *YS1*

que codifica este transportador. *YS1* codifica una proteína de 682 aminoácidos con 12 dominios transmembrana, y pertenece a una nueva subclase de la familia de transportadores oligopeptídicos OPT (Yen *et al.*, 2001). La expresión del gen *YS1* está incrementada en condiciones de deficiencia de hierro, tanto en la raíz como en la parte aérea. La acumulación de mRNA del gen *YS1* en la parte aérea de la planta en deficiencia de Fe sugiere otra posible función del transportador YS1 en el transporte de Fe a lo largo de la planta (Curie y Briat, 2003).

Búsquedas de secuencias homólogas a *YS1* en *Arabidopsis* han demostrado la existencia de 8 secuencias con alta homología a *YS1*, alrededor del 80%, en el genoma de esta planta. Se les ha llamado *YSL* (yellow-stripe-like) y se han clasificado dentro de la misma subclase de la familia OPT (Curie *et al.*, 2001; Yen *et al.*, 2001). Este descubrimiento es sorprendente, ya que *Arabidopsis* pertenece a las plantas de Estrategia I y entre las plantas superiores sólo las gramíneas sintetizan y excretan fitosideróforos, el substrato del transportador YS1. Como todas las plantas producen nicotianamina, y esta molécula es muy similar tanto en estructura como en su capacidad para unir Fe a los fitosideróforos, se podría especular con una posible función transportadora de complejos Fe-nicotianamina de las proteínas YSL en plantas no gramíneas. Además, la nicotianamina se ha encontrado en el floema, dónde es probable que forme quelatos con varios metales, incluyendo Fe, Zn, Ni y Cu, y participe en la homeostasis de estos metales a distintos niveles: transporte a larga distancia, compartimentalización o señalización del contenido de metales (Pich *et al.*, 1994; Stephan *et al.*, 1994).

4.2 Estrategia I

Las plantas dicotiledóneas y monocotiledóneas no gramíneas necesitan reducir Fe(III) antes de incorporarlo al interior de la raíz. Esta estrategia incluye: 1) la excreción de protones por una ATPasa de tipo P, 2) reducción del Fe(III) a Fe (II) por una reductasa Fe(III)-quelato; y 3) transporte del Fe (II) al interior de la raíz por un transportador específico.

En la Figura 1-4 se muestra el modelo propuesto para la adquisición de Fe por plantas de estrategia I. Los pasos serían los siguientes: 1) adsorción de los quelatos de Fe(III) en la raíz, 2) debilitamiento de los enlaces quelato-Fe(III), 3) reducción del Fe(III) a Fe(II), 4) disociación del quelato y 5) transporte del Fe(II) a través de un transportador de membrana.

En condiciones de deficiencia de Fe, las plantas de Estrategia I desarrollan una serie de respuestas que afectan a la morfología y fisiología de las raíces, todas ellas encaminadas a desarrollar mecanismos para aumentar la capacidad de absorción del Fe del suelo.

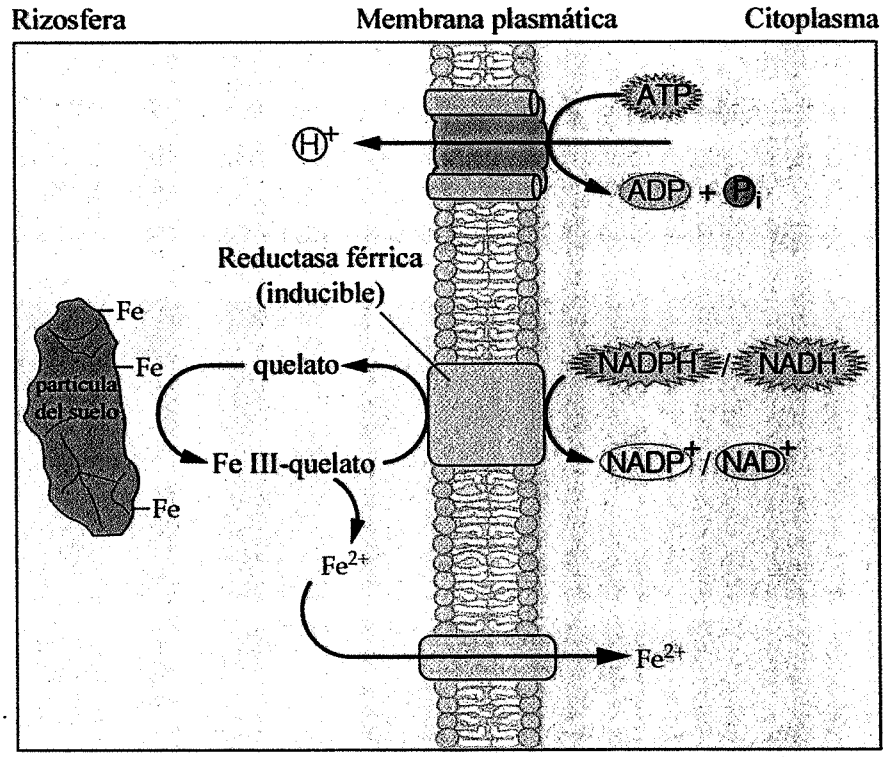

Figura 1-4. Estrategia I (Buchanan *et al.*, 2000).

Hasta el momento se han realizado pocos estudios integrados de las respuestas inducidas por la deficiencia de Fe en plantas de Estrategia I, considerando tanto aspectos fisiológicos como moleculares en una misma especie. Muchos de los estudios descritos en los párrafos siguientes se han realizado sobre aspectos puntuales de la Estrategia I. En nuestro laboratorio se han realizado estudios de la respuesta de la Estrategia I a la deficiencia de Fe en plantas de *Beta vulgaris* (Susín *et al.*, 1993, 1994, 1996; González-Vallejo, 2000; López-Millán *et al.*, 2000a, b, 2001a, b), pero en este modelo no son fáciles los análisis de expresión de proteínas, ya que es muy escasa la información de su genoma disponible en bases de datos públicas.

4.2.1 Cambios morfológicos en la raíz inducidos por la deficiencia de hierro

En condiciones de deficiencia de Fe la estructura radicular de muchas especies de estrategia I sufre cambios tanto a nivel macroscópico como microscópico. Estos cambios morfológicos van encaminados al aumento de la superficie de contacto entre la raíz y el suelo, incrementando de esta forma la posibilidad de adquisición de Fe por la planta. Entre los cambios macroscópicos, se produce una disminución en el crecimiento de la raíz primaria (Hutchinson, 1967; Brown y Ambler, 1974; Römheld y Marschner, 1981) acompañada por un aumento en el número de raíces laterales (Moog *et*

al., 1995; Pinton *et al.*, 1998). Estos cambios son evidentes después de un largo tiempo en deficiencia de Fe, mientras que otros cambios macroscópicos como la formación de pelos radiculares (Dell'Orto *et al.*, 2002) y el engrosamiento de las zonas subapicales de la raíz (Fig. 1-5) (Welkie y Miller, 1993; Landsberg, 1996, López-Millán *et al.*, 2000a) ocurren antes de que se observe una disminución en el crecimiento de la raíz.

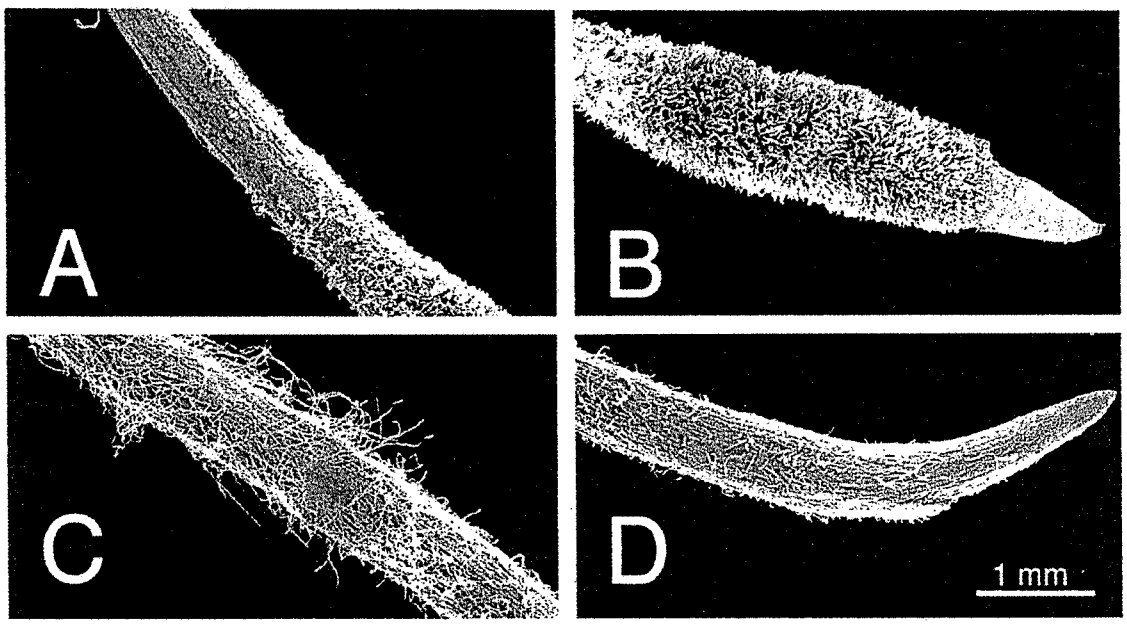

Figura 1-5. Microscopía electrónica de barrido de puntas de raíz, mostrando los segmentos distales de la raíz de plantas de remolacha deficientes en Fe a 5-10 mm (A), 0-5 mm (B) de la punta, y controles a 5-10 mm (C), 0-5 mm (D) de la punta (López-Millan *et al.*, 2000a).

El engrosamiento de las puntas de raíz no se observa en todas las especies (Wei *et al.*, 1997). Este engrosamiento es debido, por una parte, al aumento del tamaño de las células corticales y, por otra, a un incremento del número de células en la rizodermis e hipodermis (Landsberg, 1996; Kramer *et al.*, 1980). El engrosamiento de las raíces coincide espacialmente con aquellas zonas donde se produce la inducción en la reducción de Fe (Bell *et al.*, 1988) y la extrusión de protones (Alcántara *et al.*, 1991).

Los cambios microscópicos consisten en la formación de células de transferencia tanto en la rizodermis como en la hipodermis (Landsberg, 1996) aumentando así la superficie de contacto entre la pared celular y el citoplasma (Welkie y Miller, 1993; Landsberg, 1994; Schmidt y Bartels, 1996). Las células de transferencia se caracterizan por la existencia de multitud de invaginaciones, protuberancias en la pared celular más próxima al exterior, y por tener un citoplasma denso con numerosas mitocondrias y protoplastidios voluminosos (Landsberg, 1994). La función de estas células de transferencia aún no se conoce exactamente, aunque algunos autores proponen que esté relacionada con la inducción de la acidificación de la

rizosfera (Schmidt *et al.*, 2003). La frecuencia de las células de transferencia en raíces deficientes en Fe es mayor en las zonas acidificantes de la raíz que en las zonas no acidificantes. Además, las células de transferencia inducidas por deficiencia de Fe presentan mayor cantidad de enzima ATPasa que las células ordinarias de la epidermis (Schmidt *et al.*, 2003).

Experimentos de "split root" realizados en raíces de tomate muestran que la mitad de la raíz crecida sin Fe presenta un número de células de transferencia cuatro veces mayor que en la mitad crecida con Fe (Schmidt *et al.*, 2003). Sin embargo, respuestas como la extrusión de protones y actividad reductasa indican un comportamiento distinto, con una mayor inducción en la mitad de la raíz crecida con Fe que en la mitad crecida sin Fe (Schmidt *et al.*, 1996; Schikora y Schmidt, 2001). Aunque las bases moleculares de este comportamiento no se conocen hasta el momento, estos experimentos sugieren que los cambios morfológicos inducidos por la deficiencia de Fe están regulados a nivel local por la concentración de Fe (Schmidt *et al.*, 2003).

4.2.2 Cambios fisiológicos

- *Inducción de la actividad reductasa*

En las plantas de Estrategia I, la reducción del Fe(III) en la membrana plasmática es un paso obligatorio antes de la adquisición y transporte de este microelemento al interior de la planta (Chaney *et al.*, 1972). En deficiencia de Fe, la capacidad de reducción aumenta hasta alcanzar un máximo de actividad que varía dependiendo de la especie. Hasta el momento, todas las plantas pertenecientes a esta estrategia muestran un aumento de la actividad reductasa que oscila entre 5 y 20 veces (Moog y Brüggemann, 1994; Susín *et al.*, 1996; Sueyoshi *et al.*, 1997; López-Millán *et al.*, 2005). El tiempo en el que se produce la inducción también varía entre especies: en tomate, por ejemplo, este máximo de actividad se observa a los 8-10 días (Brown y Jolley, 1988, Zouari *et al.*, 2001), en judía a los 6-8 días (Schmidt, 1993) y en *Medicago* a los 7-9 días (López-Millán *et al.*, 2005). La reducción de Fe en raíces se ajusta a una cinética de tipo Michaelis-Menten con un pH óptimo para la reducción de Fe(III)-EDTA de 5,5 (Rosenfield *et al.*, 1991; Schmidt y Janiesch, 1991), y una Km que oscila entre 28 μM en soja (Cornett y Johnson, 1991) y 230 μM en tomate (Brüggemann *et al.*, 1990). Además, en algunas especies como tomate es necesaria la presencia de una cantidad mínima de Fe para la inducción de la actividad reductasa férrica (Romera *et al.*, 1996a, b; Zouari, 1996; Gogorcena *et al.*, 2000; Zouari *et al.*, 2001). Esta actividad reductasa se localiza generalmente en la superficie de las partes subapicales de las raíces que muestran engrosamiento, así como en los pelos radiculares (Moog y Brüggemann, 1994).

La reductasa férrica está codificada por un gen (*FRO*) que pertenece a una superfamilia de flavocitocromos cuyos miembros contienen en su secuencia sitios de unión a FAD y NADPH, en concordancia con su función en la transferencia de electrones desde los nucleótidos de piridina citosólicos a los quelatos férricos del lado opuesto de la membrana. Los genes de reductasa férrica caracterizados hasta la fecha son: *AtFRO2* en *Arabidopsis thaliana* (Robinson *et al.*, 1999), *LeFRO1* en tomate (Li *et al.*, 2004), *PsFRO1* en guisante (Waters *et al.*, 2002) y *MtFRO1* en *Medicago truncatula* (López-Millán *et al.*, 2005). Estos genes codifican polipéptidos de entre 712 y 725 aminoácidos con un peso molecular deducido entre 80,5 y 81,5 kDa y un punto isoeléctrico teórico de aproximadamente 9,4. En general, las proteínas descritas hasta el momento poseen seis dominios hidrofóbicos en el extremo N-terminal y dos en el C-terminal, todos ellos formando hélices α transmembrana (Fig. 1-6). Los sitios de unión de los cofactores se encuentran en el "loop" del lado citoplasmático que une las hélices α 6 y 7 (Robinson *et al.*, 1999).

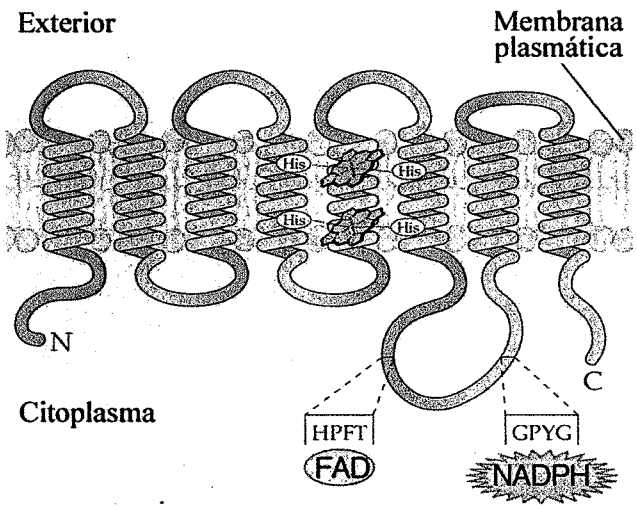

Figura 1-6. Estructura molecular de la reductasa férrica (Buchanan *et al.*, 2000).

En todas las especies para las cuales se conoce el gen de la reductasa (*Arabidopsis*, *Medicago*, tomate y guisante) se ha descrito un aumento inducido por la deficiencia de Fe, tanto en la actividad de esta enzima como en la expresión del gen correspondiente en raíces (Robinson *et al.*, 1999; Waters *et al.*, 2002; Li *et al.*, 2004; López-Millán *et al.*, 2005). Sin embargo, al contrario de lo que ocurre en *Arabidopsis* y *Medicago*, donde la expresión de *AtFRO2* y *MtFRO1* está restringida a raíz, *LeFRO1* se expresa en raíz, hoja, cotiledones, flores y frutos jóvenes de tomate (Li *et al.*, 2004) y *PsFRO1* se expresa en raíz, hoja y nódulos de guisante (Waters *et al.*, 2002). Estos datos de expresión sugieren una regulación distinta de estos genes en hoja y raíz, y/o la existencia de más de una reductasa indicando que *LeFRO1*

y *PsFRO1* participarían tanto en adquisición de Fe en raíz como en la distribución de Fe por la planta. Más aún, experimentos realizados con los mutantes de guisante *brz* y *dgl*, que tienen una regulación anormal de la adquisición de Fe, con una inducción constitutiva de la actividad reductasa (Grusak *et al.*, 1990a; Grusak y Pezeshgi, 1996), sugieren que la regulación del gen *PsFRO* es distinta en hojas y raíces. En estos mutantes, la expresión de *PsFRO1* está inducida en raíz, mientras que en hoja la expresión depende de la concentración de Fe (Waters *et al.*, 2002).

- *Acidificación de la rizosfera*

La acidificación de la rizosfera, al contrario de lo que ocurre con la reducción férrica, no es evidente en todas las especies de Estrategia I y, en aquellas especies que la muestran, esta respuesta depende de muchos factores como el balance de incorporación cationes/aniones, la composición de los exudados de la raíz y el tipo de nutrición nitrogenada.

La solubilidad del Fe en el suelo depende principalmente del pH, disminuyendo más de 1000 veces por cada aumento de unidad de pH. Por lo tanto, debilitar el enlace Fe-O por acidificación de la rizosfera es un método eficiente para incrementar la disponibilidad de Fe. La excreción neta de protones en deficiencia de Fe ha sido descrita en muchas especies (girasol, remolacha, pepino, tomate) y ha sido atribuida a un aumento de la actividad ATPasa de la membrana plasmática (Römheld *et al.*, 1984; Susín *et al.*, 1994; Dell'Orto *et al.*, 2000; Schmidt *et al.*, 2003). En raíces de tomate, la cantidad de la proteína H^+-ATPasa aumenta principalmente en las células de transferencia formadas en la rizodermis bajo condiciones de deficiencia de Fe (Schmidt *et al.*, 2003).

La ATPasa de membrana plasmática, perteneciente a la familia de ATPasas tipo P, es un polipéptido de aproximadamente 100 kDa (Palmgren, 2001). La Ca^{2+}-ATPasa es la primera ATPasa de tipo P resuelta por rayos X (Toyoshima *et al.*, 2000) y consta de diez dominios α-hélice transmembrana (Fig. 1-7). La región citoplasmática está divida en tres dominios: el dominio A incluye la región N-terminal y el "loop" citosólico, el dominio P es el de fosforilación y el dominio N contiene el sitio de unión a ATP (Palmgren, 2001). En pepino se han encontrado dos isoformas de la ATPasa (*CsHA1* y *CsHA2*). La expresión de una de ellas, *CsHA1*, aumenta en raíz en condiciones de deficiencia de Fe, mientras que la otra isoforma *CsHA2*, que se expresa tanto en raíz como en hoja, no se ve afectada por el estado nutricional de Fe de la planta (Santi *et al.*, 2005). En *Arabidopsis*, la familia de ATPasas de membrana plasmática está formada por 12 miembros cuya función, en la mayoría de los casos, no ha sido determinada hasta la fecha (Palmgren, 2001). La expresión de, al menos, 4 isoformas, entre ellas la *AtAHA2*, aumenta en raíces en condiciones de deficiencia de Fe (Santi *et al.*,

2005). La *AtAHA2* se expresa preferentemente en pelos radiculares y, además de en la adquisición de Fe, podría participar en la adquisición de otros nutrientes (Sussmann, 1994).

Por otro lado, el aumento de la excreción de protones podría tener otras funciones además de aumentar la solubilidad del Fe en la rizosfera. La afinidad del quelato de Fe por la reductasa aumenta en condiciones de pH bajo, probablemente debido a una neutralización de las cargas negativas superficiales del sitio de reducción, que podría evitar la repulsión de los quelatos de Fe cargados negativamente (Schmidt y Janiesch, 1991; Cohen *et al.*, 1997).

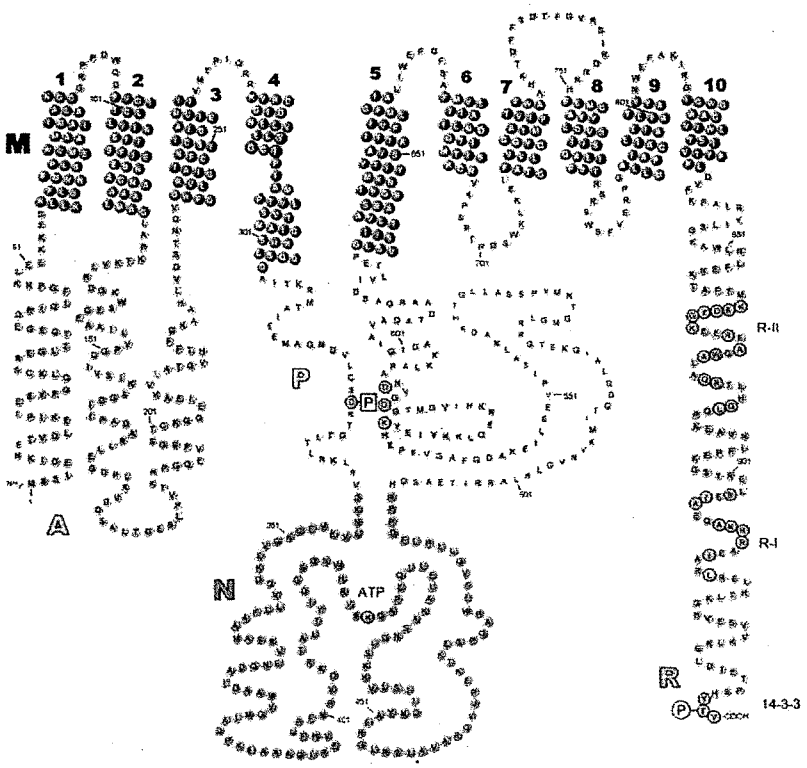

Figura 1-7. Estructura de la ATPasa de tipo P (Palmgren, 2001).

- *Transportador de Fe*

Una vez que el Fe es reducido, éste debe ser transportado al interior de la raíz. Datos bioquímicos indican que este transporte muestra una cinética de tipo Michaelis-Menten y está inducido en condiciones de deficiencia de Fe (Cohen *et al.*, 1998). Estudios moleculares en estos últimos años han identificado la familia de transportadores de metales ZIP ("ZNT-IRT like protein") que actúa no sólo en el transporte de este elemento en la membrana plasmática de raíz, sino también en su distribución en la planta. El primer miembro identificado de esta familia como transportador de Fe, codificado por el gen *IRT1*, se caracterizó en *Arabidopsis, y* corresponde a un

polipéptido de 347 aminoácidos con 8 dominios transmembrana (Eide *et al.*, 1996, Vert *et al.*, 2002) (Fig 1-8). IRT1 es un transportador de Fe(II) pero también puede transportar Mn(II), Zn(II), Cd(II) y Co(II) (Korshunova *et al.*, 1999; Rogers *et al.*, 2000). Este gen se expresa en la epidermis de la raíz y su expresión se induce después de 1 ó 2 días de crecimiento en condiciones de deficiencia de Fe, pero cuando las plantas son sometidas a experimentos de adición de Fe, su inducción desaparece en 12 - 24 horas, para evitar la acumulación perjudicial del metal y mantener así su homeostasis (Connolly *et al.*, 2002).

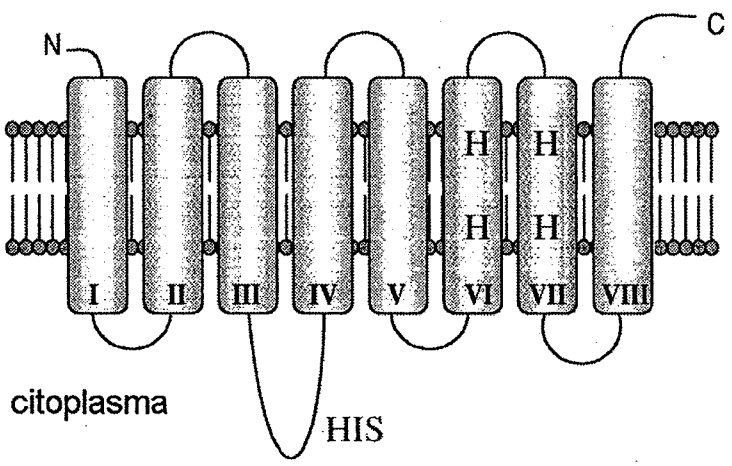

Figura 1-8. Predicción de la estructura de los transportadores de metales ZIP.

Otros genes homólogos han sido caracterizados en guisante (*RIT1*: Cohen *et al.*, 1998), y tomate (*LeIRT1* y *LeIRT2*: Eckhardt *et al.*, 2001). Todos ellos se expresan en raíz, pero sólo *RIT1* y *LeIRT1* se inducen por deficiencia de Fe.

Además de *IRT1*, otros transportadores de Fe de alta afinidad han sido clonados en *Arabidopsis* (Curie *et al.*, 2000; Thomine *et al.*, 2000). Estos transportadores pertenecen a la familia NRAMP ("Natural Resistance Associate Macrophage Proteins"), se expresan en raíz y parte aérea, pero su papel fisiológico todavía no ha sido completamente aclarado. Algunos de ellos, como AtNRAMP 1, 3 y 4, se inducen en condiciones de deficiencia de Fe.

4.2.3 Excreción de compuestos de bajo peso molecular

Las raíces de plantas pueden excretar, ya sea de forma activa o pasiva, gran variedad de compuestos orgánicos, entre los que se encuentran azúcares reductores, aminoácidos y ácidos orgánicos. Las cantidades excretadas pueden suponer hasta un 20% del carbono asimilado (Jones y Darrah, 1995). El tipo de exudados radiculares está determinado genéticamente, aunque

existen factores medioambientales que pueden causar una alteración en la composición de estos exudados. La tasa de exudación y su composición dependen del pH, temperatura y tipo de suelo, intensidad de la luz, así como de la edad y estado nutricional de la planta y de la presencia de microorganismos (Jones, 1998). La exudación de estos compuestos está estimulada en condiciones de deficiencia de Fe.

- *Fenoles*

Las plantas deficientes en Fe producen y excretan diferentes compuestos de naturaleza fenólica (Brown y Ambler, 1974). Entre los compuestos identificados se encuentra el ácido caféico, el ácido *p*-cumárico (Olsen *et al.*, 1981), el ácido fenólico y el ácido clorogénico (Hether *et al.*, 1984). Inicialmente se atribuyó a estos compuestos una función reductora del Fe(III). Sin embargo, varios estudios han mostrado que las cantidades excretadas no son suficientes para explicar la tasa de reducción encontrada en las plantas deficientes (Chaney *et al.*, 1972; Barret-Lennard *et al.*, 1983; Bienfait *et al.*, 1983), y que la adición de estos compuestos no sólo no afecta sino que incluso disminuye la actividad reductasa de Fe(III)-EDTA de las raíces (Römheld y Marschner, 1983).

Probablemente, el papel principal de los fenoles consista en la inhibición de la degradación de los ácidos orgánicos, cuyo papel en la nutrición férrica como quelantes de Fe es muy importante (Schmidt, 1999). Una función alternativa fue propuesta por Sijmons *et al.* (1985), al relacionar la excreción de estos compuestos con la pérdida de suberina, recubrimiento protector de las células corticales de la raíz, que presentan las raíces deficientes en Fe.

- *Flavinas*

En condiciones de deficiencia de Fe, algunas especies acumulan y excretan flavinas (Welkie y Miller, 1993). La flavina mayoritaria es la riboflavina (Kannan y Seshyri, 1988; Shinmachi *et al.*, 1994, 1995; Welkie, 1996) y, en algunas plantas como remolacha y espinaca, los sulfatos de riboflavina (Susín, 1994; Susín *et al.*, 1993, 1994). A pH alto, las flavinas se acumulan en la zona subapical de la raíz (Susín *et al.*, 1993) siendo excretadas al medio cuando las plantas crecen a pH bajo (Susín *et al.*, 1994a, b).

Las plantas que producen flavinas como remolacha (Welkie y Miller, 1988; Susín *et al.*, 1993, 1994; Susín, 1994), tabaco (Welkie y Miller, 1988), lechuga (Welkie y Miller, 1992), melón, alfalfa, pimiento (Shinmachi *et al.*, 1995) y pepino (Shinmachi *et al.*, 1992) son generalmente muy eficientes en la adquisición de Fe (Welkie y Miller, 1993). El papel de las flavinas en la deficiencia de Fe es todavía desconocido. Sin embargo, el hecho de que la acumulación de flavinas tenga lugar simultáneamente al incremento en la

actividad reductasa sugiere que estos compuestos podrían ser parte integral de los sistemas de reductasa férrica de las raíces (Cakmak *et al.*, 1987; Susín *et al.*, 1993). Además, el gen de la reductasa férrica pertenece a la familia de los flavocitocromos y contiene un sitio de unión a FAD (Robinson *et al.*, 1999).

Otra posible función de los sulfatos de riboflavina, una vez excretados a la rizosfera, podría ser una acción antimicrobiana en las proximidades de la raíz, disminuyendo la posibilidad de que los microorganismos del entorno compitan con la planta por la adquisición de Fe (Susín *et al.*, 1993).

La ruta de síntesis de la riboflavina, precursor del mononucleótido de flavina (FMN) y del dinucleótido de flavina y adenina (FAD), se puede ver en la figura 1-9. El compuesto de partida de la síntesis es el GTP, y mediante cinco pasos enzimáticos se obtiene la riboflavina. La DMRL sintasa (2.5.1.9), que cataliza el penúltimo paso de la biosíntesis de riboflavina, es un péptido de 16 a 17 kDa que ha sido clonado en espinaca, tabaco y *Arabidopsis thaliana* (Jordan *et al.*, 1999). Los sulfatos de riboflavina son posiblemente sintetizados por una enzima sulfotransferasa, similar a las que tienen como sustrato flavonoides, que transfiere el azufre desde un donador como adenosina 3'-fosfato 5'-fosfosulfato o adenosina 3'-fosfosulfato hasta el aceptor riboflavina, siendo el primero de estos donadores el más usado por las plantas (Varin *et al.*, 1987).

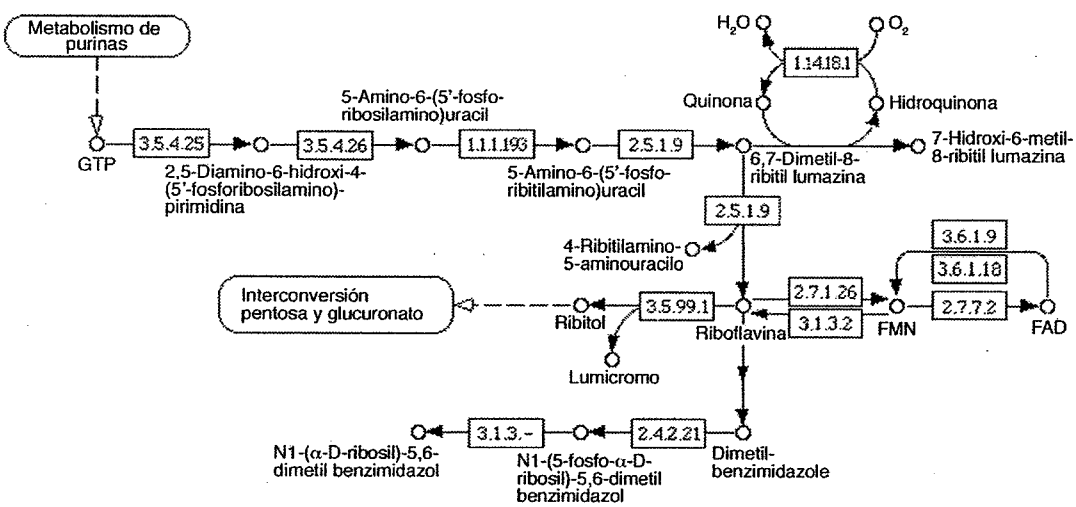

Figura 1-9. Metabolismo de la riboflavina.

- *Ácidos orgánicos*

En condiciones de deficiencia de Fe, las plantas dicotiledóneas acumulan en las raíces y excretan ácidos orgánicos, principalmente citrato y malato (Brown, 1966; de Vos *et al.*, 1986; Brancadoro *et al.*, 1995). Dependiendo de sus propiedades de disociación y del número de grupos carboxílicos, los

ácidos orgánicos pueden variar su carga negativa y, por tanto, quelar distintos metales de la solución del suelo. Por este motivo, los ácidos están implicados en un gran número de procesos en el suelo como la movilización y toma de nutrientes (por ejemplo Fe y P) por las plantas y microorganismos, la detoxificación de metales por las plantas (Zn y Al), la proliferación de microorganismos en la rizosfera y la disolución de minerales en el suelo (Jones, 1998).

En condiciones de deficiencia de Fe, la función más probable de estos ácidos consiste en la solubilización de Fe (III). Cuando el pH del suelo es bajo, tanto citrato como malato forman complejos estables con el Fe(III), favoreciendo su disolución en la solución del suelo (Jones *et al.*, 1996). En suelos calcáreos, con pH alto, la movilización del Fe por malato y citrato es lenta, puesto que los complejos que se forman son inestables y se degradan rápidamente (Jones *et al.*, 1996; Gerke, 1997). Sin embargo, en estas condiciones, la combinación del poder de acidificación de la ATPasa de la raíz con el poder quelante del citrato (que aumenta conforme disminuye el pH) podrían constituir un mecanismo viable para movilizar el Fe de la rizosfera (Jones, 1998). Usando un modelo de simulación por ordenador, Jones *et al.* (1996) estimaron que la concentración de Fe(III)-citrato en la interfase raíz-suelo podía llegar a ser de 0,1-50 μM. Por lo tanto, la concentración de Fe unida a ácidos orgánicos podría ser adecuada para satisfacer las necesidades de las plantas.

La excreción de estos ácidos orgánicos tiene lugar probablemente por difusión pasiva, gracias al gradiente de potencial electroquímico de la membrana plasmática (Jones y Darrah, 1995). Sin embargo, también se ha sugerido la posible existencia de un canal o transportador acoplado con la ATPasa de la membrana plasmática (Dinkelaker *et al.*, 1995; Fox *et al.*, 1996; Yamaguchi *et al.*, 2005).

4.2.4 Síntesis de proteínas en raíz

Las respuestas a la deficiencia de Fe implican cambios en la expresión de genes y un aumento general en el contenido de proteína celular (Sijmons y Bienfait, 1983; Pontiggia *et al.*, 2003). Varios trabajos sobre la deficiencia de Fe han demostrado que la actividad de un gran número de enzimas aumenta bajo estas condiciones, y el incremento, frecuentemente, se corresponde con un aumento en el contenido proteico además de con la posible existencia de regulación enzimática (Schmidt y Buckhout, 1997; Pontiggia *et al.*, 2003). Este aumento se ha demostrado por Western-blot para IRT1, PEPC y ATPasa (Dell'Orto *et al.*, 2000; De Nisi y Zocchi, 2000; Andaluz *et al.*, 2002; Connolly *et al.*, 2002; Vert *et al.*, 2003). Además, Schmidt (1999), usando el inhibidor de síntesis de proteína cicloheximida,

demostró que es necesaria la síntesis proteica *de novo* para aumentar la actividad de la reductasa férrica. Más aún, utilizando microscopía electrónica se ha demostrado que las puntas de raíz engrosadas tienen un citoplasma denso y rico en orgánulos y que el número de polisomas presentes en raíces deficientes en Fe es casi el doble que en raíces control, hechos que demuestran la existencia de una mayor actividad biosintética (Landsberg, 1994; Dell'Orto *et al.*, 2002; Pontiggia *et al.*, 2003). Otro resultado que apoya el incremento en la síntesis proteica, es el incremento observado en la cantidad total de aminoácidos libres, en particular los ácidos glutámico y aspártico (Pontiggia *et al.*, 2003).

La aplicación de nuevas técnicas de proteómica (Cánovas *et al.*, 2004), tales como la electroforesis bidimensional y las técnicas espectroscopia de masas, permitirá la obtención y el análisis de mapas proteicos de raíces controles y deficientes en Fe, y aportará una visión más global de los cambios que experimenta la raíz en su adaptación a este estrés ambiental.

5. TRANSPORTE DE HIERRO

5.1 Transporte en la raíz

Una vez dentro de las células, el Fe(II) debe ser protegido del oxígeno para evitar la generación de radicales libres que producen estrés oxidativo. Hasta la fecha, se desconoce la naturaleza de la molécula o moléculas quelantes de Fe en la raíz, y de hecho, distintas moléculas podrían tener esta función dependiendo de la localización subcelular del Fe. Según Hell y Stephan (2003), aunque algunos ácidos orgánicos y aminoácidos son apropiados para quelar el Fe(II), el papel más importante en el tráfico de Fe en el citoplasma lo podría tener la nicotianamina (NA). Estos autores se basan en varias razones:

- La NA forma complejos estables tanto con el Fe(III) como con el Fe(II) a pHs neutros o ligeramente alcalinos (Stephan *et al.*, 1996). Además, aunque la constante de formación del complejo Fe(III)-NA es mucho mayor que la de Fe(II)-NA, cinéticamente el complejo Fe(II)-NA es más estable en condiciones aeróbicas (von Wirén *et al.*, 1999).
- La NA parece estar presente en todas las plantas superiores y se encuentra en todos los tejidos (Scholz *et al.*, 1992).
- Los complejos Fe-NA no actúan bien como sustratos para la reacción de Fenton (von Wirén *et al.*, 1999).
- El mutante de tomate *chloronerva*, deficiente en NA, muestra tanto precipitación de Fe en vacuolas y mitocondrias (Liu *et al.*, 1998) como elevadas actividades de enzimas antioxidantes (Herbik *et al.*, 1996).

En las puntas de raíz de girasol y cebada, la concentración de NA aumenta en aquellas zonas de la raíz donde se produce la adquisición de Fe (Stephan y Scholz, 1990). Además, la concentración de NA se correlaciona con la localización y concentración de Fe en guisante y tomate (Pich *et al.*, 2001).

5.2 Transporte en el xilema

La forma por la que el Fe es transportado al interior del xilema no ha sido aclarada todavía, pero probablemente se realiza a través de canales iónicos que están controlados por el voltaje de la membrana (Gaymard *et al.*, 1998; Köhler *et al.*, 2002). Recientemente se ha identificado un gen, *FRD3* (Rogers y Guerinot, 2002; Green y Rogers, 2004), perteneciente a la familia MATE (Multi Antimicrobial Extrusion), que podría estar implicado en el transporte de Fe a la parte aérea de la planta. Este gen se expresa en el periciclo y otros tejidos vasculares de raíz, y su expresión aumenta en condiciones de deficiencia de Fe. No se conoce exactamente cuál es el papel de *FRD3* en la homeostasis del Fe, pero se ha especulado con dos posibles funciones: la carga y descarga en la savia de xilema bien de Fe o de una molécula necesaria para su transporte, y la participación en la señalización del estado nutricional de Fe en la planta (Rogers y Guerinot, 2002; Green y Rogers, 2004). Una vez que el Fe está dentro del xilema, sería oxidado de nuevo y está aceptado que se trasporta como complejo Fe(III)-citrato (Tiffin, 1966; López-Millán *et al.*, 2000b; Abadía *et al.*, 2002). El tipo de complejo en el que se encuentra el Fe(III) podría variar con la edad de las plantas y también en situaciones de estrés, ya que la composición y pH de la savia del xilema podría variar en dichos casos. Utilizando programas de especiación química se ha demostrado que el Fe en xilema de remolacha y tomate estaría principalmente formando complejos con citrato, a pesar de que el malato fue el ácido orgánico mayoritario, tanto en plantas control como deficientes en Fe (López-Millán *et al.*, 2000b; White *et al.*, 1981a, b). En condiciones control, el Fe se encontraría mayoritariamente (61%) en forma de $FeCitOH^-$, mientras que en situación de estrés el dímero $FeCit_2^{3-}$ sería la especie mayoritaria (96%).

5.3 Transporte al interior de las hojas

El mecanismo de transporte de Fe desde la savia de xilema hasta las hojas todavía no se conoce en profundidad. Inicialmente, el Fe en el apoplasto debe ser reducido antes de entrar a la célula del mesófilo. Para esta reducción se propuso la existencia de una enzima reductasa férrica en la membrana plasmática de las células del mesófilo que podría ser similar a la

presente en la membrana plasmática de la raíz (Brüggeman *et al.*, 1993). Aunque esta idea de un reducción enzimática en hoja ha producido controversia (Schmidt, 1999), la actividad reductasa Fe(III)-citrato ha sido claramente demostrada tanto en discos de hoja (Larbi *et al.*, 2001) como en protoplastos (González-Vallejo, 2000). Más aún, el gen *FRO1* de guisante se ha encontrado expresado en hoja y su expresión se induce en condiciones de deficiencia de Fe (Waters *et al.*, 2002). Por otro lado, se ha propuesto que el citrato de Fe(III) podría ser fotoreducido *in vivo* en la hoja por luz ultravioleta y/o azul (Jolley *et al.*, 1987), dado que la citada reacción se puede producir *in vitro* (Bienfait y Scheffers, 1992). En todo caso, la reducción de quelatos férricos en hoja está claramente estimulada por luz (Brüggemann *et al.*, 1993; González-Vallejo *et al.*, 2000). Una vez en el citoplasma de la célula del mesófilo, el Fe podría estar quelado de nuevo con NA (Hell y Stephan, 2003) que actuaría como molécula transportadora de Fe a aquellos compartimentos donde se necesita. De hecho, en el mutante *chloronerva* no se ha podido detectar inmunológicamente fitoferritina (Becker *et al.*, 1995), aunque se vieron precipitados de Fe en el cloroplasto (Liu *et al.*, 1998). Esto indicaría la función del NA como mediador entre las distintas formas de almacenamiento y utilización de Fe.

5.4 Transporte al cloroplasto

El cloroplasto es el destino final de una gran parte del Fe de la planta (80%, Young y Terry, 1982). El transporte de Fe al interior del plastidio es de gran importancia en fisiología de plantas, y, paradójicamente, está poco documentado. Los datos disponibles hasta ahora sobre caracterización del transporte de Fe hacia el interior del cloroplasto a través de la envoltura del mismo (Bughio *et al.*, 1997a, b; Mori, 1998), indican que es un transporte activo y dependiente de luz. Estudios recientes parecen indicar que el transporte se realiza a través de mecanismos uniporte no específicos, estimulados por potencial de membrana (Shingles *et al.*, 2002). Este transporte se inhibe completamente por Zn(II), Cu(II) y Mn(II). Curie *et al.* (2000) han descrito la existencia de un péptido señal de transporte a la membrana del cloroplasto en el extremo N-terminal de la proteína NRAMP1, perteneciente a la familia NRAMP (Natural Resistance-Associated Macrophage Protein), sugiriendo un posible papel de este transportador en el transporte de Fe al interior del cloroplasto. Estudios con cloroplastos aislados de plantas de cebada control sugieren, que previamente al transporte, es necesaria una reducción mediada por una reductasa de Fe(III) no dependiente de ATP (Bughio *et al.*, 1997b). Más aún, en *Arabidopsis* se han descrito al menos 8 miembros de la familia FRO de

reductasas férricas y alguno de ellos podría estar implicado en este proceso (Yi y Guerinot, 1996).

Una vez que el Fe alcanza su destino final, si no va a ser utilizado, es necesario que sea acumulado en forma no tóxica y soluble, para que posteriormente pueda ser liberado según las necesidades metabólicas de la planta. Esta función la realiza una proteína denominada ferritina (Briat, 1996; Briat y Lobréaux, 1997) que se encuentra en el estroma del cloroplasto y en plastidios tales como proplastidios, etioplastos y amiloplastos (Briat y Lobréaux, 1997). Así, se ha descrito que en cebada el 75% del Fe cloroplástico se encuentra en el estroma mientras que el resto se encuentra en la membrana tilacoidal (Bughio *et al.*, 1997a). La ferritina es un complejo proteico multimérico con 24 subunidades que es capaz de almacenar hasta 4.500 átomos de Fe en su cavidad central (Fig. 1-10). La abundancia de la ferritina está controlada por un mecanismo regulador preciso que pone de manifiesto la necesidad de un fuerte control homeostático en la célula (Briat *et al.*, 1999).

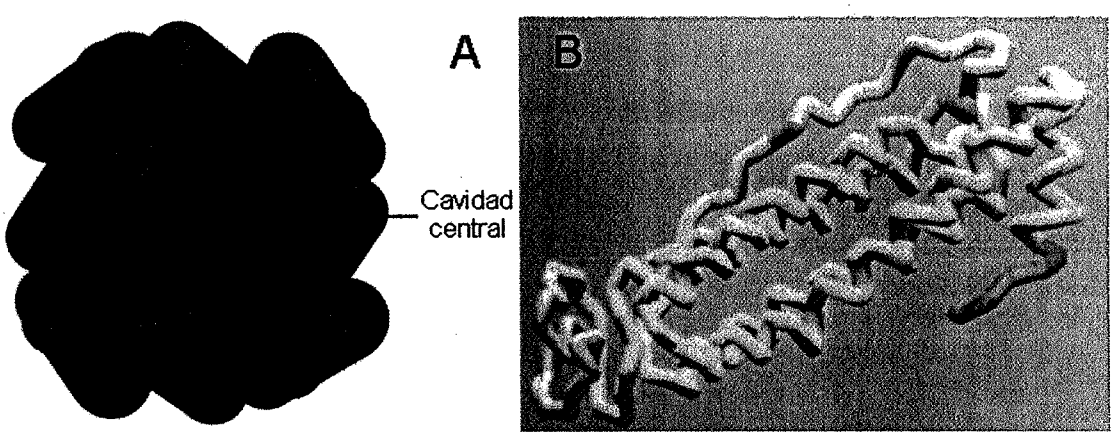

Figura 1-10. Estructura de la ferritina. A. Representación esquemática del complejo multimérico. B. Modelo estructural de una subunidad de ferritina (Briat, 1997).

5.5 Transporte en el floema

El floema es el tejido vegetal encargado del transporte a larga distancia, desde los órganos de producción, principalmente hojas maduras, hasta los tejidos en crecimiento y órganos reproductivos o de almacenamiento, de una amplia variedad de compuestos. En angiospermas está constituido por tubos cribosos, parénquima floemático y, en algunos tejidos, fibras floemáticas. En el floema secundario, los elementos de los tubos cribosos se encuentran asociados a células parenquimáticas especializadas denominadas células de compañía (Azcón-Bieto y Talón, 2000). En los elementos de los tubos cribosos existen unas punteaduras agrupadas en los polos de la célula formando unas estructuras denominadas placas cribosas (Fig. 1-11). Los

elementos de los tubos cribosos son las células más características de este tejido. Durante su madurez funcional estas células pierden el núcleo aunque conservan el citoplasma. Las células de compañía mantienen vivo dicho citoplasma permitiendo el transporte de sustancias.

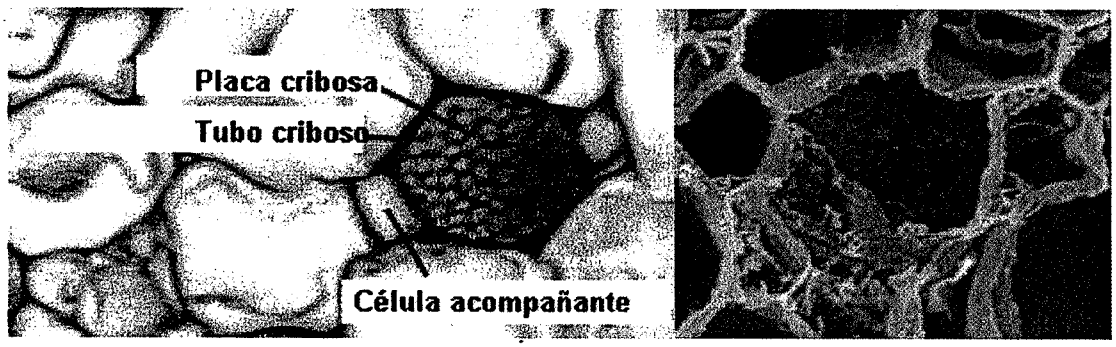

Figura 1-11. Corte transversal del tubo criboso y su célula acompañante. A. Microscopía óptica. B.microscopía electrónica de barrido (http://www.biologia.edu.ar).

Aunque la translocación de Fe desde las hojas maduras a las partes de la planta en crecimiento a través del simplasto y el floema se conoce desde hace mucho tiempo (Edding y Brown, 1967), la movilidad del Fe en el floema está pobremente documentada. Una de las moléculas identificadas como posible transportador de metales en el floema es la nicotianamina (NA) (Stephan y Scholz, 1993), aunque también se ha sugerido que el Fe pueda estar unido a un péptido de bajo peso molecular formando un complejo férrico de 2,4 kDa (Maas *et al.*, 1988). Recientemente, Krüger *et al.* (2002) han purificado una proteína del floema de *Ricinus communis*, de 17 kDa de peso molecular, que es capaz de unir *in vivo* Fe(III), pero no Fe(II). *In vitro*, dicha proteína puede unir Fe(III), Cu(II), Zn(II) y Mn(II). Estos autores han clonado un cDNA, *ITP* (Iron Transporter Protein), que codifica una proteína de 96 aminoácidos perteneciente a la familia "Late Embryogenesis Abundant" (LEA). Este gen se expresa en semillas y hojas maduras y un 67% de sus aminoácidos está constituido por histidina, lisina, ácido glutámico y glicina.

Debido a que en floema existe una concentración baja (4%) pero significativa del ión ferroso en equilibrio con el ión férrico y a la mayor afinidad de NA por el ión ferroso al pH ligeramente alcalino del floema (Maas *et al.*, 1988), se ha especulado sobre el hecho de que la NA podría actuar como lanzadera, quelando el Fe del complejo Fe-ITP durante los procesos de carga y descarga del floema y manteniendo, por tanto, un nivel basal de Fe(II). Para que esta hipótesis sea cierta es necesaria la existencia de:

1. uno o varios transportadores de Fe(II)-NA en las células adyacentes del floema. Unos buenos candidatos para esta función serían los

transportadores "Yellow Stripe Like" (YSL) (Curie *et al.*, 2001), de los que se han encontrado 8 homólogos en *Arabidopsis* (DiDonato *et al.*, 2004; Schaaf *et al.*, 2005) y 18 en arroz (Gross *et al.*, 2003).

2. un sistema de oxido-reducción que debería funcionar dentro del floema para oxidar el Fe(II)-NA generando el Fe(III) que se uniría a la proteína ITP y para reducir el Fe(III)-ITP a Fe(II) permitiendo su unión a NA. Actualmente no existe candidato para esta actividad oxido-reductora, aunque en calabaza (*Cucurbita maxima)* se ha descrito la existencia de una proteína, la citocromo b_5 reductasa, que se encuentra anclada a la membrana a través de su dominio N-terminal, cuyo corte produce una proteína soluble. Esta proteína presenta actividad Fe(III)-citrato reductasa *in vitro*, y es capaz de entrar a los tubos cribosos del floema. Además, su transcrito está inducido por deficiencia de Fe y reprimido por exceso de Fe (Xoconostle-Cazares *et al.*, 2000).

El estudio de los exudados de floema, usando las nuevas técnicas de proteómica, ampliará los datos disponibles sobre las proteínas solubles en el floema. Además, se podrán realizar estudios específicos sobre el transporte de micronutrientes en este medio.

6. CAMBIOS EN EL METABOLISMO INDUCIDOS POR DEFICIENCIA DE HIERRO

La respuesta a la deficiencia de Fe es más compleja que la simple activación de los mecanismos de adquisición de Fe por la raíz. Además de estos mecanismos, se producen cambios metabólicos a nivel de planta entera dirigidos a mantener las actividades enzimáticas implicadas en la adquisición, transporte y utilización de Fe.

6.1 Metabolismo energético

Para mantener la activación de los procesos de reducción y excreción de protones bajo condiciones de deficiencia de Fe, es necesario incrementar las tasas de regeneración de NAD(P)H y ATP. Tanto la proporción $NADPH:NADP^+$ (Sijmons *et al.*, 1984; Schmidt y Schuck, 1996) como la concentración de ATP (Espen *et al.*, 2000; López-Millán *et al.*, 2000a) en especies como judía, *Plantago lanceolata*, remolacha y pepino, son más altas en condiciones de deficiencia de Fe. Se ha demostrado también que después de la adición de compuestos férricos aumenta el estado oxidado de los pares $NADH/NAD^+$ y $NADPH/NADP^+$ en plantas de judía (Sijmons *et al.*, 1984) y *Plantago lanceolata* (Schmidt y Schuck, 1996) crecidas en deficiencia de Fe. En condiciones aeróbicas, la recarga de estos substratos

requiere la aceleración del metabolismo unido a la ruta respiratoria. De este modo, se ha demostrado que la tasa de oxígeno incorporado por las raíces aumenta en deficiencia de Fe (Espen *et al.*, 2000; López-Millán *et al.*, 2000a), aunque es difícil asociar esta mayor utilización de oxígeno únicamente a la cadena oxidativa de transporte electrónico, ya que también están presentes rutas oxidativas alternativas (López-Millán *et al.*, 2000a) o, incluso, parte del oxígeno podría estar siendo utilizado directamente por la reductasa férrica cuando las plantas crecen en completa ausencia de Fe. Observaciones por microscopía electrónica de segmentos apicales de raíz mostraron que en secciones de puntas deficientes el número de mitocondrias aumenta (Landsberg, 1994; Dell'Orto *et al.*, 2002; Schmidt *et al.*, 2003). Por último, apoyando también la tesis de un control respiratorio, análisis por micromatrices ("microarrays") de genes inducibles por deficiencia de Fe en *Arabidopsis* revelan que existe una inducción de componentes de la cadena de transferencia electrónica mitocondrial, principalmente citrocromo C reductasa y oxidasa (Thimm *et al.*, 2001).

Por otro lado, López-Millán *et al.* (2000a) mostraron que, en condiciones de Fe limitado, algunas enzimas asociadas con el metabolismo anaeróbico, como la lactato deshidrogenasa y la piruvato descarboxilasa, presentan un incremento en su actividad. Este comportamiento ha sido apoyado por análisis de micromatrices (Thimm *et al.*, 2001), que muestran una inducción de las enzimas de metabolismo anaeróbico lactato deshidrogenasa, piruvato descarboxilasa y alcohol deshidrogenasa. Estos resultados podrían interpretarse como un sistema de by-pass para mantener el flujo de carbono y producción de energía por reacciones glicolíticas cuando, por alguna razón, el oxígeno es un factor limitante.

6.2 Metabolismo de carbohidratos

La glucosa es la principal fuente para la síntesis de substratos energéticos y para el aporte de esqueletos carbonados a las raíces. En un tejido metabólicamente activo, el elevado requerimiento de glucosa se mantiene mediante la degradación del almidón almacenado en raíces o por traslocación de fotosintatos desde la parte aérea. Esto ocurre, por ejemplo, en judía (de Vos *et al.*, 1986) donde la concentración de azúcares en el floema de plantas deficientes es doble de la que se encuentra en las controles. También en raíces de pepino deficientes en Fe se ha descrito una disminución en la concentración de almidón, que ocurre al mismo tiempo que un aumento en la concentración de carbohidratos sencillos, principalmente glucosa-6-fostato y, en menor grado, fructosa-6-fosfato (Espen *et al.*, 2000). Además, la actividad de enzimas participantes en la glicólisis, como la gliceraldehido-3-fosfato deshidrogenasa (Sijmons y

Bienfait, 1983; Rabotti *et al.*, 1995; Espen *et al.*, 2000), la piruvato quinasa y la fructosa-6-fosfato quinasa (Espen *et al.*, 2000), también aumentan en deficiencia de Fe. Estos resultados parecen indicar que la adaptación a la deficiencia de Fe implica, por parte de las raíces, una activación de las reacciones glicolíticas y una disminución de la síntesis de carbohidratos. La activación de la glicólisis proporciona una serie de elementos necesarios para la activación de las respuestas características de la Estrategia I (ATP para mantener el aumento de actividad de la ATPasa, equivalentes de reducción para la reductasa férrica y fosfoenolpiruvato) y, finalmente, contribuye a la regulación del pH citosólico.

Además, otras rutas metabólicas y actividades enzimáticas citosólicas encaminadas a aumentar la producción de equivalentes reductores necesarios para mantener el aumento de actividad de la reductasa férrica, están activadas durante la deficiencia de Fe. Así en deficiencia de Fe, se han encontrado aumentos de actividad en la enzima glucosa-6-fosfato deshidrogenasa (G6PDH), perteneciente a la ruta de las pentosas fosfato (Sijmons y Bienfait, 1983; Rabotti *et al.*, 1995; López-Millán *et al.*, 2000a), la malato deshidrogenasa (Sijmons y Bienfait, 1983; Rabotti *et al.*, 1995, López-Millán *et al.*, 2000a), y la isocitrato deshidrogenasa (IDH) (López-Millán *et al.*, 2000a).

6.3 Fosfoenolpiruvato carboxilasa

Entre las actividades metabólicas que están aumentadas en deficiencia de Fe, la fosfoenolpiruvato carboxilasa (PEPC) merece una mención especial, ya que, en muchos casos, su activación no sólo es comparable sino aún mayor que la de otras respuestas características de la Estrategia I, como por ejemplo la actividad reductasa férrica. La PEPC es una enzima muy abundante en plantas y cataliza la fijación de bicarbonato a fosfoenolpiruvato para producir oxalacetato y fósforo inorgánico. En plantas C3 y tejidos no fotosintéticos, la PEPC actúa como fuente anaplerótica de reposición de intermediarios para el ciclo de Krebs y de esqueletos carbonados para la síntesis de aminoácidos, y en la regulación del pH citosólico.

En condiciones de deficiencia de Fe, la actividad de la enzima PEPC, en base a peso fresco, aumenta 4 veces en raíces de pepino (De Nisi y Zocchi, 2000) y 60 veces en puntas amarillas de raíz de remolacha (López-Millán *et al.*, 2000a). Este aumento en la actividad puede ser debido a una alta regulación alostérica de la enzima similar a la descrita en otros casos (Chollet *et al.*, 1996) y/o a un aumento de la cantidad de la proteína (De Nisi y Zocchi, 2000, Andaluz *et al.*, 2002), quizá mediado por una posible

inducción de la transcripción (se ha realizado un comunicación a un Congreso en 2004 en dicho sentido, De Nisi *et al.*, 2004).

El aumento de la actividad PEPC en raíz de pepino deficiente en Fe ocurre principalmente en las capas externas de las células corticales que, a su vez, son muy activas en la extrusión de protones (De Nisi *et al.*, 2002). Así mismo, el aumento en la actividad PEPC coincide con una acumulación de ácidos orgánicos en raíz deficiente (López-Millán *et al.*, 2000a; Abadía *et al.*, 2002). Se han establecido dos hipótesis para explicar estas correlaciones:

- Una primera hipótesis se basa en la teoría "pH-stat" formulada por Davies en 1973. Esta teoría propone que la alcalinización del citoplasma asociada con la extrusión de H^+ activaría la PEPC y, en consecuencia, aumentaría la concentración de ácidos orgánicos. Este aumento en la concentración de ácidos mantendría el balance iónico en el citoplasma, re-equilibrando el pH citosólico en su valor fisiológico. Estudios *in vivo* con ^{31}P-NMR han demostrado que el pH citosólico aumenta ligeramente bajo deficiencia de Fe (Espen *et al.*, 2000). Sin embargo, la acumulación de ácidos orgánicos en deficiencia de Fe no está necesariamente acoplada a la extrusión de H^+ (Bienfait, 1989; Landsberg, 1981), lo que plantea dudas sobre la validez de esta hipótesis.
- La segunda hipótesis sugiere un papel más complejo para la PEPC. La activación de la excreción de H^+, como una de las principales respuestas a la deficiencia de Fe, requiere no sólo producción de ATP como combustible de la ATPasa, sino también producción de H^+ para ser excretado por la enzima. La glicólisis podría ser la ruta que satisficiese ambos requerimientos. De hecho, tres reacciones glicolíticas son consideradas protogénicas, las catatalizadas por la hexoquinasa, la fosfofructoquinasa (PFK) y la gliceraldehido-3-fosfato deshidrogenasa (G3PDH). Para mantener la tasa de glicólisis lo suficientemente alta, el fosfoenolpiruvato (PEP) debe ser consumido con el fin de desplazar el equilibrio y, además, evitar la inhibición alostérica sobre la enzima piruvato quinasa (PK). En plantas donde la actividad ATPasa es alta, la actividad PEPC también está aumentada y como consecuencia la tasa de glicólisis también se incrementa. Así, de acuerdo con lo expuesto anteriormente, se han encontrado aumentos en las acitividades de la PFK en pepino (Espen *et al.*, 2000) y de G3PDH en pepino (Rabotti *et al.*, 1995), judía (Bianfait *et al.*, 1983) y tomate (Herbik *et al.*, 1996) cuando las plantas se cultivaron en deficiencia de Fe.

El PEP producido por el aumento de la actividad glicolítica puede ser utilizado por dos enzimas: la PEPC y la PK. La ventaja de la PEPC sobre la piruvato quinasa (PK) en el consumo de PEP no se ciñe exclusivamente a la termodinámica, sino también a su capacidad de producir ácidos orgánicos protogénicos (Davies, 1973; Lance y Rustin, 1984). Además, la PEPC podría

actuar como by-pass frente al posible control negativo ejercido por el citrato sobre la PK. Este modelo asume que la excreción de H^+ sería la fuerza conductora para la activación de la glicólisis y que la PEPC está activada como consecuencia de la acumulación de PEP. Aunque también se puede plantear de otro modo, considerando que la PEPC es el punto clave en la respuesta a la deficiencia de Fe y su activación produce un aumento de la glicólisis, que a su vez induciría una activación de la ATPasa.

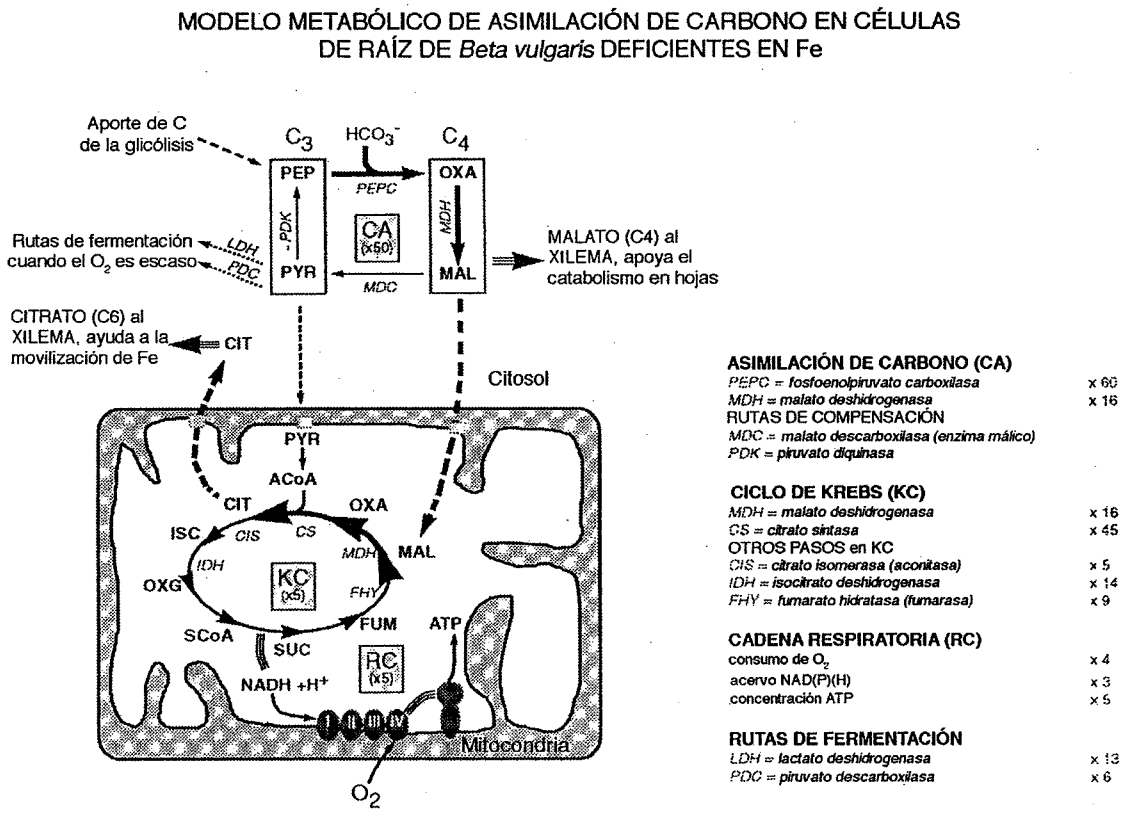

Figura 1-12. Modelo metabólico de la asimilación de Fe (López-Millán *et al.*, 2000a).

Independientemente de la hipótesis, la activación de la PEPC produce un aumento en la concentración de oxalacetato y/o malato. Estos compuestos son utilizados como fuente de carbono en el ciclo de Krebs (Fig. 1-12). Esta función anaplerótica de reposición de intermediarios del ciclo de Krebs es importante para producir tanto ATP como ácidos orgánicos, que son exportados desde la mitocondria al citosol. Estos ácidos orgánicos pueden realizar distintas funciones:

- pueden ser liberados a la rizosfera y utilizados posteriormente para quelar y facilitar la adquisición de Fe del suelo,
- pueden ser translocados al xilema donde quelarían el Fe, facilitando así su transporte a la parte aérea (Tiffin, 1966; López-Millan *et al.*, 2000b). En las hojas cloróticas, los ácidos orgánicos podrían ser utilizados

también como fuente anaplerótica de carbono para mantener procesos básicos como la respiración y el crecimiento (Abadía *et al.*, 2002), ya que la fotosíntesis en estas hojas deficientes en Fe está muy afectada (Terry, 1980).

- pueden participar en la síntesis de NADH y NADPH, a través de las actividades enzimáticas de la IDH y G6PDH. Estos nucleótidos podrían actuar como fuente de poder reductor para la reductasa férrica de raíz.

El aumento en la actividad de la PEPC en las raíces deficientes en Fe puede ser debido a distintos factores: inducciones de la transcripción por el estado nutricional de la planta, modificaciones post-transcripcionales como la fosforilación (Vidal y Chollet, 1997) u otras todavía no identificadas, y/o regulaciones alostéricas de la enzima PEPC (Chollet et al., 1996). Un estudio más detallado de esta enzima permitirá conocer los mecanismos que regulan esta importante proteína de la respuesta de la Estrategia I a la deficiencia de Fe.

7. CAMBIOS EN LA FOTOSÍNTESIS INDUCIDOS POR LA DEFICIENCIA DE HIERRO

La clorosis debida a la baja concentración de clorofilas y carotenoides por área foliar (Morales *et al.*, 1990, 1994; Abadía y Abadía, 1993) es una de las principales características de la deficiencia de hierro. Las hojas deficientes en Fe reducen el número de membranas tilacoidales por cloroplasto (Spiller y Terry, 1980) así como el número de ciertos componentes de las membranas: transportadores electrónicos de la cadena fotosintética, como el PSII, citocromo f, PSI y ferredoxina (Spiller y Terry, 1980; Terry y Abadía, 1986); y clorofilas y carotenoides (Morales *et al.*, 1990, 1994; Abadía y Abadía, 1993). Se ha descrito que la deficiencia de Fe en remolacha produce mayores cambios en el cloroplasto que en el resto de los orgánulos celulares (Platt-Aloia *et al.*, 1983). Estos cambios consisten en la reducción de los apilamientos tilacoidales y en la presencia de glóbulos osmiofílicos en el estroma (Spiller y Terry, 1980). En los tilacoides de plantas deficientes se ha observado una reducción del 75 % en la cantidad de galactolípidos (Abadía *et al.*, 1988) y reducciones en la relación MGDG/DGDG de los tilacoides (Nishio *et al.*, 1985; Abadía *et al.*, 1989), hecho que está de acuerdo con la disminución del grado de apilamiento de las membranas, observado en los cloroplastos de plantas deficientes en Fe (Fig. 1-13).

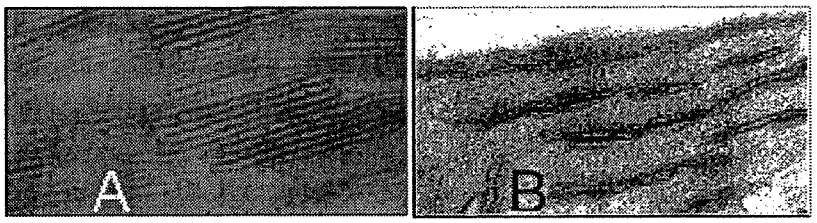

Figura 1-13. Detalle del grado de apilamiento de tilacoides de melocotonero en condiciones control (A) y de deficiencia de Fe (B) (Morales *et al.*, 2000a).

En cuanto a los pigmentos fotosintéticos, no todos disminuyen en igual proporción, ya que existe una disminución preferente de Chl *b* y, por lo tanto, de antena extrínseca LHC. El gran descenso observado en el contenido de Chl en las plantas deficientes en Fe ha sido explicado de diversas formas. Algunos autores relacionan la disminución del contenido de Chl en las plantas deficientes en Fe con la existencia de pasos dependientes de este elemento en la ruta biosintética de la misma (Pushnik *et al.*, 1984; ver referencias en Terry y Abadía, 1986). Otra posible explicación de la disminución de Chl podría ser la carencia de proteínas a las que unirse, ya que la mayor parte de los pigmentos fotosintéticos en las membranas tilacoidales aparecen formando complejos pigmento-proteína. Además del descenso en el contenido de Chl, también se produce una disminución en las concentraciones foliares de carotenoides (Terry, 1980; Morales *et al.*, 1990, 1994, 2000b), aunque en menor grado que en la concentración de Chl. No todos los carotenoides disminuyen de igual forma, produciendose un menor descenso en xantofilas que en ß-caroteno.

Por otro lado, la disminución del contenido de pigmentos en las hojas de plantas deficientes en Fe puede restringir la inserción estable de proteínas a la membrana tilacoidal produciendo en consecuencia una disminución en el contenido proteico de la misma (Paulsen *et al.*, 1993). Aparte de la disminución de proteínas tilacoidales, también se ha demostrado la existencia de un nuevo pigmento-proteína inducido por la deficiencia de hierro en la cianobacteria *Synechococcus* sp (Riethman y Sherman, 1988; Burnap *et al.*, 1993). Esta proteína, CP43', está codificada por el gen *ISIA* y tiene gran homología con la proteína del fotosistema II CP43. Bibby *et al.* (2001) en *Synechocystis* sp. y Boekema *et al.* (2001) en *Synechococcus* sp mostraron que la proteína CP43' se asocia para formar un anillo de 18 moléculas de CP43' alrededor de un trímero de fotosistema I (PSI). La utilización de esta proteína como una antena extra del PSI aumenta la flexibilidad del LHC de cianobacterias y parece compensar el descenso de los niveles de ficobilisomas y PSI en respuesta a la deficiencia de Fe (Bibby *et al.*, 2001; Boekema *et al.*, 2001). En remolacha se han encontrado indicios de la existencia de un nuevo complejo pigmento-proteína y un relativo enriquecimiento de las antenas internas del fotosistema II (Quílez *et al.*,

1992; Morales *et al.*, 2001). La aplicación de las nuevas técnicas de proteómica (Whitelegge, 2003) permitirá ampliar la información sobre la adaptación de las membranas tilacoidales a la deficiencia de Fe.

En condiciones de deficiencia de Fe la tasa fotosintética está disminuida (Terry, 1980), y se han encontrado evidencias de que este descenso se debe a una disminución en la regeneración de la ribulosa 1,5-bifosfato (RuBP), y no a una modulación de la actividad de la enzima ribulosa 1,5-bisfosfato carboxilasa/oxigenasa (Rubisco) (Arulanantham *et al.*, 1990). Los niveles de ATP, NADPH, triosa-P, fructosa bifosfato y fructosa-6-fosfato no están muy afectados por la deficiencia de Fe en hojas, sugiriendo que el efecto de la baja capacidad bioquímica en la regeneración de la RuBP se debe a alguna enzima situada entre la fructosa-6-fostato (F6P) y la RuBP, y no a una limitación en las concentraciones de ATP y NADPH. Algunas enzimas del ciclo de Calvin fueron estudiadas en hojas de plantas de remolacha control y deficiente en Fe. Las actividades de la Rubisco, 3-fosfoglicerato quinasa, gliceraldehido 3-fosfato deshidrogenasa, fructosa 1,6-bisfosfatasa y sedoheptulosa 1-7 bisfosfatasa no están muy afectadas por la deficiencia de Fe, mientras que la actividad de la Ru5P quinasa disminuye de forma apreciable en deficiencia de Fe, sugiriendo que esta enzima podría ser la responsable de la baja regeneración de la RuBP (Arulanantham *et al.*, 1990). Sin embargo, Winder y Nishio (1995) demostraron que la deficiencia de Fe reduce tanto la activación de la Rubisco como la expresión de la proteína.

La aplicación de nuevas técnicas de proteómica permitirá la obtención de mapas proteicos de los tilacoides de plantas controles y deficientes en Fe y aportará una visión más global de los cambios que ocurren en el aparato fotosintético tilacoidal en su adaptación a este estrés ambiental.

8. REGULACIÓN DE LAS RESPUESTAS ANTE LA DEFICIENCIA DE HIERRO A NIVEL DE PLANTA

A pesar de las continuas fluctuaciones de las condiciones medioambientales, la planta es capaz de mantener una concentración estable de Fe. Esta homeostasis se consigue con un delicado balance entre las cantidades de Fe incorporado, utilizado y almacenado. Debido, por una parte, al efecto tóxico del Fe como catalizador del estrés oxidativo, y por otra, al defecto en el crecimiento unido a la deficiencia de Fe, este balance en la concentración de Fe requiere una regulación extremadamente precisa a nivel de órgano, tejido y célula (Curie y Briat, 2003). Esta regulación podría tener dos sistemas de control: señales sistémicas que controlasen el

contenido global de Fe en la planta, y señales locales que controlasen el contenido de Fe a nivel de cada célula.

Una señal sistémica permitiría la comunicación entre los distintos órganos de las plantas, para evitar desequilibrios en el aporte de nutrientes y así integrar las demandas nutricionales de toda la planta. La naturaleza de esta señal (o señales) en el caso de la nutrición férrica es todavía desconocida, pero un complejo de Fe que permitiese su transporte estable en el floema podría contribuir a la regulación sistémica de las respuestas de raíz (Schmidt, 2003). Se han identificado distintas moléculas que podrían participar en esta función:

- Un posible candidato es el producto del gen *FER*, recientemente identificado en tomate. Este gen codifica un factor de transcripción bHLH (Ling *et al.*, 2002), cuya ausencia en el mutante *fer* de tomate provoca una pérdida completa de las respuestas fisiológicas y morfológicas a la deficiencia de Fe (Ling *et al.*, 1996). Aunque se sabe que FER está implicado en la cascada reguladora que dirige la expresión de genes implicados en la respuesta a la deficiencia de Fe, no se conoce en que punto de la cascada actúa. La expresión de FER es independiente del estatus de Fe y se encuentra en la epidermis y periciclo de raíz (Ling *et al.*, 2002).
- Otro posible candidato es el producto del gen de *Arabidopsis FRD3*. El mutante *frd3* expresa constitutivamente las proteínas de respuesta a deficiencia de Fe provocando hiperacumulación de hierro en raíces y hojas (Rogers y Guerinot, 2002). *FRD3* se expresa constitutivamente en raíz y aumenta su expresión en condiciones de deficiencia de Fe. La función fisiológica de *FRD3* debe ser elucidada todavía, pero una de las hipótesis sobre su función propone que *FRD3* es necesario para la importación al xilema de un factor necesario para el transporte de Fe (Green y Rogers, 2004). Sin embargo, se ha demostrado recientemente, mediante experimentos de injertos cruzados entre el mutante *frd3* y el silvestre de *Arabidopsis*, que el fenotipo de la planta injertada depende del genotipo de la raíz y no del genotipo de la parte aérea. Estos resultados contradicen la hipótesis de una participación de *FRD3* en la señalización proveniente de parte aérea (Green y Rogers, 2004).
- Un tercer candidato es la proteína ITP (Iron Transporter Protein). Esta proteína une Fe(III) en el floema (Krüger *et al.*, 2002) y podría participar en la señalización del estado nutricional de Fe.
- Por último, el propio Fe podría actuar como señal del estado nutricional de la planta, uniéndose a algún receptor que desencadenase la respuesta correspondiente para mantener la homeostasis.

Una señal local permitiría una respuesta inmediata de las células de la raíz a las necesidades nutricionales de la planta. En raíces de plantas de

tomate crecidas durante un breve espacio de tiempo, de 1 a 3 h, en un medio sin Fe, potasio o fósforo, se induce la expresión de genes relacionados con el transporte de estos nutrientes (Wang *et al.*, 2002) y con cascadas de señalización como factores de transcripción, MAP (Mitogen Activated Protein) quinasas, MAP quinasa quinasas y proteínas de la familia 14-3-3. Asimismo, en raíces de plantas de *Arabidopsis* deficientes en Fe, se ha descrito recientemente la inducción de un gen, *FIT1* (Fe-deficiency Induced Transcription Factor 1), que regula la expresión del transportador *IRT1* y la reductasa férrrica *FRO2* (Colangelo y Guerinot, 2004). La inducción de *IRT1* y *FRO2* tiene lugar tras cultivar las plantas en solución sin Fe durante 24 h, mientras que la desactivación ocurre 24 h después del aporte de Fe (Connolly *et al.*, 2002, 2003).

En general, la homeostasis de Fe se puede mantener a través de un control transcripcional, post-transcripcional y/o post-traduccional.

- Hasta el momento, no se ha descrito ningún mecanismo de control de la transcripción de genes como el sistema IRE/IRP de animales (Klausner *et al.*, 1993) o el Aft1 p de levadura (Yamaguchi-Iwai *et al.*, 1995), ya que no se ha encontrado ningún gen homólogo a *AFT1* en las bases de datos de *Arabidopsis*. Sin embargo, se ha propuesto que FIT1 (Colangelo y Guerinot, 2004) y/o FER (Ling *et al.*, 2002) puedan regular la transcripción de los genes de respuesta a la deficiencia de Fe. La trascripción de genes de ferritina, tanto en maíz como en *Arabidopsis*, depende de la combinación positiva y negativa de promotores *cis*, que producen acumulación de mRNA de ferritina en respuesta al aumento en el contenido de Fe (Petit *et al.*, 2001; Murgia *et al.*, 2002).
- Un ejemplo de regulación post-transcripcional lo encontramos en *Arabidopsis*, donde el gen *IRT1* se expresa tanto en raíces deficientes en Fe de plantas silvestres como en raíces y parte aérea de plantas transgénicas 35S-IRT1, en condiciones control y de deficiencia de Fe. Sin embargo, análisis por Western-blot muestran que la acumulación de proteína solo se produce en raíces, tanto de las plantas silvestres como transgénicas, en condiciones de deficiencia de Fe (Connolly *et al.*, 2002).
- El tercer tipo de regulación, la post-traduccional, ha sido propuesta también para el gen *IRT1* de *Arabidopsis* (Colangelo y Guerinot, 2004). En el transportador de zinc ZRT1, perteneciente a la misma familia que IRT1, la modificación por ubiquitina de una lisina posiblemente localizada en un "loop" citosólico, mediaría la endocitosis y degradación de este transportador (Gitan y Eide, 2000).

Capítulo 2

OBJETIVOS

1. Estudiar la actividad y expresión de distintas enzimas implicadas en la respuesta a la deficiencia de Fe, utilizando como especies modelo remolacha (*Beta vulgaris* L.) y *Medicago truncatula*.

2. Caracterizar los cambios inducidos por la deficiencia de Fe en el proteoma de puntas de raíz de las plantas pertenecientes a la Estrategia I, utilizando como especie modelo remolacha (*Beta vulgaris* L.).

3. Caracterizar los cambios inducidos por la deficiencia de Fe en el proteoma de tilacoides aislados de la planta modelo remolacha (*Beta vulgaris* L.).

4. Caracterizar el proteoma del floema aislado de la planta modelo *Lupinus texensis* y estudiar las proteínas implicadas en el transporte a larga distancia de Fe y Zn.

Capítulo 3

RESPONSES OF *Medicago truncatula* ROOTS TO IRON DEFICIENCY

Abstract: *Medicago truncatula* plants have been used as a model plant to study some of the major responses of roots to iron deficiency. At different time points after imposing the deficiency the activities of iron reductase in intact roots and phosphoenolpyruvate carboxylase in root extracts and the expression patterns of their corresponding genes, *MtFRO2* and *MtPEPC*, were studied. The capacity for root acidification of the nutrient solution and the concentrations of flavins in roots were also determined, as well as the expression profile of the genes *Mtha1*, encoding for ATPase, *MtribA* and *MtDMRLs*, two genes encoding enzymes related to flavin synthesis, and *MtSULT1*, a gene encoding for a putative flavin sulfotransferase. Our results indicate that in roots of *Medicago truncatula* grown under iron deficiency PEPC activity is regulated at the transcriptional level, similarly to what occurs with the root iron reductase and ATPase. The flavin-related genes *MtribA, MtDMRLs* and *MtSULT1* were also found to be upregulated by Fe status and flavin concentrations were higher in Fe deficient roots, providing further support for the hypothesis that flavins could be involved in the mechanism of iron reduction.

Key words: iron deficiency, *Medicago truncatula*, Strategy I

1. INTRODUCTION

Iron is an essential micronutrient for plants and the study of its roles in plant metabolism is currently a very active research field in plant nutrition (Marschner, 1995; Fox and Guerinot, 1998). Although Fe is the fourth most abundant element in the earth's crust, plant Fe deficiency is a worldwide problem, especially in high-pH calcareous soils. In these soils Fe is present in oxidized forms with low solubility that are not readily available to plants

(Lindsay and Schwab, 1982). Plants can be broadly classified into two groups based on their root mechanisms for Fe uptake: Strategy I plants, which include dicotyledonous and non-Graminaceae monocotyledonous species, and Strategy II plants, which include Graminaceae species. Strategy II plants release phytosiderophores (PS) in response to Fe deficiency stress. These phytosiderophores solubilize Fe(III) from soil inorganic compounds by chelation, and then the Fe(III)-PS complexes are taken up through specific transporter systems in the root plasma membrane (Marschner and Römheld, 1994; Mori, 1999).

When grown under Fe deficiency, Strategy I plants develop a series of morphological and biochemical changes that increase their capacity for Fe uptake. Morphological changes include swelling of root tips and formation of lateral roots, root hairs and transfer cells (Landsberg, 1982; Schmidt, 1999). These changes lead to an increase of the root surface that allows plants to maximize Fe uptake. Biochemical changes can include i) an enhanced excretion of protons to the rhizosphere (mediated by a plasma membrane-bound H^+-ATPase), which serve to lower soil pH and increase Fe(III) solubility (Dell'Orto *et al.*, 2002; Schmidt *et al.*, 2003); ii) the induction of a plasma-membrane ferric reductase (FC-R) enzyme that reduces Fe(III) to Fe(II) in root epidermal cells (Moog and Brüggemann 1994; Schmidt, 1999); iii) the activation of a plasma membrane transport system for Fe(II) uptake (Chaney *et al.*, 1972; Eide *et al.*, 1996; Fox and Guerinot, 1998), and iv) the excretion to the growth medium of compounds such as phenolics, organic acids and flavins which facilitate reduction and solubility of external Fe (Welkie and Miller, 1993; Susín *et al.*, 1994).

Some of the key components of Strategy I mechanisms have been recently identified at the molecular level. The acidification is most likely a result of the activation of one or more members of the H^+-ATPase family in plants (Palmgren, 2001) such as the *AHA2* gene from *Arabidopsis* (Harper *et al.*, 1990; Santi *et al.*, 2004) and the *CsHA1* gene from cucumber. The plasma membrane FC-R is encoded by the genes *AtFRO2* in *Arabidopsis* (Robinson *et al.*, 1999), *PsFRO1* in *Pisum sativum* (Waters *et al.*, 2002), *LeFRO1* in *Lycopersicon esculentum* (Li *et al.*, 2004) and *MtFRO2* in *Medicago truncatula* (López-Millán *et al.*, 2005). Iron transporter genes probably involved in root uptake have been cloned from several plant species, and include *IRT1* and *IRT2* in *Arabidopsis* (Eide *et al.*, 1996; Vert *et al.*, 2002), *RIT1* in *P. sativum* (Cohen *et al.*, 1998), *LeIRT1* and *LeIRT2* in *L. esculentum* (Eckhardt *et al.*, 2001) and *MtZIP6* in *M. truncatula* (López-Millán *et al.*, 2004).

Genes encoding for GTP cyclohydrolase II (*ribA*) and 6,7-dimethyl-8-ribityllumazine synthase (DMRL synthase), enzymes that catalyze the first and the last step in riboflavin synthesis, respectively, have been

characterized in *Spinacia oleracea* (Jordan *et al.*, 1999), and identified in *A. thaliana* (*DMRL*: At2g20690, *ribA*: AJ000053), *L. esculentum* (*ribA*: AJ002298) and *Nicotiana tabacum* (*DMRL*: AAD44809), although no report is yet available on the effect of Fe deficiency in the expression of these genes.

On the other hand, the metabolism of roots in Strategy I plants is highly affected by Fe deficiency. Several changes at the metabolic level have been reported, including an accumulation of organic acids, mainly malate and citrate (reviewed in Abadía *et al.*, 2002), shifts in the redox state of the cytoplasm (Schmidt, 1999; López-Millán *et al.*, 2000a) and increases in the activity of PEPC and in several other enzymes of the Krebs cycle (Landsberg, 1986; Rabotti *et al.*, 1995; López-Millán *et al.*, 2000a) and the glycolitic pathway (Sijmons and Bienfait, 1983; Rabotti *et al.*, 1995; Espen *et al.*, 2000). Increases in PEPC activity in root extracts of Fe-deficient plants have been reported in pepper (Landsberg, 1986), kiwifruit (Rombolà, 1998), cucumber (Rabotti *et al.*, 1995; De Nisi and Zocchi, 2000) and sugar beet (López-Millán *et al.*, 2000a; Andaluz *et al.*, 2002). The increase in PEPC activity correlates with the organic acid accumulation in Fe deficient roots (López-Millán *et al.*, 2000a; Abadía *et al.*, 2002) and is mainly localized to the external layers of the cortical cells of iron deprived root apical sections which are very active in proton extrusion (De Nissi *et al.*, 2002). So far, there are several hypotheses to explain such metabolic changes (de Vos *et al.*, 1986; Landsberg, 1986), all of them giving a key role of PEPC in the root response to Fe deficiency. A relatively large number of PEPC cDNA sequences have been reported in a wide range of plant species including *M. truncatula*, but changes in the expression pattern of this gene in Fe deficient conditions have been reported only recently (De Nisi *et al.*, 2004).

M. truncatula is an emerging model legume with a number of genetic and molecular tools available. A better understanding of the proteins involved in root Fe acquisition and Fe homeostasis in this organism will strengthen our ability to enhance the Fe efficiency of other plants, especially that of different agronomic legumes. The aim of this work was to study the development of some of the major Strategy I responses to Fe deficiency in *M. truncatula* roots. We have used a time window that includes the maxima for FC-R activity found in early studies with this plant species, that occurs at 9 days after the onset of the deficiency (López-Millán *et al.*, 2005). At different time points after the onset of Fe deficiency, the activities of FC-R and PEPC and the expression patterns of their corresponding genes, *MtFRO2* and *MtPEPC*, were studied. Root acidification of the nutrient solution and root concentrations of flavins were also determined, as well as the expression profile of the genes *Mtha1*, *MtribA*, *MtDMRL* and *MtSULT1*.

2. MATERIALS AND METHODS

2.1 Plant Material

Medicago truncatula (ecotype A17) plants were grown in a controlled environment chamber with a photosynthetic photon flux density (PPFD) at leaf height of 350 μmol m^{-2} s^{-1} PAR and a 16 h- 22 °C / 8 h- 20 °C, day / night regime. *M. truncatula* seeds were scarified by nicking the seed coat, then soaked overnight in distilled water and germinated on filter paper for four days in darkness. The standard solution for hydroponically grown plants contained: (in mM) 0.6 K_2SO_4, 0.5 $Ca(NO_3)_2$, 1.0 NH_4NO_3, 0.3 KH_2PO_4, 0.2 $MgSO_4$, and (in μM) 25 $CaCl_2$, 25 H_3BO_3, 2 $MnSO_4$, 2 $ZnSO_4$, 0.5 $CuSO_4$, 0.5 H_2MoO_4, 0.1 $NiSO_4$, and 15 Fe(III)-EDTA. All hydroponic solutions were buffered with 1 mM MES/KOH, pH 5.5. Plants (35) were grown for 10 days in 10 L of standard solution with 15 μM Fe(III)-EDTA. After this time, treatments were applied by using fresh nutrient solutions with 0.5 or 15 μM Fe, and plants were grown under these new conditions for 10 more days. Nutrient solutions were renewed weekly. Samples for the different physiological and molecular analysis were taken on days 7, 8, 9 and 10 after treatment initiation. The experiment was replicated 3 times with different batches of plants.

2.2 Root iron reductase assay

Root Fe reductase was measured with intact plants. At different times, whole plants were placed in aluminium foil-wrapped beakers containing the assay solution (100 μM Fe(III)-EDTA, 100 μM bathophenanthroline disulphonate (BPDS) and 1 mM MES pH 5.5), and Fe reductase activity was determined *in vivo* by following at 535 nm the formation of the Fe(II)-BPDS complex from Fe(III)-EDTA (Bienfait *et al.*, 1983). Reactions were run for 1 h in the dark and blanks without plants were used to correct for any non-specific photoreduction.

2.3 PEPC activity

PEPC (PEPC; EC 4.1.1.31) activity was measured in root extracts. Extracts were made by grinding 100 mg FW of root material in a mortar with 1 mL of extraction buffer containing 30 mM sorbitol, 1% BSA and 1% PVP in 100 mM HEPES-KOH, pH 8.0. The slurry was centrifuged for 15 min at 10000 *g* and 4 °C, the supernatant was collected and the enzyme activity measured immediately. PEPC activity was determined in a coupled enzymatic assay with malate dehydrogenase according to Vance *et al.*

(1983) with 75 µl of extract in 2 mM PEP, 10 mM $NaHCO_3$, 5 mM $MgCl_2$, 0.16 mM NADH, and 100 mM Bicine [N, N′-bis(2-hydroxyethylglycine)]-HCl, pH 8.5.

2.4 External acidification of the medium

For a quantitative determination of H^+ extrusion, each plant was placed for 24 h in a normal growth chamber regime, in a beaker containing 100 mL of nutrient solution (pH 5.5) without MES buffer. After this time, the final pH of the solution was measured using a Metrohm 719 S Titrino pH-meter (Herisau, Switzerland).

2.5 Flavin concentrations

Root material (ca. 100 mg FW) was frozen in liquid N_2 and ground in a mortar with 0.1 M ammonium acetate, pH 6.1. Extracts were centrifuged for 5 min at 14000 *g* and the supernatant stored at –80 °C until analysis. Flavin compounds were analysed by HPLC using a 100 x 8 mm Waters Radial-Pak C18 radial compression column (Waters Corp., Milford, MA, USA) (Susín *et al.*, 1993). Samples were injected with a Rheodyne injector (50 µL loop). Mobile phase (water:methanol 70:30, v:v) was pumped at a flow rate of 1 mL min^{-1}. Flavins were detected at 445 nm. Peaks corresponding to FMN and FAD were identified by comparison of their retention times with those of standards from SIGMA (Saint Louis, MI, USA). Quantification was made with known amounts of each compound using peak areas.

2.6 Gene expression analysis

Database searches were performed with TBLASTX (Altschul and Lipman, 1990) using previously identified PEPC and DMRL synthase sequences from *A. thaliana, L. esculentum, P. sativum, Medicago sativa* and *S. oleracea*. Two putative tentative consensum (TC) sequences from *M. truncatula* encoding possible orthologs for PEPC and DMRL synthase proteins were identified. Sequences obtained were aligned using the ClustalW program. Based on these alignments, specific primers were designed to amplify the complete cDNA sequence of PEPC and DMRL synthase. Primers used were, for PEPC, f-ATGGCAAACAAGATGGAAA AAATGGC and r-TTAACCAGTGTTCTGCAT; and for DMRL synthase, f-ATGGCTTTATCTGTTTCCACC and r-CTAATTCAGATGCTCGAA. After PCR amplification, products were sequenced and RT-PCR specific primers were designed based on the sequences obtained for PEPC and DMRL and also on the known *M. truncatula* cDNA sequences for Fe

reductase (AY439088), ATPase (AJ132892), GTP cyclohydrolase II (TC100898) and a putative sulfotransferase (TC96336) (Table 3-1).

Table 3-1. Forward and reverse specific primers utilized for the RT-PCR amplification of the *MtFRO1*, *MtPEPC*, *Mtha1*, *MtDMRLs*, *MtribA*, and *MtSULT1* cDNAs and size of the fragment amplified.

	Forward (5'-3')	Reverse (5'-3')	Fragment Size (bp)	µL RT reaction	PCR cycles	$T_{anneling}$ (°C)
Actin	AAGAGYTAYGAR YTNCCWGATGG	TTRATCTTCATGC TRCTRCTWGGAGC	290	1	25	55
MtFRO1	GGTGACACGTGGA TCATCTG	TTGCAATCCACAG GAACAAA	239	2	28	55
MtPEPC	ATGGCAAACAAGA TGGAAAAAATGGC	CATTATATGGGAC ACGTTCGT	825	3	35	65
Mtha1	GCACAAGTATGAG ATTGTGAAGA	ATCACCAGTCATG CCACAAA	68	2	30	55
MtDMRLs	ATGGCTTTATCTGT TTCCACC	CTAATTCAGATGC TCGAA	666	2	30	55
MtribA	TGCAATGGTTAAGG GTGACA	CCAATCCAATACC CCTTCCT	200	2	30	55
MtSULT1	ATGGCATCAACAAA TCTCACACA	TATGGGCATACTT TAAATGAAATACC	1013	2	25	55

Total RNA was isolated from roots with the Rneasy Plant Mini kit (Qiagen, Maryland, USA). One plant per treatment was used to extract RNA, and two different batches of plants were analyzed. A third pooled sample was also obtained by combining RNA from the two batches of plants. A sample aliquot containing 3 µg of total RNA was subjected to reverse transcription with 25 µg/mL oligo (dT) primer, 0.05 mM dNTP mix and 15 units Cloned AMV Reverse Transcriptase (Invitrogen, Carlsbad, CA, USA) in a final volume of 20 µL, according to the manufacturer's instructions. PCR reactions were carried out with the volumes of resulting cDNA solution indicated in Table 3-1, using 0.5 µM of the specific primers indicated in Table 3-1. Additional reaction components were standard buffer (75 mM Tris HCl pH 9.0, 1.5 mM $MgCl_2$, 50 mM KCl, 20 mM $(NH_4)_2SO_4$), 0.2 mM dNTP's and 0.5 units DNA polymerase (Biotools, Madrid, Spain). PCR reactions were carried out for 5 min at 95 °C, followed by the number of cycles indicated in Table 3-1, each consisting of 45 s at 95 °C, 45 s at the anneling temperature indicated in Table 3-1 and 1 min at 70 °C. A final period of 10 min at 70 °C was used. RT-PCR reactions were carried out twice for each one of the three types of samples (individual plant batches and the two-batch pooled sample). Actin was used as housekeeping gene.

3. RESULTS

M. truncatula plants grown in hydroponics with 0.5 μM Fe developed visible symptoms of leaf chlorosis gradually, whereas those of plants grown with 15 μM Fe remained green. A picture of the plants at day 7 after the onset of the deficiency is shown in Fig. 3-1.

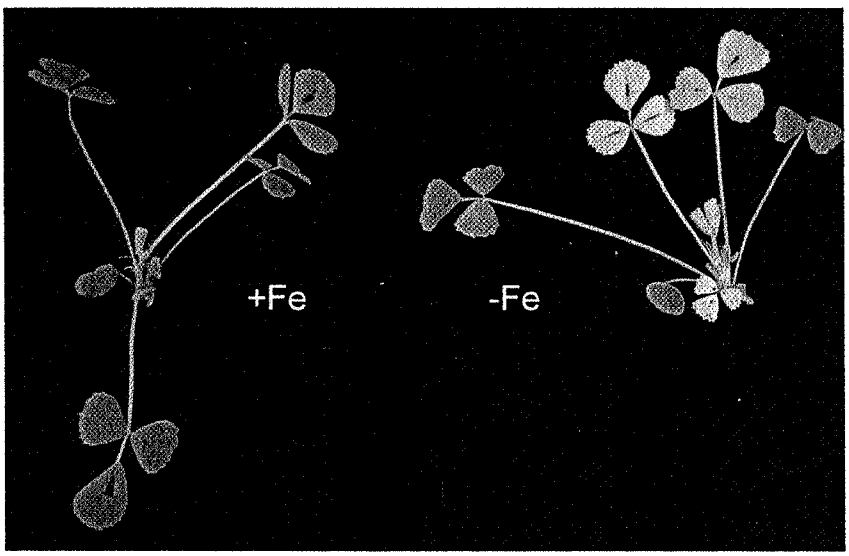

Figure 3-1. Medicago truncatula plants after 7 days of growth with 15 μM (Fe-sufficient, +Fe) and 0.5 μM Fe(III)-EDTA (Fe-deficient, -Fe).

3.1 Morphological root responses

Roots of *M. truncatula* plants grown in hydroponic culture, consisted of principal roots and a system of secondary new roots (Fig. 3-2). Roots of Fe sufficient plants, grown with 15 μM Fe, were white in color, whereas roots of Fe-deficient plants, grown with 0.5 μM for 7 days, had a yellowish color (Fig. 3-2). Root morphology was affected by Fe deficiency, and compared to control plants, roots of Fe-deficient plants had a higher amount of secondary roots (see inserts in Fig. 3-2), and swollen root tips were also apparent. These morphological root changes are often an integral part of the response of Strategy I plants (Welkie and Miller, 1993; Schikora and Schmidt, 2001).

3.2 Root iron reductase activity and expression

The time window used to assay FC-R activity was from 7 to 10 days. This window includes the time when the maximal FC-R activity is induced by Fe-deficiency in *M. truncatula* (maximum at 9 days; López-Millán *et al.*, 2005) and other herbaceous species, including tomato (maximum at 8-10 days; Zouari *et al.*, 2001) and sugar beet (maximum at 9-10 days; Susín *et*

al., 1996). Only in woody species the development of FC-R activity with Fe-deficiency takes longer (maxima at 30 days; Gogorcena *et al.*, 2001).

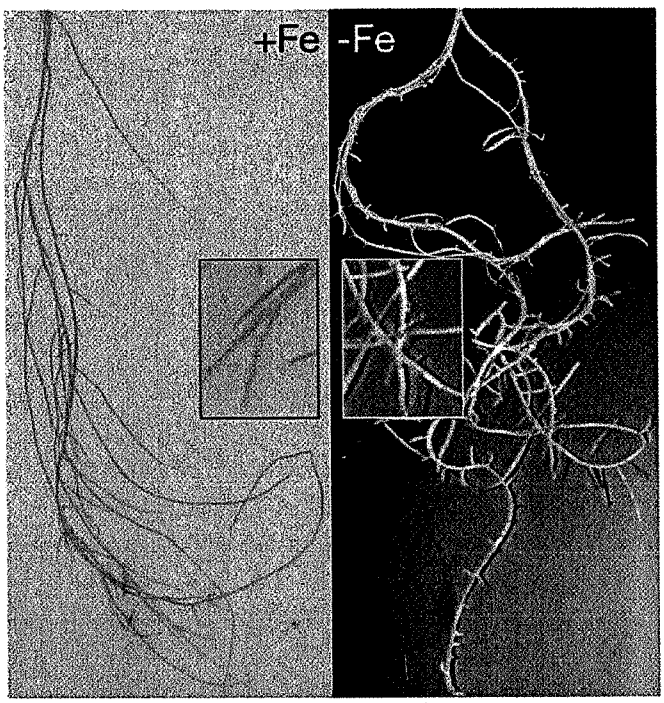

Figure 3-2. Roots of *Medicago truncatula* plants grown in nutrient solution for 7 days with 15 μM (Fe-sufficient, +Fe) or 0.5 μM Fe(III)-EDTA (Fe-deficient, -Fe). Inserts show a detail of secondary roots.

In control plants grown with 15 μM Fe, *in vivo* root FC-R activities did not change significantly over time in the time window used, ranging from 0.10 to 0.19 μmol Fe reduced g^{-1} FW h^{-1}. In Fe-deficient plants, grown with 0.5 μM Fe, root FC-R activity was significantly higher than in the controls, ranging from 0.53 to 0.90 μmol Fe reduced g^{-1} FW h^{-1}. In the time window used root FC-R activities in Fe-deficient plants were maximal at day 9, although changes over time were not statistically significant. On days 8-9, the *in vivo* root FC-R activity was approximately 4-fold higher in Fe-deficient than in control plants (Fig. 3-3A). These values are within the range found in other plant species (Moog and Brüggemann, 1995; Zouari *et al.*, 2001), although they are significantly lower than those found in the model plant species sugar beet (approximately 0.6 and >8 μmol Fe reduced g^{-1} FW h^{-1} in Fe-sufficient and deficient plants, respectively; Susín *et al.*, 1996; López-Millán *et al.*, 2000a). In *M. truncatula* FC-R activity was detected along the whole root system, as judged from agar plate assays (data not shown).

To study the correlation between enzymatic activity and gene expression, transcript levels of FC-R (*MtFRO1*-AY439088) were estimated by semi-quantitative RT-PCR in control and Fe-deficient plants at different time

points, on days 7, 8, 9 and 10 after the beginning of treatments. As estimated by RT-PCR, *MtFRO2* transcript abundances were always higher in roots from Fe-deficient as compared to control plants. The expression of *MtFRO2* was maximal at days 7 and 8 in both control and Fe-deficient plants, and then decreased over time (Fig. 3-3B).

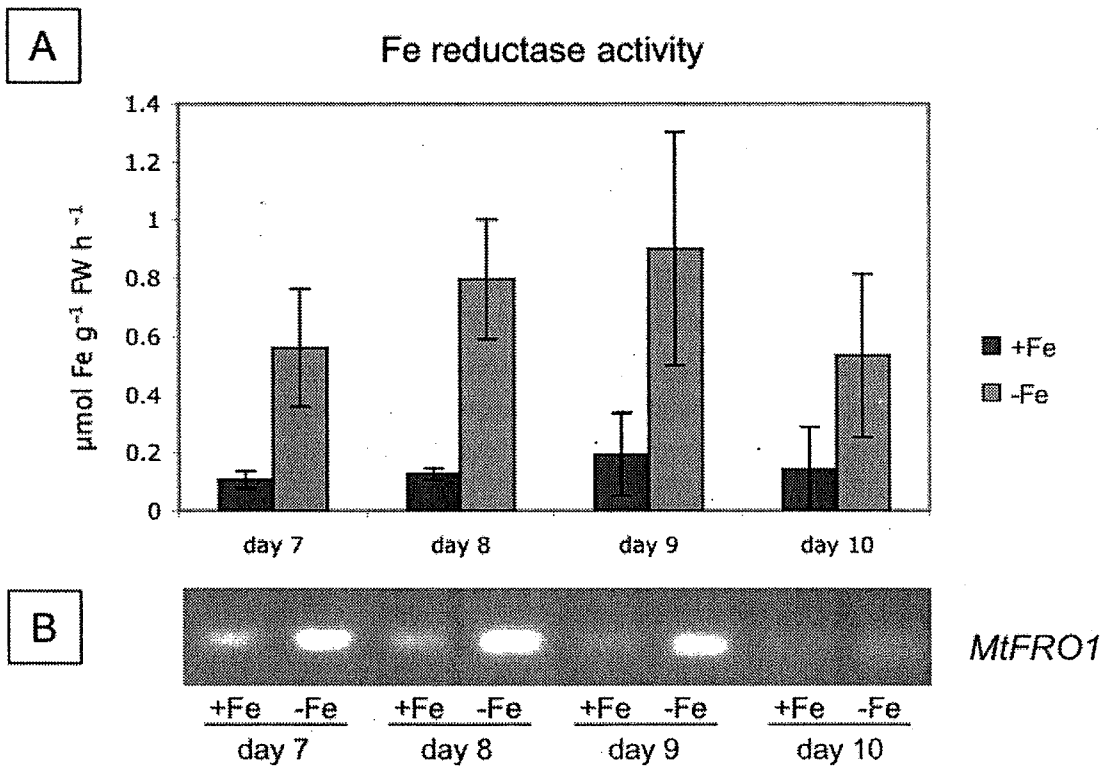

Figure 3-3. **A**- Root Fe reductase activity (µmol Fe reduced g^{-1} FW h^{-1}) in roots from *M. truncatula* plants grown at 15 (+Fe) and 0.5 (-Fe) µM Fe supplied to the nutrient solution. Activity was measured on days 7, 8, 9 and 10 after treatment initiation. **B**- Semi-quantitative RT-PCR analysis of the *MtFRO1* transcript in roots from *M. truncatula* plants grown at 15 (+Fe) and 0.5 (-Fe) µM Fe supplied to the nutrient solution, at days 7, 8, 9 and 10 after treatment initiation.

3.3 PEPC activity and expression

In control plants, PEPC activity in root extracts did not change significantly in the time window used, ranging from 0.41 to 0.68 µmol g^{-1} FW min^{-1}. In Fe-deficient plants, PEPC activity in root extracts was significantly higher than in the controls, ranging from 1.30 to 1.87 µmol g^{-1} FW min^{-1}. In root extracts of Fe-deficient plants PEPC activity was maximal at day 8, although changes over time were not statistically significant. On day 8, PEPC activity was 2.9-fold higher in root extracts of Fe-deficient than in those obtained from control plants (Fig. 3-4A). Induction of PEPC activity with Fe-deficiency was less strong in *M. truncatula* than in sugar beet (sugar

beet plants had PEPC activities of approximately 0.2 and 5-13 μmol g^{-1} FW min^{-1} in Fe-sufficient and Fe-deficient plants, respectively; Andaluz *et al.*, 2002; López-Millán et al., 2000a).

To identify potential PEPC open reading frames (ORFs) in *M. truncatula*, we performed database searches looking for ESTs and TCs with sequence similarity to previously reported genes from different species, including *A. thaliana*, *Lupinus albus*, *L. esculentum*, *M. sativa*, *N. tabacum*, *P. sativum*, *Saccharum sp.* and *S. oleracea*. We identified a TC in The Institute for Genomic Research (TIGR) *M. truncatula* gene index, MtGI TC101015, containing a full-length ORF, which probably represents a PEPC ortholog. A PCR product of approximately 2.3 kb was amplified and sequencing was carried out. The translated amino acid sequence for the PEPC ORF displayed 91% identity at the amino acid level to the *Glycine max* PEPC gene, and more than 80% to the *L. esculentum*, *P. sativum*, *L. albus*, *Saccharum sp*, and *M. sativa* PEPC genes. We assigned the name *MtPEPC* to the corresponding gene in *M. truncatula*.

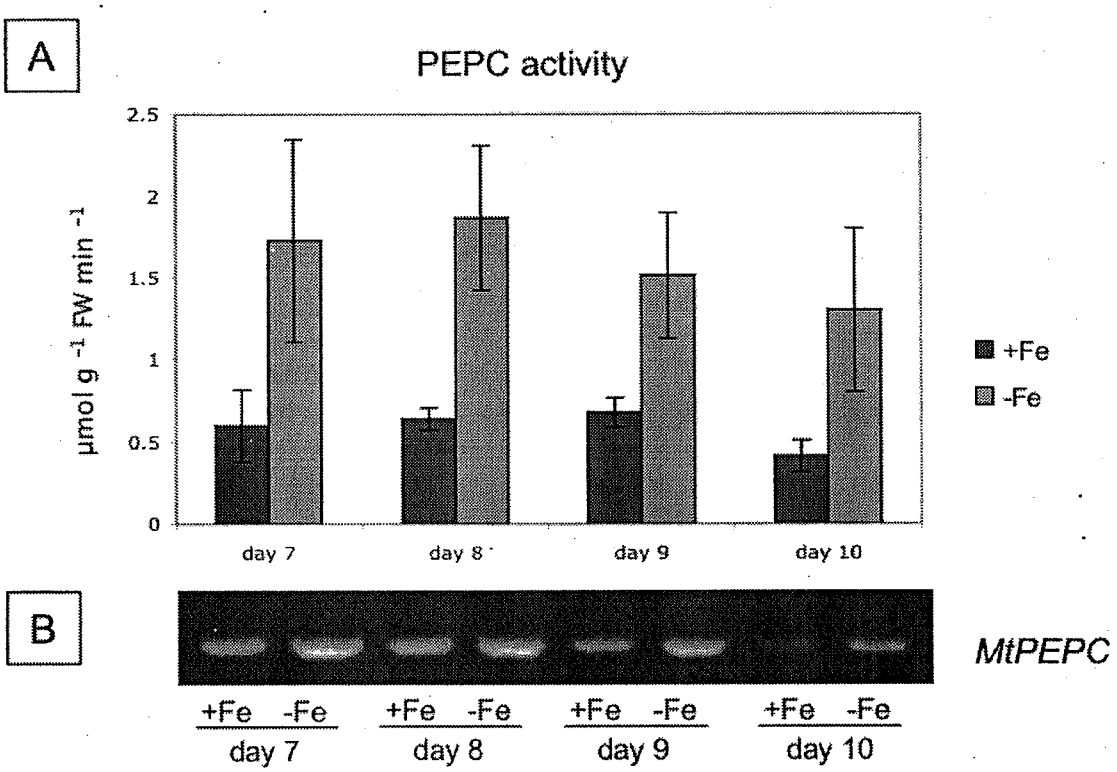

Figure 3-4. **A-** PEPC activity (μmol g^{-1} FW min^{-1}) in roots from *M. truncatula* plants grown at 15 (+Fe) and 0.5 (-Fe) μM Fe supplied to the nutrient solution. Activity was measured at days 7, 8, 9 and 10 after treatment initiation. **B-** Semi-quantitative RT-PCR analysis of the *MtPEPC* transcript in roots from *M. truncatula* plants grown at 15 (+Fe) and 0.5 (-Fe) μM Fe supplied to the nutrient solution, at days 7, 8, 9 and 10 after treatment initiation.

To study the correlation between enzymatic activity and gene expression in *M. truncatula* roots, transcript levels of PEPC (*MtPEPC*-TC101015) were estimated by semi-quantitative RT-PCR in control and Fe-deficient plants at different time points, on days 7, 8, 9 and 10 after the beginning of treatments. As estimated by RT-PCR, *MtPEPC* transcript abundances were always higher in roots from Fe-deficient as compared to control plants. The expression of *MtPEPC* was maximal at days 7 and 8 in both control and Fe-deficient plants, and then decreased over time (Fig. 3-4B).

3.4 Root ATPase activity and expression

In control plants, *in vivo* root proton extrusion did not change significantly in the time window used, ranging from 0.19 to 0.34 μmol H^+ g^{-1} FW h^{-1}. In Fe-deficient plants, root proton extrusion was significantly higher than in the controls, ranging from 0.80 to 3.58 μmol H^+ g^{-1} FW h^{-1} with a maximum at day 7. At this time point proton extrusion was approximately 19-fold higher in Fe-deficient than in control plants (Fig. 3-5A). The measured proton extrusion rates in *M. truncatula* plants are higher than those reported for Fe-deficient *Quercus suber* (8.7-26.2 nmol H^+ $plant^{-1}$ min^{-1}, equivalent to 0.13-0.35 μmol H^+ g^{-1} FW h^{-1}; Gogorcena *et al.*, 2001).

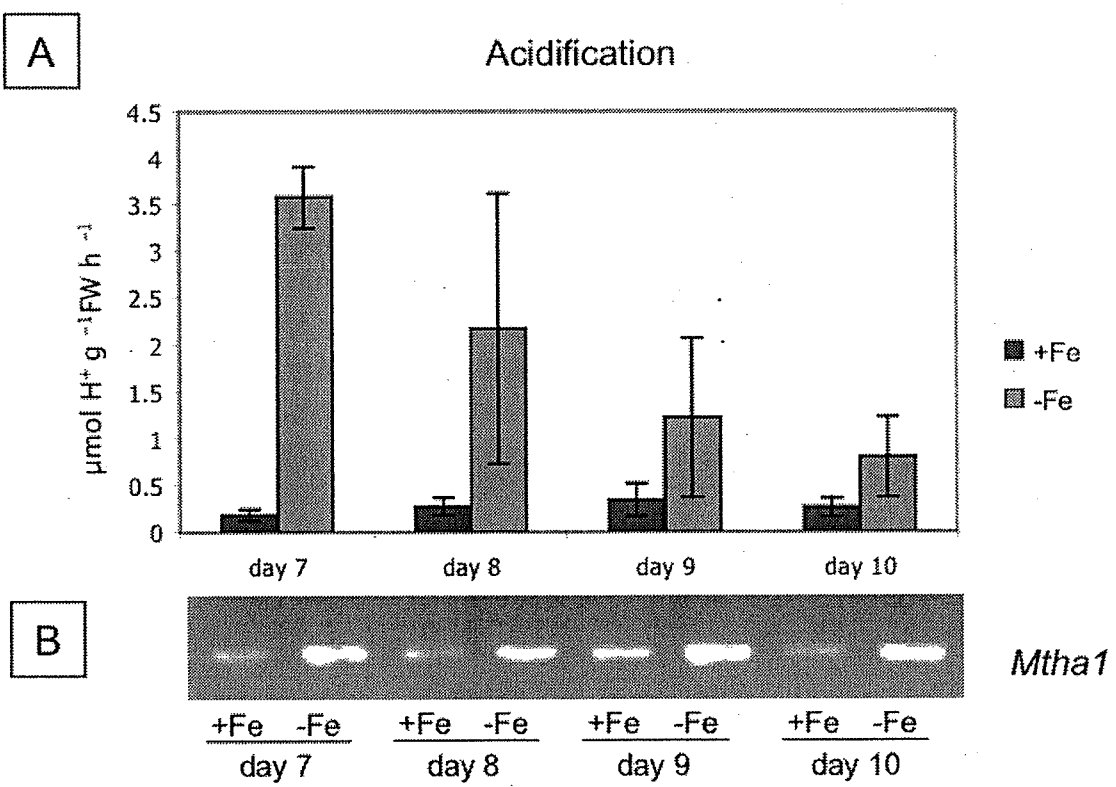

Figure 3-5. **A-** Acidification capacity (μmol H^+ g^{-1} FW h^{-1}) of *M. truncatula* plants grown at 15 (+Fe) and 0.5 (-Fe) μM Fe supplied to the nutrient solution. Proton extrusion was measured at days 7, 8, 9 and 10 after treatment initiation. **B-** Semi-quantitative RT-PCR

analysis of the *Mtha1* transcript in roots from *M. truncatula* plants grown at 15 (+Fe) and 0.5 (-Fe) μM Fe supplied to the nutrient solution, at days 7, 8, 9 and 10 after treatment initiation.

To study the correlation between enzymatic activities and gene expression in *M. truncatula* roots, transcript levels of ATPase (*Mtha1*-AJ132892) were estimated by semi-quantitative RT-PCR in control and Fe-deficient plants at different time points, on days 7, 8, 9 and 10 after imposing the treatments. As estimated by RT-PCR, *Mtha1* root transcript abundance was significantly higher in Fe deficient than in control roots at all the time points measured, and did not change over time in Fe-sufficient or Fe-deficient *M. truncatula* plants (Fig. 3-5B).

3.5 Flavin concentrations and expression of flavin synthesis enzymes

Flavin compounds in root extracts were quantified by HPLC. Peaks corresponding to FMN, riboflavin, and to an unidentified flavin (with two absorption maxima at 372 and 425 nm; data not shown) were found in Fe-deficient roots, whereas only traces of these compounds were detected in control roots. In the time window used, FMN and riboflavin concentrations in Fe-deficient roots were higher on day 7, and then decreased over time (from 64 to 21 nmol g^{-1} FW and from 100 to 28 nmol g^{-1} FW, respectively; Fig. 3-6A). The unidentified flavin was estimated to decrease also 2-fold in the same time period (data not shown). Assuming riboflavin is mostly located in the cytoplasm, riboflavin concentrations in *M. truncatula* roots at day 7 were equivalent to a concentration of approximately 100 μM. These concentrations are similar to the riboflavin concentrations found in sugar beet, and much lower than the concentrations of riboflavin sulfates, that may reach mM levels (Susín *et al.*, 1993).

To identify potential DMRL synthase open-reading frames in *M. truncatula*, we performed database searches looking for ESTs and TCs with sequence similarity to previously reported genes from different species, including *A. thaliana*, *L. esculentum*, *P. sativum*, *M. sativa*, *L. albus*, *Saccharum sp.*, *N. tabacum* and *S. oleracea*. We identified a TC in the TIGR *M. truncatula* gene index, MtGI TC107317, containing a full-length ORF, which probably represents a DMRL synthase ortholog. A PCR product of approximately 687 bp was amplified and sequencing was carried out. The translated amino acid sequence for the DMRL synthase open-reading frame displayed 61% identity at the amino acid level to the *A. thaliana* DMRL synthase gene, and 57% to those of *S. oleracea* and *N. tabacum*. We assigned the name *MtDMRLs* to the corresponding gene.

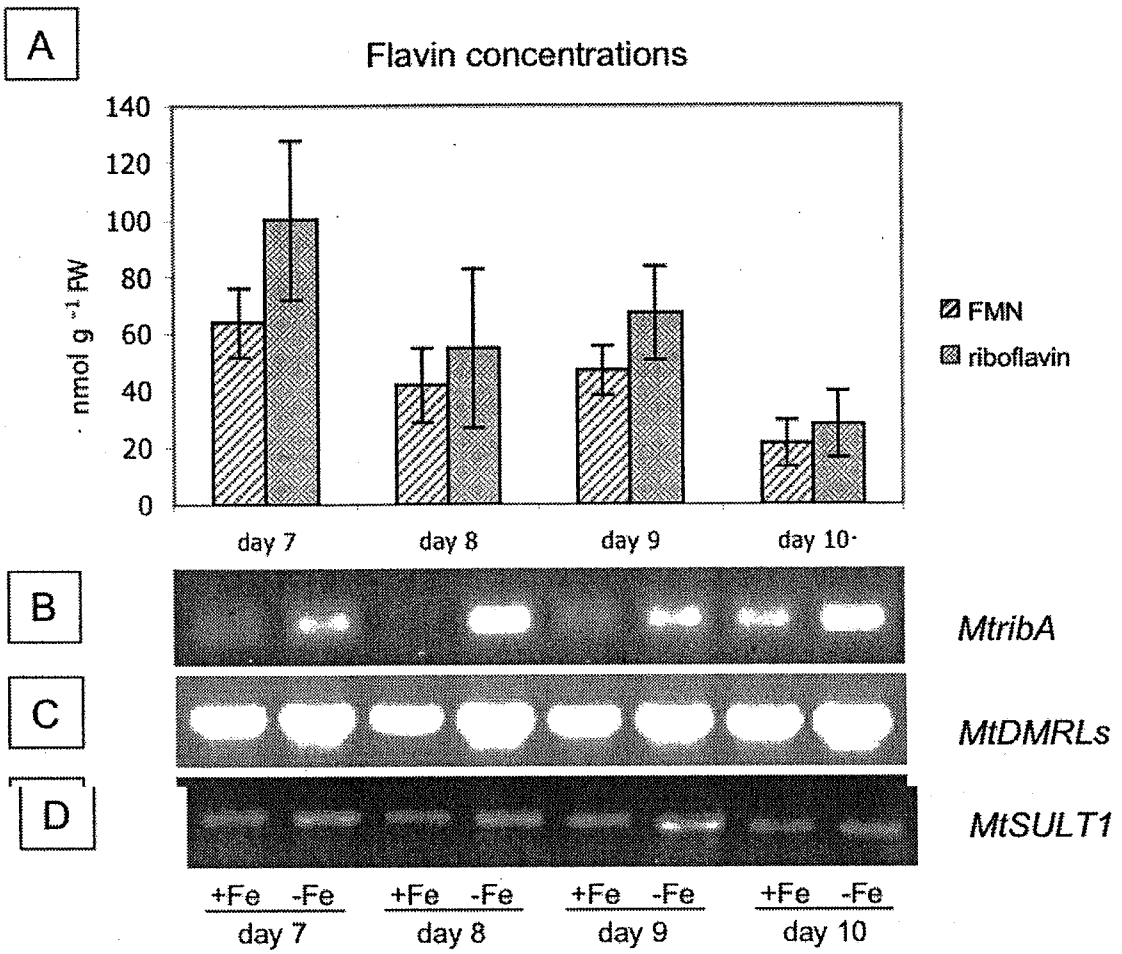

Figure 3-6. **A-** Flavin concentration (nmol g^{-1} FW) of FMN and riboflavin in roots from *M. truncatula* plants grown at 0.5 μM Fe supplied to the nutrient solution. Activity was measured at days 7, 8, 9 and 10 after treatment initiation. **B, C, D** Semi-quantitative RT-PCR analysis of the *MtribA*, *MtDMRLs* and *MtSULT1* transcripts, respectively, in roots from *M. truncatula* plants grown at 15 (+Fe) and 0.5 (-Fe) μM Fe to the nutrient solution, at days 7, 8, 9 and 10 after treatment initiation.

To study the correlation between flavin biosynthesis-related enzymatic activities and gene expression in *M. truncatula* roots, transcript levels of *MtDMRLs*-TC107317 and two other enzymes involved in flavin biosynthesis, GTP cyclohydrolase II (*MtribA*- TC100898) and a putative sulfotranferase (*MtSULT1*-TC96336), were estimated by semi-quantitative RT-PCR in control and Fe-deficient plants at different time points, on days 7, 8, 9 and 10 after beginning of treatments. The expression of the three genes (*MtribA*, *MtDMRLs* and *MtSULT1*) was always significantly higher in Fe-deficient than in Fe-sufficient roots, and did not change over time (Fig. 3-6B, C, D).

4. DISCUSSION

Most of the studies with Fe-deficient plants have focused on very specific aspects of their physiology or molecular biology. In the present work we report background information on some of the most important responses induced by Fe deficiency in roots of *Medicago truncatula*, a Strategy I model plant species. Data indicate that *M. truncatula* constitutes a good model for Strategy I, since most of the physiological responses described so far in Strategy I are developed by this species, including flavin accumulation and the consequent yellowing of root tips.

Our data demonstrate an up-regulation of the PEPC transcript in response to Fe-deficiency, which occurs concomitantly with the increase in PEPC activity in root extracts. A report indicating an up-regulation of PEPC in Fe-deficient *Cucumis sativus* was recently presented in a Symposium (De Nisi *et al.*, 2004). An increase in PEPC activity in root extracts with Fe deficiency has been described before in root extracts from pepper (Landsberg, 1986), kiwi (Rombolà, 1998), cucumber (Rabotti *et al.*, 1995; De Nisi and Zocchi, 2000) and sugar beet (López-Millán *et al.*, 2000a; Andaluz *et al.*, 2002). The amount of root PEPC protein with Fe-deficiency has been demonstrated to increase in cucumber (De Nisi and Zocchi, 2000) and sugar beet (Andaluz *et al.*, 2002). Also, post-translational upregulation by phosphorylation of the N-terminus does not appear to occur under Fe deficiency in sugar beet (Andaluz *et al.*, 2002). The increase measured in PEPC carboxylase activity in Fe-deficient *M. truncatula* roots (approximately 3-fold over control values) is similar to the increase measured in iron reductase (4-fold, see below) supporting the key role of this enzyme in the response to Fe-deficiency. The increase in PEPC activity is known to be localized mainly to the external layers of the cortical cells of Fe-deprived root apical sections, which are very active in proton extrusion (De Nissi *et al.*, 2002). It has been proposed that cytoplasm alkalinisation associated with proton extrusion would activate PEPC activity (pH-stat theory, Davis, 1973). However, the up-regulation of PEPC transcripts under Fe-deficiency and the fact that the induction of PEPC activity and acidification capacity were not parallel in time suggests that the increase in PEPC activity is not exclusively due to an effect of a cytoplasmatic pH change.

Another response of Fe-deficient *M. truncatula* plants consists in the accumulation of flavins in roots, including riboflavin, FMN and a so far unidentified compound. Also, we have found, for the first time to our knowledge, an increase with Fe deficiency in the expression of the first and last genes of the riboflavin biosynthesis pathway, *MtribA* and *MtDMRLs*. An accumulation of flavin compounds with Fe deficiency, including riboflavin

and riboflavin 3'- and 5' sulfate, has been described previously in different plant species (Welkie and Miller, 1988, 1992; Susín *et al.*, 1993, 1994). The exact role of flavins in Fe deficiency is still unresolved. It has been hypothesized, based on the similar location of flavin accumulation and Fe reduction and on the fact that the FC-R is a flavin-containing protein, that flavin accumulation may be an integral part of the Fe reducing system in roots from Strategy I plants (Cakmak *et al.*, 1987; López-Millán *et al.*, 2000a). The time-dependent expression pattern of *MtribA* and *MtDMRLs* is parallel to that of *MtFRO*, suggesting that flavin compounds could play an important, and still to be elucidated role, in the mechanism for Fe reduction. On the other hand, a mRNA (*MtSULT1*) encoding for a *M. truncatula* putative root sulfo-transferase was also found to be up-regulated by Fe deficiency. This enzyme, belonging to the secondary metabolism, might participate in the sulfation of riboflavin, yielding the unknown flavin that was detected in Fe-deficient roots. A detailed study of both *MtSULT1* and the unknown flavin is being carried out in our laboratory.

Increases of root FC-R activity and transcript abundance of the corresponding gene, *MtFRO1,* were found in *M. truncatula* grown under Fe-deficiency as compared to the controls. An increase in the activity of FC-R, which could be the rate-limiting physiological process in root Fe-acquisition (Grusak *et al.*, 1990b; Connolly *et al.*, 2003), has been demonstrated in a number of plant species (see Schmidt 1999, for a review). The 4-fold increases found in FC-R activity in *M. truncatula* were similar to those found in other species, 3-fold in *L. esculentum* (Zouari *et al.*, 2001), 5-fold in *P. sativum* (Waters *et al.*, 2002) and *M. truncatula* (López-Millán *et al.*, 2004) and 11-fold in *B. vulgaris* (López-Millán *et al.*, 2000a). Concomitant increases in the expression of the corresponding FC-R genes *AtFRO2*, *AtFRO3*, *LeFRO1* and *PsFRO1* have been described in roots from *A. thaliana*, *L. esculentum* and *P. sativum* grown under Fe-deficiency (Robinson *et al.*, 1999; Wintz *et al.*, 2003; Li *et al.*, 2004; Waters *et al.*, 2002). Furthermore, *A. thaliana* lines with an inactivated *AtFRO2* gene have reduced FC-R activity, are chlorotic, and grow slowly without elevated Fe supply (Robinson *et al.*, 1999). FC-R activity and gene expression did not correlate exactly, since at day 10 the expression of *MtFRO1* was significantly reduced, while FC-R activity was still quite high.

In Fe-deficient *M. truncatula* roots we found an increase in ATPase activity and transcript abundance as compared to Fe-sufficient roots, confirming the result found in other plant species (Dell'Orto *et al.*, 2000 and 2002; Schmidt *et al.*, 2003; Santi *et al.*, 2005). Assays of acidification in agar plates showed that in *M. truncatula* proton extrusion was located in the whole root, as it also occurs with the FC-R (data not shown). In *M. truncatula* grown without Fe for 7 days the increase in proton extrusion was

higher than that found for FC-R activity, conversely to what occurs in *Q. suber* (Gogorgena *et al.*, 2001). The early development of the ATPase activity in Fe-deficient *M. truncatula* roots support the need to carry out studies using shorter times after the onset of the deficiency.

In summary, our results indicate that in *Medicago truncatula* roots grown in Fe-deficient conditions, the *in vivo* root FC-R and ATPase activities, the activity of PEPC in root extracts as well as the concentrations of flavins in roots were significantly higher as compared to those found in Fe-sufficient plants. Also, the corresponding genes *MtFRO1*, *Mtha1*, *MtPEPC*, *MtribA* and *MtDMRLs* showed higher expression in Fe-deficient as compared to Fe-sufficient roots. These results suggest that adaptation to Fe deficiency is mediated by transcriptional up-regulation of these genes by Fe deficiency. Also, expression for each of these genes did not follow exactly the same changes in pattern over time, suggesting that although their response is more or less coordinated different signals may control each of the adaptation mechanisms.

Capítulo 4

INCREASES IN PHOSPHOENOL PYRUVATE CARBOXYLASE ACTIVITY IN IRON DEFICIENT SUGAR BEET ROOTS: ANALYSIS OF SPATIAL LOCALIZATION AND POST-TRANSLATIONAL MODIFICATION

Abstract: Root tips of Fe-deficient and Fe-sufficient sugar beet plants grown in hydroponics have been used to study the changes in the amount and activity of the cytosolic enzyme phosphoenolpyruvate carboxylase (PEPC, EC 4.1.1.31). Phosphoenolpyruvate carboxylase activity in extracts of the yellow Fe-deficient root tips was, at pH 7.3, 30-fold higher (when expressed on a FW basis) and 7.1-fold higher (when expressed on a protein basis) than that found in the extracts of Fe-sufficient root tips. The amount of phosphoenolpyruvate carboxylase protein determined by immuno-blotting was, on a protein basis, 35-fold larger in the yellow zone of Fe-deficient root tips than in the Fe-sufficient root tips. The inhibition of the phosphoenolpyruvate carboxylase activity by 500 μM malate was 41 and 58% in the extracts Fe-deficient and Fe-sufficient roots. The possibility that post-translational regulation of phosphoenolpyruvate carboxylase may occur mediated through phosphorylation, was studied by immunological detection of phosphoserine residues in root tip extracts.

Key words iron deficiency, malate, phosphoenol pyruvate carboxylase, root tips, sugar beet

1. INTRODUCTION

Iron deficiency is a widespread agricultural problem in many crops, especially in calcareous soils. In these soils, total Fe is high but occurs in chemical forms not available to plant roots (Lindsay and Schwab, 1982)

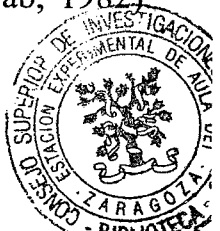

The adaptive response of the so-called Strategy I plants, which include dicotyledonous and non-graminaceous monocotyledonous plant species, involves root morphological and physiological changes (Marschner *et al.*, 1986). Among the morphological changes there is an increased formation of lateral roots, root hairs and transfer cells. All these changes increase the root surface available for Fe uptake (Landsberg, 1982). The physiological responses of Strategy I plants include higher rates of proton extrusion, which decreases the pH of the rhizosphere, a release of reducing and/or chelating substances such as phenolics and flavins and a two step mechanism for Fe uptake, in which Fe (III) is first reduced by a plasma membrane-bound ferric-chelate reductase (FC-R) and subsequently absorbed as Fe(II) (for reviews see Welkie and Miller 1993; Moog and Brüggemann, 1994).

The metabolism of roots is highly affected by Fe deficiency. Several changes at the metabolic level have been reported to occur in Fe-deficient roots, including an accumulation of organic acids, mainly malate and citrate (reviewed in Abadía *et al.*, 2002), shifts in the redox state of the cytoplasm (Schmidt, 1999; López-Millán *et al.* 2000a) and an increase in the activities of PEPC and several enzymes of the Krebs cycle (Landsberg, 1986; Rabotti *et al.*, 1995; López-Millán *et al.* 2000a) and of the glycolitic pathway (Rabotti *et al.*, 1995; Espen *et al.*, 2000).

The role of the organic acids in the Fe deficiency responses in not well established (Schmidt, 1999; López-Millán *et al.*, 2000a; Abadía *et al.*, 2002), although is commonly accepted that citrate could play an important role in Fe transport via xylem to the shoot (Tiffin, 1966). Two hypotheses have been put forward so far to explain the accumulation of organic acids in Fe-deficient roots. Landsberg (1986) reported that organic acid increases coincided with the enhanced proton extrusion found in Fe-deficient roots. This may occur through cytoplasm alkalinisation associated to proton efflux, which could activate phosphoenolpyruvate carboxylase (PEPC) activity (Rabotti *et al.*, 1995; Espen *et al.*, 2000). The second hypothesis (de Vos *et al.*, 1986) suggested that Fe deficiency may cause an alteration in the glycolytic pathway, as reported in fungi. Under Fe deficiency, phosphofructokinase would lose its regulation by citrate and pyruvate kinase would be inhibited by citrate, causing an accumulation of PEP, that in turn, via PEPC activity, would cause root organic acid concentrations to increase. In any case, Fe deficiency could cause an increase in root PEPC activity leading to organic acid accumulation. This increase in PEPC activity has been described previously in root extracts of Fe-deficient plants (Huffaker *et al.*, 1959; Landsberg 1986; Rabotti *et al.*, 1995; Rombolà, 1998; López-Millán *et al.*, 2000a).

The aim of this work was to determine whether PEPC activity was enhanced in root tips of Fe-deficient sugar beet plants. The amount of PEPC

in Fe-deficient and Fe-sufficient root tip extracts was determined by immuno-blotting and PEPC phosphorylation was investigated by immunochemical detection of phospho-serine residues. Inhibition of PEPC by malate was studied to assess the regulation of the enzyme activity under Fe deficiency conditions.

2. MATERIALS AND METHODS

2.1 Plant Material

Sugar beet (*Beta vulgaris* L. Monohil hybrid from Hilleshög, Landskröna, Sweden) was grown in a growth chamber with a PPFD of 350 μmol m^{-2} s^{-1} PAR at a temperature of 25 °C, 80% humidity and a photoperiod of 16 h light/8 h dark. Seeds were germinated and grown in vermiculite for 2 weeks. Seedlings were grown for 2 more weeks in half-strength Hoagland nutrient solution with 45 μM Fe(III)-EDTA and then transplanted to 20 L plastic buckets (four plants per bucket) containing half-strength Hoagland nutrient solution with either 0 or 45 μM Fe(III)-EDTA. The pH of the Fe-free nutrient solutions was buffered at approximately 7.7 by adding 1 mM NaOH and 1 g L^{-1} of $CaCO_3$. Root tips from plants grown for 10 days in the presence or absence of Fe(III)-EDTA were used in all experiments.

Root sections were taken approximately 0-5 and 5-10 mm from the root apex with a surgical blade (López-Millán *et al.*, 2000a). The 0-5 mm section (YZ) from the zero-Fe treatment had root hairs and was yellow due to the presence of flavins, whereas the 5-10 mm section (WZ) in the zero-Fe treatment and both the 0-5 mm and 5-10 mm sections in the control treatments had practically no root hairs and were white.

2.2 Protein quantification

Extracts for protein quantification were made according to Granier (1988) with the solubilisation buffer of Herbik *et al.* (1996). Samples were washed twice with TCA to avoid interferences by SDS and 2-mercaptoethanol. Aliquots of the extracts were incubated with 12% TCA (1 h at 4 °C) and centrifuged for 15 min at 10000 *g* at 4 °C. In the second washing step the pellet was resuspended with 6% TCA, centrifuged at 10000 *g* for 15 min at 4 °C and solubilised with ultrapure water. Proteins were quantified with the Bio-Rad DC Protein System Assay using BSA as standard.

2.3 Enzyme Assays

Extracts for measuring enzyme activity were made by grinding 100 mg FW of root material in a mortar with 1 mL of extraction buffer containing 30 mM sorbitol, 1% BSA and 1% PVP in 100 mM HEPES-KOH, pH 8.0. The slurry was centrifuged for 15 min at 10000 *g* and 4 °C, the supernatant collected and enzyme activity measured immediately. Phosphoenolpyruvate carboxylase (PEPC; EC 4.1.1.31) activity was measured in a coupled enzymatic assay with malate dehydrogenase, according to Vance *et al.* (1983), with 75 µL of extract in 1 mL of 2 mM PEP, 1 mM $NaHCO_3$, 5 mM $MgCl_2$, 0.16 mM NADH, 50 mM HEPES, pH 7.3. The endogenous root malate concentration (approximately 5.95 and 0.37 µmol g^{-1} FW in –Fe and control roots, respectively; see López-Millán *et al.*, 2000a), will give (with a ratio 100 mg/mL extract and then 75 µL extract/mL of assay) final malate concentrations in the assay medium of approximately 45 and 3 µM for Fe-deficient and control roots, respectively. These concentrations are much lower than the inhibition assay carried out with 500 µM malate. The addition of the protease inhibitor chymostatin (10 µg mL^{-1}) did not increase PEPC activities.

2.4 Immunoblotting

Extracts for immunoblotting were made according to Granier (1988) with the solubilisation buffer of Herbik *et al.* (1996). Root soluble protein was boiled for 5 min at 95 °C. Electrophoresis was carried out with a discontinuous system (Laemmli, 1970). The resolving gel contained 8% acrylamide and the stacking gel 7.2 % acrylamide in a Tris-glycine buffer. Proteins were electrophoresed for 2 h at 20 mA constant current and 25 °C in a discontinuous PAGE system. Semidry electroblotting onto nitrocellulose membranes was carried out at 50 mA for 2 h, using a Semiphor TE70 apparatus (Hoefer Scientific Instruments, San Francisco, CA, USA) according to the manufacturer's instructions. Blots were blocked for 45 min with 20 mM Tris, 0.9% NaCl and 5% BSA and then washed with 20 mM Tris, 0.9% NaCl and 0.1% BSA. For the identification of PEPC, blots were incubated for 2 h with a 1:1000 dilution of rabbit IgG against the phosphorylation site of PEPC and washed as above. The PEPC antibody was a polyclonal antibody obtained against a synthetic peptide of 23 aminoacids from the N-terminal sequence of sorghum PEPC (from Dr. J. Vidal, Orsay, France). A second incubation with a 1:2000 dilution of goat anti-rabbit IgG (H+L) horseradish peroxidase conjugate from BioRad was performed for 45 min. After thorough washing with 20 mM Tris and 0.9% NaCl, PEPC was detected with 20 mM Tris, 0.9% NaCl, 9 mg mL^{-1} chloronaftol in ethanol

and 17 µL H_2O_2. Quantification of PEPC was performed using a Molecular Imager FX apparatus (BioRad, San Francisco, USA).

Phosphoserine residues were identified by incubating the blot for 3 h with a 1:50 dilution of rabbit IgG against phosphoserine residues from SIGMA, St. Louis, USA. After washing the blot a second incubation was carried out for 1 h using a 1:2500 dilution of anti-Rabbit IgG-phosphatase. After thorough washing with 20 mM Tris and 0.9% NaCl, phosphoserine residues were detected with 0.2 M Tris, pH 9.6, 1 mM $MgCl_2$, 4 mg mL^{-1} BCIP and 1 mg mL^{-1} NBT in DMF.

3. RESULTS AND DISCUSSION

The amount of soluble protein in root tips was 2.85 and 1.18 mg protein g^{-1} FW in the yellow tip and the white adjacent zone of Fe-deficient roots, respectively. These values were approximately 4.2- and 2.4-fold higher than that found in the Fe-sufficient root tips, that was approximately 0.68 mg protein g^{-1} FW.

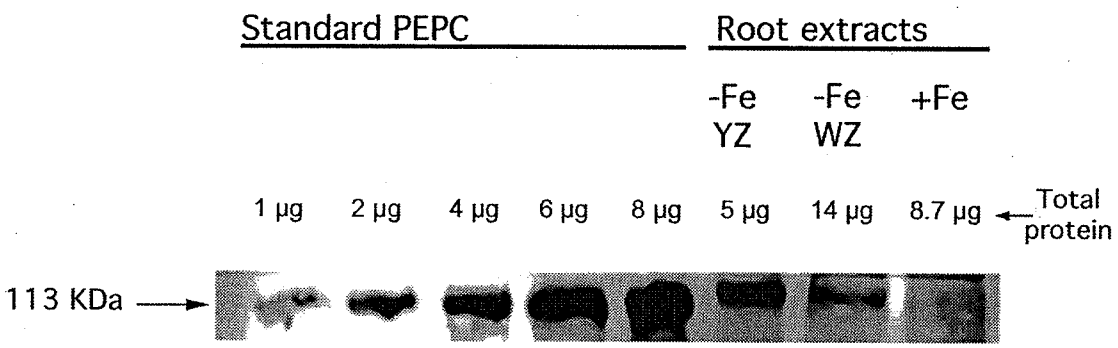

Figure 4-1. Protein immunoblot of partially purified PEPC (from SIGMA) and sugar beet root extracts. Extracts were made from the yellow (-Fe, YZ) and white parts (-Fe, WZ) of Fe-deficient root tips and from Fe-sufficient root tips (+Fe). PEPC was labelled using PEPC antibody.

The antibody against the phosphorylation site of PEPC immunodecorated a single 113-kDa polypeptide in sugar beet root tip extracts. The amount of PEPC was 34.7- and 6.5-fold higher in the yellow and white zones of Fe-deficient root tips, respectively, than in the Fe-sufficient root tips (Fig. 4-1). The activity of PEPC in root extracts was much higher in the yellow zone of Fe-deficient root tips than in the control. These increases were 29.6-fold when expressed on a FW basis and 7.1-fold when expressed on a protein basis (Table 4-1). An increase in PEPC activity in root extracts of Fe-deficient plants was first described by Huffaker *et al.* (1959). Later, increases in PEPC activity in root extracts under Fe deficiency of 1.85-, 2.3,

4 to 6 and 7- to 14-fold were reported in pepper (Landsberg, 1986), kiwifruit (Rombolà, 1998), cucumber (Rabotti *et al.*, 1995; De Nisi and Zocchi, 2000) and sugar beet (López-Millán *et al.*, 2000a), respectively. The increase in PEPC activity in Fe-deficient roots coincides spatially with areas having increased FC-R activity (López-Millán *et al.*, 2000a). Similar data were reported for the swollen root tip area of Fe-deficient pepper plants (Landsberg, 1986). The white parts of Fe-deficient roots did not have major increases neither in the total amount of PEPC (Fig. 4-1) nor in FC-R activity (López-Millán *et al.*, 2000a).

Table 4-1. Phosphoenolpyruvate carboxylase activity in root extracts from Fe-deficient and Fe-sufficient sugar beet. Enzyme assays were done at pH 7.3. Data are means ± SE of 10 replicates. Values in the same column followed by a different letter are statistically significant at $p \leq 0.05$ (*t* Student's test).

	μmol g^{-1} FW min^{-1}	μmol mg^{-1} protein min^{-1}
-Fe	5.04±0.42 a	1.77±0.42 a
+Fe	0.17±0.02 b	0.25±0.02 b
-Fe /+Fe	29.6	7.1

Increases of PEPC activity could be also mediated by post-translational regulation through phosphorylation as it occurs in the leaves of C4 and CAM species (see Chollet *et al.*, 1996, for a review) and in proteid roots of P-stressed plants (Gilbert *et al.*, 1998). The activity of PEPC in presence of 500 μM malate decreased from 4.57 to 2.72 nmol g^{-1} FW min^{-1} in extracts of the yellow zone of Fe-deficient roots and from 0.21 to 0.09 nmol g^{-1} FW min^{-1} in extracts of Fe-sufficient roots (Table 4-2). Inhibition by malate was therefore 58% in Fe-sufficient roots and 41% in Fe-deficient yellow root tips (Table 4-2). The relatively small but significant difference in PEPC sensitivity to malate could be explained by the presence of some endogenous malate in the assay medium of the Fe-deficient roots (approximately 45 μM). This could make the PEPC activity in Fe-deficient root extracts apparently less sensitive to malate. Post-translational regulation of PEPC through phosphorylation was also studied by immunological detection of phosphorylated residues of serine in the 113-kDa band, previously identified as PEPC. Phosphoserine residues were not detected in the PEPC region in any of the root extracts analysed (Fig. 4-2). These data suggest that post-translational regulation by phosphorylation may not occur in Fe-deficient roots. However this does not necessarily exclude phosphorylation because the steric conformation of the target protein may hinder the interaction of the antibody with the phosphoserine residues. Therefore, a more detailed analysis should be carried out with additional experiments, including ^{32}P labelling of PEPC protein, studies with inhibitors of protein kinases and phosphatases and PEPC-kinase tests.

Table 4-2. Inhibition of phosphoenolpyruvate carboxylase activity in root extracts from Fe-deficient and Fe-sufficient sugar beet by 500 μM malate. Enzymes assays were done at pH 7.3. Data (in μmol g^{-1} FW min^{-1}) are means ± SE of 5 replicates. Values in the same column followed by a different letter are statistically significant at $p \leq 0.05$ (*t* Student's test).

	Activity		% Inhibition
	0 μM malate	500 μM malate	
-Fe	4.57± 0.56 a	2.72± 0.33 a	40.5 a
+Fe	0.21± 0.03 b	0.09± 0.02 b	58.4 b

Other factors could further enhance PEPC activity in root cells. For instance, a cytoplasmic pH increases could boost PEPC activity, since the optimum pH for the enzyme is quite high. Espen *et al.* (2000) have recently shown with ^{31}P-NMR techniques, however, than in Fe-deficient cucumber roots cytosolic pH may increase only by approximately 0.02-0.06 units with respect to the controls, whereas the vacuolar pH increased by 0.03-0.20 units. This may be the consequence of a very efficient PEPC-mediated cytosolic pH regulation. The PEPC increase in Fe-deficient sugar beet root tips does not appear to depend on bicarbonate since root tips of plants grown without Fe in the absence of $CaCO_3$ also had PEPC activities 40-fold higher (on a FW basis and at pH 8.5) than the controls (not shown in the present work; López-Millán *et al.*, 2000a).

The possible functions of the increase in PEPC with Fe deficiency are still unclear. A metabolic model for C assimilation has been proposed recently to be triggered by Fe deficiency in sugar beet roots (López-Millán *et al.*, 2000a). In this model, PEPC catalyzes the carboxylation of PEP to oxalacetate, which could be then reduced to malate via cytosolic MDH. Malate could be transported to the mitochondria via the malate-oxalacetate shuttle and converted to citrate by CS. Part of this C could be used, through an increase in mitochondrial activity in transfer cells, to increase the capacity to produce reducing power (Bienfait, 1996), whereas another part would be exported to the shoot via xylem (Bialzyck and Lechowski, 1992; López-Millán *et al.*, 2000b). A possible function of the export of organic acids to the leaves is the use of these C compounds for the maintenance of basic processes such as respiration. PEP needed to maintain PEPC activity could possibly come via glycolysis from compounds previously synthesized and/or stored within the plant. Both phloem (de Vos *et al.*, 1986; Maas *et al.*, 1988), and root sugar concentrations (Thoiron and Briat, 1999) have been reported to increase with Fe-deficiency. The activities of some enzymes involved in the glycolytic pathway have also been shown to increase in Fe-deficient roots (Espen *et al.*, 2000; see Abadía *et al.*, 2002, for a review).

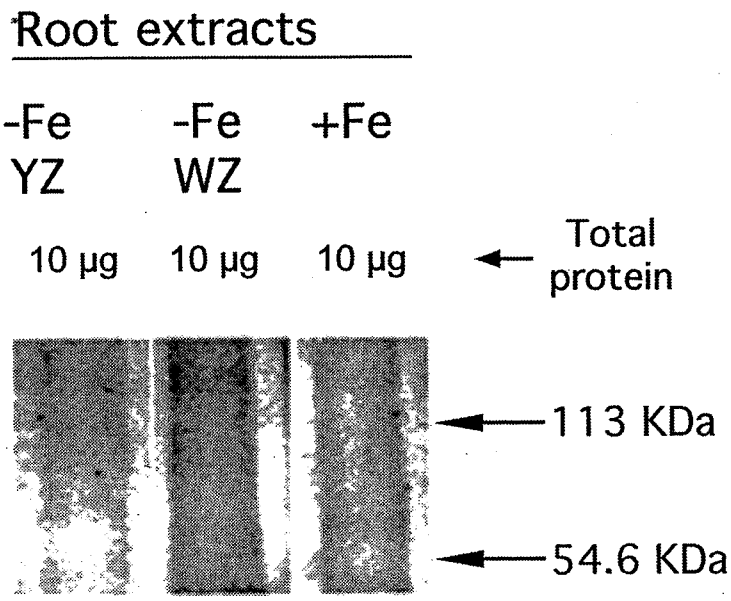

Figure 4-2. Protein immunoblot of root tip extracts. Extracts were made from the yellow (-Fe, YZ) and white parts (-Fe, WZ) of Fe-deficient root tips and from Fe-sufficient root tips (+Fe). Phosphoserine residues were labelled using phosphoserine antibody from Sigma.

Also, increased biosynthesis of carboxylates (particularly of citrate) and of phenolics (derived from organic acid metabolism) under Fe deficiency may be important for increased root exudation of these compounds, mediating Fe(III) mobilization in the rizhosphere, its transfer to the root surface and the subsequent reduction to Fe (II) and uptake. Exudation is further promoted by proton extrusion (Römheld and Marschner, 1983), and protons may be provided by enhanced biosynthesis of organic acids. Increased PEPC activity may be related to Fe-deficiency inhibition of NO_3^- uptake, resulting in excess uptake of cations over anions which could be balanced by proton extrusion (Cakmak and Marschner, 1990).

In summary, PEPC is a key enzyme in root responses to Fe deficiency that could enhance C fixation in roots and contribute to organic acid export from the roots to the leaves via xylem. The increase in PEPC activity measured in yellow root tip extracts is mainly due to an increase in the amount of the enzyme induced by Fe deficiency. Other factors like post-translational regulation by phosphorylation do not seem to control PEPC activity.

Capítulo 5

PEPC REGULATION IN *Beta vulgaris* ROOTS

Abstract: Root tips from sugar beet plants grown in hydroponics have been used to study the effects of iron deficiency on the activity and regulation of the PEPC enzyme. Western-blots indicate that the amount of PEPC was increased in Fe-deficient root tip extracts as compared to the controls and decreased after 24 and 72 h of Fe-resupply. PEPC was very low in gels from both roots of Fe-sufficient plants and the new white root tip parts of Fe-deficient plants resupplied with Fe for 72 h. PEPC transcription was found to be up-regulated by Fe deficiency. PEPC phosphorylation was studied by different strategies, including biochemical methods for the estimation of phosphorylation state as well as phosphorylation assays with ^{32}P-ATP, both *in vitro* and *in gel*. The ratios obtained with the biochemical assay phosphorylation test in Fe-deficient roots were very similar to those obtained in Fe-sufficient roots, and PEPC phosphorylation was not detected by *in vitro* phosphorylation assays. These data suggest that PEPC phosphorylation does not take place in Fe deficient sugar beet roots. The possibility that some other regulatory mechanism might take place in Fe-deficient roots should be envisaged.

Key words: iron deficiency, PEPC, regulation, roots

1. INTRODUCTION

The metabolism of plant roots is highly affected by Fe deficiency. The response of dicotyledonous and non-grass monocotyledonous plant species to Fe deficiency (known as Strategy I), includes various mechanisms for increasing Fe availability as well as root uptake of rhizospheric Fe (reviewed in Schmidt, 1999). In addition to an enhanced Fe uptake system, several changes at the metabolic level have been reported to occur in roots in order to improve Fe acquisition, transport and utilization in an Fe-deficient environment. These changes include the accumulation of organic acids, mainly malate and citrate (reviewed in Abadía *et al.*, 2002), shifts in the

redox state of the cytoplasm (Schmidt, 1999; López-Millán *et al.*, 2000a) and increases in the activity of the cytosolic enzyme phosphoenolpyruvate carboxylase (PEPC) and several other enzymes of the Krebs cycle, including citrate synthase, isocitrate dehydrogenase, fumarase, malate dehydrogenase, and aconitase (Landsberg, 1986; Rabotti *et al.*, 1995; López-Millán *et al.*, 2000a), and other enzymes of the glycolytic pathway, such as glyceraldehyde 3-phosphate dehydrogenase (Sijmons and Bienfait, 1983; Rabotti *et al.*, 1995; Espen *et al.*, 2000), piruvate kinase and fructose 6-phosphate kinase (Espen *et al.*, 2000).

An increase in PEPC activity in root extracts of Fe-deficient plants was first described by Huffaker *et al.* (1959). Further studies reported on increases induced by Fe deficiency in PEPC activity in root extracts of pepper (Landsberg, 1986), kiwifruit (Rombolà, 1998), cucumber (De Nisi and Zocchi, 2000; Rabotti *et al.*, 1995) and sugar beet (López-Millán *et al.*, 2000a; Andaluz *et al.*, 2002). The increase in PEPC activity correlates with the accumulation of organic acids in Fe deficient roots (López-Millán *et al.*, 2000a; Abadía *et al.*, 2002) and it is mainly localized to the external layers of the cortical cells of Fe-deprived root apical sections, which are very active in proton extrusion (De Nisi *et al.*, 2002).

In Fe-deprived plants, the increase measured in root PEPC activity can be the result of different regulation systems, including transcriptional, translational and post-translational mechanisms. An increase in the amount of protein in Fe deficient conditions has been measured by immuno-blotting detection in root extracts of cucumber (De Nisi and Zocchi, 2000) and sugar beet (Andaluz *et al.*, 2002). Only very recently, studies have demonstrated that PEPC transcripts are up-regulated by Fe deficiency in *Cucumis sativus* (abstract by De Nisi *et al.*, 2004) and *Medicago truncatula* roots (Andaluz *et al.*, 2005), and also that increases in transcript abundance occurred in parallel to increases in root extract PEPC activity. Also, a common post-translational regulation mechanism for PEPC regulation consists on the phosphorylation of serine residues in the N-terminal of PEPC, which leads to increases in enzyme activity (Chollet *et al.*, 1996). This regulatory mechanism has been described in soybean nodules (Schuller and Werner, 1993; Zhang *et al.*, 1995), seeds (wheat, Osuna *et al.*, 1996; barley, Osuna *et al.*, 1999; *sorghum*, Nhiri *et al.*, 2000) and leaves of C4 (see for review Vidal and Chollet, 1997) and C3 plant species (tobacco, Wang and Chollet, 1993; wheat, Duff and Chollet, 1995). However, studies in sugar beet by immunoblotting detection of phosphorylated residues (Andaluz *et al.*, 2002) and in cucumber by incorporation of γ-^{32}ATP (De Nisi and Zocchi, 2000), have been unsuccessful in detecting changes in phosphorylation of root PEPC in Fe-deficient plants.

The aim of this study was to investigate the possible ways of regulation of PEPC activity in Fe-deficient plants. The regulation of protein amount by Fe status was determined by PEPC immunoblotting in root tip extracts from Fe-sufficient, Fe-deficient and Fe-resupplied plants. Transcriptional regulation was evaluated by semi-quantitative RT-PCR in root tips from Fe-sufficient, Fe-deficient and Fe-resupplied plants. Finally, the possibility that a post-translational regulation by phosphorylation may occur was assessed by estimating the apparent phosphorylation state of root PEPC and by *in vitro* and *in gel* phosphorylation assays with Fe-sufficient and Fe-deficient root tip extracts.

2. MATERIALS AND METHODS

2.1 Plant material

Sugar beet (*Beta vulgaris* L. Monohil hybrid from Hilleshög, Landskröna, Sweden) was grown in a growth chamber with a photosynthetic photon flux density of 350 μmol m^{-2} s^{-1} photosynthetically active radiation and a 16 h, 23°C / 8 h, 18°C, day/night regime. Seeds were germinated and grown in vermiculite for two weeks. Seedlings were grown for an additional two weeks in one-half-strength Hoagland nutrient solution (Terry, 1980) with 45 μM Fe(III)-EDTA, and then transplanted to 20 L plastic buckets (four plants per bucket) containing one-half-strength Hoagland nutrient solution with either 0 or 45 μM Fe(III)-EDTA. The pH of the Fe-free nutrient solutions was buffered at approximately 7.7 by adding 1 mM NaOH and 1 g L^{-1} of $CaCO_3$. This treatment simulates conditions usually found in the field leading to Fe deficiency (Susín *et al.*, 1994). In the Fe-resupply experiment, plants grown for 10 days in absence of Fe were transferred to one-half-strength Hoagland nutrient solution, pH 5.5, with 45 μM Fe(III)-EDTA. Root tips were sampled at 0 (before adding Fe), 24 and 72 h after Fe resupply. After 72 h of resupply, root length had increased approximately by 4 mm, and therefore two types of samples were taken, one from the newly developed 4-mm white root tip zone and a second one from the still swollen yellow zone (see figures in López-Millán *et al.*, 2001b).

2.2 Preparation of root extracts

Root tips (100 mg) were homogenised thoroughly at 4°C in a mortar with 1 mL of 0.1 M Tris-HCl buffer (pH 7.5) containing 20% (v/v) glycerol, 1 mM EDTA, 10 mM $MgCl_2$, 14 mM 2-mercaptoethanol, 1mM phenylmethylsulphonyl fluoride (PMSF), 10 μg mL^{-1} chymostatin, 10 μg

mL^{-1} leupeptin, 2 μg mL^{-1} pepstatin, and 10 mM KF. Homogenates were then centrifuged at 15000 *g* for 3 min, and supernatants were immediately used. Protein quantification was performed by the method of Bradford (1976) using BSA as a standard.

2.3 Immunoblotting

Root tip homogenates were electrophoresed on 8% acrylamide gels (Laemmli, 1970) and blotted onto nitrocellulose membranes (Protan, Schleiber & Schuell, Dassel, Germany) using a Semiphor TE70 apparatus (Hoefer Scientific Instruments, San Francisco, CA, USA). Blots were blocked for 45 min with 20 mM Tris-HCl pH 7.5, 150 mM NaCl and 5% BSA and then washed with 20 mM Tris-HCl pH 7.5, 150 mM NaCl and 0.1% BSA.

For PEPC identification, blots were incubated for 2 h in a 1:1000 dilution of rabbit IgG against whole PEPC (provided by Prof. C. Echevarría, from the Department of Plant Biology, University of Seville), and washed as indicated above. A second incubation with a 1:2000 dilution of goat anti-rabbit IgG (H+L) horseradish peroxidase conjugate (Bio-Rad, Hercules, CA, USA) was performed for 45 min. After thorough washing with 20 mM Tris-HCl pH 7.5, 150 mM NaCl, PEPC bands were detected by the peroxidase assay (Ngo and Lenhoff, 1980).

2.4 PEPC gene expression analysis

Database searches were performed with TBLASTX (Altschul and Lipman, 1990) using previously identified PEPC sequences from *A. thaliana, Lycopersicon esculentum, Pisum sativum, Medicago sativa, Lupinus albus*, *Saccharum sp., Nicotiana tabacum,* and *Spinacia oleracea.* One TC (TC1867) encoding a possible ortholog for PEPC was identified in the TIGR *Beta vulgaris* Gene Index (BvGI). Sequences were aligned using the ClustalW program (Higgins *et al.*, 1994). Based on these alignments, specific primers were designed to amplify a fragment of 166 bp from *Beta vulgaris* PEPC cDNA sequence. Primers used were f-GTCCTTTGGGGA ACACTTCA and r-CAGCGTATATGCTTGGCAGA.

Total RNA was isolated from roots with the Rneasy Plant Mini kit (Qiagen, Maryland, USA) according to the manufacturer's instructions. One plant per treatment was used to extract RNA, and two different batches of plants were analyzed. A sample aliquot containing 3 μg of total RNA was subjected to reverse transcription with 25 μg/mL oligo (dT) primer, 0.05 mM dNTP mix and 1 unit of Superscript II Reverse Transcriptase (Invitrogen, Carlsbad, USA) in a final volume of 20 μL, according to the

manufacture's instructions. PCR reactions were carried out with 2 µL of resulting cDNA solution, using 0.5 µM of the specific primers. Additional reaction components were standard buffer (75 mM Tris HCl pH 9.0, 1.5 mM $MgCl_2$, 50 mM KCl, 20 mM $(NH_4)_2SO_4$), 0.2 mM dNTP's and 0.5 units DNA polymerase (Biotools, Madrid, Spain). PCR reactions were carried out with the following conditions: 95 °C for 5 min, 26 cycles consisting of 95 °C for 45 s, 55 °C for 45 s and 70 °C for 45 s, and a final period of 10 min at 70 °C. RT-PCR reactions were carried twice for each sample. Actin was used as housekeeping gene.

2.5 Determination of activity and apparent phosphorylation state of PEPC

PEPC activity was measured spectrophotometrically at 30°C at optimal (8.0) and suboptimal (7.3 and 7.1) pH values, using the NAD-malate dehydrogenase coupled assay described by Echevarría *et al.* (1994). The assay mixture contained in a total volume of 1 mL, 50 mM Hepes-KOH (pH 8.0, 7.3 or 7.1), 2.5 mM PEP, 5 mM $MgCl_2$, 1 mM $NaHCO_3$, 0.2 mM NADH and 10 units of malate dehydrogenase. Assays were initiated by addition of 75 µL of crude root extract.

The PEPC apparent phosphorylation state was estimated by 3 different biochemical tests, referred to as velocity test, APS-IgG test and malate sensitivity test. The velocity test consists on estimating the ratio between maximal PEPC activity at pH 8.0 and sub-optimal PEPC activity at pH 7.1 (Echevarría *et al.*, 1994, Osuna *et al.*, 1996). For the APS-IgG-binding assay, 40 µL of crude extract were incubated for 10 min at 0°C with 10 µL of affinity-purified APS-IgG, and then the activity at pH 7.1 was recorded. The apparent phosphorylation state according to the APS-IgG test was then calculated by estimating the ratio between PEPC activity at pH 7.1 in the extract containing a saturating amount of the APS-IgG and the PEPC activity at pH 7.1 in absence of APS-IgG (Pacquit *et al.*, 1995, Osuna *et al.*, 1996). In the malate sensitivity test, the IC_{50} (50 % inhibition of initial PEPC activity by L-malate) was calculated by measuring PEPC activity at pH 7.3 in presence of different concentrations (0-300 µM) of L-malate (Jiao *et al.*, 1991).

2.6 *In vitro* phosphorylation assays

In vitro phosphorylation was determined by ^{32}P incorporation from [γ-^{32}P] ATP into PEPC. Homogenates from Fe-sufficient and Fe-deficient root tips with PEPC activity of 0.01 and 0.1 U, respectively, were incubated at 30°C for 45 min with 0.25 mM AP_5A (to inhibit endogenous adenylate

kinase activity), a phosphocreatine (4 mM)-creatine phosphokinase (10 U) ADP-scavenging system, 25 μM ATP and 1 μCi [γ-^{32}P] ATP (Amersham, Uppsala, USA) in a final volume of 150 μL. The assay was stopped by addition of 37.5 μL of buffer containing 100 mM Tris-HCl, pH 8.8, 25% glycerol, 1% SDS and 10% 2-mercaptoethanol. Controls were carried out by adding 0.1 U of exogenous, non-phosphorylated PEPC from sugar beet leaves. A negative control was used by adding non-phosphorylated PEPC and a saturating amount of the APS-IgG (20 μg) to the extract of Fe-deficient roots and pre-incubating the mixture for 30 min at 0°C before the phosphorylation assay. The Ca-dependence of the PEPC kinase was studied by adding 5 mM EGTA to the phosphorylation mixture. After the assay, homogenates were boiled for 2 min at 90°C, and then subjected to SDS-PAGE in a 10% acrylamide gel. Gels were Coomasie-stained and autoradiographed to analiyze PEPC phosphorylation with a phosphor imager (Fujix BAS 1000, Fuji, Japan).

2.7 *In gel* phosphorylation assay.

Fe-sufficient and Fe-deficient root extracts containing 500 μg of protein were mixed with SDS-sample buffer containing 100 mM Tris-HCl, pH 8.8, 25% glycerol, 1% SDS and 10% 2-mercaptoethanol, and boiled for 2 min. Electrophoresis was performed in 15% acrylamide gels polymerized in presence of immuno-purified PEPC (0.3 mg mL^{-1}), at 18 mAmp for 1.5 h at room temperature. After electrophoresis, the gel was subjected to a denaturation/renaturation treatment as described in Wang and Chollet (1993). The *in gel* kinase assay was performed in 3.5 mL 40 mM Hepes-NaOH, pH 8.0, 2 mM DTT, 5 mM $Mg(CH_3COO)_2$, 0.1 mM EGTA and 0.1 μM [γ-^{32}P] ATP (50 μCi). After the assay, the activity gel was extensively washed at room temperature with 5 % (w/v) trichloroacetic acid and 1 % (w/v) Na pyrophosphate until ^{32}P radioactivity was no longer measured in the washing solutions. The gel was then vacuum dried and autoradiographed onto a Kodak X- Omat AR film at –70.

2.8 Glucose 6-phosphate concentration

Glucose 6-phosphate concentration in root tip extracts was measured in an enzymatic assay. Extracts were made by grinding 100 mg fresh weight of root tips in a mortar with 2 mL of 100 mM HEPES (pH 8.0) containing 30 mM sorbitol, 10 mM $CaCl_2$, 1% (w/v) BSA and 1% PVP. The slurry was centrifuged for 15 min at 10000 *g* and 4°C, and the supernatant was collected and analyzed immediately. Glucose 6-phosphate dehydrogenase (EC 1.1.1.49) activity was determined by measuring the increase in A_{340} due to

the enzymatic reduction of $NADP^+$ (Bergmeyer *et al.*, 1974) with increasing concentrations of glucose 6-phosphate as a substrate (0 to 1 mM). Glucose 6-phosphate concentration in the extract was determined by using a standard addition curve.

3. RESULTS

3.1 Western blotting

A Coomasie blue-stained, 1-D gel of root tip extracts from Fe-sufficient, Fe-deficient and Fe-deficient sugar beet plants resupplied with Fe for 24 and 72 h is shown in Fig. 5-1A. The antibody against the whole PEPC protein detects a single polypeptide of apparent molecular mass of 110 kDa in sugar beet extracts from yellow root tips of Fe-deficient and Fe-deficient plants resupplied with Fe for 24 and 72 h plants (Fig. 5-1B). No signal was detected in control root tip extracts from Fe-sufficient plants (Fig. 5-1B). The amount of PEPC was maximal in Fe-deficient root tip extracts and was lower after Fe-resupply (24 and 72 h). Also, in 72 h Fe-resupplied plants PEPC was not detected in extracts of the root tip new white part, similarly to what occurs in Fe-sufficient plants.

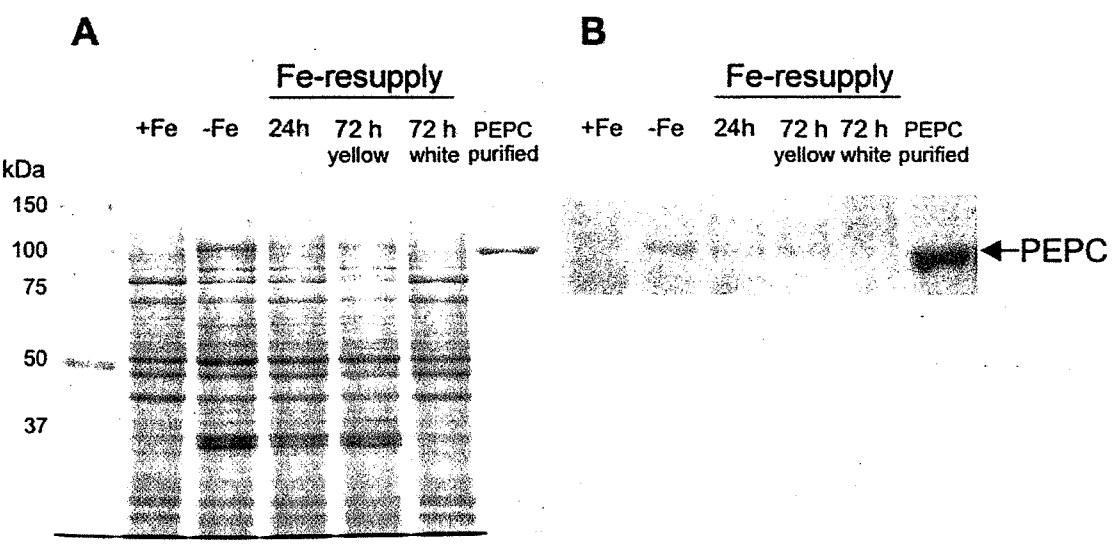

Figure 5-1. Coomasie-stained 1-D SDS-PAGE (Fig.1A) and PEPC immunoblot (Fig. 1B) of sugar beet root tip extracts and 4 µg partially purified maize PEPC (from SIGMA). Extracts were made from the Fe-sufficient (+Fe), Fe-deficient (-Fe) and Fe-resupplied (24 and 72 h) root tips. In 72 h Fe-resupplied root tips, yellow (72 h yellow) and new white (72 h white) zones were studied.

3.2 PEPC gene expression analysis

To identify potential PEPC open reading frames in *Beta vulgaris*, we performed database searches looking for ESTs and TCs with sequence similarity to previously reported genes from different species, including *A. thaliana*, *L. esculentum*, *P. sativum*, *M. sativa*, *L. albus*, *Saccharum sp.*, *N. tabacum* and *S. oleracea*. One TC, TC1867, was identified in the TIGR *B. vulgaris* gene index (BvGI) as a probable ortholog of the PEPC gene. TC1867 contains a fragment of PEPC (485 pb) corresponding to the 3' end that covers 46% of complete PEPC protein sequence with ca. 70% identity with previously known PEPC sequences from other species. The corresponding gene was named *BvPEPC*.

As estimated by semi quantitative RT-PCR, *BvPEPC* transcript abundance was much higher in the yellow root tip from Fe-deficient plants as compared to root tips from control plants. In the yellow root zones of Fe-resupplied plants (24 and 72 h after Fe addition) the expression of *BvPEPC* gene was similar to that observed in Fe-deficient yellow root tips, whereas in the new white root tip 72 h after Fe resupply expression was intermediate between that of Fe-sufficient root tips and that of Fe-deficient ones (Fig. 5-2).

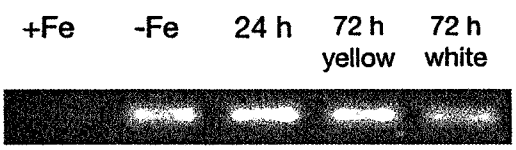

Figure 5-2. Semi-quantitative RT-PCR analysis of the *BvPEPC* transcript in roots from *B. vulgaris* plants grown at Fe-sufficient (+Fe), Fe-deficient (-Fe) and Fe resupplied (24 and 72 h) root tips. In 72 h Fe-resupplied root tips, yellow (72 h yellow) and new white (72 h white) zones were studied.

3.3 PEPC activity

The activity of the PEPC enzyme in root extracts, expressed on FW basis, was 52.4- and 59.0-fold higher in Fe-deficient as compared to Fe-sufficient plants, at optimal (pH 8.0) and suboptimal (pH 7.3) assay conditions, respectively. These data are in good agreement with data previously reported in this species, showing increases between 60- and 30-fold (López-Millán *et al.*, 2000a and Andaluz *et al.*, 2002, respectively). When data were expressed on a protein basis, increases in PEPC activity in root extracts with Fe-deficiency were approximately 12- and 14-fold at pH 8.0 and pH 7.3, respectively (Table 5-1). Increases reported previously were 7-fold at pH 7.3 (Andaluz *et al.*, 2002).

Table 5-1. PEPC activity in root tip extracts from Fe-sufficient and Fe-deficient sugar beet plants. Data are means ± SD of 3 replicates.

	pH 8.0		pH 7.3	
	µmol g^{-1} FW min^{-1}	µmol mg^{-1} prot min^{-1}	µmol g^{-1} FW min^{-1}	µmol mg^{-1} prot min^{-1}
+Fe	0.14±0.02	0.10±0.01	0.07±0.03	0.05±0.02
-Fe	7.49±1.33	1.22±0.28	4.25±1.01	0.69±0.20
-Fe/+Fe	52.4	11.8	59.0	13.6

3.4 Phosphorylation experiments

3.4.1 Biochemical phosphorylation assays

The apparent phosphorylation state of PEPC in sugar beet root tip extracts was estimated by using three different methods. Ratios of approximately 3.0 for Fe-sufficient and 3.4 for Fe-deficient root tips were obtained by using the velocity test (Table 5-2). When using the APS-IgG test rations obtained were 2.3 and 1.5 for Fe-sufficient and Fe-deficient root extracts, respectively. The IC_{50} calculated with the malate test was 0.21 for Fe-sufficient and 0.22 for Fe-deficient root tips. No statistically significant differences were found in any case. These data indicate that the phosphorylation state of PEPC was quite similar in both treatments.

Table 5-2. Apparent phosphorylation state of PEPC estimated by the velocity test, the APS-IgG test and the malate sensitivity test. Data are means ± SD of 3 replicates. Values in the same column followed by the same letter are statistically not significant at $p \leq 0.05$ (*t* Student's test).

	Velocity test (ratio)	APS-IgG test (ratio)	IC 50 (mM)
+Fe	2.98±0.67a	2.33±0.05a	0.21±0.04a
-Fe	3.37±0.93a	1.53±0.32a	0.22±0.03a

3.4.2 *In vitro* phosphorylation assay

In vitro phosphorylation of PEPC was studied in root extracts from Fe-sufficient and Fe-deficient plants (Figs. 5-3A and 5-3B). The autoradiographic pattern revealed the presence of various protein bands that incorporated ^{32}P during incubation in the presence of [γ-^{32}P] ATP (Fig. 5-3A). Two of them, with apparent molecular masses of 110 and 60 kDa, coincide with the electrophoretic mobility of two polypeptides increasing when exogenous PEPC was added to the extracts, which would correspond to PEPC and a fragment of this protein. APS-IgGs was used to assess the presence of phosphorylated PEPC among these radiolabeled polypeptides, since this antibody blocks specifically the PEPC phosphorylation site used by the PEPC kinase (Pacquit *et al.*, 1995). Addition of APS-IgGs to the *in vitro* phosphorylation assay impaired the phosphorylation of the

polypeptides at 110 and 60 kDa (Fig 5-3A, lane 5). When exogenous non-phosphorylated PEPC from sugar beet leaves was supplemented to the phosphorylation assay, PEPC kinase activity increased in both Fe-sufficient and Fe-deficient root extracts (Fig. 5-3A, lanes 2 and 4, respectively). These results and the fact that the intensity of the PEPC phosphorylated band was similar in Fe sufficient and Fe-deficient roots (Fig 5-3A, lanes 1 and 3, respectively) would suggest that PEPC kinase activity does not change in Fe deficient roots. The Ca-dependence of the PEPC kinase was studied by the addition of 0.5 mM EGTA to the phosphorylation assay. The intensity of the PEPC band was similar in both assays, with and without EGTA (Fig 5-3A, lanes 6 and 4, respectively), suggesting that the sugar beet root PEPC kinase is not a Ca-dependent enzyme.

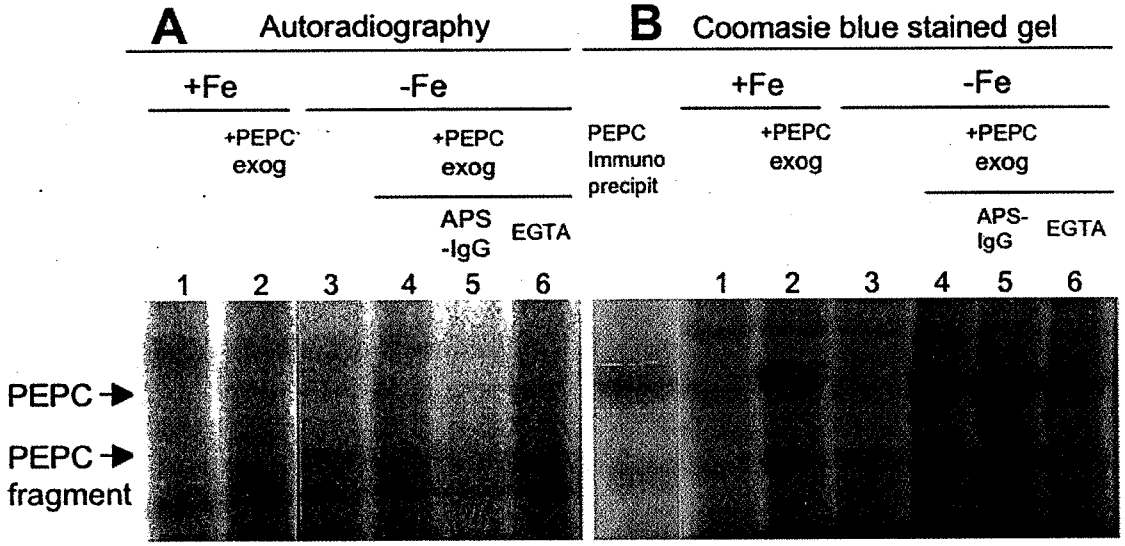

Figure 5-3. In vitro phosphorylation of PEPC in root tip extracts from Fe-sufficient (lanes 1 and 2) and Fe-deficient (lanes 3-6) plants. A) Autoradiographed gel, B) Coomasie blue stained gel. Lanes 1 and 3: Fe-sufficient and Fe-deficient root tip protein extracts, respectively. Lanes 2 and 4: Fe-sufficient and Fe-deficient root tip protein extracts plus exogenous PEPC. Lane 5: Fe-deficient root tip protein extract plus exogenous PEPC and APS-IgG. Lane 6: Fe-deficient root tip protein extract plus exogenous PEPC and EGTA.

3.5 *In gel* phosphorylation assay.

In gel phosphorylation experiments showed three protein kinase bands with apparent molecular masses of 45, 37 and 30 kDa (Fig. 5-4) in root tips of Fe-sufficient sugar beet plants and a single band of 45 kDa in root tips from Fe-deficient plants. The intensity of the 45 kDa band was much lower in gels from Fe-deficient root extracts as compared to those from extracts of Fe-sufficient root tips.

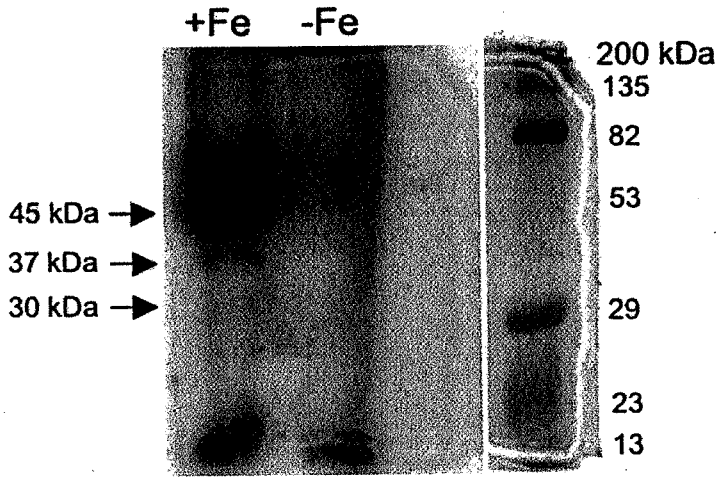

Figure 5-4. In gel assay of PEPC kinase activity from Fe-sufficient and Fe-deficient roots of sugar beet plants. The gel was polymerized with 0.3 U mL^{-1} of exogenous PEPC and the total protein per lane was 0.5 mg.

3.6 Glucose 6-phosphate concentration

Glucose 6-phosphate concentrations in the root tips were estimated to be 0.15 and 0.56 μmol g^{-1} FW in Fe-sufficient and Fe-deficient root tips, respectively. These values would result in final glucose 6-phosphate concentrations of approximately 0.8 and 1.1 μM in assays from in Fe-sufficient and Fe-deficient root tips.

4. DISCUSSION

In the present work we have studied the changes in PEPC activity in extracts from root tips of sugar beet as affected by Fe deficiency. The PEPC activity increases with Fe deficiency found in this study (52 to 59-fold on a FW basis) are similar to those reported previously for this species (López-Millán *et al.*, 2000a; Andaluz *et al.*, 2002). The increase found in PEPC activity in sugar beet is much higher than those found in other species such as pepper (Landsberg, 1986), kiwifruit (Rombolà, 1998), *Medicago truncatula* (Andaluz *et al.*, 2005) and cucumber (Rabotti *et al.*, 1995; De Nisi and Zocchi, 2000), where the increases, measured on a FW basis, were approximately 1.9-, 2.3-, 3.0- and 4.0 to 6.0-fold, respectively.

The *BvPEPC* gene was found by RT-PCR to be over-expressed in sugar beet roots with Fe deficiency. A similar increase in the transcripts of the *MtPEPC* with Fe deficiency has been found in the model plant *M. truncatula* (Andaluz *et al.*, 2005). Also, a report indicating an up-regulation of PEPC in Fe-deficient *Cucumis sativus* was recently presented in a Symposium (De

Nisi *et al.*, 2004). The transcript intensity of *BvPEPC*, however, did not fully match the changes in PEPC enzyme activity (see below). After 72 h of Fe-resupply, the expression of *BvPEPC* in the yellow root parts was maintained, whereas the expression in newly-grown white root tips was quite low, similar to that found in Fe-sufficient root tips.

Upon Fe resupply, PEPC was rapidly switched off, since both the amount and activity of PEPC decreased markedly. The amount of the PEPC protein decreased significantly 24 h after Fe resupply (Fig. 5-1), and it was no longer detected in the newly-grown white root tips sampled 72 h after Fe resupply. These data are in good agreement with previous reports indicating that the enzymatic activity of PEPC in root extracts of Fe-deficient plants decrease approximately by 50% 24 h after Fe resupply, to reach values similar to those found in controls after 96 h (López-Millán *et al.*, 2001b). The transcript intensity of *BvPEPC*, however, did not change in the yellow part of Fe-deficient root tips 72 after Fe resupply, whereas the PEPC enzyme activity was considerably decreased (López-Millán *et al.*, 2001b), suggesting that some kind of post-transcriptional regulation could be taking place in this area of the root tip.

Data presented here support that PEPC phosphorylation does not take place in Fe deficient sugar beet roots, confirming previous reports with cucumber (De Nisi and Zocchi, 2000) and sugar beet (Andaluz *et al.*, 2002). The ratios obtained with the apparent phosphorylation test in extracts from Fe-deficient roots were very similar to those found in extracts from Fe-sufficient roots, and PEPC phosphorylation was not detected by *in vitro* phosphorylation assays. Furthermore, *in gel* phosphorylation experiments indicate that PEPC kinase concentrations in Fe-deficient root extracts were much lower than in those from Fe-sufficient roots. This indicates that the widespread mechanism of PEPC post-translational regulation, consisting in the reversible phosphorylation of the N-terminal domain found in leaves from C4 and CAM species (see Vidal and Chollet, 1997, for a review), does not occur in Fe-deficient sugar beet roots. In this mechanism, light-dark (C4 species) or night-day (CAM species) regimes induce the phosphorylation-dephosphorylation of photosynthetic PEPC by a Ca-independent PEPC kinase and a type-2A protein phosphatase, respectively. Phosphorylated PEPC is more active, less sensitive to the negative effector malate and more sensitive to the positive effector glucose-6-phosphate (Chollet *et al.*, 1996). A similar regulation has also been found in non-photosynthetic tissues such as nodules and seeds (Zhang *et al.*, 1995; Osuna *et al.*, 1996; Osuna *et al.*, 1999, Nhiri *et al.*, 2000).

When expressed on a protein basis, the increase in PEPC activity in root extracts with Fe deficiency was approximately 12 to 14-fold, much lower than that expected from the measured increase in PEPC protein amount

(approximately 35-fold, also on a protein basis, in Andaluz *et al.*, 2002). These data suggest the existence of some factors influencing PEPC activities in root extracts, possibly linked to changes ocurring in the assay medium due to the different composition of the root extracts from Fe-deficient and control roots. This issue could be important, because any effect found in root extracts could be even more important in intact roots. A positive allosteric regulation of PEPC occurs with glucose 6-P and triose-P in algae (Schuller *et al.*, 1990a) and soybean nodules (Schuller *et al.*, 1990b). Iron deficiency causes a 5-fold increase in glucose 6-P, as it could be expected from the enhancement of the glycolytic pathway with Fe deficiency (Sijmons y Bienfait, 1983; Rabotti *et al.*, 1995; Espen *et al.*, 2000). However, the resulting increase in glucose 6-P in the PEPC assays would be lower than 2 μM, a value unlikely to affect significantly the root extract results .(for instance, a 500 μM glucose 6-P concentration would lead to an approximate 15% increase in PEPC activity). A possible explanation for a PEPC activity decrease in Fe-deficient root extracts is an increase in malate concentrations, since this compound is known to be a strong inhibitor of PEPC (Vidal and Chollet, 1997). However, the increase in root malate with Fe deficiency (from 0.4 to 6.0 mM; López-Millán *et al.*, 2000a) would result in increases in malate concentrations in the PEPC assays only up to 45 μM, which could decrease measured PEPC by a moderate 10%. Also, fumarate root concentrations, which increase with Fe deficiency up to approximately 0.9 mM (López-Millán *et al.*, 2000a), would result in increases in fumarate concentrations in the PEPC assays only up to 6 μM. Again, this could decrease slightly measured PEPC (by less than 5%, results not shown). Preliminary experiments in our lab indicated that extracts from Fe-deficient and Fe-sufficient root tips cause a marked decrease in the activity of purified PEPC enzyme (34 and 25% respectively), supporting the existence of a strong PEPC repressor in roots. However, this would not explain why the large Fe-deficiency induced amount of PEPC protein could result in only a moderate increase in PEPC activity. Another possibility could be the occurrence of different active PEPC forms in Fe-deficient and control roots. The presence of a single PEPC band in Western blotting experiments with Fe-deficient roots does not support the presence of forms with different gross molecular mass, but does not exclude the presence of other protein modifications.

In summary, the increase in sugar beet root PEPC activity induced by Fe deficiency is mediated through increases in both the amount of PEPC transcripts and the amount of protein. In addition our data suggest that some kind of post-transcriptional regulation, different from PEPC phosphorylation, could modulate PEPC activity in Fe-deficient yellow root tips and in their extracts.

Capítulo 6

PROTEOMIC PROFILES OF *Beta vulgaris* ROOT TIPS AND CHANGES INDUCED IN RESPONSE TO IRON DEFICIENCY

Abstract: The proteomic profile of root tips and the changes induced in that proteome by iron deficiency have been studied by using root tip extracts from *Beta vulgaris* plants grown in hydroponics. Two-dimensional electrophoresis, IEF-SDS PAGE, has been employed to obtain proteome maps. Approximately 150 spots were detected in 2-D gels form root tips of iron deficient and control plants. Iron deficiency induced significant changes in intensity in a large number of these polypeptides, mainly associated to the carbohydrate catabolism. A protein not present in Fe-sufficient roots, DMRL synthase, was in high amounts in root tips from Fe-deficient sugar beet plants and was also found to be transcriptionally regulated by Fe status.

Key words: DMRL synthase, iron deficiency, root proteome

1. INTRODUCTION

Iron is an essential micronutrient for plants, and plays a key role in plant metabolism processes as important as photosynthesis, N fixation and respiration (Marschner, 1995). Iron in calcareous soils, although abundant, is often not soluble and therefore is unavailable for the roots (Lindsay and Schwab, 1982). Plants can be classified in two groups depending on the mechanisms of Fe uptake and on the physiological responses to Fe deficiency: Strategy I plants, which include dicotyledonous and non-Graminaceae monocotyledonous species, and Strategy II plants, which include Graminaceae species. When grown under a limited Fe supply, Strategy II plants excrete phytosiderophores, which solubilize Fe and make

ferric ions available for root absorption (Marschner *et al.*, 1986; Marschner and Römheld, 1994).

Plants classified as Strategy I plants develop a series of biochemical and morphological changes in roots that lead to an increased capacity for Fe uptake when plants are Fe-deprived (see Schmidt, 1999, for a review); these responses at the uptake level are accompanied by several metabolic changes that support this adaptation mechanism to Fe deficiency (Rabotti *et al.*, 1995; Espen *et al.*, 2000; López-Millán *et al.*, 2000a). Morphological changes include root tip swelling, development of transfer cells and an increase in the number of lateral roots (Kramer *et al.*, 1980; Landsberg, 1982). These changes allow for an increase in the root surface in contact with the external medium, as a strategy for a maximization of Fe uptake from the soil (Kramer *et al.*, 1980; Landsberg, 1982). Among the biochemical changes found, there is an induction of the two-step, Fe-uptake system that consists on a plasma membrane ferric reductase that reduces extracellular Fe(III) (Moog and Brüggemann, 1994; Susín *et al.*, 1996; Robinson *et al.*, 1999; Schmidt, 1999) and a plasma membrane Fe (II) transporter that translocates the reduced iron to the root cell (Eide *et al.*, 1996; Fox and Guerinot, 1998). Biochemical responses also include a higher proton extrusion activity, probably associated to an induction of a plasma membrane H^+-ATPase in rhizodermal cells (Schmidt *et al.*, 2003, Santi *et al.*, 2005); this activity causes an acidification of the rhizosfere pH that enhances the solubility of Fe in the soil. Some Strategy I plants are also able to accumulate and release reducing and/or chelating substances, such as phenolics and flavins, which may have some role in Fe acquisition (Welkie and Miller, 1960; Susín *et al.*, 1994). Most of these changes are localized to root tips (López-Millán *et al.*, 2000a).

At the general metabolic level, increases in activity of PEPC (Rabotti *et al.*, 1995; López-Millán *et al.*, 2000a), several enzymes of glycolytic pathway such as pyruvate kinase, phosphofructokinase, fructose 1,6-bisphosphate aldolase and glyceraldehyde 3-phosphate dehydrogenase, (Rabotti *et al.*, 1995; Espen *et al.*, 2000) and of the citric acid cycle such as aconitase, fumarase, malate dehydrogenase and citrate synthase (Landsberg, 1986; Rabotti *et al.*, 1995; López-Millán *et al.*, 2000a) have been found to increase in different plant species under Fe deficiency. Also, Fe deficiency induces an accumulation of organic acids, mainly malate and citrate, in roots and leaves (Abadía *et al.*, 2002). The induction of the carbon metabolism (glycolysis and citric acid cycle) in Fe-deficient roots not only would provide a source of reducing power, protons and ATP for the ferric reductase and the H^+-ATPase enzymes, but also suggests the existence of a non-autotrophic, anaplerotic carbon fixation by roots (López-Millán *et al.*, 2000a). Carbon fixed anaplerotically in roots of Fe-deficient plants could be

exported via xylem (Bialzyk and Lechowski, 1992; López-Millán *et al.*, 2000b) and then used for basic maintenance processes in leaves with drastically reduced photosynthetic rates (Terry, 1980).

Whereas biochemical activities of all the enzymes involved in this adaptation mechanism in roots of Fe-deficient plants have been widely studied, the knowledge on the changes of the proteomic profile of roots with Fe deficiency is, as far as we know, quite scarce. This type of studies would provide a holistic view of most of the metabolic processes involved in the adaptation of Strategy I plants to Fe deficiency. The most used method to obtain proteomic profiles, IEF-SDS PAGE, has already been used to study the proteome of *Medicago truncatula* roots (Mathesius *et al.*, 2001; Watson *et al.*, 2003) but to our knowledge no data are still available the changes in the *M. truncatula* root proteome induced by Fe deficiency.

The aim of this work was to characterize the proteomic profile of root tips and the changes induced in root proteome in response to Fe deficiency. The study of the root proteome has been carried out using root tips from sugar beet plants grown in Fe-sufficient and Fe-deficient conditions in hidroponics by 2-D IEF-SDS PAGE.

2. MATERIALS AND METHODS

2.1 Plant Material

Sugar beet (*Beta vulgaris* L. Monohil hybrid from Hilleshög, Landskröna, Sweden) was grown in a growth chamber with a photosynthetic photon flux density of 350 μmol m^{-2} s^{-1} photosynthetically active radiation and a 16 h, 23°C / 8 h, 18°C, day/night regime. Seeds were germinated and grown in vermiculite for two weeks. Seedlings were grown for an additional two weeks in one-half-strength Hoagland nutrient solution (Terry, 1980) with 45 μM Fe(III)-EDTA and then transplanted to 20 L plastic buckets (four plants per bucket) containing one-half-strength Hoagland nutrient solution with either 0 or 45 μM Fe(III)-EDTA. The pH of the Fe-free nutrient solutions was buffered at approximately 7.7 by adding 1 mM NaOH and 1 g L^{-1} of $CaCO_3$. This treatment simulates conditions usually found in the field leading to Fe deficiency (Susín *et al.*, 1994). In the Fe-resupply experiment, plants grown for 10 days in absence of Fe were transferred to one-half-strength Hoagland nutrient solution, pH 5.5, with 45 μM Fe(III)-EDTA. Control and Fe-deficient root tips were excised ten days after the onset of the treatment. Fe-resupplied root tips were sampled at 0 (before adding Fe), 24 and 72 h after the Fe addition. After 72 h of resupply, root length increased approximately by 4 mm, leading to the development of a

new white root tip, while the swollen root zone was left behind (López-Millán *et al.*, 2001b). Therefore, samples at 72 h were taken from the newly developed white root tip zone and the swollen yellow zone (López-Millán *et al.*, 2001b).

2.2 Protein extraction

Protein extracts were obtained according to Meyer *et al.* (1988). Root tips (300 mg) were ground in a mortar with liquid nitrogen, and homogenized in 5 mL of solution A (50% (v/v) phenol in Tris HCl 0.1 M pH 8.0, 5 mM ß-mercaptoethanol) stirring for 30 min at 4°C. The homogenate was filtered (PVDF, 0.45 µm) and centrifuged for 15 min at 5000 *g*. The phenol phase was re-extracted for 30 min with one volume of solution B (Tris 0.1 M pH 8.0 saturated with phenol, 5 mM ß-mercaptoethanol) and centrifuged as described before. The phenol phase was collected and proteins precipitated by adding four volumes of 0.1 M ammonium acetate in cold methanol following an incubation for at least 4 h at –20°C. Samples were then centrifuged at 5000 *g* for 15 min and pellets were washed three times in cold methanol, dried with N_2 gas and resuspended in sample rehydration buffer containing 8 M urea, 2% (w/v) CHAPS, 50 mM DTT, 2 mM PMSF and 0.2% (v/v) 3-10 ampholytes (Amersham, Uppsala, Sweden). After rehydration, samples were incubated at 28°C for 1 h and then centrifuged at 15000 *g* for 10 min at 20°C. Protein concentration was measured with RC DC Protein Assay Bio-Rad based on Lowry *et al.* (1951) method.

2.3 Two-Dimensional Separation

A first dimension isoelectric focusing separation was carried out on 7 cm ReadyStrip IPG Strips (BioRad), with a linear pH gradient pH 5-8. Gels were loaded with equal amounts of protein. Strips were rehydrated for 16 h in 125 µL of rehydration buffer containing 100 µg of root extract proteins and supplemented with a trace of bromophenol blue. After this time, strips were loaded in a PROTEAN IEF Cell (BioRad, Hercules, CA, USA) and focused at 20°C, for a total of 14000 Vh. After IEF, strips were equilibrated for 10 min in equilibration solution I (6 M urea, 0.375 M Tris, pH 8.8, 2% (w/v) SDS, 20% (v/v) glycerol, 2% (w/v) DTT) and for another 10 min in equilibration solution II (6 M urea, 0.375 M Tris pH 8.8, 2% (w/v) SDS, 20% (v/v) glycerol, 2.5% (w/v) iodoacetamide).

For the second dimension, polyacrylamide gel electrophoresis (SDS-PAGE), IPG strips were placed onto 12% SDS-polyacrylamide gels (8 x 10 x 0.1 cm) and sealed with melted 0.5 % agarose. SDS-PAGE was carried out at 20 mA per gel for 1.5 h hour, and gels were subsequently stained with

Commassie-blue and analysed with the PDQuest 7.1 program (BioRad). 2-D gels were made from independent root tip preparations from different batches of plants.

2.4 *In gel* digestion of proteins and sample preparation for mass spectrometric analysis

Protein spots were excised manually and then digested automatically using a Proteineer DP protein digestion station (Bruker-Daltonics, Bremen, Germany). The digestion protocol used was that of Schevchenko *et al.* (1996) with minor variations. For peptide mass fingerprinting and LIFT TOF-TOF (Suckau *et al*, 2003) spectra acquisition, an aliquot of a-cyano-4-hydroxycinnamic acid in 33% aqueous acetonitrile and 0.1% trifluoroacetic acid was mixed with an aliquot of the above digestion solution and the mixture was deposited onto AnchorChip MALDI probes (Bruker-Daltonics).

2.5 MALDI peptide mass fingerprinting, LIFT TOF-TOF acquisition and database searching

Peptide mass fingerprint spectra were measured on a Bruker Ultraflex MALDI TOF-TOF mass spectrometer (Bruker-Daltonics) (Suckau *et al*, 2003) in positive ion reflector mode. Mass measurements were performed either automatically through fuzzy logic-based software or manually. Each spectrum was internally calibrated with mass signals of trypsin autolysis ions, and the typical mass measurement accuracy was ±25 ppm. The measured tryptic peptide masses were transferred (through the MS BioTools program from Bruker-Daltonics) as inputs to search the NCBInr database, using Mascot software (Matrix Science, London, UK). When available, MS-MS data from LIFT TOF-TOF spectra were combined with MS peptide mass fingerprint data for database searching.

2.6 DMRL synthase gene expression analysis

Database searches were performed with TBLASTX (Altschul and Lipman, 1990) using previously identified DMRL synthase sequences from *A. thaliana,* (NM129967), *Nicotiana tabacum* (AF148648) and *Spinacia oleracea* (AF147203). No DMRL synthase sequence from *Beta vulgaris* were obtained, thus primers were designed based on DMRL synthase sequence from *Spinacia oleracea* (AF147203), the closest phylogenetically related specie to *Beta vulgaris*. Primers used to amplify the complete cDNA sequence of DMRL synthase were f-ATGGCTTCATTTGCAGCTTCT and r-TTAGGCCTTCAAATGATGTTC.

Total RNA was isolated from roots with the Rneasy Plant Mini kit (Qiagen, Maryland, USA). One plant per treatment was used to extract RNA, and two batches of plants were analysed. A sample aliquot containing 3 µg of total RNA was subjected to reverse transcription with 25 µg/mL oligo (dT) primer, 0.05 mM dNTP mix and 1 unit of Superscript II Reverse Transcriptase (Invitrogen, Carlsbad, USA) in a final volume of 20 µL, according to the manufacture's instructions. PCR reactions were carried out with 2 µL of resulting cDNA solution, using 0.5 µM of the specific primers. Additional reaction components were standard buffer (75 mM Tris HCl pH 9.0, 1.5 mM $MgCl_2$, 50 mM KCl, 20 mM $(NH_4)_2SO_4$), 0.2 mM dNTP's and 0.5 units DNA polymerase (Biotools, Madrid, Spain). PCR reactions were carried out with the following conditions: 95 °C for 5 min, 30 cycles consisting of 95 °C for 45 s, 55 °C for 45 s and 70 °C for 1 min, and a final period of 10 min at 70 °C. RT-PCR reactions were carried twice for each sample set. Actin was used as housekeeping gene.

2.7 Flavin concentrations

Root material (ca. 100 mg FW) was frozen in liquid N_2 and ground in a mortar with 0.1 M ammonium acetate, pH 6.1. Extracts were centrifuged for 5 min at 14000 *g* and the supernatant stored at –80 °C until analysis. Flavin compounds including FMN and riboflavin were analysed by HPLC using a 100 x 8 mm Waters Radial-Pak C18 radial compression column (Waters Corp., Milford, MA, USA). Samples were injected with a Rheodyne injector (50 µL loop). Mobile phase (water:methanol 70:30, v:v) was pumped at a flow rate of 1 mL/min (Susín *et al.*, 1993). Flavins were detected at 445 nm. Peaks corresponding to FMN and FAD were identified by comparison of their retention times with those of standards from SIGMA (Saint Louis, Missouri, USA). Quantification was made with known amounts of each compound using peak areas.

3. RESULTS

3.1 IEF-PAGE electrophoresis

Root tip extracts from sugar beet plants grown in Fe-sufficient and Fe-deficient conditions were separated by 2-D IEF-SDS PAGE electrophoresis and gels were analysed to study the changes induced by Fe deficiency in the polypeptidic pattern. Real scans of typical 2-D gels obtained with extracts from Fe-sufficient and Fe-deficient plants are shown in Figs. 6-1A and 6-1B, respectively. Gels obtained with different root tip extract preparations

isolated from different batches of plants were very similar. The number of polypeptides detected in gels of root tip extracts from Fe-sufficient and Fe-deficient plans was 141 and 148, respectively (Figs. 6-1A and 6-1B).

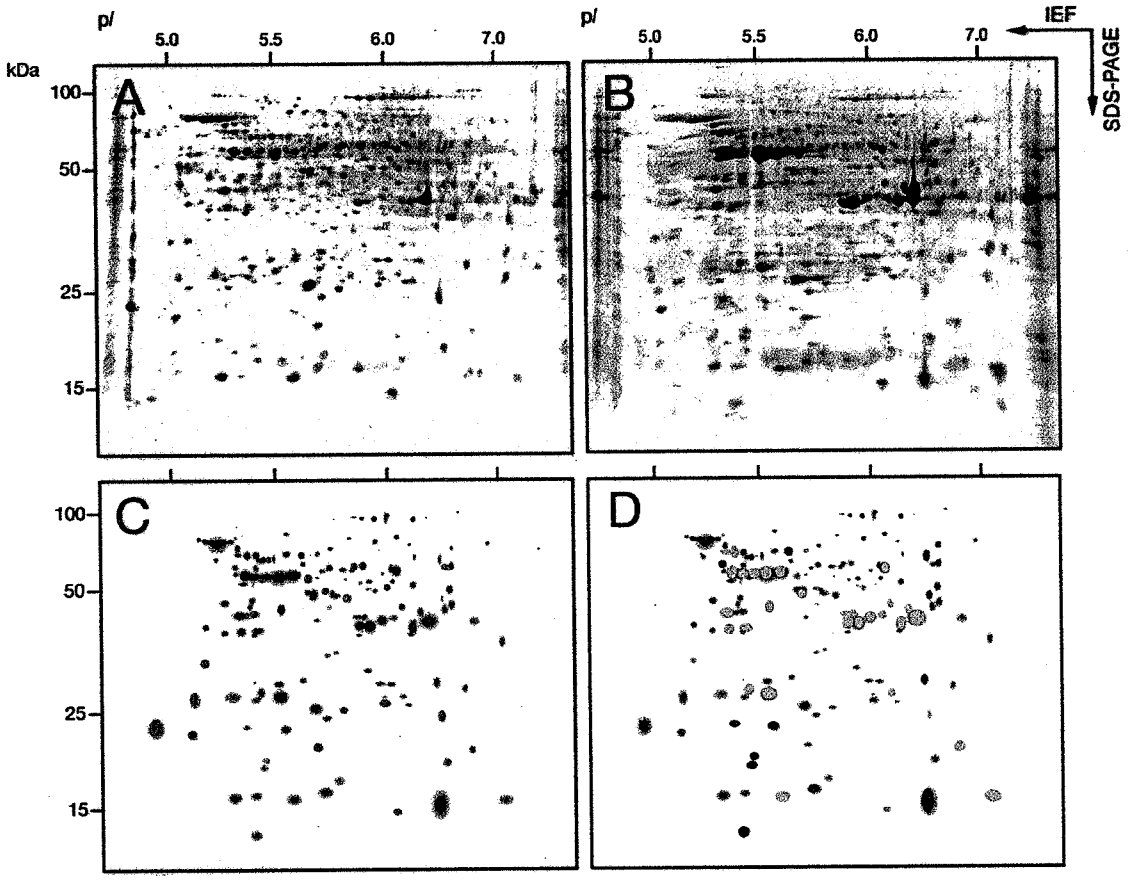

Figure 6-1. 2-D IEF-SDS PAGE root tip proteome maps of root tips from Fe-sufficient and Fe-deficient *Beta vulgaris* plants. Proteins were separated in the first dimension in linear (pH 5-8) IPG gel strips and in the second dimension in 12% acrylamide vertical gels. Scans of real typical gels of root tips from Fe-sufficient and Fe-deficient plants are shown in A and B, respectively. To facilitate visualization of the spots studied, a virtual composite image (C and D) was created containing all spots present in the real gels A and B. Then, spots whose intensities decrease or disappear completely with Fe deficiency were labelled with blue and green marks, respectively (C), and those increasing with Fe deficiency or only present in Fe-deficient gels were labelled with orange and red marks, respectively (D).

Averaged 2-D polypeptide maps of root tip extracts from Fe sufficient and Fe-deficient plants were made from three independent preparations, each from a different batch of plants. To better describe the changes in polypeptide composition we built a composite averaged virtual map containing all spots present in both Fe-deficient and control root tip extracts (Figs. 6-1C and 6-1D). The comparison of averaged maps indicated that Fe deficiency caused increases and decreases in signal intensity in 29 (orange marks in Fig. 6-1D) and 13 spots (blue marks in Fig 6-1C), respectively.

Furthermore, 6 and 13 spots were only detected in Fe-sufficient (green marks in Fig. 6-1C) and Fe-deficient plants (red marks in Fig. 6-1D), respectively. All polypeptides in the composite averaged map are depicted again in Fig. 6-2A, to permit annotation of those polypeptides where homologies were found by using MALDI TOF (marked by squares in Fig. 6-2A). These polypeptides were numbered from 1 to 29 as described in Fig. 6-2B, and the homologies are described in detail in Table 6-1.

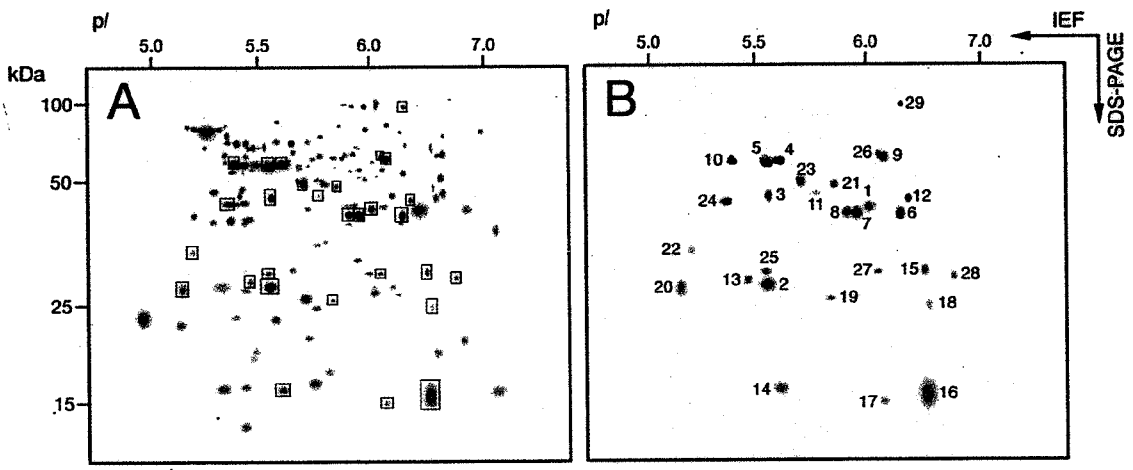

Figure 6-2. Virtual composite image, showing all polypeptides present in root tips from Fe-deficient and Fe-sufficient plants. In A, polypeptides which had significant homologies with proteins in the databases (using MALDI MS and MASCOT) are annotated by squares. The same polypeptides are numbered in B, and homologies are described in detail in Table 6-1.

From the 29 spots that increased in signal in root tip extracts of Fe-deficient as compared to Fe-sufficient controls, 20 were excised and analysed by MALDI MS. Since the sugar beet genome has not been sequenced yet and very few sequences are available in the databases, identification was performed by homology searches with proteins from other plant species. From the 20 spots analyzed, 14 proteins were identified (proteins labelled 1 to 14 in Fig. 6-2B and Table 6-1). These include proteins related to glycolysis such as fructose 1,6-bisphosphate aldolase from *Arabidopsis thaliana* (spot 1), triose-phosphate isomerase from *Coptis japonica* (spot 2), 3-phosphoglycerate kinase from *Triticum aestivum* (spot 3) and enolase from *Mesenbryanthenum crystallinum* and *Lactuca sativa* (spots 4 and 5, respectively). Three spots gave significant matches to malate dehydrogenase from *Beta vulgaris* and *Nicotiana tabacum* (spots 6-8), and two more polypeptides presented homology with α and ß subunits from F1 ATP synthase from *B. vulgaris* and *Sorghum bicolour*, respectively (spots 9 and 10). Other proteins that were found to increase in root tip extracts from Fe-deficient sugar beet plants as compared to the Fe-sufficient controls were fructokinase from *B. vulgaris* (spot 11) and formate dehydrogenase from

Quercus robur (spot 12). Also, one spot gave significant matches to a cytosolic peptidase At1g79210/YUP8H12R_1 from *A. thaliana* (spots 13). Spot 14 gave significant match to a glycine rich protein from *A. thaliana*, that possibly has a role in RNA transcription or processing during stress conditions.

Table 6-1. Proteins identified by MALDI-MS in 2-D IEF-SDS PAGE gels. [1]MS1 data: Protein score is –10*Log (P), where P is the probability that the observed match is a random event. Protein scores >76 are significant ($p<0.05$). [2]MS2 data: Ion score is –10*Log (P), where P is the probability that the observed match is a random event. Individual ion scores >40 indicate identity or extensive homology ($p<0.05$). In both cases, protein scores are derived from ion scores as a non-probabilistic basis for ranking protein hits.

spot	th MW	th pI	ex MW	ex pI	Mascot score	accesion n	homology	species
Increased proteins in Fe-deficiency								
1	39	7.6	42	5.9	76[1]	T48396	fructose 1,6-bisphosphate aldolase	*A. thaliana*
2	27	5.5	35	5.4	143[1]	gi|556171	triose-phosphate isomerase	*C. japonica*
3	31	4.9	45	5.4	103[1]	gi|28172909	cytosolic 3-phosphoglycerate kinase	*T. aestivum*
4	49	5.6	59	5.5	188[1]	gi|1087071	enolase	*M. crystallinum*
5	49	5.6	58	5.4	123[1]	T12341	enolase	*L. sativa*
6	36	5.9	40	6.2	140[1]	CAB61618	malate dehydrogenase	*B. vulgaris*
7	36	5.9	40	5.8	77[1]	CAB61618	malate dehydrogenase	*B. vulgaris*
8	22	7.6	40	6.0	124[1]	gi|48375044	malate dehydrogenase	*N. tabacum*
9	55	6.0	60	6.0	185[1]	O78692	F1 ATPase α subunit	*B. vulgaris*
10	49	5.1	58	5.3	170[1]	gi|4388533	F1 ATPase ß subunit	*S. bicolor*
11	36	5.2	49	5.5	299[1]	gi|1052973	fructokinase	*B. vulgaris*
12	41	6.5	44	6.3	102[1]	gi|38636526	formate dehydrogenase	*Q. robur*
13	26	5.5	35	5.4	113[1]	gi|21689609	At1g79210/YUP8H12R_1	*A. thaliana*
14	17	5.9	17	5.5	116[2]	gi|16301	glycine rich protein	*A. thaliana*
New spots in Fe-deficiency								
15	37	7.1	36	6.6	101[1]	gi|19566	glyceraldehyde 3-phosphate DH	*M. quinquepeta*
16	23	8.7	16	6.6	65[54]	Q9XH32	DMRL synthase	*S. oleracea*
Decreased proteins in Fe-deficiency								
17	16	6.3	15	6.4	166[1]	gi|3309053	nucleoside diphosphate kinase I	*M. crystallinum*
18	23	6.4	30	6.8	217[1]	gi|11496133	oxalate oxidase-like germin 171	*B. vulgaris*
19	22	6.1	32	5.7	188[1]	gi|34365651	At4g27270	*A. thaliana*
Disappeared spots in Fe deficiency								
20	23	6.4	34	5.7	217[1]	gi|11496133	oxalate oxidase-like germin 171	*B. vulgaris*
21	9	6.0	49	5.7	49[2]	gi|2956703	peroxidase	*S. oleracea*
22	29	5.1	38	5.3	69[2]	gi|5101868	caffeoyl CoA O-methyltransferase	*Z. mays*

spot	th MW	th pI	ex MW	ex pI	Mascot score	accesion n	homology	species
Spots that did not change in intensity								
23	31	4.9	49	5.7	186[1]	gi|28172909	cytosolic 3-phosphoglycerate kinase	*T. aestivum*
24	39	5.1	44	5.3	127[1]	gi|13173419	cytosolic glutamine synthetase	*B. vulgaris*
25	28	5.4	36	5.4	125[1]	gi|310587	ascorbate peroxidase	*S. oleracea*
26	59	6.6	62	6.0	62[2]	gi|12802327	mitochondrial peptidase ß subunit	*C. melo*
27	27	5.4	36	6.0	143[1]	gi|21386959	endopeptidase complex α subunit	*A. thaliana*
28	30	6.3	36	6.8	113[1]	gi|3914430	proteasome ε chain	*S. oleracea*
29	95	5.9	100	6.0	186[1]	gi|2369714	elongation factor 2	*B. vulgaris*

From the 13 new spots detected *de novo* in proteome maps from root tip extracts of Fe-deficient plants (Fig. 6-1D), the 6 more abundant were analysed by MALDI MS, resulting in only 2 positive matches (spots 15 and 16 in Fig. 6-2B and Table 6-1). Significant matches were found for glyceraldehyde 3-phosphate dehydrogenase from *Magnolia quinquepeta* (spot 15) and 6,7-dimethyl-8-ribityllumazine synthase (DMRL) from *Spinacia oleracea* (spot 16). The intensities of the remaining 7 spots detected only in Fe-deficient root tip extracts were so low that it was not possible to study them by MALDI MS.

From the 13 spots showing a decrease in signal intensity in root tip extracts from Fe-deficient plants as compared to controls (Fig. 6-1C), 3 were identified by MALDI MS. Spots 17 and 18 (Fig. 6-2B, Table 6-1) gave a significant match to nucleoside diphophate kinase I from *Mesembryanthemum crystallinum* and to oxalate oxidase-like germin from *B. vulgaris*, respectively. Spot 19 presented homology with At4g27270 protein from *A. thaliana* (Fig 6-2B and Table 6-1) whose molecular function is to interact selectively with FMN, and also presents oxidoreductase activity.

From the 6 spots that were not detected in root tip extracts from Fe-deficient plants as compared to the controls (Fig. 6-1C), 3 were identified by MALDI MS (spots 20-22 in Fig. 2B and Table 6-1). Proteins matched were oxalate oxidase from *B. vulgaris* (spot 20), peroxidase from *S. oleracea* (spot 21) and caffeoyl CoA O-metyltransferase from *Zea mays* (spot 22).

Twelve spots that did not change in intensity when the Fe deficient proteome map was compared to the Fe sufficient map (Figs. 6-1A and 6-1B) were analysed by MALDI MS, and 7 of them (spots 23-29 in Fig. 6-2B and Table 6-1) gave significant matches to already known proteins. Identified proteins were 3-phosphoglycerate kinase from *Triticum aestivum* (spot 23), glutamine synthetase from *B. vulgaris* (spot 24), and ascorbate peroxidase

from *S. oleracea* (spot 25). Three more spots gave significant matches with different peptidases, a mitochondrial processing peptidase ß subunit from *Cucumis melo*, α subunit from multicatalytic endopeptidase complex from *A. thaliana* and ε chain from proteasome from *S. oleracea* (spots 26-28). Spot 29 presented homology to the elongation factor 2 from *B. vulgaris*.

3.2 DMRL synthase protein amount analysis

To further analyse the changes induced by Fe status in the amount of DMRL synthase, root tip extracts from sugar beet plants grown in Fe-sufficient, Fe-deficient and Fe-resupplied condition were separated by 2-D IEF-SDS PAGE electrophoresis and gels were analysed. Real scans of the 2-D gel zone where DMRL synthase protein is located (16 kDa, p*I* 6.6) are shown in Fig. 6-3. As previously shown in Fig. 6-1, the DMRL synthase protein was detected *de novo* in Fe-deficient root tip extracts (-Fe, Fig. 6-3). The spot corresponding to DMRL synthase was also detected with a similar signal intensity in 2-D gels obtained from extracts of the yellow zone of the root tip from plants 24 and 72 h after Fe was resupplied to the nutrient solution (24 h and 72 h yellow, Fig. 6-3). However, the spot corresponding to DMRL synthase was not detected in 2-D gels from extracts of the new white zone of root tips from plants 72 h after Fe resupply (72 h white, Fig. 6-3), as occurs in Fe-sufficient root tip extracts (+Fe, Fig. 6-3).

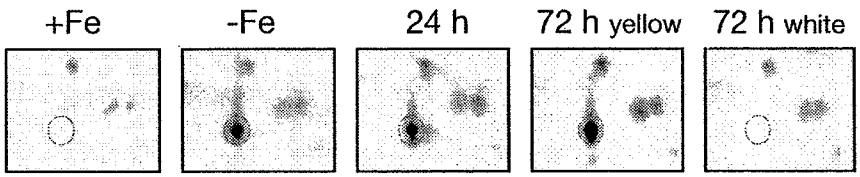

Figure 6-3. Zoom scans of real typical gels of root tips from Fe-sufficient (+Fe), Fe-deficient (-Fe) and 24 h, 72 h yellow and 72 h white Fe-resupplied plants.

3.3 DMRL synthase gene expression analysis

To identify a putative DMRL synthase cDNA in *Beta vulgaris*, primers based on DMRL synthase sequence from *Spinacia oleracea* (AF147203) were designed. A PCR product of approximately 675 bp was amplified and then sequenced (Fig. 6-4).

```
ATGGCTTCATTTGCAGCTTCTCAATCTTGTTTCCTTACTACTAATTCCAAT
M  A  S  F  A  A  S  Q  S  C  F  L  T  T  N  S  N

CTTTTACCTCTTAAACCCTCTTTTCTTCAACAATCTTCTACCTTTCTTCGC
L  L  P  L  K  P  S  F  L  Q  Q  S  S  T  F  L  R

TTTTCTGCCCCTCTTTCTTCCTCATCTTCTGTCCCAGGTTGTGGGTTAGTT
F  S  A  P  L  S  S  S  S  S  V  P  G  C  G  L  V

CATGTTGCGACAGAAAAGAAAAATCGTGCCTCATTTGCAGTGACAAATGCA
H  V  A  T  E  K  K  N  R  A  S  F  A  V  T  N  A

GTGAGGGAGTTGGAAGGATATGTCACTAAAGCCCAGAATTTTCGATTTGCC
V  R  E  L  E  G  Y  V  T  K  A  Q  N  F  R  F  A

ATTGTTGTGGCTAGGTTTAATGAATTTGTGACAAGGCGGCTAATGGAAGGA
I  V  V  A  R  F  N  E  F  V  T  R  R  L  M  E  G

GCTCTTGACACTTTCAAGAAATATTCCGTCACTGAAGATATTGATGTTGTT
 A  L  D  T  F  K  K  Y  S  V  T  E  D  I  D  V  V

TGGGTTCCTGGTGCTTATGAGCTTGGCGTTACTGCACAGGCACTGGGAAAA
W  V  P  G  A  Y  E  L  G  V  T  A  Q  A  L  G  K

TCAGGAAAATATCATGCTATTGTGTGTCTTGGAGCTGTGGTAAAAGGGGAT
S  G  K  Y  H  A  I  V  C  L  G  A  V  V  K  G  D

ACTTCACACTACGATGCTGTCGTTAACTCCGCCTCCTCTGGAATACTAACA
T  S  H  Y  D  A  V  V  N  S  A  S  S  G  I  L  T

GCTGGACTGAATTCAGGAGTACCTTGTATCTTTGGTGTCCTTACTTGTGAT
A  G  L  N  S  G  V  P  C  I  F  G  V  L  T  C  D

GACATGGATCAGGCCATTAATCGCGCTGGTGGAAAAGTAGGCAATAAGGGT
D  M  D  Q  A  I  N  R  A  G  G  K  V  G  N  K  G

TCTGAGGCAGCGCTAACAGCTATTGAGATGGCTTCGCTCTTTGAACATCAT
S  E  A  A  L  T  A  I  E  M  A  S  L  F  E  H  H

TTGAAGGCCTAA
L  K  A  *
```

Figure 6-4. DMRL synthase sequence in *Beta vulgaris*.

The translated amino acid sequence for the DMRL synthase open reading frame displayed 89%, 57% and 54% identity at the amino acid level to the *Spinacia oleracea*, *Arabidopsis thaliana* and *Nicotiana tabacum* DMRL synthase proteins (Fig. 6-5). We have assigned the name *BvDMRLs* to the corresponding DMRL gene of *B. vulgaris*.

Figure 6-5. Alignment of DMRL synthase protein from *Nicotiana tabacum* (Nt), *Arabidopsis thaliana* (At), *Beta vulgaris* (Bv) and *Spinacia oleracea* (So).

Transcriptional regulation by Fe status of *BvDMRLs* gene was estimated by semi-quantitative RT-PCR. *BvDMRLs* transcript abundances were significantly higher in root tips from Fe-deficient as compared to control plants. The expression of *BvDMRLs* gene was drastically reduced 24 h after Fe-resupply to Fe-deficient plants. Transcript abundance in root tips, both white and yellow zones, sampled 72 h after Fe-resupply showed the same very low expression level as in Fe-sufficient plants (Fig. 6-6).

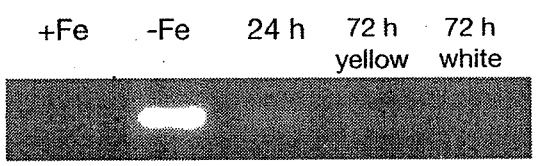

Figure 6-6. Semi-quantitative RT-PCR analysis of the *BvDMRLs* transcript in tip roots from *Sugar beet* plants. Extracts were made from the Fe-sufficient (+Fe), Fe-deficient (-Fe) and Fe-resupplied (24 and 72 h) root tips. In 72 h Fe-resupplied root tips, yellow (72 h yellow) and new white (72 h white) zones were studied.

3.4 Flavin concentrations

Flavin compounds in root tip extracts from Fe-sufficient, Fe-deficient and Fe-resupplied plants were quantified by HPLC. Peaks corresponding to FAD, riboflavin sulfates and riboflavin were found in Fe-deficient and Fe-resupplied root tip extracts, whereas only traces of these compounds were

detected in extracts of both Fe-sufficient roots and of the new white zone of 72 h Fe-resupplied root tips.

Riboflavin sulfates account for 98% of the total flavin concentration, with riboflavin accounting for the remaining 2% (the concentration of FAD was below the detection limit). Riboflavin sulfate concentration increased from 318 nmol g^{-1} FW in Fe-deficient yellow root tips to 488 nmol g^{-1} FW in the yellow zone of 72 h Fe-resupplied root tips (Fig. 6-7A). Riboflavin concentration was maximal in yellow root tips sampled 24 h after Fe-resupply (2.25 nmol g^{-1} FW) and decreased to 1.10 nmol g^{-1} FW in yellow root tips sampled 72 h after Fe resupply (Fig. 6-7B). Both in Fe-sufficient root tips and 72 Fe-resupplied white root tip parts the concentrations of flavins were below the detection limit. The concentration data of flavins in *B. vulgaris* roots are in the range reported previously in this species (Susín *et al.*, 1993).

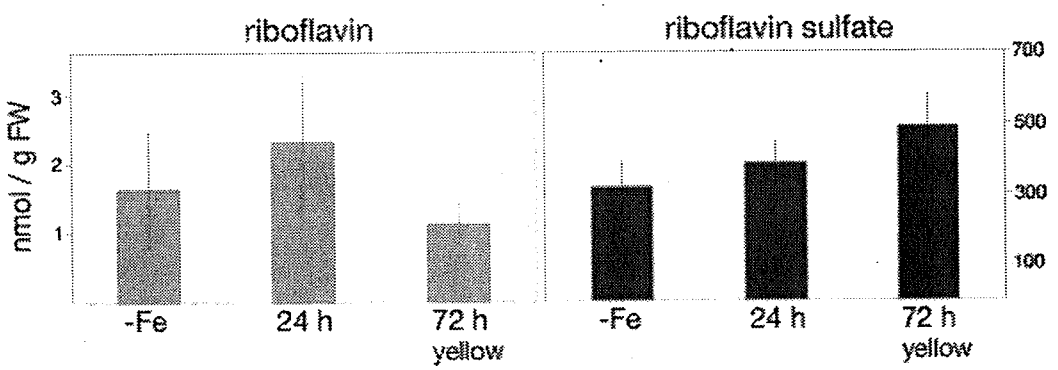

Figure 6-7. Flavin concentration (nmol g^{-1} FW) of riboflavin and riboflavin sulfates in root tips from *Beta vulgaris* plants. Extracts were made from the Fe-deficient (-Fe) and Fe-resupplied 24 (24 h) and 72 h yellow (72 h) root tips. Both in Fe-sufficient root tips and 72 Fe-resupplied white root tip parts the concentrations of flavins were below the detection limit.

4. DISCUSSION

Root tip extracts from sugar beet plants grown in hydroponics have been used to study the changes induced by Fe deficiency in the root proteome. The most widely used technique in proteomic studies, IEF-SDS PAGE, has been employed to resolve proteins from root tip extracts, obtaining proteome maps with approximately 150 spots (Fig. 6-1). Data obtained show that Fe deficiency results in relative intensity changes in a large number of these polypeptides. The study has focused in proteins in the p*I* range 5-8 and the apparent molecular mass range 10-100 kDa, and therefore changes in proteins outside these ranges have not been investigated.

Most of the proteins found to be up-regulated in sugar beet root tips by Fe deficiency were identified by MALDI MS as carbohydrate catabolism

enzymes, including 5 of the 10 enzymes of the glycolytic pathway: fructose 1,6-bisphosphate aldolase, triosephosphate isomerase, glyceraldehyde 3-phosphate dehydrogenase, 3-phosphoglycerate kinase and enolase; one of the citric acid cycle, malate dehydrogenase; and fructokinase. Increases in the activities of several glycolytic enzymes in root extracts with Fe deficiency have been previously found, including fructose 1,6-bisphosphate aldolase (Sijmons and Bienfait, 1983) and glyceraldehyde 3-phosphate dehydrogenase (Sijmons and Bienfait, 1983; Rabotti *et al.*, 1995; Espen *et al.*, 2000). Also, increases in the activities of several enzymes of the citric acid cycle in root extracts with Fe deficiency have been previously reported, including malate dehydrogenase in cucumber and sugar beet plants (Rabotti *et al.*, 1995; López-Millán *et al.*, 2000a). Results are also in agreement with microarray gene analysis in Fe-deficient *A. thaliana* roots (Thimm *et al.*, 2001). However, increased levels of protein have not been reported, as far as we know, with the only exception of glyceraldehyde 3-phosphate dehydrogenase (Herbik *et al.*, 1996). Increases in the amount of PEPC (phosphoenolpyruvate carboxilase; De Nisi and Zocchi, 2000; Andaluz *et al.*, 2002) have been found, but this enzyme, with a molecular mass of 110 kDa, was not in the range used in our 2-D gels. Up-regulation of carbohydrate catabolism in roots of plants grown in Fe deficient conditions is probably a result of an increased demand of energy and reducing power in roots needed to sustain the increased activity of H^+-ATPase and Fe-reductase (Schmidt, 1999; Thimm *et al.*, 2002). Also, two spots corresponding to different subunits of F1 ATP synthase were found to increase in 2-D gels from Fe deficient root tips, further supporting the higher energy requirement in these roots. Moreover, our results show an increase in the amount of formate dehydrogenase, an enzyme related to the anaerobic respiration, in Fe-deficient roots. Anaerobic respiration is an alternative pathway for energy production, when oxidative phosphorylation is impaired (as occurs in Fe deficient conditions), and it has been described to occur in Fe-deficient roots based both on enzyme activities (López-Millán *et al.*, 2000a) and on transcriptional up-regulation (Thimm *et al.*, 2001).

The largest change found in the proteome map of root tip extracts from sugar beet plants grown in Fe deficiency corresponds to appearance of spot number 16 (Fig. 6-3), identified by MALDI MS as DMRL synthase. This spot was detected *de novo* in Fe deficient sugar beet root tips and represented the protein with the highest concentration in these gels. This spot was already detected, but not identified, in previous studies in our laboratory (Gonzalez-Vallejo, 2000). DMRL synthase belongs to the five-step riboflavin biosynthesis pathway, and catalyses the last step of riboflavin biosynthesis. Ribloflavin is the precursor of riboflavin sulphates, flavin mononucletotide (FMN), flavin adenin dinucleotide (FAD), the last one

being a cofactor for the ferric reductase from roots. Fe-resupply assays showed that DMRL synthase concentration in yellow parts of root tips before and after Fe-resupply did not change. Accordingly, flavin compounds such as riboflavin and riboflavin sulphates were found to be accumulated in Fe-resupplied yellow root tips. However, *BvDMRLs* expression drastically decreased 24 h after the addition of Fe to Fe-deficient plants, suggesting that the turnover of this protein is slow. Accumulation in Fe-deficient roots of flavin compounds, including riboflavin and riboflavin 3'- and 5' sulfate is a characteristic response of sugar beet plants. This accumulation has already been described previously in different plant species including *N. tabacum*, *Licopersicum esculentum*, *L. sativa* and *B. vulgaris* (Welkie and Miller, 1988, 1992; Susín *et al.*, 1993, 1994). The exact role of these flavins in Fe deficiency is unknown. However, it has been hypothesised, based on the similar location of flavin accumulation and iron reduction and on the fact that the iron reductase is an flavin-containing protein, that flavin accumulation may be an integral part of the Fe-reducing system in roots from Strategy I plants (Cakmak *et al.*, 1987; López-Millán *et al.*, 2000a). In *M. truncatula* plants, in addition to *MtDMRLs*, *MtribA*, the first gene in the riboflavin biosynthesis pathway, is also transcriptionally regulated by Fe status and both *MtDMRL* and *MtribA* expression patterns over time are parallel to the *MtFRO* expression pattern, suggesting that these compounds play a role in the mechanism for Fe reduction which still needs to be elucidated (Andaluz *et al.*, 2005). On the other hand, an mRNA (*MtSULT1*) encoding for a sulfotransferase in *M. truncatula* roots was also found to be up-regulated by Fe deficiency (Andaluz *et al.*, 2005). This enzyme, belonging to the secondary metabolism, might participate in the sulfation of riboflavin yielding riboflavin sulfates. No candidates for this role have been detected so far in the proteome map of sugar beet roots.

In summary, Fe deficiency induced significant changes in the root tip sugar beet proteome, mainly associated to the carbohydrate catabolism. A protein not present in Fe-sufficient roots, DMRL synthase, was in high amounts in root tip extracts from Fe-deficient sugar beet plants and was also found to be transcriptionally regulated by Fe status.

Capítulo 7

PROTEOMIC PROFILES OF THYLAKOID MEMBRANE PROTEINS AND CHANGES IN RESPONSE TO IRON DEFICIENCY

Abstract: The proteomic profile of thylakoid membranes and the changes induced in that proteome by iron deficiency have been studied by using thylakoid preparations from *Beta vulgaris* plants grown in hydroponics. Two different 2-D electrophoresis approaches have been used to study these proteomes: isoelectrical focusing followed by SDS PAGE (IEF-SDS PAGE) and blue-native polyacrylamide gel electrophoresis followed by SDS PAGE (BN-SDS PAGE). Iron deficiency induced significant changes in the thylakoid sugar beet proteome profiles: the relative amounts of electron transfer protein complexes were reduced, whereas those of proteins participating in leaf carbon fixation-linked reactions were increased. A set of polypeptides, which includes several enzymes related to metabolism, was only detected in thylakoid preparations from Fe deficient *Beta vulgaris* leaves by using BN-SDS PAGE, suggesting that they may be associated in these thylakoids *in vivo*. The BN-SDS PAGE technique has been proven to be a better method than IEF/SDS-PAGE to resolve highly hydrophobic integral membrane proteins from thylakoid preparations, allowing for the identification of complexes and determination of their polypeptidic components.

Key words Blue Native gel, IEF-PAGE, iron deficiency, MALDI mass spectrometry, thylakoid

1. INTRODUCTION

Iron deficiency is one of the major abiotic stresses affecting many crop species, especially when they are grown in alkaline and calcareous soils (Lindsay and Schwab, 1982). Iron, although abundant, is often not soluble and therefore unavailable for plant roots in these soils, thus causing a

decrease in shoot growth rates and crop yield (Chen and Barak, 1982). When plants are grown under Fe-deficient conditions their youngest leaves develop a characteristic greenish-yellow colour, often referred to as Fe deficiency chlorosis. This yellow colour is due to decreases in the leaf concentrations of the light harvesting pigments chlorophylls and carotenoids, along with a relative enrichment in carotenoids (Terry, 1980; Morales *et al.*, 1990, 1994). Leaves of Fe-deficient plants show a marked decrease in photosynthetic rates (Terry, 1980) and decreases in photosynthetic efficiency and electron transport rates (Spiller and Terry, 1980). In addition to these changes, Fe deficiency is known to cause a reduction in the number of granal and stromal lamellae per chloroplast (Spiller and Terry, 1980; Platt-Aloia *et al.*, 1983), and decreases in the amounts of many thylakoid membrane components, including proteins, electron carriers and lipids (Terry and Abadía, 1986).

Thylakoid membranes contain the multiprotein photosynthetic complexes photosystems I and II, which include the reaction centres responsible for converting light energy into chemical bond energy, as well as a cytochrome b_6/f complex and an ATPase. Effects of Fe deficiency on these thylakoid proteins have been studied previously in sugar beet plants by 1-D SDS PAGE (Nishio *et al.*, 1985). These studies showed that Fe deficiency reduces drastically both the light harvesting and core complexes of photosystem II and photosystem I (Terry and Abadía, 1986). Photosystem I was the complex most diminished, followed by cytochrome b_6/f and photosystem II, whereas the ATPase complex was least affected (Nishio *et al.*, 1985).

The effects of Fe deficiency in the structure of antenna complexes and supercomplexes are better known in cyanobacteria (Guikema and Sherman, 1983; Pakrasi *et al.*, 1985). These studies showed that the amounts of high molecular weight complexes and supercomplexes are decreased in Fe-deficient conditions, indicating that aggregation of low molecular weight complexes into higher order structures is also affected by this nutritional stress. Moseley *et al.* (2002) suggested that responses to Fe deficiency in *Chlamydomonas* involve remodelling of the antenna complexes, disconnection of the LHCI antenna from photosystem I and establishment of a new steady state, with decreased stoichiometries of electron transfer complexes. Another change induced by Fe deficiency in the arrangement of the PSI antenna in cyanobacteria is the induction of the CP43 like protein CP43' (Riethman and Sherman, 1988; Burnap *et al.*, 1993). This protein associates with photosystem I to form a complex that consists in a ring of 18 CP43' molecules around a photosystem I trimer (Bibby *et al.*, 2001; Boekema *et al.*, 2001). The function of this protein has not been completely elucidated yet, although this new harvesting complex would increase the size of the PSI antenna and compensate for the decrease in phycobilisome and PSI levels in response to Fe deficiency (Bibby *et al.*, 2001).

The effect of Fe deficiency on leaf growth is relatively small when compared to the marked reduction in photosynthetic rates (Terry, 1979; Terry, 1980; Rombolà *et al.*, 2005). This fact agrees with the smaller decrease observed in the activities of the Calvin cycle proteins when compared to thylakoid proteins. Total activities of the enzymes glyceraldehyde-3-phosphate dehydrogenase, fructose 1,6-bisphophatase, 3-phosphoglycerate kinase and sedoheptulose 1,7-bisphosphatase were decreased by Fe deficiency by less than 15 % (Taylor *et al.*, 1982; Arulanantham *et al.*, 1990), whereas the total activity of ribulose-5-phosphate kinase decreased by 29% and that of ribulose 1,5- biphosphate carboxylase/oxygenase (Rubisco) decreased by 40%, the latter being the most affected Calvin cycle enzyme with Fe deficiency (Taylor *et al.*, 1982; Arulanantham *et al.*, 1990).

To date, isoelectric focusing followed by SDS PAGE is the most used technique to obtain proteome maps (Whitelegge, 2003). In fact, IEF-SDS PAGE has been used to separate peripheral thylakoid proteins, lumenal and stromal soluble proteins and integral membrane proteins (Kieselbach *et al.*, 2000; Peltier *et al.*, 2000, 2002; Hippler *et al.*, 2001). However, membrane proteins are poorly soluble in the solvents commonly used for IEF due to their high hydrophobicity, and they are therefore underrepresented in IEF-SDS PAGE gels. To solve this limitation, a second 2-D technique (BN-PAGE) employs the anionic dye Coomassie Brilliant Blue G-250 to transfer negative charges to membrane protein complexes while keeping them in a structurally intact form, thus making them more soluble for 2-D analysis. This technique has been previously used to characterize chloroplast protein complexes in algae (*Synechocystis*, Herranen *et al.*, 2004; *Chlamydomonas*, Rexroth *et al.*, 2003) and also in higher plants (*Spinacea oleracea*, Kügler *et al.*, 1997; *Nicotiana tabacum*, Suorsa *et al.*, 2004; *Pisum sativum*, Thidholm *et al.*, 2002; *Hordeum vulgaris*, Ciambella *et al.*, 2005; *Arabidopsis*, Heinemeyer *et al.*, 2004).

The aim of this work was to characterize the proteomic profile of thylakoids and the changes induced in the thylakoid proteome in response to Fe deficiency. The study of the photosynthetic apparatus proteome has been carried out using thylakoids from sugar beet plants grown in Fe-sufficient and Fe-deficient conditions by two different 2-D electrophoresis approaches: isoelectrical focusing followed by SDS PAGE (IEF-SDS PAGE) and blue-native polyacrylamide gel electrophoresis followed by SDS PAGE (BN-SDS PAGE) (Schägger and von Jagow, 1991).

2. MATERIALS AND METHODS

2.1 Plant Material

Sugar beet (*Beta vulgaris* L. Monohil hybrid from Hilleshög, Landskröna, Sweden) was grown in a growth chamber with a photosynthetic photon flux density of 350 μmol m^{-2} s^{-1} photosynthetically active radiation and a 16 h, 23°C / 8 h, 18°C, day/night regime. Seeds were germinated and grown in vermiculite for two weeks. Seedlings were grown for an additional two weeks in one-half-strength Hoagland nutrient solution (Terry, 1980) with 45 μM Fe(III)-EDTA, and then transplanted to 20 L plastic buckets (four plants per bucket) containing one-half-strength Hoagland nutrient solution with either 0 or 45 μM Fe(III)-EDTA. The pH of the Fe-free nutrient solutions was buffered at approximately 7.7 by adding 1 mM NaOH and 1 g L^{-1} of $CaCO_3$. This treatment simulates conditions usually found in the field leading to Fe deficiency (Susín *et al.*, 1994). Young and recently expanded leaves were sampled 10 days after treatment initiation.

2.2 Isolation of thylakoid membranes

Thylakoid membranes were obtained as described by Berthold *et al.* (1981) and Dunahay *et al.* (1984) with some modifications. Leaves (approximately 100 g FW) were homogenized in an Osterizer blender in 200 mL 400 mM NaCl, 20 mM Tricine, 2 mM $MgCl_2$, 0.2% BSA, pH 8.0. The brei was filtered through two Miracloth layers, and the filtrate centrifuged at 300 *g* for 2 min. The supernatant was then centrifuged at 10000 *g* for 10 min, and the obtained pellet was washed in 40 mL 150 mM NaCl, 20 mM Tricine, 5 mM $MgCl_2$, 0.2% BSA, pH 8.0, and subsequently centrifuged at 9000 *g* for 10 min. The resulting pellet, consisting in crude thylakoids, was resuspended in 10 mM NaCl, 5 mM $MgCl_2$, 50 mM MES, 400 mM sucrose, pH 6.0, frozen in liquid N_2 and stored at -80 °C until use. Chlorophyll was extracted in 80% acetone and quantified as described in Arnon (1949). Protein concentration was measured using the DC Protein Assay kit of BioRad (BioRad, Hercules, CA, USA) according to the manufacturer's instructions. Leaves used to obtain thylakoids had chlorophyll concentrations of approximately 375 and 50 μmol m^{-2} in Fe-sufficient and Fe-deficient leaves, respectively.

2.3 Two-dimensional electrophoresis. (IEF-SDS PAGE)

2.3.1 Protein extraction from thylakoids and solubilization

Thylakoid proteins were precipitated with 80% acetone and 0.07% ß-mercaptoethanol at -20 °C for 30 min. After centrifugation at 10000 *g* for 10 min, the supernatant was discarded and the pellet was washed with 80% acetone and 0.07% ß-mercaptoethanol. These two steps were repeated and the final pellet was dried with N_2. The sample rehydration buffer used to resuspend the proteins consisted in 2 M thiourea, 8 M urea, 20 mM Tris, 4% (w/v) CHAPS, 50 mM DTT, 0.05% (w/v) n-dodecyl ß-D-maltoside, 2 mM PMSF and 0.5% (v/v) 3-10 ampholytes (Amersham, Uppsala, Sweden). After rehydration, samples were incubated at 28°C for 1 h and then centrifuged at 15000 *g* for 10 min at 20°C. Protein concentration was measured as indicated above.

2.3.2 IEF focusing

A first dimension isoelectric focusing separation was carried out on 7 cm ReadyStrip IPG Strips (BioRad), with linear pH gradients from pH 4-7 or 5-8. Gels were loaded with equal amounts of protein. Strips were rehydrated for 16 h in 125 µL of rehydration buffer containing 170 µg of thylakoid proteins and supplemented with a trace of bromophenol blue. After this time, strips were loaded in a PROTEAN IEF Cell (BioRad, Hercules, CA, USA) and focused at 20°C, for a total of 14000 Vh. After IEF, strips were equilibrated for 10 min in equilibration solution I (6 M urea, 0.375 M Tris, pH 8.8, 2% (w/v) SDS, 20% (v/v) glycerol, 2% (w/v) DTT) and for another 10 min in equilibration solution II (6 M urea, 0.375 M Tris pH 8.8, 2% (w/v) SDS, 20% (v/v) glycerol, 2.5% (w/v) iodoacetamide).

2.3.3 SDS PAGE electrophoresis

For the second dimension polyacrylamide gel electrophoresis (SDS PAGE), IPG strips were placed onto 12% SDS-polyacrylamide gels (dimensions 8 x 10 x 0.1 cm) and sealed with melted 0.5 % agarose. SDS PAGE was carried out at 20 mA per gel for 1.5 h hour and gels were subsequently stained with Commassie-blue and analysed with the PDQuest 7.1 program (BioRad). 2-D gels were made from independent thylakoid preparations from different batches of plants.

2.4 Blue-native gel electrophoresis (BN PAGE) and SDS PAGE

BN PAGE was performed as described in Kügler *et al.* (1997) with slight modifications. Thylakoid membranes (0.5 mg chlorophyll mL^{-1}) were solubilized with 1% (w/v) n-dodecyl ß-D-maltoside, incubated on ice for 2 min and centrifuged at 18000 *g*, 4 °C for 15 min. 0.1 volumes of a solution containing 100 mM BisTris/HCl, pH 7.0, 0.5 M ε-amino-n-caproic acid, 30% (w/v) sucrose, and 50 mg mL^{-1} Serva Blue G was added to the supernatant and the mixture was loaded into a 4-10% acrylamide gradient gel. Gels were loaded with equal amounts of protein (27.5 µg of protein per lane). Electrophoresis was carried out at 2 °C, with a progressive increase in voltage from 75 to 200 V for approximately 4 h. After the run, BN PAGE lines were excised and proteins were solubilized for 30 min with a sample buffer containing 5% ß-mercaptoethanol (Laemmli, 1970).

The second dimension SDS PAGE was carried out in 15% acrylamide gels with 6 M urea. After electrophoresis, gels were silver-stained (Blum *et al.*, 1987) and analysed using the PDQuest 7.1 program (BioRad).

2.5 *In gel* digestion of proteins and sample preparation for mass spectrometric analysis

Protein spots were excised manually and then digested automatically using a Proteineer DP protein digestion station (Bruker-Daltonics, Bremen, Germany). The digestion protocol used was that of Schevchenko *et al.* (1996) with minor variations. For peptide mass fingerprinting and LIFT TOF-TOF (Suckau *et al.*, 2003) spectra acquisition, an aliquot of α-cyano-4-hydroxycinnamic acid in 33% aqueous acetonitrile and 0.1% trifluoroacetic acid was mixed with an aliquot of the above digestion solution and the mixture was deposited onto AnchorChip MALDI probes (Bruker-Daltonics).

2.6 MALDI peptide mass fingerprinting, LIFT TOF-TOF acquisition and database searching

Peptide mass fingerprint spectra were measured on a Bruker Ultraflex TOF-TOF MALDI mass spectrometer (Bruker-Daltonics) (Suckau *et al.*, 2003) in positive ion reflector mode. Mass measurements were performed either automatically through fuzzy logic-based software or manually. Each spectrum was internally calibrated with mass signals of trypsin autolysis ions, and the typical mass measurement accuracy was ±25 ppm. The measured tryptic peptide masses were transferred (through the MS BioTools program from Bruker-Daltonics) as inputs to search the NCBInr database,

using Mascot software (Matrix Science, London, UK). When available, MS-MS data from LIFT TOF-TOF spectra were combined with MS peptide mass fingerprint data for database searching.

3. RESULTS

3.1 IEF-PAGE electrophoresis.

Thylakoid proteins from sugar beet plants grown in Fe-sufficient and Fe-deficient conditions were separated by 2-D IEF-PAGE and gels were analysed to study the changes induced by Fe deficiency in the polypeptidic pattern. Real scans of typical 2-D gels obtained with thylakoids from Fe-sufficient and Fe-deficient plants are shown in Figs. 7-1A and 7-1B, respectively. Gels obtained with different thylakoid preparations isolated from different batches of plants were very similar. The number of polypeptides detected in gels of thylakoids from Fe-sufficient and Fe-deficient plants was 110 and 138, respectively (Figs. 7-1A and 7-1B).

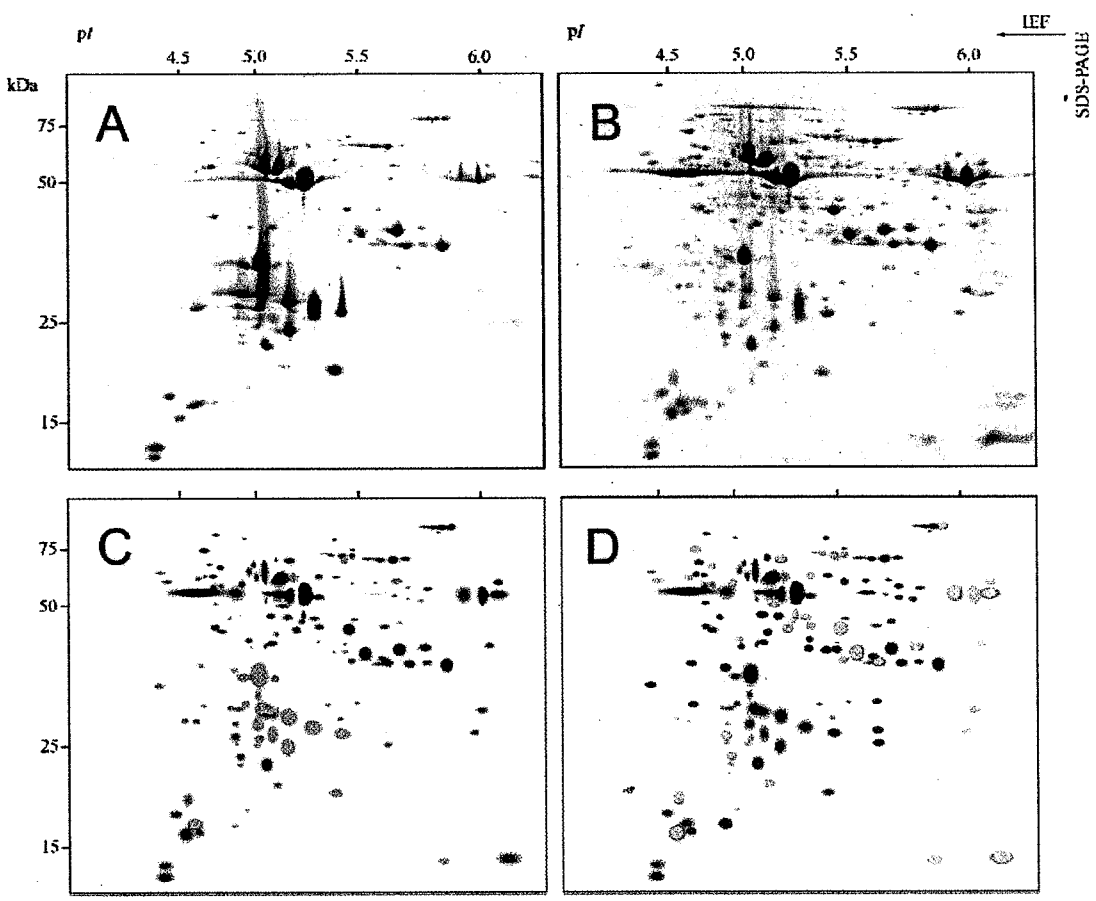

Figure 7-1. 2-D IEF-SDS PAGE thylakoid proteome maps of thylakoid preparations from Fe-sufficient and Fe-deficient *Beta vulgaris* plants. Proteins were separated in the first dimension

in linear (pH 4-7) IPG gel strips and in the second dimension in 12% acrylamide vertical gels. Scans of real typical gels of thylakoids from Fe-sufficient and Fe-deficient plants are shown in A and B, respectively. To facilitate visualization of the spots studied, a virtual composite image (C and D) was created containing all spots present in the real gels A and B. Then, spots whose intensities decrease or disappear completely with Fe deficiency were labelled with blue and green marks, respectively (C), and those increasing with Fe deficiency or only present in Fe-deficient thylakoids were labelled with orange and red marks, respectively (D).

Averaged 2-D polypeptide maps of thylakoids from Fe sufficient and Fe-deficient plants were made from three independent thylakoid preparations, each from a different batch of plants. To better describe the changes in polypeptide composition we have built a composite, averaged virtual map containing all spots present in both Fe-deficient and control thylakoids (Figs. 7-1C and 7-1D). The comparison of averaged maps indicated that Fe deficiency caused decreases and increases in signal intensity in 18 (blue spots in Fig. 7-1C) and 37 spots (orange spots in Fig. 7-1D), respectively. Furthermore, 5 and 33 spots were only detected in Fe-sufficient (green spots in Fig. 7-1C) and Fe-deficient plants (red spots in Fig. 7-1D), respectively, whereas 18 spots did not change in signal intensity. All polypeptides in the composite, averaged map are depicted again in Fig. 7-2A, to permit annotation of those polypeptides where homologies were found by using MALDI-TOF (marked by squares in Fig. 7-2A). These polypeptides were numbered from 1 to 50 as described in Fig. 7-2B, and the hits are described in detail in Table 7-1.

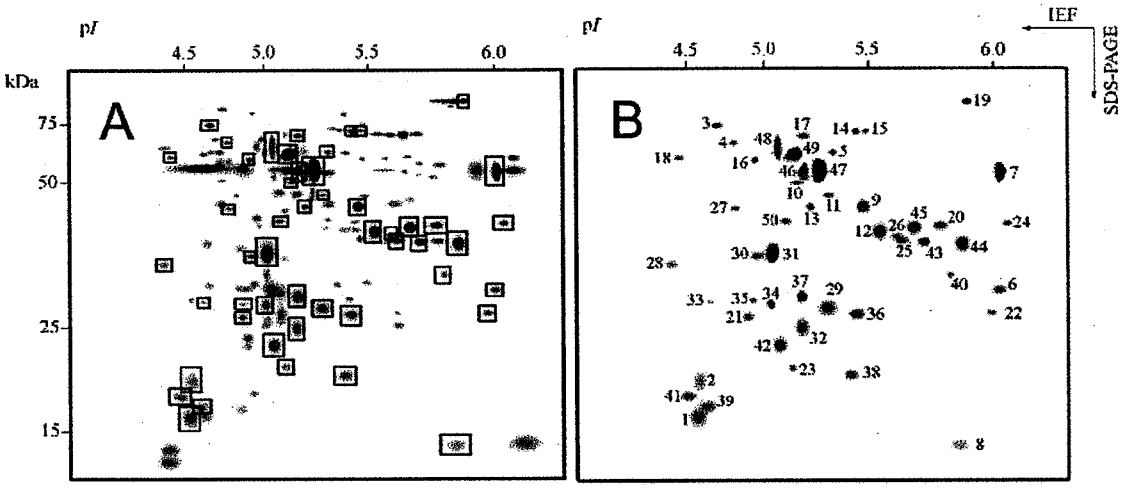

Figure 7-2. Virtual composite image, showing all polypeptides present in thylakoids from Fe-deficient and Fe-sufficient plants. In A, polypeptides which had significant homologies with proteins in the databases (using MALDI-MS and MASCOT) are annotated by squares. The same polypeptides are numbered in B, and homologies are described in detail in Table 1.

From the 37 spots that increased in signal in thylakoids of Fe-deficient as compared to Fe-sufficient controls, 27 were excised and analysed by

MALDI-MS. Since the sugar beet genome has not been sequenced yet and very few sequences are available in the databases, identification was performed by homology searches with proteins from other plant species. From the 27 spots analyzed, 25 proteins were identified (proteins labelled 1 to 25 in Fig. 7-2B and Table 7-1). These include proteins related to regulation of protein biosynthesis pathways such as GTP binding protein (spot 1), ribosomal protein L12 and Hsp70 from spinach (spots 2 and 3) and α and ß subunits of the 60 kDa chaperonin (spots 4 and 5). Ten spots gave significant matches to Calvin cycle proteins, i.e. carbonic anhydrase (spot 6), large and small subunits of Rubisco (spots 7 and 8, respectively), Rubisco activase from two different species (spots 9 and 10), phosphoglycerate kinase (spot 11), plastidic aldolase (spot 12), phosphoribulokinase from *Beta vulgaris* (spot 13), and two transketolases from *Spinacea oleracea* (spots 14 and 15). Other proteins that were found to increase in thylakoid preparations from Fe-deficient sugar beet plants as compared to the Fe-sufficient controls were different ATPase subunits (spots 16 and 17), a calreticulin (spot 18), a P-protein precursor (spot 19), malate dehydrogenase (spot 20), a peroxiredoxin (spot 21), superoxide dismutase (spot 22), a ß-type cyclin protein (spot 23), mRNA binding protein CSP41 fragment (spot 24), and an unnamed protein product from *Spinacia oleracea* with the conserved domain for ferredoxin-NADP oxidoreductases (spot 25).

From the 33 new spots detected *de novo* in proteome maps from thylakoids of Fe-deficient plants (Fig. 7-1D), the 6 more abundant were analysed by MALDI-MS, resulting in 3 positive matches (spots 26-28 in Fig. 7-2B and Table 7-1). Significant matches were found for cysteine synthase and sedoheptulose-1,7-bisphosphatase from *Spinacia oleracea* (spots 26 and 27, respectively) and RNA-binding protein from *Arabidopsis thaliana* (spot 28). Since the intensities of the remaining 27 spots detected only in Fe-deficient thylakoids and the 5 polypeptides detected only in Fe-sufficient thylakoids were very low, it was not possible to study them by MALDI-MS.

Among the 18 spots showing a decrease in signal intensity in thylakoids from Fe-deficient plants as compared to the controls (Fig. 7-1C), 11 were identified by MALDI-MS. Three of them gave significant matches to proteins from the water-oxidizing complex of PSII (spots 29-31 in Fig. 7-2B and Table 7-1). The spot 29 presented homology with the polypeptide of 23 kDa from *Arabidopsis thaliana*, and the spots 30 and 31 presented homology with the polypeptide of 33 kDa from *Nicotiana tabacum*. Six more polypeptides (spots 32-37) gave significant matches with different chlorophyll *a/b* binding proteins from diferent species and 2 more spots showed homology to the Fe-S Rieske protein from the cytochrome b_6/f (spot 38) and to the ATP synthase subunit 9 of CF_0 (spot 39).

Eighteen spots did not change in intensity when the Fe deficient proteome map was compared to the Fe sufficient map (Figs. 7-1A and 7-1B), and 11 of them (spots 40-50 in Fig. 7-2B and Table 7-1) gave significant matches in MALDI-MS. One of them (spot 40) was a protein kinase, 4 (spots 41-44) matched hypothetical proteins with unknown function, 2 of them (spots 43 and 44) containing a conserved domain of ferredoxin-NADP oxidoreductases. Five more spots (spots 45-49) gave significant matches with different subunits of ATPase synthase and one protein (spot 50) gave a significant match to the putative PSII stability/assembly factor HCF136.

Table 7-1. Proteins identified by MALDI-MS in 2-D IEF-SDS PAGE gels. [1]MS1 data: Protein score is –10*Log (P), where P is the probability that the observed match is a random event. Protein scores >65 are significant ($p<0.05$). [2]MS2 data: Ion score is –10*Log (P), where P is the probability that the observed match is a random event. Individual ion scores >40 indicate identity or extensive homology ($p<0.05$). In both cases, protein scores are derived from ion scores as a non-probabilistic basis for ranking protein hits.

spot	th MW	th pI	ex MW	ex pI	Mascot score	accesion n	homologies	specie
Increased proteins in Fe-deficiency								
1	73	6.1	16	4.5	77[1]	Q682V3	putative GTP-binding protein	*A. thaliana*
2	20	5.5	20	4.5	69[1]	R7SP12	ribosomal protein L12 chl	*S. oleracea*
3	76	5.2	73	4.6	333[1]	gi|2654208	heat shock 70 protein	*S. oleracea*
4	62	4.8	58	5.3	142[1]	gi|21554572	60 kDa chaperonin α subunit	*A. thaliana*
5	63	5.8	66	5.2	171[1]	gi|806808	60 kDa chaperonin ß subunit	*P. sativum*
6	36	5.7	29	6.0	114[1]	gi|214169	carbonic anhydrase	*F. brownii*
7	52	6.2	51	6.0	130[2]	gi|6689241	Rubisco large subunit	*S. bandeirae*
8	14	5.8	14	4.8	80[1]	8RUBS	Rubisco small subunit	*S. oleracea*
9	41	6.0	42	5.4	121[1]	O82428	Rubisco activase	*D. glomerata*
10	51	8.6	48	5.1	149[1]	gi|2707330	Rubisco activase	*L. pennellii*
11	50	8.5	47	5.3	108[1]	T03660	phosphoglycerate kinase chl	*N. tabacum*
12	43	6.9	37	5.5	74[1]	Q95XX4	plastidic aldolase	*N. tabacum*
13	31	5.1	42	5.2	71[1]	Q9SPH7	phosphoribulokinase fragment	*B. vulgaris*
14	80	6.2	70	5.4	270[1]	gi|2529342	transketolase	*S. oleracea*
15	80	6.2	66	5.6	126[1]	gi|2529342	transketolase	*S. oleracea*
16	54	5.1	55	4.9	322[1]	gi|2493132	V-ATPase subunit ß isoform 2	*H. vulgaris*
17	69	4.9	66	5.2	289[1]	gi|1418409	V-type ATPase	*B. vulgaris*
18	48	4.4	56	4.4	186[1]	gi|3288109	calreticulin	*B. vulgaris*
19	113	6.5	92	5.8	177[2]	gi|2894362	P-Protein precursor	*S. tuberosum*
20	36	8.9	38	5.7	65[2]	gi|52139816	malate dehydrogenase	*L. esculentum*
21	29	5.2	26	4.8	197[1]	gi|11558244	peroxiredoxin	*P. vulgaris*
22	25	8.8	26	6.0	146[1]	gi|3108345	superoxide dismutase	*R. sativus*
23	20	9.5	21	5.1	71[1]	Q7DN57	ß-type cyclin	*C. roseus*

spot	th MW	th p*I*	ex MW	ex pI	Mascot score	accesion n	homologies	specie
24	45	6.1	38	6.0	65[2]	gi|7484674	mRNA-bindig protein CSP41, chl	*S. oleracea*
25	41	8.7	35	5.6	145[2]	gi|21247	unnamed protein product	*S. oleracea*
New sopts in Fe-deficiency								
26	39	8.7	36	5.6	133[1]	gi|1066153	cysteine synthase	*S. oleracea*
27	42	5.9	42	4.8	157[1]	gi|2529376	sedoheptulose-1,7-bisphosphatase	*S. oleracea*
28	36	4.6	32	4.4	114[1]	gi|475720	RNA-binding protein 3	*A. thaliana*
Decreased proteins in Fe-deficiency								
29	28	6.9	27	5.3	112[2]	gi|21592906	23 kDa OEC of PSII	*A. thaliana*
30	35	5.9	33	4.9	215[1]	gi|505482	33 kDa OEC of PSII	*N. tabacum*
31	35	5.9	34	5.0	89[1]	T02066	33 kDa OEC of PSII	*N. tabacum*
32	16	5.1	25	5.1	83[2]	gi|33772151	LhcI type I CAB protein	*M. domestica*
33	22	4.8	27	4.6	127[1]	gi|48375048	LhcII type III CAB protein	*N. tabacum*
34	28	5.6	27	5.0	118[1]	gi|3126854	LhcII type I CAB protein	*O. sativa*
35	29	5.6	27	4.8	85[2]	gi|115796	LHCII type I, CP29	*O. sativa*
36	29	8.6	26	5.4	150[1]	gi|20260044	LhcI type III	*A. thaliana*
37	30	6.0	28	5.2	128[1]	gi|21593520	CP26	*A. thaliana*
38	24	7.6	20	5.4	99[2]	gi|19995	Rieske FeS	*N. tabacum*
39	24	6.0	17	4.6	91[2]	gi|394755	CF_0 II ATP synthase subunit 9	*S. oleracea*
Spots that did not change in intensity								
40	76	8.6	31	5.7	78[1]	Q84RT2	protein kinase	*O. sativa*
41	76	6.2	18	4.4	69[1]	Q7XE68	Hipotetical protein	*O. sativa*
42	100	4.9	23	5.0	67[1]	Q9LIW7	Hipotetical protein	*O. sativa*
43	41	8.7	35	5.7	118[2]	gi|21247	unnamed protein product	*S. oleracea*
44	41	8.7	34	5.8	104[2]	gi|21247	unnamed protein product	*S. oleracea*
45	52	5.2	51	5.2	147[2]	gi|4995854	H(+)-transporting ATP synthase	*T. hirsuta*
46	60	6.0	52	5.0	176[1]	gi|19685	ATP synthase β subunit	*N. plumbaginifolia*
47	55	5.4	60	5.0	161[1]	gi|6723751	ATP synthase α subunit	*O. elata*
48	41	5.6	38	5.6	177[1]	gi|20654	ATP synthase γ subunit	*P. sativum*
49	56	5.1	58	5.1	168[1]	gi|67825	ATPase a chain	*S. oleracea*
50	45	9.0	40	5.1	216[1]	gi|54291349	PSII stab/assemb factor HCF136	*O. sativa*

3.2 Blue Native-SDS PAGE electrophoresis

Thylakoid proteins isolated from Fe deficient and sufficient sugar beet plants were first submitted to BN PAGE, a technique capable to separate intact protein complexes in the first dimension. Five green bands and one blue band were always detected in gels obtained with thylakoids from Fe-deficient and Fe-sufficient plants (Figs. 7-3A and 7-3B, respectively). The 5

green bands, with apparent molecular masses of approximately 890, 695, 475, 255 and 145 kDa (named I, II, III, V and VI in Figs. 7-3A and 7-3B), contained pigment-protein complexes and decreased in intensity with Fe deficiency. Conversely, the blue band, with an apparent mass of 325 kDa (named IV in Figs. 7-3A and 7-3B), showed an increase in relative intensity with Fe deficiency (gels were always loaded on an equal protein basis).

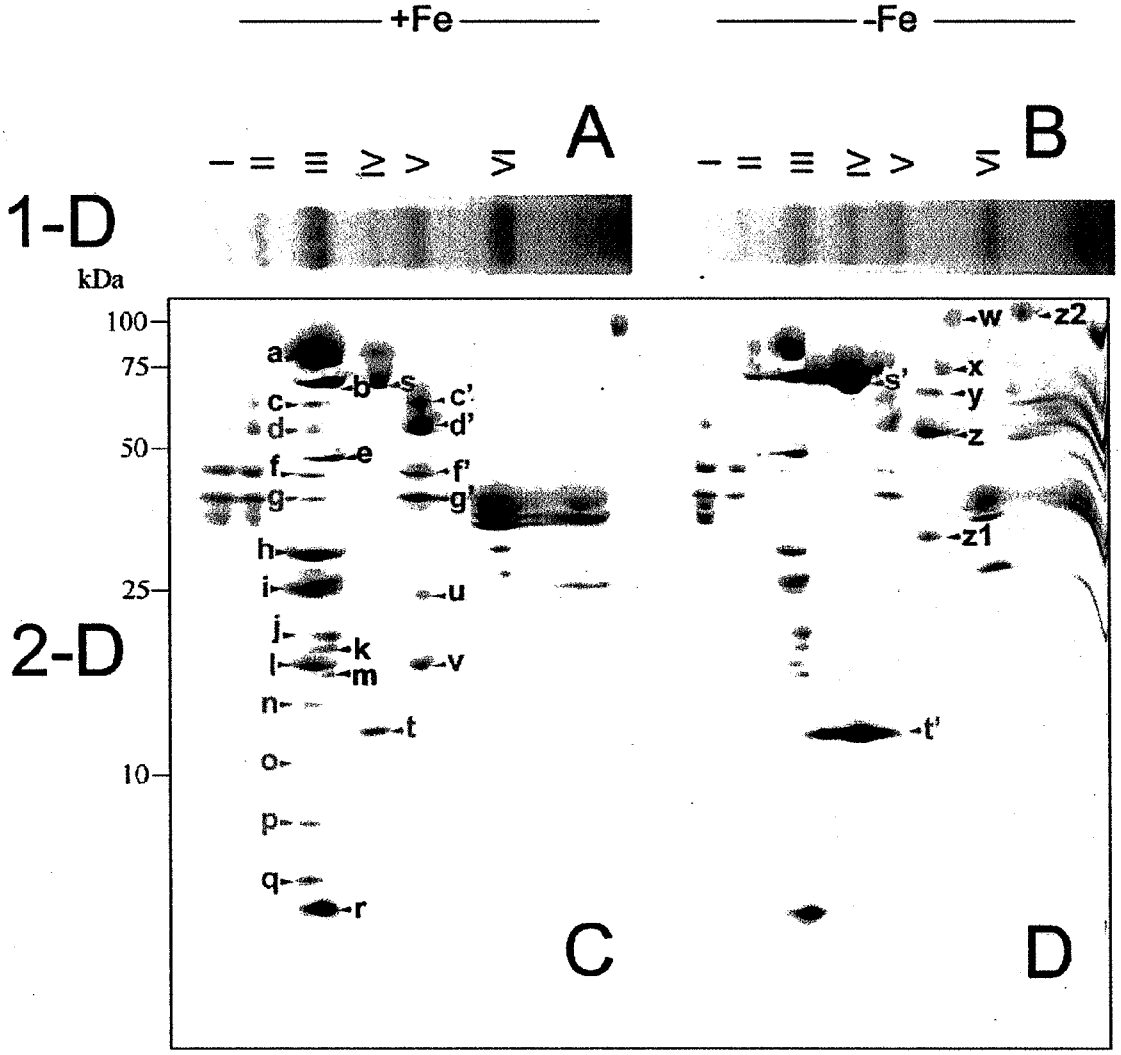

Figure 7-3. 1-D Blue Native electrophoresis (BN PAGE) (A-B), and 2-D BN-SDS PAGE (C-D) of Fe-sufficient and Fe-deficient thylakoid preparations from *Beta vulgaris* plants. Typical scans of real gels obtained with thylakoids from Fe-sufficient (A and C) and Fe-deficient (B and D) plants are shown. Some polypeptides decreasing or disappearing with Fe-deficiency are marked with blue and green letters (in C) respectively, whereas some polypeptides that increase and appear with Fe deficiency are marked with orange (in C and D) and red letters (in D), respectively. Significant homologies obtained for some of these spots with MALDI-TOF are described in detail in Table 7-2.

For the second dimension, BN PAGE gels were excised, layered onto PAGE gel slabs, SDS PAGE was run and gels were silver-stained. Two-D,

BN-SDS PAGE proteome maps corresponding to thylakoids isolated from Fe-sufficient and Fe-deficient plants are shown in Figs. 7-3C and 7-3D, respectively. Some of the spots were excised and analysed by MALDI-MS (these analyzed spots are marked by letters in Figs. 7-3C and 7-3D and Table 7-2).

Table 7-2. Proteins identified by MALDI-MS in 2-D BN-SDS PAGE gels. [1]MS1 and [2]MS2 data as indicated in Table 7-1.

spot label	theor. MW (kDa)	exp. MW (kDa)	MASCOT score	accesion n	homology	species
a	80	76	110[1]	gi|22091504	PsaA	*C. laciniata*
b	43	67	187[1]	gi|6686965	ATP synthase ß subunit	*B. lanuginosa*
c	56	61	112[1]	gi|72703	PsbB CP47	*S. oleracea*
c'	56	61	110[1]	gi|11497552	PsbB CP47	*S. oleracea*
d	45	53	92[1]	gi|27435881	PsbC CP43	*H. canadensis*
d'	50	55	115[1]	gi|13625479	PsbC CP43	*N. tabacum*
e	42	47	59[2]	gi|20654	ATP synthase γ subunit	*P. sativum*
f	25	44	138[1]	gi|33317759	PsbD D2	*D. purpusii*
f'	14	44	140[1]	gi|22858680	PsbD D2	*U. adpressa*
g	39	39	124[1]	gi|16904360	PsbA D1	*A. powellii*
g'	39	39	118[1]	gi|16904360	PsbA D1	*A. powellii*
h	29	30	148[1]	gi|20260044	Lhca type III	*A. thaliana*
l	13	18	149[1]	gi|6006283	PsaL	*A. thaliana*
o	15	12	54[2]	gi|21287	PsaH	*S. oleracea*
q	14	7	65[2]	gi|539055	PsaK	*H. vulgare*
r	8	6	49[2]	gi|3603009	ATPase CF0 subunit III	*G. theta*
s	50	68	185[1]	gi|34576609	Rubisco large subunit	*B. vulgaris*
s'	50	68	191[1]	gi|34576610	Rubisco large subunit	*B. vulgaris*
t	20	13	50[2]	gi|20341	Rubisco small subunit	*O. sativa*
t'	20	13	152[1]	gi|347451	Rubisco small subunit	*O. sativa*
u	25	25	100[2]	gi|19995	Rieske FeS	*N. tabacum*
v	12	18	64[2]	gi|11598	PetD	*H. vulgare*
x	58	72	121[1]	gi|15809972	glycine hydroxymethyl transferase	*A. thaliana*
y	48	63	194[1]	gi|12963877	glutamine synthetase GS2	*B. vulgaris*
z	39	53	160[1]	gi|1781348	plastidic aldolase	*S. tuberosum*
z1	36	33	178[1]	gi|8954289	carbonic anhydrase	*V. radiata*
z2	81	92	115[1]	gi|2529342	transketolase	*S. oleracea*

The first two green bands in the 1-D gels, with apparent masses of approximately 890 and 695 kDa (I and II in Figs. 7-3A and 7-3B), would correspond to different supercomplexes of photosystems I and II (Ciambella *et al.*, 2005). These two bands were resolved in 5 spots each in both treatments, which generally showed a decrease in intensity with Fe deficiency (Figs. 7-3C and 7-3D). Some of the polypeptides present in bands I and II had similar apparent masses than other identified as PSI and PSII components in smaller complexes (see below).

Band III, with a molecular weight of approximately 475 kDa (Figs. 7-3A and 7-3B), was resolved in the second dimension in 18 and 13 spots in Fe-sufficient and Fe-deficient thylakoid membranes (Fig. 7-3B). These polypeptides have been marked in Figs. 7-3C and 7-3D with letters in alphabetical order (from higher to lower apparent molecular mass). From these, 5 polypeptides (spots d, g, n, o and p, labelled in green in Fig. 7-3C) were not detected in Fe-deficient thylakoids, whereas 8 more polypeptides (spots a, c, f, h, I, j, l and q, labelled in blue in Fig. 7-3C) decreased in intensity in with Fe deficiency. Five of the polypeptides that decrease or disappear with Fe deficiency were identified as the components of the PSI-LHCI complex, i.e. PsaA, PsaL, PsaH, PsaK and Lhca type III (spots a, l, o, q and h, respectively; Fig. 7-3C and Table 7-2). Also, four more spots in this class were identified as PSII components, CP47, CP43, D2 and D1 (spots c, d, f and g, respectively; Fig. 7-3C and Table 7-2). The remaining 4 spots (spots i, j, n and p) could not be identified. Five polypeptides in band III that did not change in signal intensity (spots b, e, k, m and r in Fig. 7-3C) were also analysed, finding homologies in three of them with proteins from the ATPase complex such subunits γ, ß of CF_1 and subunit III of CF_0, (spots b, e and r, respectively; Fig. 7-3C and Table 7-2). The results are in good agreement with Ciambella *et al.* (2005), that found band III was composed of a PSI-LHCI complex, a dimeric form of the PSII core complex and an ATPase complex. Iron deficiency caused a relative decrease of the PSI and PSII components, whereas the ATPase components of this complex did not change in intensity.

The blue band IV had a mass of approximately 325 kDa (Figs. 7-3A and 7-3B), and was resolved in the second dimension SDS PAGE electrophoresis in two spots, with masses of 68 and 13.2 kDa, both in Fe deficient and Fe sufficient thylakoids (Figs. 7-3C and 7-3D, respectively). Using MALDI-TOF, we obtained similar matches for the spots of both Fe-sufficient and Fe-deficient thylakoids, with homologies with the large and small subunits of Rubisco from *Oryza sativum* and *Beta vulgaris* (spots s and t in Fe-sufficient thylakoids and s' and t' in Fe-deficient thylakoids; Figs. 7-3C and 7-3D and Table 7-2). Therefore, band IV contained mainly Rubisco, and its relative intensity increased with Fe deficiency.

The green band V had a mass of approximately 285 kDa (Figs. 7-3A and 7-3B) and was resolved in 6 spots in 2-D gels from both Fe deficient and Fe sufficient plants (Figs. 7-3C and 7-3D, respectively). Homology searches indicated that 4 of these polypeptides (spots named c', d', f' and g' in Figs. 7-3C and 7-3D and Table 7-2) presented homology with proteins from the PSII complex homologous to those identified in band III (this was the reason to use similar letters to name the spots) including CP47, CP43, D2 and D1. Two more spots had homologies with the cytochrome b_6/f components Rieske FeS and PetD (spots u and v, respectively in Fig. 7-3C). Therefore, band V contained PSII and cytochrome b_6/f polypeptides, with all of them decreasing in intensity with Fe deficiency.

The green band VI of approximately 145 kDa (Figs. 7-3A and 7-3B) was resolved after 2-D in 4 spots, in both treatments, with their relative intensities decreasing with Fe deficiency (Fig. 7-3C-D). This band has been described as composed by LHC components (Ciambella *et al.*, 2005).

A group of six new spots was detected in SDS PAGE gels from Fe deficient thylakoids (Fig. 7-3D). This group of proteins (labelled with red letters as w, x, y, z, z1 and z2 in Fig. 7-3D), was not detected in the 1-D BN PAGE electrophoresis gel. Five of the proteins presented significant homologies (Table 7-2) with glycine hydroxymethyltransferase, glutamine synthethase GS2, plastidic aldolase, carbonic anhydrase and a transketolase (spots x, y, z, z1 and z2, respectively, in Fig. 7-3D). All these polypeptides were not detected in Fe-sufficient thylakoids (Fig. 7-3C), and all of them are enzymes related to amino acid metabolism. As judged by their position in the 2-D gels (Fig. 7-3D), they may be associated in one or possibly two multi-enzyme complexes in Fe-deficient thylakoid membranes. For three of these proteins (plastidic aldolase, carbonic anhydrase and transketolase) relative increases with Fe deficiency were also detected with the other 2-D technique, IEF-SDS PAGE.

4. DISCUSSION

Thylakoid preparations from sugar beet plants grown in hydroponics have been used to study the changes induced by Fe deficiency in the thylakoid proteome. The most widely used technique in proteomic studies, IEF-SDS PAGE (Whitelegge, 2003), has been employed elsewhere to separate thylakoid proteins from the algae *Chlamydomonas reinhardti* (Hippler *et al.*, 2001) and several higher plant species, including *Arabidopsis thaliana* (Kieselbach *et al.*, 2000), *Pisum sativum* (Peltier *et al.*, 2000), and *Nicotiana benthamiana* (Pérez-Bueno *et al.*, 2004). The use of this technique has been reported to result in a significant exclusion of integral membrane

proteins, due to their poor solubility in the neutral or zwitterionic detergents employed in the first IEF dimension (Molloy, 2000; Santoni *et al.*, 2000). Results show that several LHC proteins with a short number of transmembrane domains are detectable in 2-D IEF-SDS PAGE separations of *Beta vulgaris* thylakoids, although many integral membrane proteins with a large number of spanning domains were not detectable (Fig. 7-1). Similar results have been reported with thylakoids from *Chlamydomonas* (Hippler *et al.*, 2001), where only a few integral membrane proteins such as LHC and PsaA were detected, whereas most of the proteins with a high number of transmembrane domains belonging to the PSII complex were not detected.

The 2-D IEF-SDS PAGE technique, however, is very powerful to separate other thylakoid polypeptides, permitting to obtain proteome maps with more than 100 spots (Fig. 7-1). Data obtained show that Fe deficiency results in relative intensity changes in a large number of these polypeptides, including decreases in the levels of many components of the protein complexes that participate in photosynthetic electron transport, whereas the level of some proteins involved in carbon fixation-related reactions is increased. Some proteins found to be relatively up-regulated by Fe deficiency were identified by MALDI-MS as photosynthetic enzymes, including the small and large subunits of Rubisco, Rubisco activase, carbonic anhydrase, phosphoglycerate kinase, plastidic aldolase, phosphoribulokinase, transketolase and sedoheptulose-1, 7-bisphosphatase.

To avoid some of the limitations imposed by 2-D IEF-SDS PAGE, a second 2-D technique, called BN-SDS PAGE, has been used to investigate mitochondrial protein complexes and supercomplexes (Schägger *et al.*, 1994) and more recently thylakoid proteins (Rexroth *et al.*, 2003; Suorsa *et al.*, 2004; Ciambella *et al.*, 2005). This technique also allows for the evaluation of polypeptide modifications, altered protein-protein interactions and complex assembly in the first dimension (BN PAGE), and differences in the subunit composition of these complexes in the second dimension (SDS PAGE). Results indicate that resolving *Beta vulgaris* thylakoids by BN-SDS PAGE allows for the detection of a large number of transmembrane proteins (Table 7-2) as recently shown in *Hordeum vulgare* (Ciambella *et al.*, 2005). This technique also supports the relative decrease in the level of many photosynthetic electron transport components, as well as the relative increase in Rubisco and other proteins involved in other biochemical processes. The identified spots that were shown to be down-regulated by Fe deficiency by both 2-D techniques corresponded to proteins belonging to the antenna and core complex of both PSI and PSII, the oxygen evolving complex, and the cytochrome b_6/f complex (Tables 7-1 and 7-2). These results are in good agreement with the decreases observed by 1-D electrophoresis in the amounts of the different proteins participating in electron transport (Spiller

and Terry, 1980; Terry, 1980; Nishio *et al.*, 1985; Terry and Abadía, 1986) and with the limited photosynthetic rate and efficiency reported to occur in Fe-deficient plants.

Proteome maps obtained by 2-D BN-SDS PAGE revealed the induction of a new protein set in Fe-deficient conditions, which is not detected in Fe-sufficient thylakoids and includes five polypeptides with homologies to carbonic anhydrase, plastidic aldolase, glutamine synthetase and glycine hydroxymethyltransferase. These enzymes are involved in amino acid metabolism, and specially in the amino keto-alcohol metabolic equilibrium. Evidence that Calvin cycle enzymes can assemble into stable multienzyme complexes bound to stromal-faced thylakoid membranes has been obtained elsewhere in *Spinacia oleracea* (Süss *et al.*, 1993), *Pisum sativum* (Anderson *et al.*, 1996), *Nicotiana tabacum* (Jebanathirajah and Coleman, 1998) and *Chlamydomonas reinhardtii* (Süss *et al.*, 1995), and the association of these enzymes with thylakoid membranes has been proposed to provide direct access to required cofactors such as ATP and NADPH, and to prevent interferences by other metabolic pathways (Süss *et al.*, 1993; Anderson *et al.*, 1996). Proteomic data shown here suggest that the five enzymes mentioned may be associated *in vivo* to thylakoid membranes, perhaps constituting an enzymatic network associated to the chlorotic thylakoid membranes and involved in amino acid and keto acid metabolism. This may be related to the known fact that the plastoquinone pool in the thylakoid membranes of Fe-deficient plants is in the reduced state under dark conditions (Belkhodja *et al.*, 1988). It is hypothesized that the presence of the new set of possibly associated proteins may be related to the oxidative equilibrium of Fe-deficient thylakoids.

In summary, Fe deficiency induced significant changes in the thylakoid sugar beet proteome: the relative amount of electron transfer complexes was reduced, whereas proteins participating in carbon-linked reactions showed an increased level. A new protein set, which includes several proteins usually located in the chloroplast stroma, has been detected in thylakoid preparations from Fe-deficient *Beta vulgaris* leaves by using the BN-SDS PAGE 2-D technique, and increases in some of these proteins were also detected with the IEF-SDS PAGE 2-D technique. To our knowledge, this is the first time that both 2-D methods have been compared in a single study to assess the effect of an environmental stress on the composition of the thylakoid membrane proteome. Our data confirm that BN-SDS PAGE is more adequate than IEF-SDS PAGE to resolve highly hydrophobic integral membrane proteins from thylakoid preparations, although the very high resolving power of the latter makes it a complementary technique that provides useful information on the effects of Fe deficiency on many other membrane proteins.

Capítulo 8

PROTEOMIC ANALYSIS OF *Lupinus texensis* PHLOEM: STUDY OF IRON AND ZINC TRANSPORTER PROTEINS

Abstract: Sieve tube exudates from *Lupinus texensis* plants have been used to study the composition of the phloem sap proteome, with the particular aim to identify putative Fe and Zn transporters in this plant compartment. The mechanisms of long-distance transport of metals through the phloem system have not been characterized yet. Sieve element exudates were collected from *Lupinus texensis* plants after the emergence of inflorescence, using an incision method. We used metal affinity chromatography, followed by 1-D gel electrophoresis of the fractions obtained and 2-D gel electrophoresis, in order to identify soluble proteins from sieve element sap involved in Fe and Zn transport. Specific staining methods for gel blots were used to find putative Fe and Zn transporter proteins. Further analysis by MALDI and ESI MS was carried out to characterize proteins from sieve element exudates. Two *Lupinus texensis* phloem sap proteins that could be involved in Fe transport and three more that could be involved in Zn transport were found.

Key words: iron transporter, *Lupinus texensis*, phloem, zinc transporter

1. INTRODUCTION

The phloem tissue is composed of an intimately associated complex of two cell types, companion cells and sieve elements, which form a cellular conduit throughout the plant body called sieve tube (see for review Oparka and Santa Cruz, 2000; van Bel, 2003). Sieve elements are communicated through perforated end walls known as sieve plates. During development, these sieve elements suffer selective cytoplasmic degradation, losing many of their organelles, included the nucleus. The only organelles that remain in the sieve elements are located in a thin layer composed of smooth

endoplasmic reticulum, mitochondria and starch-storing plastids, which is located against the cell wall of the sieve elements. This appears to provide the only means of membrane continuity between sieve elements and companion cells. Sieve elements and companion cells form a structural and molecular complex, in which the companion cell synthesizes the needed macromolecules for maintaining the functionality of both cell types. Connection between these cells through plasmodesmata allows for the loading and unloading of the sieve tube.

The function of the phloem is long-distance transport of a diverse range of compounds between source and sink tissues in the plant. Photo-assimilates are exported from photosynthetically active leaves to sink organs to maintain the growth of the plant (Fiehn, 2003). Low molecular weight signaling molecules such as hormones, systemic wound signals and even herbicides and pathogens use this pathway in their distribution throughout the plant (Thompson and Schulz, 1999; van Bel, 2003). Research on phloem exudates has also demonstrated the presence of numerous proteins, which could be synthesized in companion cells and are subsequently translocated into the sieve elements (Oparka and Santa Cruz, 2000). Endogenous mRNAs are also transported in phloem exudates (Ruiz-Medrano *et al.*, 2001; Lucas *et al.*, 2001) and could play a role in long-distance regulation of gene-specific expression patterns in widely separated tissues, acting, for instance, as co-suppressors for gene silencing in plants (Palauqui *et al.*, 1996). The movement of all these components through the sieve tube occurs by mass flow and is driven by pressure gradients between source and sink regions of the plant (Münch, 1930).

The mechanisms of metal transport in the plant phloem, including the nature of the compounds that could be associated with these metals, are poorly known. Nevertheless, the binding of metals to transport molecules is mandatory, due to the fact that they are are highly reactive and can damage plant membranes and components. Iron is especially problematic, since this element could easily induce the generation of highly reactive oxygen species through the Fenton reaction (Guerinot and Yi, 1994). Moreover, the pH of the sieve element sap, approximately 7.5, could cause the precipitation of Fe with anionic compounds also found in the phloem. Recently, Krüger *et al.* (2002) have shown that Fe(III) is transported into the phloem sap of castor bean seedling bounded to a protein called ITP (Iron Transport Protein). Also, it has been suggested that Fe could be loaded and unloaded from sieve elements complexed by the non-proteogenic aminoacid nicotianamine (NA) in the form of an Fe(II)-NA complex (Hell and Stephan, 2003). NA would function as a shuttle, chelating Fe(II) from the complex Fe(III)-ITP during these processes. Identification of a metal-nicotianamine trasporter, *OsYSL2*, in phloem companion cells of *Oryza sativa* (Koike *et al.*, 2004) would

support this hypothesis. Iron(II) and Mn(II) bounded to NA have been demonstrated to be transported by OsYSL2. However, the redox system needed to oxidize the Fe(II) and generate the Fe(III) for binding to ITP, must still be elucidated.

Different techniques have been employed so far to resolve the proteome of sieve tube exudates. One-D gel electrophoresis was used in studies with exudates of *Triticum aestivum* (Fisher *et al.*, 1992; Schobert *et al.*, 1998), *Cucurbita maxima* (Schobert *et al.*, 1998; Dannenhoffer *et al.*, 2001; Walz *et al.*, 2002), *Cucumis sativus* (Walz *et al.*, 2002), *Oryza sativa, Yucca filamentosa, Ricinus comunis, Robinia pseudoaccia* and *Tilia platyphyllos* (Schobert *et al.*, 1998). Microtrap/microbore HPLC separation was also used in *Perilla ocymoides* and *Lupinus albus* phloem sap studies (Hoffman-Bennig *et al.*, 2002). In addition, the most widely used technique in proteomic studies, IEF-SDS PAGE, has been used to study exudates of *T. aestivum* (Fisher *et al.*, 1992), *O. sativa* (Hayashi *et al.*, 1993; Ishiwatari *et al.*, 1995), *C. maxima* (Haebel and Kehr, 2001) and *R. communis* (Krüger *et al.*, 2002; Barnes *et al.*, 2004). The proteins identified so far could be grouped in different classes, including sugar metabolism, signal transduction, redox regulation, protein metabolism, macromolecular trafficking, defence and cell structure (Hayashi *et al.*, 2000).

In the present work, *Lupinus texensis* was chosen as model plant for phloem extraction due to simplicity to obtain sieve element exudates. Collection and analysis of phloem sap is complicated in other species due to the fact that the sieve tube could seal itself upon wounding, with no exudate being secreted. In some plant species, including as *R. communis*, *Cucumis sativus* and *Lupinus* sp., the sealing process is slow and exudates can be obtained readily (Sakuth *et al.*, 1993; Schobert *et al.*, 1995; Marentes and Grusak, 1998; Kehr *et al.*, 1999). In other plant species, methods involving aphids (Fisher *et al.*, 1992; Nakamura *et al.*, 1995) or exudation into an EDTA containing solution to prevent sealing of sieve tubes (King and Zeevaart, 1974) can be used.

In this study, sieve element exudates were collected from *Lupinus texensis* plants after the emergence of influorescence, using an incision method. To separate soluble proteins from sieve element sap we used metal affinity chromatography followed by 1-D gel electrophoresis of the fractions obtained, as well as 2-D gel electrophoresis. Specific staining methods have been used to find putative Fe- and Zn-transporter proteins. Further analysis by MALDI and ESI MS were carried out in an attempt to identify proteins from sieve element exudates.

2. MATERIALS AND METHODS

2.1 Plant Material

Seeds of *Lupinus texensis* were imbibed and germinated on wet Whatman No. 1 paper sheets, in the dark and at room temperature. At day 5, five germinated seeds were transferred to a 10 L container and grown in a controlled environment chamber with a photosynthetic photon flux density of 350 μmol m^{-2} s^{-1} PAR, and a 16 h- 22 °C / 8 h- 20 °C, day / night regime. The standard solution for hydroponics contained (in mM): 0.6 K_2SO_4, 0.5 $Ca(NO_3)_2$, 1.0 NH_4NO_3, 0.3 KH_2PO_4, 0.2 $MgSO_4$, and (in μM) 25 $CaCl_2$, 25 H_3BO_3, 2 $MnSO_4$, 2 $ZnSO_4$, 0.5 $CuSO_4$, 0.5 H_2MoO_4, 0.1 $NiSO_4$ and 45 Fe(III)-EDTA. All hydroponics solutions were buffered by the addition of 1 mM MES, pH 5.5. Plants were maintained for one month in 10 L of standard solution, and solutions were changed weekly. After this time, each plant was transferred to plastic pots containing 1:1 vermiculite: potting soil (Floradur, Oldenburg, Germany) mix, and grown there for approximately another month until the development of the inflorescence. Plants were fertilized with a modified Hoagland-type nutrient solution according to Marentes *et al.* (1997). Two batches of plants were used in the analyses.

2.2 Sieve element exudate collection

Lupinus texensis sieve element exudates were collected from plants every other day during 3 weeks after the emergence of the inflorescence.

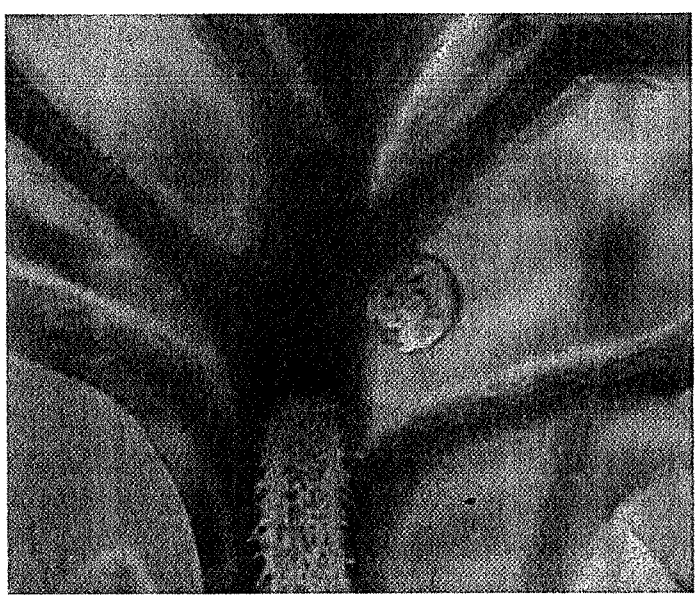

Figure 8-1. Droplet of phloem exudate from *Lupinus texensis*.

About 3 h after the beginning of the photoperiod, shallow incisions were made with a medical lancet device (BD, NJ, USA), using the 6th depth setting in the device, at the base of the attached inflorescence. Droplets of exudate (Fig. 8-1) were collected for approximately 20 min using a plastic micropipette. The first droplets were discarded to minimize contamination with other plant fluids. Samples were kept on ice during the entire collection period, and stored at –80 °C until further analysis was performed. pH and sucrose concentrations in exudates were measured prior to protein analysis.

2.3 Two-dimensional electrophoresis (IEF-PAGE)

2.3.1 Protein extraction from sieve element exudates and solubilization

Sieve element exudate was pooled from different plants. Proteins were precipitated from 1 mL of exudates by adding 10 mL 80% acetone and 0.07% ß-mercaptoethanol at -20 °C. After 2 h, the sample was centrifuged at 10000 *g* for 10 min, the supernatant was discarded and the pellet was washed with 80% acetone and 0.07% ß-mercaptoethanol. These two steps were repeated and the final pellet was dried with N_2. The sample rehydration buffer used to resuspend the proteins consisted on 2 M thiourea, 8 M urea, 20 mM Tris, 4% (w/v) CHAPS, 50 mM DTT, 0.05% ß-DDM, 2 mM PMSF and 0.5% (v/v) ampholytes of pH range 3-10 (Amersham, Uppsala, Sweden). After rehydration, samples were incubated at 28°C for 1.5 h and then centrifuged at 15000 *g* for 10 min at 20°C.

2.3.2 IEF focusing

A first dimension, isoelectric focusing (IEF) was carried out on 7 cm ReadyStrip IPG Strips (BioRad), with linear pH gradients 3-10 and 5-8. Strips were rehydrated for 16 h in 125 µL of the sample in rehydration buffer containing a trace of bromophenol blue. After this time, strips were loaded in a PROTEAN IEF Cell (BioRad, Hercules, CA, USA) and focused at 20°C, for a total of 14000 Vh. After IEF, strips were equilibrated for 10 min in equilibration solution I (6 M urea, 0.375 M Tris, pH 8.8, 2% (w/v) SDS, 20% (v/v) glycerol, 2% (w/v) DTT) and for another 10 min in equilibration solution II (6 M urea, 0.375 M Tris pH 8.8, 2% (w/v) SDS, 20% (v/v) glycerol, 2.5% (w/v) iodoacetamide).

2.3.3 SDS-PAGE electrophoresis

For the second dimension, polyacrylamide gel electrophoresis (SDS PAGE), IPG strips were placed onto 12% SDS-polyacrylamide gels (dimensions 8 x 10 x 0.1 cm) and sealed with melted 0.5 % agarose. SDS-PAGE was carried out at 20 mA per gel for 1.5 h hour and gels were subsequently silver-stained and analyzed with the PDQuest 7.1 program (BioRad). 2-D gels were made from independent sieve element exudates from two different batches of plants. A 2-D SDS PAGE standard (Bio-Rad) was used for the estimation of molecular weight and p*I*.

2.4 Protein blotting and staining

For electroblotting to PVDF membranes (Immobilon PSQ; Millipore) proteins were transferred from the 2-D PAGE gel using a semi-dry transfer unit (Hoefer Scientific instruments, San Francisco, USA) with transfer buffer 0.025 M Tris pH 8.3, 0.192 M glycine, 25% (v/v) methanol. The Ferene S method (Krüger *et al.*, 2002), based on the formation of a specific Fe colored complex, was used to detect Fe-containing proteins. The blotted membrane was incubated overnight at room temperature in a freshly prepared solution containing 0.75 mM Ferene (3-[2-pyridyl]-5,6-bis(2-[5-furylsulfonic acid])-1,2,4-triazine disodium salt; Sigma), 15mM thioglycolic acid and 2% (v/v) acetic acid. A second method based on the catalytic ability of Fe in redox processes was also used with some modifications to detect possible Fe-containing proteins, as described by Krüger *et al.* (2002). The blotting membrane was incubated at 35 °C for 2 h with 50 mM sodium acetate/acetic buffer pH 5.5 containing 80 mM diaminobenzoic acid dihydrochloride (Serva). After this period, 100 mM hydrogen peroxide was added and the membrane was incubated at 35°C overnight. The membrane was washed twice with water and then destained with 7% (v/v) acetic acid. Myoglobin was used as a positive staining control in both methods.

2.5 *In gel* digestion of proteins and sample preparation for mass spectrometric analysis

Protein spots were excised manually from 2-D gels and then digested automatically using a Proteineer DP protein digestion station (Bruker Daltonics, Bremen, Germany). The digestion protocol used was that of Schevchenko *et al.* (1996) with minor variations. For peptide mass fingerprinting and LIFT TOF-TOF spectra acquisition (Suckau *et al.*, 2003), an aliquot of α-cyano-4-hydroxycinnamic acid in 33% aqueous acetonitrile and 0.1% trifluoroacetic acid was mixed with an aliquot of the above

digestion solution and the mixture was deposited onto AnchorChip MALDI probes (Bruker-Daltonics).

2.6 MALDI peptide mass fingerprinting, LIFT TOF/TOF acquisition and database searching

Peptide mass fingerprint spectra were measured on a Bruker Ultraflex MALDI TOF-TOF mass spectrometer (Bruker Daltonics) (Suckau *et al.*, 2003) in positive ion reflector mode. Mass measurements were performed either automatically through fuzzy logic-based software or manually. Each spectrum was internally calibrated with mass signals of trypsin autolysis ions, and the typical mass measurement accuracy was ±25 ppm. The measured tryptic peptide masses were transferred (through the MS BioTools program from Bruker Daltonics) as inputs to search the NCBInr database, using Mascot software (Matrix Science, London, UK). When available, MS-MS data from LIFT TOF-TOF spectra were combined with MS peptide mass fingerprint data for database searching.

2.7 ESI-MS/MS analysis

Protein spots were excised manually from 2-D gels and then digested automatically using a Proteineer DP protein digestion station (Bruker Daltonics, Bremen, Germany). The digestion protocol used was that of Schevchenko et al. (1996) with minor variations. All LC-MS/MS analyses were performed using LC Packings nanoLC system (Dionex, Amsterdam, The Netherlands) and the HCTPlus ion-trap MS (Bruker Daltonics, Bremen, Germany). Samples were concentrated and de-salted on a C18 trap column (PepMap C18; Dionex) using the FAMOS autosampler and switching valve modules (Dionex). Peptide separation was achieved on a reverse phase C18 column (C18 PepMap100 15 cm x 75 μm i.d) using a 30 min linear gradient of 2-40% ACN *vs* 0.1% formic acid. An electrospray voltage of 1500 V and a cone voltage of 30 V were used. Peptide ions detected were submitted to high resolution scans to determine their charge state and M_r. MS/MS spectra were acquired in the information dependent acquisition mode.

2.8 Protein metal affinity purification

For affinity purification of metal (Zn and Fe) chelating proteins, a Hi-TRAP chelating HP column (1 mL bed volume; Amersham Biosciences, Uppsala, Sweden) containing chelating sepharose was rinsed with 5 mL of water, and the matrix was loaded with either Fe(III) or Zn(II) ions by the application of 0.5 mL of 0.1 M $FeCl_3$ or $ZnCl_2$, according to the

manufacturer's instructions. Metal excess was removed by washing with 5 mL of water followed by equilibration of the column with elution buffer containing 2.5 mM phosphate buffer, 62.5 mM NaCl, 10 mM imidazole, pH 7.4. One mL of pooled sieve element exudate from different plants was diluted in 2.5 mL 20 mM HEPES, pH 7.2, 0.15 mM NaCl, filtered and loaded to the column by recirculation for 30 min using a peristaltic pump with a 1 mL min^{-1} rate. The column was washed with 5 mL of elution buffer and proteins were eluted progressively with 1 mL of increasing concentrations of imidazole in elution buffer. Imidazole concentrations started at 50 µM, and continued at 100, 150, 200 and 250 mM. Finally, 5 mL of 400 M imidazole were used. Proteins in the different fractions were precipitated overnight in a Corex tube with an excess of 80% acetone and 0.07% ß-mercaptoethanol at -20 ºC and after centrifugation at 10000 *g* for 10 min, the supernatant was discarded and the pellet was dried with N_2. The sample rehydration buffer used to resuspend the proteins consisted on 2 M thiourea, 8 M urea, 20 mM Tris, 4% (w/v) CHAPS, 50 mM DTT, 0.05% ß-DDM, 2 mM PMSF. After rehydration, samples were incubated at 29ºC for 1.5 h and centrifuged at 15000 *g* for 10 min at 20ºC and then separated by SDS-PAGE and silver stained.

2.9 Organic acid analysis

Organic acid analyses were carried out by HPLC-MS. The HPLC system (Alliance 2795, Waters Corp., Milford, MA, USA) was fitted with an Aminex HPX-87H column (300 mm x 7.8 mm) (BioRad, Hercules, CA), that was maintained at 30ºC. Chromatographic separations were performed isocratically, using 0.5 % (v/v) formic acid as mobile phase with a flow rate of 0.6 mL min^{-1}. Detection and determination of organic acids were carried out by using exact mass measurements, performed with a coaxial multipass time of flight mass spectrometer (TOF MS). The effluent from the HPLC was driven to the MS device through an Apollo Electrospray Ionization Source (ESI; BioTOF II, Bruker Daltonics, Billerica, MA, USA). The apparatus was used in the negative ion mode and with the following operating parameters: accelerating potential 4 kV, spray tip potential 3.5 kV; flow rate 50 µL min^{-1}, with N_2 as drying and nebulizing gas in the ESI source. The mass axis was externally calibrated using a mixture of sucrose, malic and quinic acids, that cover the 100-400 mass/charge (m/z) range. The orifice voltage was –70 V. Spectra were acquired in the mass range from 80 to 1200 m/z at a scan rate of 1 spectrum/s.

2.10 Sugar analysis

Sugar analyses were performed with an HPLC system (Waters, Milford, MA) equipped with a 515 pump and a differential refractive index detector (Waters 2410). Sugars were separated in an Aminex HPX-87C (300 x 7.8 mm) column, maintained at 85°C. Chromatographic separations were performed isocratically at a solvent flow rate of 0.6 mL min^{-1}, using MilliQ water as mobile phase.

3. RESULTS

3.1 IEF-PAGE electrophoresis

Proteins from *Lupinus texensis* sieve element exudates were separated by 2-D IEF-PAGE and gels were analysed to study the proteome profile. A real scan of a typical 2-D gel obtained with sieve element exudate is shown in Fig. 8-2A. Gels obtained with exudates from different sets of plants were very similar. In each gel, approximately 250 polypeptides can be detected after silver staining.

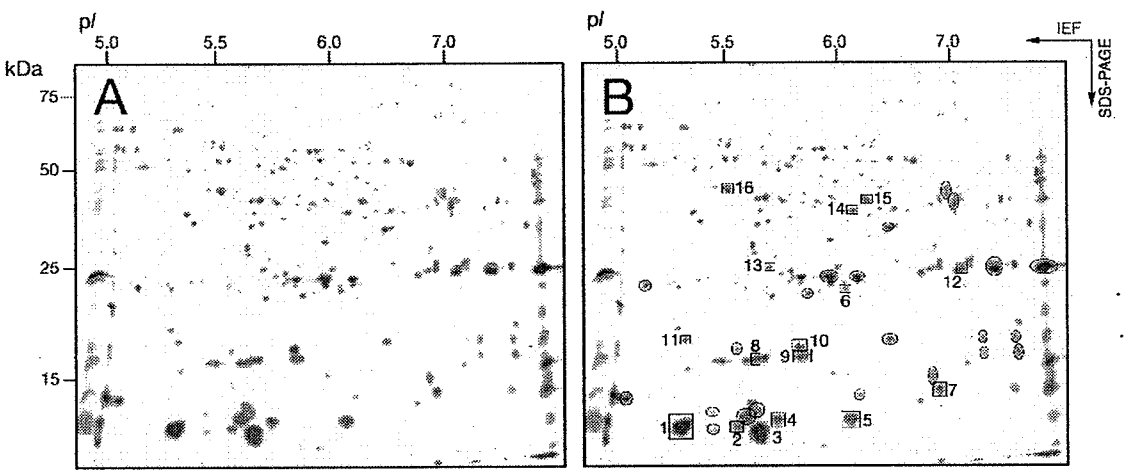

Figure 8-2. IEF-SDS PAGE phloem proteome maps of exudates from *Lupinus texensis* plants. Proteins were separated in the first dimension in linear (pH 5-8) IPG gel strips and in the second dimension in 12% acrylamide vertical gels. Scans of real typical gels of phloem exudates are shown in A and B. Spots enclosed in squares and circles in B were excised and analysed by MALDI MS. Polypeptides which had significant homologies with proteins included in the databases (using MALDI-MS and MASCOT) are marked by squares and numbered in B. Homologies are described in detail in Table 8-1.

Table 8-1. Proteins identified by MALDI-MS in 2-D IEF-SDS PAGE gels. [1]MS1 data: Protein score is –10*Log (P), where P is the probability that the observed match is a random event. Protein scores >76 are significant ($p<0.05$). [2]MS2 data: Ion score is –10*Log (P),

where P is the probability that the observed match is a random event. Individual ion scores >40 indicate identity or extensive homology ($p<0.05$). In both cases, protein scores are derived from ion scores as a non-probabilistic basis for ranking protein hits.

spot	th MW (kDa)	th *pI*	ex MW (kDa)	ex *pI*	MASCOT score	accesion n	homology	species
1	13	5.6	13	5.4	88[2]	gi|1255954	thioredoxin	*R. communis*
2	13	5.6	13	5.7	53[2]	gi|1255954	thioredoxin	*R. communis*
3	13	4.8	11	5.8	72[2]	gi|14485509	thioredoxin h	*P. sativum*
4	11	6.1	12	5.8	74[2]	gi|288188	cysteine proteinase inhibitor	*V. unguiculata*
5	11	9.1	12	6.2	78[2]	gi|288188	cysteine proteinase inhibitor	*V. unguiculata*
6	11	4.9	23	6.2	67[2]	gi|8099682	cysteine proteinase inhibitor	*M. esculenta*
7	13	9.3	14	7.1	139[2]	gi|30699363	ubiquitin-conjugating enzyme	*A. thaliana*
8	17	5.7	17	5.7	174[1]	gi|2225885	eukaryotic initiation factor 5A5	*S. tuberosum*
9	17	5.7	17	5.7	145[1]	gi|2225885	eukaryotic initiation factor 5A5	*S. tuberosum*
10	17	5.3	18	5.9	134[1]	gi|53748427	eukaryotic initiation factor 5A-1	*P. major*
11	19	5.7	19	5.5	100[2]	gi|296358	probable glutathione peroxidase	*C. sinensis*
12	20	6.3	25	7.2	125[1]	gi|4336905	Ran-related GTP binding protein	*Z. mays*
13	28	5.9	27	5.8	67[2]	gi|1523789	L-ascorbate peroxidase	*A. thaliana*
14	36	6.0	37	6.3	152[1]	gi|27462764	malate dehydrogenase	*L. albus*
15	39	6.2	39	6.4	193[1]	gi|3021338	fructose-1,6-bisphosphate aldolase	*C. arietinum*
16	42	5.3	36	5.5	191[1]	gi|9965319	actin	*S. italica*

Thirty-seven from these spots, chosen among those with higher signal intensities, were excised and analysed by MALDI MS (spots enclosed in squares and circles in Fig. 8-2B). Since the *Lupinus texensis* genome has not been sequenced yet and very few sequences for this species are available in the databases, identification was performed by carrying out homology searches with proteins in the databases from other plant species. From the 37 spots analysed, 16 proteins were identified (spots enclosed in squares and labelled 1-16 in Fig. 8-2B and Table 8-1). Three of those spots corresponded to two thioredoxins from *Ricinus communis* and thioredoxin h from *Pisum sativum* (spots 1-3) and two more spots gave significant matches to a cysteine proteinase inhibitor from *Vigna unguiculata* and *Manihot esculenta* (spots 4-6). Spot 7 showed homology with a putative ubiquitin-conjugating enzyme from *Arabidopsis thaliana* and three more spots gave significant matches with the eukaryotic initiation factors 5A5 (spots 8 and 9) and 5A1 (spot 10). Other spots with significant matches were a probable glutathione peroxidase (CIT-SAP) from *Citrus sinensis* (spot 11), a Ran-related GTP

binding protein from *Zea mays* (spot 12), L-ascorbate peroxidase from *A. thaliana* (spot 13), malate dehydrogenase from *Lupinus albus* (spot 14), fructose-1,6-bisphosphate aldolase from *Cicer arietinum* (spot 15) and actin from *Setaria italica* (spot 16).

3.2 Staining of iron containing proteins

Two-D gels such as those shown in Fig. 8-1 were blotted to PVDF membranes, and possible Fe-binding proteins in sieve element exudates were localized in the blots by using two different staining methods, Ferene S and a second method based on the catalytic properties of Fe in redox processes.

The Ferene S staining method revealed the presence in sieve element exudates of a single protein able to bind Fe. Comparisons of the 2-D gel (Fig. 8-3A) and the stained membrane (Fig. 8-3B) indicated that the protein stained with Ferene in the blot corresponded to a spot in the 2-D gel with an unidentified protein with an apparent MW of 13 kDa and a p*I* of 5.7 (spot marked by an elipse in Fig. 8-3A). The second staining method is less specific, because it is based in the oxidation of diaminobenzoic acid in the presence of hydrogen peroxide, that results in a destaining of the membrane in those places where redox-active metal-binding proteins are present. This staining protocol revealed the presence in blots from sieve element exudates of 9 redox-active metal-binding proteins (Fig. 8-3C). Comparisons of the blotted membrane and the 2-D gel indicated that destained spots in the membrane (Fig. 8-3C) corresponded to proteins in the 2D gel (spots labelled with squares a-i in Fig. 8-3A) with experimental MW values and p*I*s listed in Table 8-2. Some of them had been identified by MALDI MS, such as the three thioredoxin spots and the two cysteine proteinase inhibitors. Spot c, with an apparent MW of 12.9 and a p*I* of 5.7, corresponded to the only protein detected by the Ferene method.

Table 8-2. Homologies and experimental MW and p*I*s of the spots revealed in the blotted membrane method based on the redox properties of metals.

spot	homology	MW (kDa)	p*I*	Detection in Ferene
a	thioredoxin	12.0	5.4	No
b	thioredoxin	12.2	5.6	No
c	Not found	12.9	5.7	Yes
d	thioredoxin	11.2	5.8	No
e	Cysteine proteinase inhibitor	12.5	6.7	No
f	Cysteine proteinase inhibitor	16.6	7.4	No
g	Not found	18.0	7.4	No
h	Not found	24.4	6.7	No
i	Not found	38.6	7.2	No

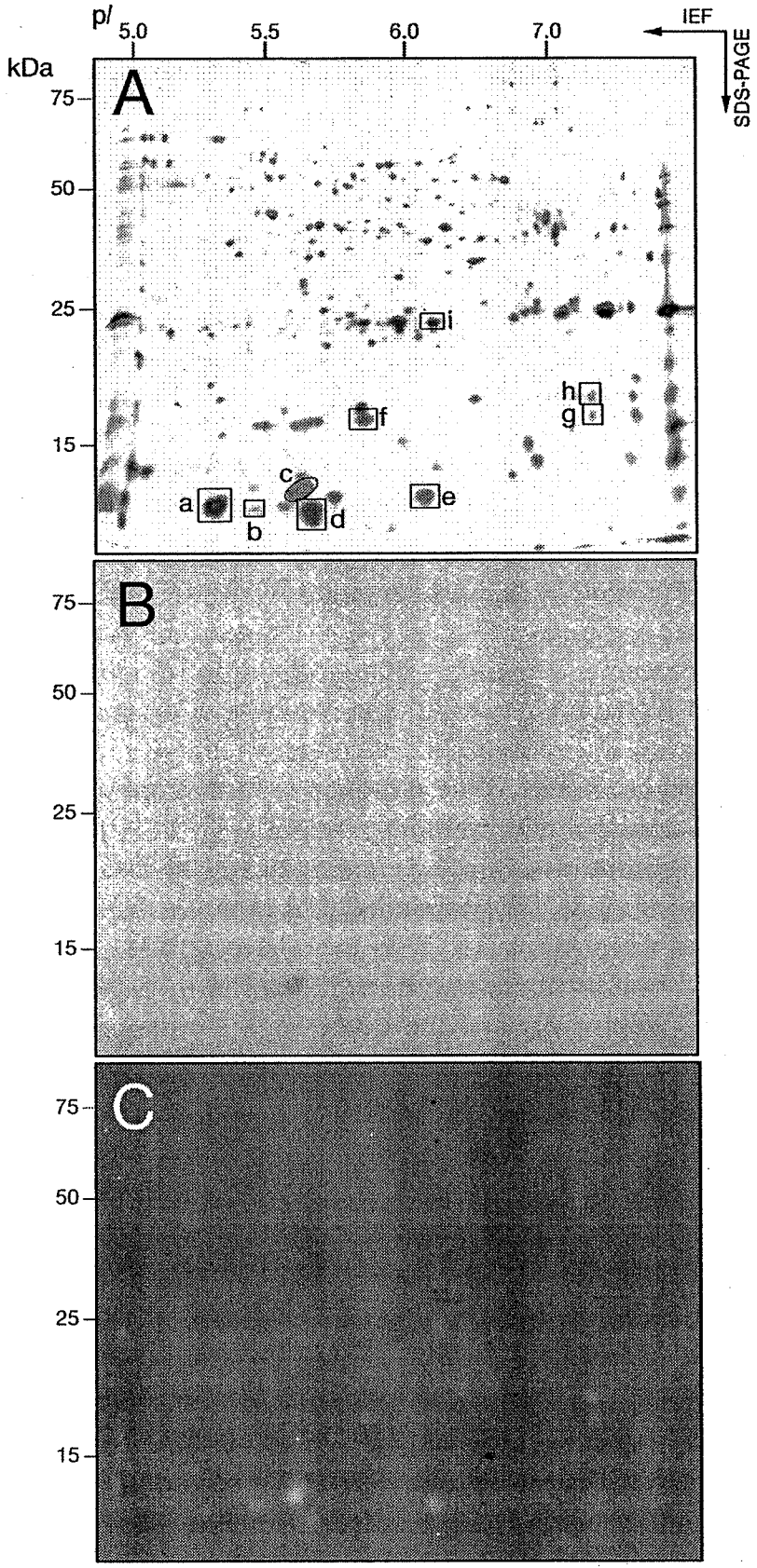
p/
5.0
5.5
6.0
7.0
IEF
SDS-PAGE
kDa
A
B
C
75
50
25
15
a
b
c
d
e
f
g
h
i

Figure 8-3. Comparisons of a 2-D gel (Fig. 8-3A) and membrane blots from similar gels, stained with Ferene (Fig. 8-3B) and a second method based on redox properties (Fig. 8-3C). Spots revealed with the method based on the redox properties are enclosed and labeled in Fig. 8-3A, and the spot detected with both methods (c) is enclosed in an elipse. Homologies are described in Table 8-2.

3.3 ESI MS-MS analysis of the iron-binding protein

The spot corresponding to a putative Fe-binding protein detected by both staining methods (Figs. 8-3B and 8-3C) was further analysed by ESI MS-MS. This protein was digested with trypsin, and the tryptic digest was studied by MS-MS. Fourteen different peptides in the digest, with double charged precursor ions at 510.22, 618.27, 722.66, 726.14, 778.40, 885.75, 897.55, 904.41, 926.20, 934.00, 940.32, 1013.61, 1069.46 and 1116.21 m/z were studied by *de novo* sequencing. Sequences of the protein fragments are shown in Table 8-3. The sequence deduced from these 14 peptides was blasted to the NCBI nr database, and only four of them, with m/z 722.66, 778.40, 897.55 and 1069.46, gave significant matches. Homologies were with an ABC transporter from *Arabidopsis thaliana*, a hypothetical protein and a starch synthase fragment from *Oryza sativa* and a phloem specific protein from *Vicia faba* (Q41666).

Table 8-3. Sequences of the protein fragments from spot c.

	sequence	Acc n	homology	%id	E
510.22	ND(GC)GLFHR		no significant hits		
618.27	LRCTPYQEVK		no significant hits		
722.66	YSAWLRLPCNI	Q7PC81	PDR15 ABC transporter *A. thaliana*	100	0.36
726.14	VVYEEDELEGLR		no significant hits		
778.40	YEENEIAGYG	Q6Z0B1	Hypothetical protein OSJBN	70.0	26
885.75	ELSMNLLTDTRHS(PR)		no significant hit		
897.55	DFNDGYNTEVQR	Q508U7	Starch synthase fragment *O. sativa*	63.6	36
904.41	SGVSG		no significant hits		
926.20	YYLEYQQVPVYNNR		no significant hits		
934.00	VVYEDVVDIE		no significant hits		
940.32	RRVYEEGGAAGNVE		no significant hits		
1013.61	MSGDAGNT		no significant hits		
1069.46	ERVQVNEYEQV	Q41666	Phloem specific protein *V. faba*	72.7	31
1116.21	SETNIIGVISSSE		no significant hits		

3.4 Metal (iron and zinc) affinity chromatography

Affinity Hi-Trap chromatography with immobilized Fe showed the presence of only one protein that was weakly retained in the column and eluted in the first step (50 mM imidazole) of the elution gradient (Fig. 8-4). Silver staining revealed a very low intensity band in the 1-D SDS-PAGE gel, with an apparent MW of 16.5 kDa.

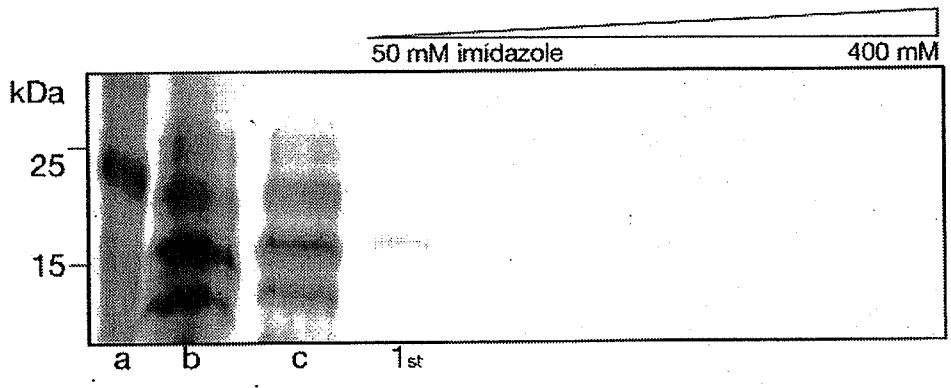

Figure 8-4. 1-D electrophoresis of fractions from Fe-affinity Hi-Trap chromatography. a) MW markers, b) and c) washes. 1st, first fraction eluted with 50 mM of imidazole.

Three proteins were retained in the Zn affinity Hi-Trap column as revealed by 1-D SDS-PAGE analysis of the different elution fractions (Fig. 8-5). A protein with an apparent MW of 15.5 kDa eluted in the second, third and fourth fractions, with a maximum in the second one, and was the more abundant among the three proteins. A second protein of 19.5 kDa apparent MW was eluted in the third, fourth and fifth fractions, with a maximum in the fourth one. A third protein with an apparent MW of 23.3 kDa was detected in the second, third and fourth fractions, with a maximum in the third one.

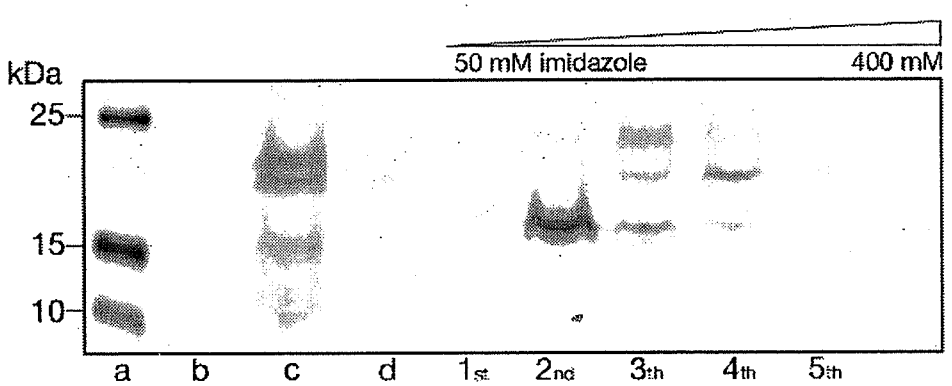

Figure 8-5. 1-D electrophoresis of fractions from Zn-affinity Hi-Trap chromatography. a) MW markers, b), c) and d) washes. 1st-5th, fractions eluted with the gradient of imidazole.

3.5 Organic acid and sugar analysis

The major sugar in sieve sap was sucrose, with a concentration of 227 mM, whereas much lower concentrations (lower than 14 mM) of other sugars were also present (Fig. 8-6).

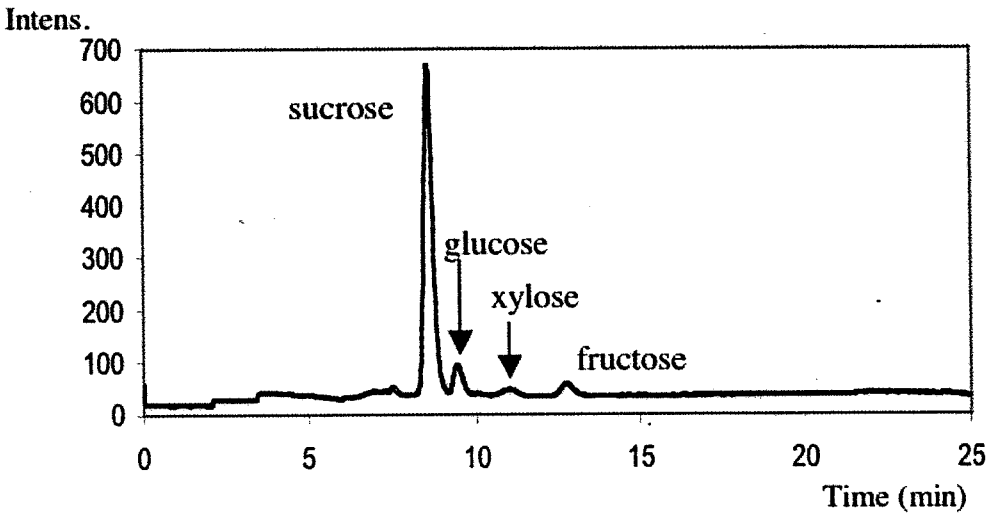

Figure 8-6. HPLC chromatogram of sugars from *Lupinus texensis* sieve sap.

A number of organic acids were found in sieve element sap from *Lupinus texensis* (Fig. 8-7). Succinic, malic, ascorbic and citric acids showed the highest concentrations, and total organic acid concentration was 15.37 mM (Table 8-4).

Table 8-4. Concentrations of organic acids in sieve element sap from *Lupinus texensis*.

acid	concentration (mM)
malic	5.47 ± 1.45
succinic	5.38 ± 1.03
ascorbic	1.95 ± 0.30
citric	1.10 ± 0.28
2-oxoglutaric	0.44 ± 0.07
dehydroascorbic	0.31 ± 0.06
oxalacetic	0.18 ± 0.03
Cis-aconitic	0.18± 0.01
fumaric	0.18 ± 0.06
oxalic	0.10 ± 0.03
gliceric	0.05 ± 0.01
malonic	0.02 ± 0.01
citramalic	0.01 ± 0.00

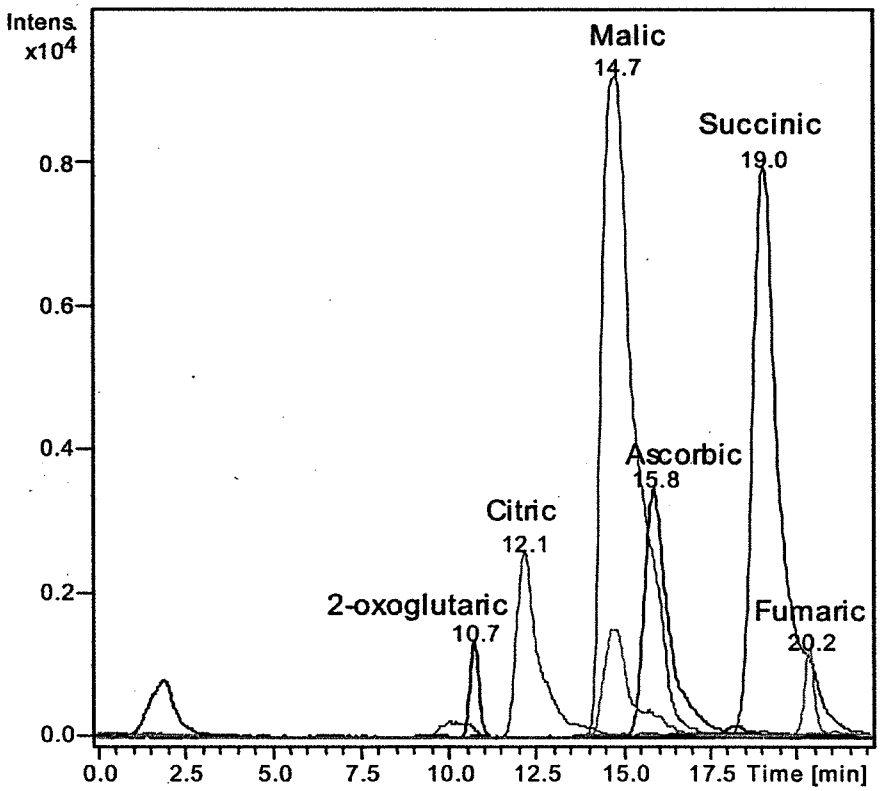

Figure 8-7. Chromatogram of sieve sap of *Lupinus texensis*, showing peaks for major carboxylates: malic (m/z 133), succinic (m/z 117), ascorbic (m/z 175), citric (m/z 191), 2-oxoglutaric (m/z 145) and fumaric (m/z 115).

4. DISCUSSION

Sieve tube exudates from *Lupinus texensis* plants have been used to study the proteome profile of phloem sap, with the particular aim to identify putative Fe and Zn transporters in this plant compartment. The long distance transport of metals through the phloem system is not well characterized yet, and the present work reports new data on this important issue. With the 2-D method used, proteins that can be detected should be in the ranges 8-80 kDa and 5-8 p*I*.

A possible candidate for Fe transport in mature sieve tubes has been detected by metal-specific staining of membrane blotted 2-D gels. The 2-D IEF-SDS PAGE technique allowed us to resolve more than 250 polypeptides in 2-D gels from phloem exudates. From these proteins, only one, with a molecular weight of 12.9 kDa and p*I* of 5.7 was revealed as an Fe-containing protein by the Ferene S staining method and as a redox active protein by a second staining method based on the redox properties of metal containing proteins. This spot was analysed by MALDI MS, and no homology with proteins present in the databases was found. This protein was further

analysed by ESI-MS/MS, by *de novo* sequencing of 14 peptides found in tryptic digests of this spot. Only four of these peptides (with the sequence presented in Table 8-3) gave a significant match to already known proteins, an ABC transporter from *A. thaliana*, a hypothetical protein and a starch synthase fragment from *O. sativa* and a phloem specific protein from *V. faba* (Q41666). ABC transporters have highly ABC conserved domains and an ATP binding site formed by boxes named Walker A and Walker B. The alignment of the sequenced peptide correspond to 10 amino acids in the N-terminal sequence between the Walker A box and the ABC signature sequence. A protein with an apparent molecular weight of 12.9 kDa could have approximately 130 aminoacids, whereas the coverage of the sequenced protein fragments in this spot would account for approximately 144 aminoacids. This would suggest that the eliptical spot could contain more than one protein. Further experiments are needed to study this protein.

A second protein that could be involved in Fe transport has been identified by using Fe-affinity chromatography and gradual elution with imidazole, followed by 1-D SDS of the eluted fractions. This protein, with an apparent MW of 16.5 kDa was weakly retained in the column that contained immobilized Fe. This protein could be the iron transport protein (ITP) already described by Krüger *et al.*, (2002) in castor bean seedlings phloem, which had a MW of 17 kDa and binds Fe *in vivo*. *In vitro*, ITP binds preferentially Fe(III) but no Fe(II) and also complexes Cu^{2+}, Zn^{2+}, and Mn^{2+}. The *ITP* gene belongs to the large family of late-embryogenesis-abundant (LEA) proteins, called dehydrins. This protein can be difficult to detect in 2-D gels due to its high experimental p*I*, higher than 7.3 (Krüger *et al.*, 2002).

Three proteins possibly involved in Zn transport in phloem exudates have been detected using Zn-affinity chromatography and 1-D SDS PAGE analysis. These proteins, with apparent MW of 15.5, 19.5 and 23.3 kDa, were retained with different strength in the Zn affinity Hi-Trap column and subsequently eluted from the chromatographic system in different fractions. Little is known about Zn transport in the mature sieve tube sap. So far, Zn has been reported to be associated with the low molecular weight fraction of sieve tube exudates in experiments carried out with ^{65}Zn (van Goor and Wiersma, 1976; Krüger *et al.*, 2002), probably complexed to organic compounds in a negatively charged complex with a MW between 1 and 1.5 kDa (van Goor and Wiersman, 1976). To our knowledge, data presented here constitute the first report on the existence of putative Zn binding proteins, and therefore probable Zn transporters, in the phloem sap.

The less specific, 2-D blot staining method based on the redox properties of metal containing proteins revealed the existence of 6 additional spots, which might be candidates for metal-associated activities (including transport) in sieve tube exudates. Three of these spots (spots a, b and d in

Fig. 8-3A) corresponded to thioredoxins and two (spots e and f in Fig. 8-3A) corresponded to cysteine proteinase inhibitors. The signals detected in the blot for these latter spots could be due to the redox properties of the cysteine residues present in these proteins, and therefore it is possible that these proteins are not involved in metal transport. All these 6 spots did not give any staining with the Ferene S method. Two more spots with positive staining in the redox-based method (spots h and i in Fig. 8-3A) were analysed by MALDI but no homologies with known proteins were found.

The large majority of the 250 polypeptides resolved by 2-D IEF-SDS PAGE of phloem exudates have no known relationship with metal transport. Since mature sieve tubes lack the machinery needed for transcription and translation of proteins, these proteins are most likely synthesized in the companion cells and then transported to the sieve tubes (see van Bel, 2003 for a review). Polypeptides identified in 2-D gels from *Lupinus texensis* sieve tube exudates included proteins related to oxidative stress and signal trafficking, such as glutathione peroxidase, ascorbate peroxidase and three spots corresponding to thioredoxin, which were also among the spots with highest signal intensity. The presence of oxidative stress related elements such as thioredoxin h (Isiwatari *et al.*, 1995; Schobert *et al.*, 1998), peroxidases (Walz *et al.*, 2002) and ascorbic acid (Franceschi and Tarlyn, 2002) in mature sieve tube elements has already been described in several plant species. Data presented here confirmed the high concentration of ascorbic acid in phloem sap. Elements protecting against oxidative stress could be present in the phloem sap as a response to wounding and pathogens, which constitute two commonly used methods for phloem sap sampling. Also, it has also been proposed that the presence in mature sieve elements of oxidative defense molecules could constitute a mechanism to protect this plant compartment as well as the adjacent tissues from oxidative damage, since the enucleated cells lack the mechanisms to trigger this cellular response (Walz *et al.*, 2002). On the other hand, the phloem pathway provides a perfect conduit for long-distance signals, and proteins related to signal trafficking, such as eukaryotic initiation factors 5A5 and 5A1, ubiquitin, and a GTP binding protein were identified in our 2-D phloem exudate gels. Several proteins manufactured in companion cells or in source tissues probably exert a distant effect on cellular mechanisms through its transport in this plant compartment. In such way, several works are underway to study the function of phloem specific proteins in long distance signaling (Ruiz-Medrano *et al.*, 2001; Lucas *et al.*, 2001). Moreover, it has been described that remote control by mRNA is mainly inferred by long-distance transmission of signals through the mature sieve elements inducing post-transcriptional gene silencing in the target tissue (van Bel, 2003).

In summary, our results show the presence in phloem exudates of two proteins possibly involved in Fe transport and three proteins possibly involved in Zn transport in the phloem sap of *Lupinus texensis*. One of those Fe transport proteins could be the ITP protein described by Krüger *et al.*, (2002), but to our knowledge, the other possible Fe and Zn transporters have not been described until now.

Capítulo 9

DISCUSIÓN GENERAL

ÍNDICE

1. RESPUESTAS DE LA RAÍZ A LA DEFICIENCIA DE HIERRO

La mayoría de los estudios realizados en plantas deficientes en hierro se han centrado en aspectos muy específicos, desde enfoques ya sea de

fisiología o de biología molecular. En este trabajo se ha intentado conseguir una visión integrada de algunas de las respuestas más importantes inducidas por la deficiencia de hierro en dos especies modelo, *Medicago truncatula* y *Beta vulgaris*, ambas pertenecientes a la Estrategia I. *Beta vulgaris* se ha utilizado habitualmente como planta modelo de Estrategia I, ya que es una de las plantas más eficientes en la toma y utilización de hierro en condiciones de deficiencia en dicho elemento, y por ello ya existen numerosos datos sobre su fisiología y bioquímica (Susín *et al.*, 1993, 1994, 1996; López-Millán *et al.*, 2000a, b, 2001a, b). Los datos obtenidos en este trabajo demuestran que la especie *M. truncatula* constituye también un buen modelo para la Estrategia I, ya que muchas de las respuestas fisiológicas frente a la deficiencia de Fe descritas hasta el momento se desarrollan también en esta especie, incluyendo la acumulación de flavinas y el consiguiente amarilleamiento de las puntas de raíz.

1.1 Acumulación de flavinas en las raíces con la deficiencia de hierro

Una respuesta característica de las plantas de *M. truncatula* y *B. vulgaris* deficientes en Fe es la acumulación de flavinas en raíces. Esta acumulación de flavinas inducida por la deficiencia de Fe ha sido previamente descrita en tabaco, tomate, lechuga y remolacha, e incluye, dependiendo de las especies, tanto riboflavina como los sulfatos 3' y 5' de riboflavina (Welkie y Miller, 1988, 1992; Susín *et al.*, 1993, 1994). En este trabajo se ha detectado la presencia de una flavina, que aún no ha podido ser identificada, en *M. truncatula*. El papel exacto de las flavinas en deficiencia de Fe no se conoce todavía. Una primera hipótesis, basada por un lado en que la localización de la acumulación de flavinas y la reducción de Fe es similar, y, por otro, en el hecho de que la reductasa de Fe es una proteína que contiene flavinas, sugiere que la acumulación de flavinas podría ser una parte integral del sistema de reducción de Fe en las plantas de Estrategia I (Cakmak *et al.*, 1987; López-Millán *et al.*, 2000a). Los resultados obtenidos en plantas de *M. truncatula* indican por primera vez que tanto el primero como el último gen de la ruta de biosíntesis de riboflavina, *Mtriba* y *MtDMRLs*, se sobreexpresan con la deficiencia de Fe. Además, los patrones de expresión de dichos genes en el periodo estudiado son paralelos al patrón de expresión del gen que codifica la reductasa, *MtFRO*. Esto sugiere que las flavinas podrían tener un papel importante, todavía desconocido, en el mecanismo de reducción de Fe. Por otra parte, un mRNA (*MtSULT1*) que codifica una posible sulfotransferasa de raíz de *M. truncatula* también se sobreexpresa en deficiencia de Fe. Esta enzima, perteneciente al metabolismo secundario,

podría participar en la sulfatación de riboflavina generando la flavina desconocida que fue detectada en raíces deficientes en Fe de *M. truncatula.*

El cambio más importante causado por la deficiencia de Fe en los geles 2-D de puntas de raíz de *B. vulgaris*, correspondió a un spot detectado *de novo* en los geles de raíces deficientes en Fe, e identificado por MALDI MS como la DMRL sintasa. Geles bidimensionales de extractos de puntas obtenidas 24 y 72 h después del aporte de Fe a las plantas deficientes, mostraron que en las puntas amarillas de la raíz la concentración de la proteína no variaba con el aporte de Fe, mientras que en las puntas blancas obtenidas 72 h tras dicho aporte no se detectó esta proteína. Apoyando estos datos, en las puntas de raíz amarillas de las plantas suplementadas con Fe se encontraron tanto riboflavina como sulfatos de riboflavina acumulados. Dado que la expresión del gen *BvDMRLs* disminuyó drásticamente sólo 24 h después del aporte de Fe a las plantas deficientes, la tasa de recambio de esta proteína es posiblemente baja.

En resumen, en condiciones de deficiencia de Fe, las concentraciones de flavinas medidas en extractos de raíz de *M. truncatula* y *Beta vulgaris*, fueron significativante más altas que las encontradas en condiciones control, y también la expresión de algunos genes relacionados con la biosíntesis de flavinas también fue mayor en las raíces deficientes en Fe que en las raíces de plantas control. Estos resultados demuestran que es necesario más trabajo para elucidar el papel real de las flavinas en la Estrategia I frente a la deficiencia de Fe.

1.2 Cambios en actividad y expresión de la reductasa férrica de la raíz con la deficiencia de hierro

Una de las respuestas más importantes de las raíces de plantas de Estrategia I frente a la deficiencia de Fe consiste en la inducción de una reductasa de Fe (FC-R) localizada en la membrana plasmática de las células de la raíz. Evidencias obtenidas en trabajos con guisante sugieren que la actividad enzimática FC-R podría ser el factor limitante en el proceso fisiológico de la adquisición de Fe en raíz (Grusak *et al.*, 1990; Connolly *et al.*, 2003). En este trabajo se ha encontrado, en plantas de *M. truncatula*, que tanto la actividad FC-R *in vivo* como la abundancia de los transcritos de *MtFRO1* fueron mayores en las plantas crecidas en deficiencia de Fe que en las plantas control. La actividad FC-R se detectó a lo largo de todo el sistema radicular mediante ensayos en placa de agar (datos no mostrados). Un aumento en la actividad de esta enzima con la deficiencia de Fe ha sido demostrado en un amplio número de especies vegetales (ver revisión de Schmidt, 1999). El aumento encontrado en la actividad de la FC-R de plantas de *M. truncatula*, de unas 4 veces frente al control, es similar a los

aumentos previamente descritos en otras especies: 3 veces en tomate (Zouari *et al.*, 2001), 5 veces en *Pisum sativum* (Waters *et al.*, 2002) y 11 veces en *B. vulgaris* (López-Millán *et al.*, 2000a). En un estudio previo con *M. truncatula* se obtuvo un aumento de la actividad de FC-R de 5 veces frente al control (López-Millán *et al.*, 2005). En diversos trabajos, se han descrito aumentos en la expresión de los genes de FC-R, incluyendo *AtFRO2*, *AtFRO3*, *LeFRO1* y *PsFRO1* en raíces de *A. thaliana*, *L. esculentum* y *P. sativum* crecidas en condiciones de deficiencia de Fe (Robinson *et al.*, 1999; Wintz *et al.*, 2003; Li *et al.*, 2004; Waters *et al.*, 2002). Líneas de *A. thaliana* en las se ha introducido un gen *AtFRO2* inactivado tienen disminuida la actividad FC-R, son cloróticas y crecen lentamente a no ser que se produzca un elevado aporte de Fe (Robinson *et al.*, 1999). En *M. truncatula* la actividad FC-R y la expresión de la reductasa de Fe no se correlacionan exactamente, ya que en 10 días tras el inicio de la deficiencia la expresión de *MtFRO1* disminuye considerablemente, mientras que la actividad FC-R es todavía bastante alta.

En resumen, en *M. truncatula* cultivada en solución nutritiva en condiciones de deficiencia de Fe, tanto la actividad FC-R medida en raíz *in vivo* como la expresión del gen *MtFRO1*, aumentaron frente a los controles. Estos datos indican que la especie *M. truncatula* puede ser utilizada como una especie modelo para el estudio detallado de la reducción de Fe en la Estrategia I.

1.3 Cambios en actividad y expresión de la ATPasa de la raíz con la deficiencia de hierro

Las especies de Estrategia I cultivadas en deficiencia de Fe causan una disminución del pH del medio, debido a la extrusión de protones, mediada por un aumento de la actividad H^+-ATPasa (Dell'Orto *et al.*, 2002; Schmidt *et al.*, 2003). En este trabajo, se ha encontrado en raíces de *M. truncatula* deficientes en Fe un aumento de la actividad y de la expresión de la ATPasa en comparación con las raíces de plantas control, lo que está de acuerdo con los datos encontrados en otras especies vegetales (Dell'Orto *et al.*, 2000, 2002; Schmidt *et al.*, 2003; Santi *et al.*, 2005). Los ensayos de acidificación en placas de agar mostraron que en *M. truncatula* la extrusión de H^+ está localizada en todo el sistema radicular (datos no mostrados). En *M. truncatula*, a los 7 días tras el inicio de la deficiencia de Fe el aumento en la extrusión de H^+ fue mayor que el aumento encontrado en la actividad FC-R. En otras especies, como *Quercus suber*, ocurre lo contrario (Gogorcena *et al.*, 2001). La expresión del gen *Mtha1* en raíces de *M. truncatula* también fue mayor en las raíces deficientes en Fe que en las raíces de plantas control, al igual que lo que ocurre en *Cucumis sativus* (Santi *et al.*, 2005).

En resumen, tanto la actividad ATPasa medida *in vivo* en las raíces de *M. truncatula* como la expresión del gen *Mtha1* fue mayor en las raíces deficientes en Fe que en las raíces de plantas control. Esta enzima es posiblemente uno de los puntos claves de la Estrategia I en esta especie. El rápido desarrollo de la actividad ATPasa en las raíces de *M. truncatula* deficientes en Fe apoya la necesidad de un estudio del aumento de actividad de esta enzima en estadíos más tempranos de la deficiencia de Fe.

1.4 Cambios en actividad y expresión de la PEPC en la raíz con la deficiencia de hierro

En extractos de raíces de *M. truncatula* deficientes en Fe se han encontrado incrementos de actividad de la enzima PEPC de aproximadamente 3 veces, en base a peso fresco, en comparación con los controles (Andaluz *et al.*, 2005). También se ha medido esta actividad en extractos de puntas de raíz de remolacha, obteniendo aumentos de actividad de aproximadamente 50 veces, en base a peso fresco, similares a los encontrados previamente en dicha especie (López-Millán *et al.*, 2000a). Se han descrito previamente aumentos en la actividad PEPC en extractos de raíz con la deficiencia de Fe en pimiento (Landsberg, 1986), kiwi (Rombolà, 1998), pepino (Rabotti *et al.*, 1995; De Nisi and Zocchi, 2000) y *B. vulgaris* (López-Millán *et al.*, 2000a).

Se han realizado experimentos de Western-blot con anticuerpos tanto frente al sitio de fosforilación de la PEPC (Andaluz *et al.*, 2002) como frente a la proteína PEPC entera, detectando en ambos casos un único polipéptido de aproximadamente 110 kDa en los extractos de puntas de raíz de plantas de remolacha. La cantidad de proteína fue 35 y 7 veces más alta en la zona amarilla y blanca de las puntas de raíz deficientes en Fe, respectivamente, en comparación con las puntas control (Andaluz *et al.*, 2002). Los datos obtenidos indican que la cantidad de proteína PEPC está muy regulada por el estatus nutricional de Fe, ya que la misma disminuyó significativamente sólo 24 h tras el aporte de Fe a las plantas deficientes. Además, esta banda ya no se pudo detectar en las nuevas puntas de raíz blancas crecidas tras 72 h del aporte de Fe. Estos resultados confirman los datos publicados anteriormente, que indicaban que la actividad enzimática de la PEPC en extractos de raíces de plantas deficientes disminuye aproximadamente un 50% tras sólo 24 h del aporte de Fe, hasta alcanzar valores muy bajos, similares a los controles, tras 96 h (López-Millán *et al.*, 2001b).

La cantidad de proteína total por peso fresco en extractos de raíz de remolacha aumenta con la deficiencia de Fe unas 3 veces (Andaluz *et al.*, 2002). Por lo tanto, cuando la actividad de la enzima PEPC se expresa en base a proteína en vez de en base a peso fresco, el aumento encontrado fue

de aproximadamente 12 a 14 veces. Dicho aumento es mucho menor que el aumento medido en la cantidad de proteína con la deficiencia de Fe, que fue de aproximadamente 35 veces. Estos datos sugieren la existencia de factores que pueden modificar la actividad PEPC en los extractos de raíz, posiblemente causados por los cambios que pueden tener lugar en el medio de ensayo debido a la diferente composición de las raíces de las plantas deficientes en Fe y las controles. Este hecho puede ser importante, ya que cualquier efecto que se encuentre en los extractos de raíz puede tener incluso mayor importancia en raíces intactas.

Una regulación alostérica de la actividad PEPC por diversos efectores positivos, como por ejemplo la glucosa 6-fosfato y la triosa fosfato, ha sido demostrada previamente en algas (Schuller *et al.*, 1990a) y nódulos de soja (Schuller *et al.*, 1990b). En las raíces de remolacha deficientes en Fe era probable que ocurriese un aumento en la concentración de estos efectores, ya que la ruta glicolítica está aumentada en dichas raíces (Sijmons y Bienfait, 1983; Rabotti *et al.*, 1995; Espen *et al.*, 2000). De acuerdo con esta hipótesis, se ha obtenido un aumento de unas 5 veces en la cantidad de glucosa 6-fosfato en extractos de puntas de raíces de remolacha deficientes en Fe en comparación con los controles. Sin embargo, este aumento llevaría a un pequeño aumento de la concentración de glucosa 6-fosfato en el ensayo de actividad de la PEPC, inferior a 2 μM. Es improbable que este hecho afecte significativamente a las medidas de actividad en los extractos de raíz, ya que una concentración de 500 μM de glucosa 6-fosfato produce un aumento en la actividad PEPC de aproximadamente un 15%. Una posible explicación para los relativamente bajos valores de la actividad PEPC en los extractos de raíces de remolacha deficientes en Fe sería un aumento de las concentraciones de malato, ya que este compuesto es un fuerte inhibidor de la PEPC (Vidal y Chollet, 1997). Sin embargo, el aumento en la concentración de malato en las raíces de remolacha deficientes en Fe (de 0.4 a 6.0 mM; López-Millán *et al.*, 2000a) solo aumentaría la concentración de malato en el extracto del ensayo hasta 45 μM. Esta concentración de malato solamente podría producir una disminución de la actividad PEPC de aproximadamente un 10%. Además, la concentración de fumarato en la raíz, que en plantas de remolacha deficientes en Fe aumenta hasta aproximadamente 0.9 mM (López-Millán *et al.*, 2000a), podría provocar aumentos de fumarato en el extracto del ensayo de PEPC de aproximadamente 6 μM, lo que podría producir disminuciones en la actividad de menos de un 5 %.

Por otra parte, experimentos preliminares en nuestro laboratorio demostraron que la inhibición de la actividad cuando se añadió enzima PEPC purificada al extracto de puntas de raíz deficientes en Fe y controles fue aproximadamente del 34 y 25%. Esto indica la existencia de factores que

disminuyen la actividad PEPC en los extractos de raíces de remolacha, pero no explica que el considerable aumento de la cantidad de proteína PEPC produzca sólo un aumento moderado en la actividad de la enzima. Otra posibilidad sería la existencia de diferentes formas activas de la PEPC en las raíces control y deficientes, si bien la presencia de una única banda de PEPC en los experimentos de Western-blot no apoya la presencia de diferentes tipos de PEPC con distinta masa molecular. De todas formas, esto no excluye la presencia de otras posibles modificaciones de la proteína que no lleven a grandes modificaciones en su masa molecular.

Los datos obtenidos sugieren la existencia de varios tipos de regulación de la enzima PEPC. En el presente estudio se ha demostrado la regulación transcripcional de PEPC en respuesta a la deficiencia de Fe tanto en *M. truncatula* como remolacha, ya que existe una sobreexpresión de esta enzima en respuesta a la deficiencia de Fe. Recientemente, se presentó en un Congreso la sobreexpresión de la PEPC in *Cucumis sativus* deficiente en Fe (De Nisi *et al.*, 2004). En remolacha se ha observado que tras el aporte de Fe a plantas deficientes en este elemento, la intensidad de los transcritos de *BvPEPC*, no cambia en la parte amarilla de las puntas de raíces deficientes en Fe, lo que sugiere la existencia de algún tipo de regulación post-transcripcional en este área de las puntas de raíz.

Un mecanismo ampliamente aceptado para la regulación post-traduccional de la enzima PEPC es la fosforilación reversible del dominio amino-terminal. Esta clase de regulación ha sido ampliamente estudiada en hojas de plantas C4 y CAM (ver la revisión de Vidal y Chollet, 1997). En estas plantas los ciclos luz-oscuridad (en plantas C4) o noche-día (en plantas CAM), inducen la fosforilación-defosforilación de la PEPC fotosintética por una PEPC kinasa independiente de Ca y una proteína fosfatasa de tipo 2A, respectivamente. La PEPC fosforilada es más activa, menos sensible al efector negativo malato y más sensible al efector positivo glucosa 6-fostato (Chollet *et al.*, 1996). La regulación por fosforilación también se ha encontrado en tejidos no fotosintéticos como nódulos y semillas (Zhang *et al.*, 1995; Osuna *et al.*, 1996; Osuna *et al.*, 1999; Nhiri *et al.*, 2000). Nuestros datos sugieren que en las raíces de remolacha deficientes en Fe la fosforilación de la PEPC no tiene lugar, confirmando algunos resultados preliminares obtenidos en pepino (De Nisi y Zocchi, 2000). La fosforilación de la PEPC fue estudiada por diferentes estrategias incluyendo detección inmunológica de residuos fosforilados de serina (Andaluz *et al.*, 2002), métodos rápidos de estimación del estado de fosforilación y ensayos de fosforilación *in vitro* e *in gel* con ^{32}P-ATP. En la región de la PEPC no se detectaron residuos de fosfoserina en ninguno de los extractos analizados (Andaluz *et al.*, 2002), mientras que las relaciones obtenidas en los test de fosforilación aparente en extractos de raíz de plantas deficientes fueron muy

similares a los encontrados en extractos de raíces control. Además, no se detectó la fosforilación de la PEPC en los ensayos de fosforilación *in vitro*, y los ensayos de fosforilación *in gel* indican que la concentración de quinasas en los extractos de las raíces deficientes fue más baja que la encontrada en raíces control. Estos datos sugieren que en las raíces deficientes en Fe no hay regulación post-transcripcional por fosforilación.

Otros factores podrían contribuir a aumentar la actividad PEPC en raíz. Por ejemplo, el aumento del pH citoplasmático podría estimular la actividad PEPC ya que el pH óptimo de la enzima es bastante alto. Sin embargo, Espen *et al.* (2000) demostraron por técnicas de ^{31}P-NMR que el pH citosólico en raíces deficientes en Fe de pepino aumenta solamente entre 0.02-0.06 unidades con respecto a los controles, mientras que el pH vacuolar aumentó 0.03 y 0.20 unidades. Dado que el aumento en la actividad PEPC está principalmente localizado en la capa externa de las células corticales de las secciones apicales de raíz deficientes en Fe, que son muy activas en la extrusión de protones (De Nisi *et al.*, 2002), se ha propuesto que la alcalinización del citoplasma asociada con la extrusión de protones podría aumentar la actividad de la PEPC (teoría "pH stat", Davies, 1973). Sin embargo, tanto la sobreexpresión de los transcritos de PEPC en deficiencia de Fe como el hecho de que la inducción de la actividad PEPC y la capacidad de acidificación no sean paralelos en el tiempo apoyan la hipótesis de que que el aumento en la actividad PEPC no se debe exclusivamente a cambios del pH citoplasmático.

La posible función del aumento de PEPC en la deficiencia de Fe está todavía sin resolver, si bien ya se ha propuesto un modelo metabólico para la asimilación de C en las raíces de remolacha deficientes en Fe (López-Millán *et al.*, 2000a). En este modelo, PEPC cataliza la carboxilación de PEP a oxalacetato, el cual podría ser reducido a malato a través de la malato deshidrogenasa citosólica. El malato podría ser transportado a la mitocondría a traves de la lanzadera malato-oxalacetato y convertido a citrato por la citrato sintasa. Parte de este carbono podría ser usado, a través de un aumento de la actividad mitocondrial en las células de transferencia, para aumentar la capacidad de producir poder reductor, mientras que otra parte podría ser exportado a la parte aérea vía xilema (Bialzyck and Lechowski, 1992; López-Millán *et al.* 2000b). Una posible función de los ácidos orgánicos exportados a las hojas es el uso de estos esqueletos de C para el mantenimiento de procesos básicos como la respiración. El PEP necesario para mantener la actividad PEPC podría venir de la glicólisis de compuestos previamente generados y/o almacenados dentro de la planta. En este contexto, se han encontrado aumentos con la deficiencia de Fe en la concentración de azúcares tanto en floema (de Vos *et al.*, 1986; Maas *et al.*, 1988) como en raíz (Thoiron y Briat, 1999), y las actividades de algunas

enzimas implicadas en la ruta glicolítica también aumentan en raíces deficientes en Fe (ver la revisión de Abadía *et al.*, 2002).

En resumen, en condiciones de deficiencia de Fe, el incremento en la actividad PEPC está mediado por una aumento en la expresión del gen *MtPEPC* y por un aumento en la cantidad de proteína. Además, los datos obtenidos sugieren que en las raíces deficientes en Fe puede existir algún tipo de regulación post-traduccional, distinto de la fosforilación de la enzima, que modularía a la baja la actividad de la enzima. Se podrían plantear en un futuro inmediato estudios sobre posibles cambios en la enzima PEPC en las raíces de las plantas deficientes en hierro, mediante técnicas de MS-MS que permitan el estudio de modificaciones post-traduccionales.

1.5 Cambios en el proteoma de la raíz con la deficiencia de hierro

Se han estudiado los cambios inducidos por la deficiencia de Fe en el proteoma de raíz en las raíces de puntas de remolacha crecidas en medio hidropónico. La técnica de electroforesis bidimensional, IEF-SDS PAGE, permitió la separación de proteínas de extractos de puntas de raíz, obteniendo mapas con aproximadamente 150 polipéptidos. Dadas las técnicas experimentales utilizadas, el estudio se ha centrado en proteínas pertenecientes a un rango de p*I* de 5-8 y peso molecular aparente de 10-100 kDa, rango que cubre la mayor parte de las proteínas de raíz. Los datos obtenidos muestran que la deficiencia de Fe produce cambios en la cantidad relativa de un gran número de polipéptidos.

La mayoría de las proteínas en las que se produjo un aumento de intensidad fueron identificadas por MALDI MS como enzimas del catabolismo de carbohidratos: 5 de las 10 enzimas de la ruta glicolítica, fructosa 1,6-bisfosfato aldolasa, triosafosfato isomerasa, gliceraldehido 3-fosfato deshidrogenasa, 3-fosfoglicerato quinasa y enolasa; una enzima del ciclo del ácido cítrico, la malato deshidrogenasa; y la fructoquinasa. Se había descrito previamente el aumento en la deficiencia de Fe en las actividades de varias enzimas glicolíticas, incluyendo la fructosa 1,6-bisfosfato aldolasa (Sijmons y Bienfait, 1983) y la gliceraldehido 3-fosfato deshidrogenasa (Sijmons y Bienfait, 1983; Rabotti *et al.*, 1995; Espen *et al.*, 2000). También se han descrito previamente aumentos en la actividad de la malato deshidrogenasa en plantas de pepino y *B. vulgaris* (Rabotti *et al.*, 1995; López-Millán *et al.*, 2000a). Los resultados obtenidos concuerdan con los análisis de micromatrices realizados en raíces de *Arabidopsis* deficientes en Fe (Thimm *et al.*, 2001). Sin embargo, no hay datos sobre aumentos inducidos por la deficiencia de Fe en la cantidad relativa de estas proteínas,

con la única excepción de la gliceraldehido 3-fosfato deshidrogenasa (Herbik *et al.*, 1996). En otros trabajos también se han encontrado aumentos en la cantidad de PEPC (De Nisi y Zocchi, 2000; Andaluz *et al.*, 2002), pero esta enzima, con un peso molecular de aproximadamente 110 kDa, queda fuera del rango usado en los geles de 2-D. La activación del catabolismo de carbohidratos en raíces de plantas crecidas en condiciones de deficiencia de Fe se debe probablemente a un aumento en la demanda de energía y poder reductor por parte de la raíz, necesario para mantener el aumento en las actividades H^+-ATPasa y FC-R (Schmidt, 1999; Thimm *et al.*, 2002). Además, dos polipéptidos identificados en los geles 2-D como diferentes subunidades de la ATPasa F1 también aumentan en las raíces deficientes en Fe, apoyando el alto requerimiento energético de estas raíces. Por otra parte, los resultados muestran un aumento en la cantidad de formato deshidrogenasa, una enzima relacionada con la respiración anaeróbica en las raíces deficientes en Fe. La respiración anaeróbica es una ruta alternativa para la producción de energía cuando la fosforilación oxidativa está dañada, como ocurre en condiciones de deficiencia de Fe. Se han descrito aumentos tanto en la actividad (López-Millán *et al.*, 2000a) como en la expresión (Thimm *et al.*, 2001) de este tipo de enzimas con la deficiencia de este elemento.

En resumen, la deficiencia de Fe induce cambios significativos en el proteoma de las puntas de raíz de *Beta vulgaris*, muchos de los cuales parecen estar asociados al catabolismo de carbohidratos. Además, como se ha discutido anteriormente, el cambio más importante en los geles 2-D se produjo en la proteína DMRL sintasa, que fue detectada *de novo* (y con una gran intensidad) en los geles de puntas de raíz deficientes en Fe, y que sigue presente en las puntas amarillas de las plantas deficientes en Fe tras el aporte de Fe.

2. CAMBIOS EN EL PROTEOMA DE TILACOIDES DE *Beta vulgaris* CON LA DEFICIENCIA DE HIERRO

En este trabajo hemos estudiado los cambios inducidos por la deficiencia de Fe en el proteoma de tilacoides aislados de plantas de remolacha crecidas en cultivo hidropónico. La técnica más ampliamente usada en los estudios de proteómica, IEF-SDS PAGE (Whitelegge, 2003), se ha utilizado hasta ahora para separar las proteínas tilacoidales de algas *Chlamydomonas reinhardtii* (Hippler *et al.*, 2001) y de varias especies de plantas, incluyendo *Arabidopsis thaliana* (Kieselbach *et al.*, 2000), *Pisum sativum* (Peltier *et al.*, 2000) y *Nicotianamina benthamiana* (Pérez-Bueno *et al.*, 2004). Esta técnica

tiene como inconveniente una exclusión significativa de proteínas integrales de membrana, debido a su baja solubilidad en los detergentes neutros o zwiteriónicos empleados en la primera dimensión de IEF (Molloy, 2000; Santoni *et al.*, 2000). Los resultados obtenidos en este trabajo muestran que la separación bidimensional IEF-SDS PAGE de tilacoides de remolacha permite la detección de varias proteínas de los complejos LHC con pocos dominios transmembrana. Sin embargo, no fue posible detectar proteínas con un gran número de dominios transmembrana. Se han encontrado resultados similares en tilacoides de *Chlamydomonas* (Hippler *et al.*, 2001), donde se detectaron pocas proteínas integrales de membrana como LHC y PsaA, mientras que la mayoría de las proteínas con un gran número de dominios transmembrana, pertenecientes al complejo del PS II, no pudieron ser detectadas.

Sin embargo, la técnica bidimensional IEF-SDS PAGE es una herramienta bidimensional muy potente para la separación de otros polipéptidos tilacoidales, y en este estudio ha permitido la obtención de mapas con más de 100 polipéptidos. Los datos obtenidos muestran que la deficiencia de Fe induce cambios en la intensidad de un gran número de polipéptidos, incluyendo disminuciones en la intensidad de muchos componentes de complejos proteicos que participan en el trasporte fotosintético de electrones, y aumentos en la intensidad de diversas proteínas implicadas en las reacciones relacionadas con la fijación de carbono. Algunas proteínas inducidas en deficiencia de Fe fueron identificadas por espectrometría de masas MALDI MS como proteínas estromáticas, incluyendo las subunidades grande y pequeña de la Rubisco, Rubisco activasa, anhidrasa carbónica, fosfoglicerato quinasa, aldolasa, fosforibuloquinasa, transcetolasa y sedoheptulosa 1,7-bisfosfatasa.

Para evitar alguna de las limitaciones de IEF-SDS PAGE, se ha desarrollado una segunda técnica bidimensional, llamada BN-SDS PAGE, para estudiar complejos y supercomplejos de proteínas mitocondriales (Schägger *et al.*, 1994). Esta técnica se ha empleado sólo muy recientemente para el estudio de proteínas tilacoidales (Rexroth *et al.*, 2003; Suorsa *et al.*, 2004; Ciambella *et al.*, 2005). La técnica permite la evaluación de modificaciones post-traduccionales, interacciones proteína-proteína alteradas, así como la detección de cambios en el ensamblaje de complejos (en la primera dimensión BN-PAGE), y la composición de dichos complejos (en la segunda dimensión SDS-PAGE). Nuestros resultados indican que la separación de tilacoides de remolacha mediante BN-SDS PAGE, permite la detección de un gran número de proteínas transmembrana, como recientemente se demostró en tilacoides de cebada (Ciambella *et al.*, 2005). Esta técnica corrobora los resultados encontrados por IEF-SDS PAGE, tanto para la disminución en la intensidad de muchos transportadores de electrones

fotosintéticos, como para el aumento en la intensidad de Rubisco y otras proteínas implicadas en las reacciones de fijación de carbono. Los polipéptidos identificados cuya intensidad disminuyó con la deficiencia de Fe en las dos técnicas bidimensionales usadas, correspondieron principalmente a proteínas pertenecientes a complejos de antena y centro de reacción de los complejos PSI, PSII (incluyendo el complejo productor de oxígeno OEC) y b_6/f. Estos resultados concuerdan con las disminuciones observadas por técnicas de electroforesis monodimensional en las cantidades de diferentes proteínas participantes en el transporte de electrones (Spiller and Terry, 1980; Terry, 1980; Nishio *et al.*, 1985; Terry and Abadía, 1986).

Los mapas proteicos obtenidos por 2-D BN-SDS PAGE muestran la inducción por la deficiencia de Fe de un nuevo conjunto de proteínas que no aparece en los geles de los tilacoides de plantas control. Este conjunto incluye 5 polipéptidos con homología con anhidrasa carbónica, aldolasa, glutamina sintetasa y glicina hidroximetiltransferasa. Estas enzimas están implicadas en el metabolismo de aminoácidos, y especialmente en el equilibrio metabólico amino ceto-alcohol. Se han encontrado evidencias del ensamblaje de proteínas del ciclo de Calvin en complejos multienzimáticos estables unidos a la cara estromática de la membrana tilacoidal en distintas especies vegetales como *Spinacia oleracea* (Süss *et al.*, 1993), *Pisum sativum* (Anderson *et al.*, 1996), *Nicotiana tabacum* (Jebanathirajah and Coleman, 1998) y *Chlamydomonas reinhardtii* (Süss *et al.*, 1995). Se ha propuesto que la asociación de estas enzimas con las membranas tilacoidales podría facilitar el acceso directo a cofactores como ATP y NADPH producidos durante la fotosíntesis, y prevenir interferencias de otras rutas metabólicas (Süss *et al.*, 1993; Anderson *et al.*, 1996). Los datos proteómicos mostrados sugieren que las enzimas mencionadas podrían estar asociadas *in vivo* a las membranas tilacoidales, constituyendo quizás una red enzimática asociada a las membranas tilacoidales cloróticas e implicada en el metabolismo de aminoácidos y cetoácidos. Ésto podría estar relacionado con la presencia del acervo de plastoquinonas en estado reducido, en condiciones de oscuridad, en las membranas tilacoidales de plantas deficientes (Belkhodja *et al.*, 1988). La presencia de este nuevo conjunto de proteínas, posiblemente asociadas, podría estar relacionada con el equilibrio redox de los tilacoides deficientes en Fe.

En resumen, la deficiencia de Fe induce cambios significativos en el proteoma de tilacoides de remolacha, con una disminución de la cantidad relativa de complejos de transporte electrónico y un aumento relativo de algunas proteínas implicadas en las reacciones de fijación de carbono. Además, usando la técnica 2-D BN-SDS PAGE, se ha detectado un nuevo grupo de proteínas en las preparaciones de membranas tilacoidales de hojas

de remolacha deficientes en Fe. Este grupo incluye varias proteínas localizadas normalmente en el estroma del cloroplasto.

3. COMPOSICIÓN DEL PROTEOMA DE FLOEMA DE *Lupinus texensis*

En este trabajo se ha estudiado el proteoma de exudados de floema de *Lupinus texensis*, con el objetivo de identificar posibles transportadores de Fe y Zn en este compartimento celular. El transporte a larga distancia de metales a traves del floema no está bien caracterizado todavía y el presente trabajo aporta nuevos datos sobre este importante mecanismo.

La técnica de 2-D IEF-SDS PAGE permitió la separación de más de 250 polipéptidos en geles bidimensionales de exudados de floema. Mediante tinciones específicas de metales en membranas en las que se habían transferido geles 2-D se identificó un posible candidato para el transporte de Fe en el floema. Sólo una de las proteínas separadas en los geles 2-D, con masa molecular de 12.9 kDa y un p*I* de 5,7, se detectó tanto en la tinción específica de Fe como en la tinción de proteínas redox. Este polipéptido se analizó por MALDI MS, y al no encontrar homología con ninguna proteína presente en las bases de datos, se analizó también por ESI-MS/MS. Se secuenciaron *de novo* 14 péptidos obtenidos en la digestión tríptica de este polipéptido, de los que sólo cuatro presentaron homología con proteínas conocidas, un transportador ABC de *Arabidopsis*, una proteína hipotética y un fragmento de almidón sintasa de arroz, y una proteína específica de floema de *Vicia faba*. Los transportadores ABC tienen dominios ABC altamente conservados y un sitio de unión a ATP formado por cajas llamadas Walker A y Walker B. El alineamiento del péptido secuenciado y estas proteínas se produjo en la secuencia N-terminal entre la caja Walker A y el dominio ABC.

Una segunda proteína potencialmente implicada en el trasporte de Fe se identificó usando cromatografía de afinidad de Fe y una elución gradual con imidazol, seguido de electroforesis de 1-D de las fracción eluídas. En la columna con Fe inmovilizado se retuvo una proteína con un peso molecular de aproximadamente 16,5 kDa. Esta proteína podría ser la proteína ITP (iron transport protein) descrita por Krüger *et al.* (2002) en floema de plántulas de *Ricinus communis*. La proteína ITP tiene un peso molecular de 17 kDa y une Fe *in vivo*. *In vitro*, la ITP une preferentemente Fe(III) pero no Fe (II) y también compleja Cu^{2+}, Zn^{2+} y Mn^{2+}. El gen *ITP* pertenece a una gran familia de proteínas abundantes después de la embriogénesis (LEA, late-embryogenesis-abundant) llamada dehidrinas. Esta proteína podría ser de difícil detección en los geles 2-D debido a su alto punto isoeléctrico (7,3).

Mediante cromatografía de afinidad de Zn y electroforesis 1-D SDS PAGE se detectaron en el exudado de floema tres proteínas posiblemente implicadas en el transporte de Zn. Estas 3 proteínas, con pesos moleculares aparentes de 15,9, 19,5 y 23,3 kDa, quedaron retenidas en una columna Hi-Trap de afinidad de Zn, y posteriomente eluyeron en diferentes fracciones. Se conoce muy poco sobre el transporte de Zn en el floema, pero en experimentos realizados con ^{65}Zn (van Goor and Wiersma, 1976; Krüger *et al.*, 2002) se ha descrito que dicho transporte está asociado con la fracción de bajo peso molecular de los exudados de floema, probablemente unido a compuestos orgánicos en un complejo cargado negativamente con un peso molecular de aproximadamente 1-1,5 kDa (van Goor and Wiersma, 1976). Los resultados aportados en este trabajo constituyen la primera prueba de la existencia de posibles proteínas unidas a Zn y, probablemente, transportadoras de este elemento en el floema.

El método de tinción menos específico basado en las propiedades redox de los metales contenidos en las proteínas, reveló la existencia de otros 6 polipéptidos que podrían ser candidatos para actividades asociadas a metales (incluido el transporte) en el floema. Tres de estas proteínas presentaron homología con tiorredoxinas y otras dos con inhibidores de cisteína proteinasa. Las señales detectadas en las membranas debidas a estos polipéptidos podrían deberse a las propiedades redox de los residuos de cisteína presentes en estas proteínas y no a su implicación en el transporte de metales. Estos 6 polipéptidos no se tiñeron en la tinción con Ferene, específica de proteínas que contienen Fe. Dos polipéptidos más fueron detectados con el método basado en la reacción redox y analizados por MALDI MS pero no se obtuvieron homologías.

La gran mayoría de los 250 polipéptidos separados por 2-D IEF-SDS PAGE en el exudado de floema no tienen relación con el transporte de metales. Como los tubos cribosos carecen de la maquinaria necesaria para la transcripción y traducción de proteínas, estas proteínas probablemente se habrán sintetizado en las células de compañía y después transportado a los tubos cribosos (van Bel, 2003). Los polipéptidos identificados en geles 2-D de exudados de floema en *Lupinus texensis* incluyen proteínas relacionadas con el estrés oxidativo y la circulación de señales como glutation peroxidasa, ascorbato peroxidasa y tiorredoxina. Tres polipéptidos con muy alta intensidad presentaron homología con esta proteína. La presencia en el floema de elementos relacionados con el estrés oxidativo, como tiorredoxina h (Isiwatari *et al.*, 1995; Schobert *et al.*, 1998), peroxidasas (Walz *et al.*, 2002) y ácido ascórbico (Franceschi y Tarlyn, 2002) ya se han descrito en varias especies. Los datos presentados en este trabajo confirman la alta concentración de ácido ascórbico y tiorredoxinas en el floema de *Lupinus texensis*. Estos elementos, protectores frente al estrés oxidativo, podrían estar

presentes en el floema como respuesta a la herida, si bien se ha propuesto que la presencia de estas moléculas de defensa oxidativa podrían constituir un mecanismo protector de los tubos cribosos y los tejidos adyacentes, ya que las células sin núcleo de los tubos carecen de mecanismos capaces de desencadenar esta respuesta celular (Walz *et al.*, 2002). Por otra parte, el floema proporciona un conducto perfecto para el transporte de señales a larga distancia. En los geles 2-D de floema también se han identificado proteínas relacionadas con la circulación de señales, tales como factores eucarióticos de iniciación 5A5 y 5A1, ubiquitina, y una proteína de unión a GTP. Varias proteínas producidas en células de compañía o en tejidos productores ejercen probablemente un efecto a distancia a través de su transporte a través del floema. Algunos trabajos han abordado el estudio de la función de proteínas específicas de floema en la señalización a larga distancia (Ruiz-Medrano *et al.*, 2001; Lucas *et al.*, 2001). Además, se ha descrito que el control remoto por RNA mensajero se realiza principalmente por transporte a larga distancia de señales a través del floema, incluyendo el silenciamiento post-transcripcional de genes en los tejidos diana (van Bel, 2003).

En resumen, los resultados muestran que el floema de *Lupinus texensis* contiene al menos dos proteínas posiblemente implicadas en el transporte de Fe y tres proteínas posiblemente implicadas en el transporte de Zn. Una de estas proteínas transportadoras de Fe podría ser la proteína ITP descrita por Krüger *et al.* (2002), pero de los otros posibles transportadores de Fe y Zn no existen datos hasta el momento.

Capítulo 10

CONCLUSIONES

1. La expresión de los genes de la ATPasa (*Mtha1*) y la reductasa de Fe de membrana plasmática (*MtFRO1*) aumenta con la deficiencia de Fe en plantas de *Medicago truncatula.*

2. La expresión de los genes relacionados con la ruta de biosíntesis de flavinas, *Mtriba* en *Medicago truncatula*, y *MtDMRLs* y *BvDMRLs en Medicago truncatula* y *Beta vulgaris*, respectivamente, aumenta con la deficiencia de Fe.

3. El gen *MtSULT1*, correspondiente a una sulfotransferasa, está sobreexpresado en raíces de plantas deficientes en Fe de *Medicago truncatula.*

4. La técnica IEF-SDS PAGE se ha demostrado útil para la separación de polipéptidos en los tejidos estudiados obteniéndose mapas proteicos con más de 140 polipéptidos en raíz de *Beta vulgaris*, más de 110 en tilacoides de *Beta vulgaris* y más de 250 en floema de *Lupinus texensis.*

5. La deficiencia de hierro induce cambios significativos en el proteoma de puntas de raíz de *Beta vulgaris*: 13 polipéptidos disminuyeron, 29 aumentaron, 6 desaparecieron y 13 fueron detectados *de novo*.

6. El cambio más importante inducido por la deficiencia de Fe en el proteoma de raíz de *Beta vulgaris* correspondió a la proteína DMRL sintasa. Dicha proteína es mayoritaria en los geles 2-D de las puntas

amarillas (tanto de las plantas deficientes en Fe como de las plantas que han recibido un aporte de Fe tras la deficiencia), mientras que no aparece en los geles de raíces de plantas control.

7. En los extractos de puntas amarillas de raíz de *Beta vulgaris* deficientes en Fe se ha encontrado un gran aumento en la actividad PEPC con respecto a los controles. Dicho aumento fue de aproximadamente 30-50 (en base a peso fresco) y 7-14 veces (en base a proteína).

8. La expresión de los genes de la PEPC aumenta con la deficiencia de Fe en *Medicago truncatula* (*MtPEPC*) y *Beta vulgaris* (*BvPEPC*).

9. El aumento de la actividad PEPC en plantas de *Beta vulgaris* deficientes en Fe no parece estar mediado por la fosforilación de la enzima.

10. La deficiencia de hierro induce cambios significativos en el proteoma de tilacoides de *Beta vulgaris*: 18 polipéptidos disminuyeron, 37 aumentaron, 5 desaparecieron y 33 fueron detectados *de novo*.

11. La deficiencia de Fe induce disminuciones de la cantidad relativa de los complejos transportadores de electrones y aumentos en la cantidad relativa de otras proteínas.

12. Se ha detectado un nuevo grupo de proteínas en tilacoides de *Beta vulgaris* deficientes en Fe que incluye varias proteínas normalmente localizadas en el estroma del cloroplasto.

13. En los exudados de floema de *Lupinus texensis* se han detectado dos proteínas que pueden estar implicadas en el transporte de Fe y tres proteínas más que pueden estar implicadas en el transporte de Zn.

Capítulo 11

BIBLIOGRAFÍA

Abadía A, Ambard-Bretteville F, Remy R and Trémolières A 1988 Iron-deficiency in pea leaves: Effect on lipid composition and synthesis. Physiol. Plant. 72, 713-717.

Abadía A, Sanz M, de las Rivas J and Abadía J 1989 Pear yellowness: an atypicall iron chlorosis? Acta Hortic. 256, 177-181.

Abadía J 1992 Leaf reponses to Fe deficiency: a review. J. Plant Nutr. 15, 1699-1713.

Abadía J and Abadía A 1993 Iron and plant pigments. *In* Iron Chelation in Plants and Soil Microorganisms, Eds L L Barton and L Hemming. pp 327-343. Academic Press, New York.

Abadía J, López-Millán A F, Rombolà A and Abadía A 2002 Organic acids and Fe deficiency: a review. Plant Soil 241, 75-86.

Abbott A J 1967 Physiological effects on micronutrient deficiencies in isolated roots of *Lycopersicon esculentum*. New Phytol. 66, 419-437.

Alcántara E, de la Guardia M D and Romera F J 1991 Plasmmalemma redox activity and H^+ extrusion in roots of Fe-deficient cucumber plants. Plant Physiol. 96, 1034-1037.

Alhendawi R A, Römheld V, Kirkby E A and Marschner H 1997 Influence of increasing bicarbonate concentrations on plant growth, organic acid accumulation in roots and iron uptake by barley, sorghum and maize. J. Plant Nutr. 20, 1731-1753.

Altschul S F and Lipman D J 1990 Protein database searches for multiple alignments. Proc. Natl. Acad. Sci. USA 87, 5509-5513.

Andaluz S, López-Millán A F, Peleato M L, Abadía J and Abadía A 2002 Increases in phospho*enol*pyruvate carboxylase activity in iron-deficient sugar beer roots: Analysis of spatial localization and post-translational modification. Plant Soil 241, 43-48.

Andaluz S, Tacchini I, Abadía A, Abadía J and López-Millán A F 2005 Responses of *Medicago truncatula* roots to iron deficiency. Enviado a Plant Cell Physiol.

Anderson L E, Gibbons J T and Wang X 1996 Distribution of ten enzymes of carbon metabolism in pea (*Pisum sativum*) chloroplasts. Int. J. Plant Sci. 157, 525-538.

Arnon D I 1949 Copper enzymes in isolated chlorolasts- Polyphenoloxidase in *Beta vulgaris*. Plant Physiol. 24, 1-15

Arulanantham A R, Rao I M and Terry N 1990 Limiting factors in photosynthesis. VI. Regeneration of ribulose 1,5-bisphosphate limits photosynthesis at low photochemical capacity. Plant Physiol. 93, 1466-1475.

Awad F, Römheld V and Marschner H 1988 Mobilization of ferric iron chlorosis in calcareous soil by plant-borne chelators (phytosiderophores). J. Plant Nutr. 11, 701-713.

Azcón-Bieto J and Talón M 2000 Fisiología y Bioquímica Vegetal, Mac Graw Hill, Madrid.

Barnes A, Bale J, Constantinidou C, Ashton P, Jones A and Pritchard J 2004 Determining protein identity from sieve element sap in *Ricinus communis* L. by quadrupole time of flight (Q-TOF) mass spectrometry. J. Exp. Bot. 55, 1473-1481.

Barret-Lennard E G, Marschner H and Römheld V 1983 Mechanism of short term Fe(III) reduction by roots. Evidence against the role of secreted reductants. Plant Physiol. 73, 893-898.

Becker R, Fritz E and Manteuffel R 1995 Subcellular localization and characterization of excessive iron in the nicotianamine-less tomato mutant *chloronerva*. Plant Physiol. 108, 269-275.

Belkhodja R, Morales F, Quílez R, López-Millán AF, Abadía A and Abadía J 1998 Iron deficiency causes changes in chlorophyll fluorescence due to the reduction in the dark of the photosystem II acceptor side. Photosynth. Res. 56, 265-276

Bell P F, Chaney R L and Angle J S 1988 Staining localization of ferric reduction on roots. J. Plant Nutr. 11, 1237-1252.

Bergmeyer H U, Brent E, Schmidt E and Stork H 1974 D-Glucose. Determination with hexokinase and glucose-6-phosphate dehydrogenase. *In* methods of Enzymatic Analysis, Eds H U Bergmeyer, J Bergmeyer and M Graßl. pp 1196-1201. Academic Press, New York.

Berthold D A, Babcock G T and Yocum C F 1981 Highly resolved oxygen-evolving photosysthem II preparation from spinach thylakoid membranes. FEBS Lett. 134, 231-234.

Bialzyck J and Lechowski L 1992 Absorption of HCO_3^- by roots and its effect on carbon metabolism of tomato. J. Plant Nutr. 15, 293-312.

Bibby T S, Nield J and Barber J 2001 Iron deficiency induces the formation of an antenna ring around trimeric photosystem I in cyanobacteria. Nature 412, 743-745.

Bienfait H F 1989 Prevention of stress in iron metabolism of plants. Acta Bot. Neerl. 38, 105-129.

Bienfait H F 1996 Is there a metabolic link between H^+ excretion and ferric reduction by roots of Fe-deficient plants? – A viewpoint. J. Plant Nutr. 19, 1211–1222.

Bienfait H F and Scheffers M R 1992 Some properties of ferric citrate relevant to the iron nutrition of plants. Plant Soil 143, 141-144.

Bienfait H F, Bino R J, van der Bliek A M, Duivenvoorden J F and Fontaine J M 1983 Characterization of ferric reducing activity in roots of Fe-deficient *Phaseolus vulgaris*. Physiol. Plant. 59, 196-202.

Blum H, Beier H and Gross H J 1987 Improved silver staining of plant proteins, RNA and DNA in polyacrylamide gels. Electrophoresis 8, 93-99.

Boekema E J, Hifney A, Yakushevska A E, Piotrowski M, Keegstra W, Berry S, Michel K P, Pistorius E K and Kruip J 2001 A giant chlorophyll-protein complex induced by iron deficiency in cyanobacteria. Nature 412, 745-748.

Bradford N M 1976 A rapid and sensitive method for the quantitation of microgram quantities of protein utilizing the principle of protein-dye binding. Anal. Biochem. 72, 248-254.

Brancadoro L, Rabotti G, Scienza A and Zocchi G 1995 Mechanisms of Fe efficiency in roots of *Vitis* sp. in response to iron deficiency stress. Plant Soil 171, 229-234.

Briat J F 1996 Roles of ferritin in plants. J. Plant Nutr. 19, 1331-1342.

Briat J F and Lobréaux S 1997 Iron transport and storage in plants. Trends Plant Sci. 2, 187-193.

Briat J F, Lobreaux S, Grignon N and Vansuyt G 1999 Regulation of plant ferritin synthesis: how and why. Cell. Mol. Life Sci 56, 155-166.

Brown J C 1966 Fe and Ca uptake as related to root-sap and stem-exudate citrate in soybeans. Physiol. Plant. 19, 968-976.

Brown J C and Ambler J E 1974 Iron-stress response in tomato. I. Sites of Fe reduction, absorption and transport. Physiol. Plant. 31, 221-224.

Brown J C and Jolley V D 1988 Strategy I and Strategy II mechanisms affecting iron availability to plants may be established too narrow or limited. J. Plant Nutr. 11, 1077-1098.

Brüggemann W, Moog P R, Nakagawa H, Janiesh P and Kuiper P J C 1990 Plasma membrane-bound NADH: Fe^{3+}-EDTA reductase and iron deficiency in tomato (*Lycopersicum esculentum*). Is there a Turbo reductase? Physiol. Plant. 79, 339-346.

Brüggemann W, Maas-Kantel K and Moog P R 1993 Iron uptake by leaf mesophyll cells: The role of the plasma membrane-bound ferric-chelate reductase. Planta 190, 151-155.

Buchanan B B, Gruissem W and Jones R L 2000 Biochemistry and molecular biology of plants, ASPP.

Bughio N, Takahashi M, Yoshimura E, Nishizawa N K and Mori S 1997a Light-dependent iron transporter into isolated barley chloroplasts. Plant Cell Physiol. 38, 101-105.

Bughio N, Takahashi M, Yoshimura E, Nishizawa N K and Mori S 1997b Characteristics of light regulated iron transport system in barley chloroplasts. Soil Sci. Plant Nutr. 43, 959-963.

Burnap R L, Troyan T and Sherman L A 1993 The highly abundant chlorophyll-protein complex of iron-deficient *Synechococcus* sp. PCC7942 (CP43') is encoded by the *isiA* gene. Plant Physiol. 103, 893-902.

Cakmak I, Van de Wetering D A M, Marschner H and Bienfait H F 1987 Involvement of superoxide radical in extracellular ferric reduction by iron-deficient bean roots. Plant Physiol. 85, 310-314.

Cánovas F M, Dumas-Gaudot E, Recorbet G, Jorrín J, Mock H P and Rossignol M 2004 Plant proteome analysis. Proteomics 4, 285-298.

Chaney R L 1984 Diagnostic practices to identify iron deficiency in higher plants. J. Plant Nutr. 7, 47-67.

Chaney R L, Brown J C and Tiffin L O 1972 Obligatory reduction of ferric chelates in iron uptake by soybeans. Plant Physiol. 50, 208-213.

Chen Y and Barak P 1982 Iron nutrition of plants in calcareous soils. Adv. Agron. 35, 217-240.

Chollet R, Vidal J and O'Leary M H 1996 Phosphoenolpyruvate carboxylase: A ubiquitous, highly regulated enzyme in plants. Annu. Rev. Plant. Physiol. Plant Mol. Biol 47, 273-298.

Ciambella C, Roepstorff P, Aro E M and Zolla L 2005 A proteomic approach for investigation of photosynthetic apparatus in plants. Proteomics 5, 746-757.

Clark R B 1983 Plant genotype differences in the uptake, translocation, acumulation and use of mineral elements required for plant growth. Plant Soil 72, 175-196.

Cohen C K, Fox T C, Garvin D F and Kochian L V 1998 The role of iron-deficiency stress responses in stimulating heavy-metal transport in plants. Plant Physiol. 116, 1063-1072.

Cohen C K, Norwell W A and Kochian L V 1997 Induction of the root cell plasma membrane ferric reductase. An exclusive role for Fe and Cu. Plant Physiol. 114, 1061-1069.

Colangelo E P and Guerinot M L 2004 The essential basic helix-loop-helix protein FIT1 is required for the iron deficiency response. Plant Cell 16, 3400-3412.

Connolly E L, Fett J P and Guerinot M L 2002 Expression of the IRT1 metal transporter is controlled by metals at the levels of transcript and protein accumulation. Plant Cell 14, 1347-1357.

Connolly E L, Campbell N H, Grotz N, Prichard C L and Guerinot M L 2003 Overexpression of the FRO2 ferric chelate reductase confers tolerance to growth on low iron and uncovers post-transcriptional control. Plant Physiol. 133, 1102-1110.

Cornett J D and Johnson G V 1991 Ferric chelate reduction by suspension culture cells and roots of soybean: a kinetic comparison. Plant Soil 130, 75-80.

Cramer M, Lewis O and Lips S 1993 Inorganic carbon fixation and metabolism in maize roots as affected by nitrate and ammonium nutrition. Physiol. Plant. 89, 632-639.

Curie C and Briat J F 2003 Iron transport and signaling in plants. Annu. Rev. Plant Biol. 54, 183-206.

Curie C, Alonso J M, Le Jean M, Ecker J R and Briat J F 2000 Involvement of NRAMP1 from *Arabidopsis thaliana* in iron transport. Biochem. J. 347 Pt 3, 749-755.

Curie C, Panaviene Z, Loulergue C, Dellaporta S L, Briat J F and Walker E L 2001 Maize *yellow stripe1* encodes a membrane protein directly involved in Fe(III) uptake. Nature 409, 346-349.

Dannenhoffer J M, Suhr R C and Thompson G A 2001 Phloem-specific expression of the pumpkin fruit trypsin inhibitor. Planta 212, 155-162.

Davies D D 1973 Control of and by pH. Symp. Soc. Exp. Biol. 27, 513-529.

De Nisi P and Zocchi G 2000 Phospho*enol*pyruvate carboxylase in cucumber (*Cucumis sativus* L.) roots under iron deficiency: activity and kinetic characterization. J. Exp. Bot. 51, 1903-1909.

De Nisi P and Zocchi G 2002 Immunodetection of H^+-ATPase and PEPC in roots of cucumber grown under Fe-deficiency. *In* 11th International Symposium on Iron Nutrition and Interactions in Plants, Udine, Italy, 2002, pp 70.

De Nisi P, Chittò P and Zocchi G 2004 Local and systemic signals in the regulation of responses to Fe-deficiency. *In* XII International Symposium on Iron Nutrition and Interactions in Plants, Tokio, Japan, pp 26.

de Vos C R, Lubberding H J and Bienfait H F 1986 Rhizosphere acidification as a response to iron deficiency in bean plants. Plant Physiol. 81, 842-846.

Dell'Orto M, Santi S, De Nisi P, Cesco S, Varanini Z, Zocchi G and Pinton R 2000 Development of Fe-deficiency responses in cucumber (Cucumis sativus L.) roots: involvement of plasma membrane H^+-ATPase activity. J Exp Bot 51, 695-701.

Dell'Orto M, Pirovano L, Villalba J M, González-Reyes J A and Zocchi G 2002 Localization of the plasma membrane H^+-ATPase in Fe-deficient cucumber roots by immunodetection. Plant Soil 241, 11-17.

DiDonato R J Jr, Roberts L A, Sanderson T, Eisley R B and Walker E L 2004 *Arabidopsis* Yellow Stripe-Like2 (*YSL2*): a metal-regulated gene encoding a plasma membrane transporter of nicotianamine-metal complexes. Plant J. 39, 403-414.

Dinkelaker B, Hengeler C and Marschner H 1995 Distribution and function of proteoid roots and other root clusters. Bot. Acta 108, 183-200.

Duff S and Chollet R 1995 *In vivo* regulation of wheat-leaf phosphoenolpyruvate carboxylase by reversible phosphorylation. Plant Physiol. 107, 775-782.

Dunahay T G, Staehelin L A, Seibert M, Ogilvie P D and Berg S P 1984 Structural, biochemical and biophysical characterization of four oxygen-evolving photosystem II preparations from spinach. Biochim. Biophys. Acta 764, 179-193.

Echevarría C, Pacquit V, Bakrim N, Osuna L, Delgado B, Arrio-Dupont M and Vidal J 1994 The effect of pH on the covalent and metabolic control of C4 phosphoenolpyruvate carboxylase from Sorghum leaf. Arch. Biochem. Biophys. 315, 425-430.

Eckhardt U, Mas Marques A and Buckhout T J 2001 Two iron-regulated cation transporters from tomato complement metal uptake-deficient yeast mutants. Plant Mol. Biol. 45, 437-448.

Edding J L and Brown A L 1967 Absorption and translocation of foliar-applied iron. Plant Physiol. 42, 15-19.

Eide D, Brodenius M, Fett J and Guerinot M L 1996 A novel iron-regulated metal transporter from plants identified by functional expression in yeast. P. Natl. Acad. Sci. USA 93, 5624-5628.

Espen L, Dell'Orto M, De Nisi P and Zocchi G 2000 Metabolic responses in cucumber (*Cucumis sativus* L.) roots under Fe-deficiency: a ^{31}P-nuclear magnetic resonance in-vivo study. Planta 210, 985-992.

Fiehn O 2003 Metabolic networks of *Cucurbita maxima* phloem. Phytochemistry 62, 875-886.

Fisher D B, Wu Y and Ku M S B 1992 Turnover of soluble proteins in the wheat sieve tube. Plant Physiol. 100, 1433-1441.

Fox T C and Guerinot M L 1998 Molecular biology of cation transport in plants. Annu. Rev. Plant Physiol. Plant Mol. Biol. 49, 669-676.

Fox T C, Schaff J E, Grusak M A, Norvell W A, Chen Y, Chaney R L and Kochian L V 1996 Direct measurement of Fe ^{59}-labeled Fe^{2+} influx in roots of pea using a chelator buffer system to control free Fe^{2+} in solution. Plant Physiol. 111, 93-100.

Franceschi V R and Tarlyn N M 2002 L-ascorbic acid is accumulated in source leaf phloem and transported to sink tissues in plants. Plant Physiol. 130, 649-656.

Gaymard F, Pilot G, Lacombe B, Bouchez D, Bruneau D, Boucherez J, Michaux-Ferriere N, Thibaud J B and Sentenac H 1998 Identification and

disruption of a plant shaker-like outward channnel involved in K^+ release into the xylem sap. Cell 94, 647-655.

Gerke J 1997 Aluminum and iron (III) species in the soil solution including organic complexes with citrate and humic substances. Pflanzener. Bodenk. 160, 427-432.

Gilbert G A, Vance C P and Allan D L 1998 Regulation of white lupin root metabolism by phosphorus availability. *In* Phosphorus in plant biology: regulatory roles in molecular, cellular, organismic and ecosystem proceses. Eds. JP Lynch and J Deikman, pp157-167, ASPP.

Gitan R S and Eide D 2000 Zinc-regulated ubiquitin conjugation signals endocytosis of the yeast ZRT1 zinc transporter. Biochem. J. 346, 329-336.

Gogorcena Y, Abadía J and Abadía A 2000 Induction of in vivo root ferric chelate-reductase activity in the fruit tree rootstock *Prunus amygdalo-persica*. J. Plant Nutr. 23, 9-21.

Gogorcena Y, Molías N, Larbi A, Abadía J and Abadía A 2001 Characterization of the responses of cork oak (*Quercus suber*) to iron deficiency. Tree Physiol. 21, 1335-1340.

González-Vallejo E B 2000 Caracterización de mecanismos de adquisición de Fe en plantas superiores. Universidad de Zaragoza, Zaragoza, España.

González-Vallejo E B, Morales F, Cistué L, Abadía A and Abadía J 2000 Iron deficiency decreases the Fe(III)-chelate reducing activity of leaf protoplasts. Plant Physiol. 122, 337-344.

Granier F 1988 Extraction of plant proteins for two-dimensional electrophoresis. Electrophoresis 9, 712-718.

Green L S and Rogers E E 2004 *FRD3* controls iron localization in *Arabidopsis*. Plant Physiol. 136, 2523-2531.

Gries D and Runge M 1995 Responses of calcicole and calcifuge *Poaceae* species to iron-limiting conditions. Bot. Acta 108, 482-489.

Grime J P and Hutchinson T C 1967 The incidence of lime-chlorosis in the natural vegetation of England. J. Ecol. 55, 557-566.

Gross J, Stein R J, Fett-Neto A G and Fett J P 2003 Iron homeostasis related genes in rice. Genet. Mol. Biol. 26, 477-497.

Grusak M A and Pezeshgi S 1996 Shoot-to-root signal transmission regulates root Fe(III) reductase activity in the *dgl* mutant of pea. Plant Physiol. 110, 329-334.

Grusak M A, Welch R M and Kochian L V 1990a Physiological characterization of a single-gene mutant of *Pisum sativum* exhibiting excess iron accumulation. I Root iron reduction and iron uptake. Plant Physiol. 93, 976-981.

Grusak M A, Welch R M and Kochian L V 1990b Does iron deficiency in *Pisum sativum* enhance the activity of the root plasmalemma iron transport protein? Plant Physiol. 94, 1353-1357.

Guerinot M L and Yi Y 1994 Iron: nutritious, noxious, and not readily available. Plant Physiol. 104, 815-820.

Guikema J A and Sherman L A 1983 Chlorophyll-protein organization of membranes from the cyanobacterium *Anacystis nidulans*. Arch. Biochem. Biophys. 220, 155-166.

Haebel S and Kehr J 2001 Matrix-assisted laser desorption/ionization time of flight mass spectrometry peptide mass fingerprints and post source decay: a tool for the identification and analysis of phloem proteins from *Cucurbita maxima* Duch. separated by two-dimensional polyacrylamide gel electrophoresis. Planta 213, 586-593.

Harper J F, Manney L, DeWitt N D, Yoo M H and Sussman M R 1990 The *Arabidopsis thaliana* plasma membrane H(+)-ATPase multigene family. Genomic sequence and expression of a third isoform. J. Biol. Chem. 265, 13601-13608.

Hayashi H, Ueno Y and Okamoto T 1993 Oxidoreductive regulation of nuclear factor kB. J. Biol. Chem. 268, 11380-11388.

Hayashi H, Fukuda A, Suzui N and Fujimaki S 2000 Proteins in the sieve element-companion cell complexes: their detection, localization and possible functions. Aust. J. Plant Physiol. 27, 489-496.

Heinemeyer J, Eubel H, Wehmhoner D, Jansch L and Braun H P 2004 Proteomic approach to characterize the supramolecular organization of photosystems in higher plants. Phytochem. 65, 1683-1692.

Hell R and Stephan U W 2003 Iron uptake, trafficking and homeostasis in plants. Planta 216, 541-551.

Herbik A, Giritch A, Horstmann C, Becker R, Balzer H J, Bäumlein H and Stephan U W 1996 Iron and copper nutrition-dependent changes in protein expression in a tomato wild type and the nicotianamine-free mutant *chloronerva*. Plant Physiol. 111, 533-540.

Herranen M, Battchikova N, Zhang P, Graf A, Sirpio S, Paakkarinen V and Aro E M 2004 Towards functional proteomics of membrane protein complexes in *Synechocystis* sp. PCC 6803. Plant Physiol 134, 470-481.

Hether N H, Olsen R A and Jackson L L 1984 Chemical identification of iron reductants exuded by plant roots. J. Plant Nutr. 7, 667-676.

Higgins D G, Thompson J D and Gibson T J 1994 CLUSTAL W: improving the sensitivity of progressive multiple sequence alignment through sequence weighting, position-specific gap penalties and weight matrix choice. Nucleic Acids Res. 22, 4673-4680.

Higuchi K, Suzuki K, Nakanishi H, Yamaguchi H, Nishizawa N K and Mori S 1999 Cloning of nicotianamine synthase genes, novel genes involved in the biosynthesis of photosiderophores. Plant Physiol. 119, 471-479.

Hippler M, Klein J, Fink A, Allinger T and Hoerth P 2001 Towards functional proteomics of membrane protein complexes: analysis of thylakoid membranes from *Chlamydomonas reinhardtii*. Plant J. 28, 595-606.

Hoffmann-Benning S, Gage D A, McIntosh L, Kende H and Zeevaart J A D 2002 Comparison of peptides in the phloem sap of flowering and non-flowering *Perilla* and lupine plants using microbore HPLC followed by matrix-assisted laser desorption/ionization time-of-flight mass spectrometry. Planta 216, 140-147.

Huffaker R C, Hall D O, Wallace A and Rhoads W A 1959 Effects of iron and chelating agents on dark carboxylation reactions in plant homogenates. Plant Physiol. 34, 446-449.

Hutchinson T C 1967 Coralloid root systems in plants showing lime-induced chlorosis. Nature 214, 943-945.

Ishiwatari Y, Honda C, Kawashima I, Nakamura S, Hirano H, Mori S, Fujiwara T, Hayashi H and Chino M 1995 Thioredoxin h is one of the major proteins in rice phloem sap. Planta 195, 456-463.

Jebanathirajah J A and Coleman J R 1998 Association of carbonic anhydrase with a Calvin cycle enzyme complex. Planta 204, 177-182.

Jiao J, Echevarría C, Vidal J and Chollet R 1991 Protein turnover as a component in the light/dark regulation of phosphoenolpyruvate carboxylase protein-serine kinase activity in C4 plants. P. Natl. Acad. Sci. USA 88, 2712-2715.

Jolley V D, Brown J C, Pushnik J C and Miller G W 1987 Influences of ultraviolet(uv)-blue light radiation on the growth of cotton. I. Effect on iron nutrition and iron stress response. J. Plant Nutr. 10, 333-351.

Jones D L 1998 Organic acids in the rizosphere- A critical review. Plant Soil 205, 25-44.

Jones D L and Darrah P R 1995 Influx and efflux of organics acids across the soil-root interface of *Zea mays* L. and its implications in rizosphere C flow. Plant Soil 173, 103-109.

Jones D L, Darrah P R and Kochian L V 1996 Critical-evaluation of organic-acid mediated iron dissolution in the rizosphere and its potential role in root iron uptake. Plant Soil 180, 57-66.

Jordan D B, Bacot K O, Carlson T J, Kessel M and Viitanen P V 1999 Plant riboflavin biosynthesis. J. Biol. Chem. 274, 22114-22121.

Kannan S and Seshadri K 1988 Physiology responses associated with Fe-deficiency stress in different plant species. J. Plant Nutr. 11, 1185-1192.

Kehr J, Haebel S, Blechschmidt-Schneider S, Willmitzer L, Steup M and Fisahn J 1999 Analysis of phloem protein patterns from different organs of *Cucurbita maxima* Duch. by matrix-assisted laser desorption/ionization time of flight mass spectroscopy combined with sodium dodecyl sulfate polyacrylamide gel electrophoresis. Planta 207, 612-619.

Kieselbach T, Bystedt M, Hynds P, Robinson C and Schröder W P 2000 A peroxidase homoloque and novel plastocyanin located by proteomics to the *Arabidpsis* chloroplast thylakoid lumen. FEBS lett. 480, 271-276.

King R W and Zeevaart J A D 1974 Enhancement of phloem exudation from cut petioles by chelating agents. Plant Physiol. 53, 96-103.

Klausner R D, Rouault T A and Harford J B 1993 Regulating the fate of mRNA: the control of cellular iron metabolism. Cell 72, 19-28.

Köhler B, Wegner L H, Osipov V and Raschke K 2002 Loading of nitrate into the xylem: apoplastic nitrate controls the voltage dependence of X-QUAC, the main anion conductance in xylem-parenchyma cells of barley roots. Plant J. 30, 133-142.

Koike S, Inoue H, Mizuno D, Takahashi M, Nakanishi H, Mori S and Nishizawa N K 2004 OsYSL2 is a rice metal-nicotianamine transporter that is regulated by iron and expressed in the phloem. Plant J. 39, 415-424.

Korshunova Y O, Eide D, Clark W G, Guerinot M L and Pakrasi H B 1999 The IRT1 protein from *Arabidopsis thaliana* is a metal transporter with a broad substrate range. Plant Mol. Biol. 40, 37-44.

Kramer D, Römheld V, Landsberg E C and Marschner H 1980 Induction of transfer-cell formation by iron deficiency in the root epidermis of *Helianthus annuus* L. Planta 147, 335-339.

Krüger C, Berkowitz O, Stephan U W and Hell R 2002 A metal-binding member of the Late Embryogenesis Abundant Protein family transports iron in the phloem of *Ricinus communis* L. J. Biol. Chem. 277, 25062-25069.

Kügler M, Jänsch L, Kruft V, Schmitz U K and Braun H P 1997 Analysis of the chloroplast protein complexes by blue-native polyacrylamide gel electrophoresis (BN-PAGE). Photosynth. Res. 53, 35-44.

Laemmli U K 1970 Cleavage of structural proteins during the assembly of the head of bacteriophage T4. Nature 227, 680-685.

Lance C and Rustin P 1984 The central role of malate in plant metabolism. Physiol. Veg. 22, 625-641.

Landsberg E C 1981 Organic acid synthesis and release of hydrogen ions in response to iron deficiency stress of mono and dicotyledoneous plant species. J. Plant Nutr. 3, 579-591.

Landsberg E C 1982 Transfer cell formation in the root epidermis: A prerequisite for Fe-efficiency? J. Plant Nutr. 5, 415-432.

Landsberg E C 1986 Function of rhizodermal transfer cells in the Fe stress response mechanisms of *Capsicum annuum* L. Plant Physiol. 82, 511-517.

Landsberg E C 1994 Transfer cell formation in sugar beet roots induced by latent Fe deficiency. Plant Soil 165, 197-205.

Landsberg E C 1996 Hormonal regulation of iron-stress response in sunflower roots: a morphological and cytological investigation. Protoplasma 194, 69-80.

Larbi A, Morales F, López-Millán A F, Gogorcena Y, Abadía A, Moog P R and Abadía J 2001 Technical advance: Reduction of Fe(III)-chelates by mesophyll leaf disks of sugar beet. Multi-component origin and effects of Fe deficiency. Plant Cell Physiol. 42, 94-105.

Li L, Cheng X and Ling H Q 2004 Isolation and characterization of Fe(III)-chelate reductase gene *LeFRO1* in tomato. Plant Mol. Biol. 54, 125-136.

Lindsay W L and Schwab A P 1982 The chemistry of iron soils and its availability to plants. J. Plant Nutr. 5, 821-840.

Ling H Q, Pich A, Scholz G and Ganal M W 1996 Genetic analysis of two tomato mutants affected in the regulation of iron metabolism. Mol. Gen. Genet. 252, 87-92.

Ling H Q, Bauer P, Bereczky Z, Keller B and Ganal M 2002 The tomato *fer* gene encoding a bHLH protein controls iron-uptake responses in roots. P. Natl. Acad. Sci. USA 99, 13938-13943.

Liu J, Adler K and Stephan U W 1998 Iron-containing particles accumulate in organelles and vacuoles of leaf and root cells in thenicotianamine-free tomato mutant *chloronerva*. Protoplasma 201, 213-220.

Loeppert R H 1986 Reactions of iron and carbonates in calcareous soils. J. Plant Nutr. 9, 195-214.

Loeppert R H and Hallmark C T 1985 Indigenous soil properties influencing the availability of iron in calcareous soils. Soil Sci. Soc. Am. J. 49, 597-603.

López-Millán A F, Morales F, Andaluz S, Gogorcena Y, Abadía A, De Las Rivas J and Abadía J 2000a Responses of sugar beet roots to iron deficiency. Changes in carbon assimilation and oxygen use. Plant Physiol. 124, 885-898.

López-Millán A F, Morales F, Abadía A and Abadía J 2000b Effects of iron deficiency on the composition of the leaf apoplastic fluid and xylem sap in sugar beet. Implications for iron and carbon transport. Plant Physiol. 124, 873-884.

López-Millán A F, Morales F, Abadía A and Abadía J 2001a Changes induced by Fe deficiency and Fe resupply in the organic acid metabolism of sugar beet (*Beta vulgaris*) leaves. Physiol. Plant. 112, 31-38.

López-Millán A F, Morales F, Gogorcena Y, Abadía A and Abadía J 2001b Iron resupply-mediated deactivation of Fe-deficiency stress responses in roots of sugar beet. Aust. J. Plant Physiol. 28, 171-180.

López-Millán A F, Ellis R and Grusak M A 2004 Identification and characterization of several new members of the ZIP family of metal ion transporters in *Medicago truncatula*. Plant Mol. Biol. 54, 583-596.

López-Millán A F, Musetti V and Grusak M A 2005 Identification and characterization of a Fe (III)-reductase, MtFRO-1, in *Medicago truncatula*. Enviado a Funct. Biol.

Lowry O H, Rosebrough N J, Farr A L and Randall R J 1951 Protein measurement with the Folin phenol reagent. J. Biol. Chem. 193, 265-275.

Lucas W J, Yoo B C and Kragler F 2001 RNA as a long-distance information macromolecule in plants. Nat. Rev. Mol. Cell Biol. 2, 849-857.

Maas F M, van de Wetering D A M, van Beusichem M L and Bienfait H F 1988 Characterization of phloem iron and its possible role in the regulation of Fe-efficiency reactions. Plant Physiol. 87, 167-171.

Marentes E and Grusak M A 1998 Mass determination of low-molecular-weight proteins in phloem sap using matrix-assisted laser desorption/ionization time-of-flight mass spectrometry. J. Exp. Bot. 49, 903-911.

Marentes E, Shelp B J, Vanderpool R A and Spiers G A 1997 Retranslocation of boron in broccoli und lupin during early reproductive growth. Physiol. Plant. 100, 389-399.

Marschner H 1995 Mineral Nutrition of Higher Plant. Academic Press, London.

Marschner H and Römheld V 1994 Strategies of plants for acquisition of iron. Plant Soil 165, 261-274.

Marschner H, Römheld V and Kissel M 1986 Different strategies in higher plants in mobilization and uptake of iron. J. Plant Nutr. 9, 695-713.

Mathesius U, Keijzers G, Natera S H, Weinman J J, Djordjevic M A and Rolfe B G 2001 Establishment of a root proteome reference map for the model legume *Medicago truncatula* using the expressed sequence tag database for peptide mass fingerprinting. Proteomics 1, 1424-1440.

Mengel K 1994 Iron availability in plant tissues - Iron chlorosis on calcareous soils. Plant Soil 165, 275-283.

Mengel K and Geurtzen G 1986 Iron chlorosis on calcareous soils. Alkaline nutritional condition as the cause for the chlorosis. J. Plant Nutr. 9, 161-173.

Meyer I, Grosset J, Chartier Y and Cleyet-Marel J C 1988 Preparation by two-dimensional electrophoresis of proteins for antibody production: antibody against proteins whose synthesis is reduced by auxin in tobacco mesophyll protoplasts. Electrophoresis 9, 704-712.

Molloy M P 2000 Two-dimensional electrophoresis of membrane proteins using immobilized pH gradients. Anal. Biochem. 280, 1-10.

Moog P R and Brüggemann W 1994 Iron reductase systems on the plant plasma membrane- A review. Plant Soil 165, 241-260.

Moog P R and Brüggemann W 1995 Iron reductase systems on the plant plasma membrane- A review. *In* Iron nutrition in soils and plants. Ed J Abadía. pp 343-362. Kluwer Academic Publishers, Dordrecht, The Netherlands.

Moog P R, van der Kooij T A W, Brüggemann W, Schiefelbein J W and Kuiper P J C 1995 Responses to iron deficiency in *Arabidopsis thaliana*: The turbo iron reductase does not depend on the formation of root hairs and transfer cells. Planta 195, 505-513.

Morales F, Abadía A and Abadía J 1990 Characterization of the xanthophyll cycle and other photosynthetic pigment changes induced by iron deficiency in sugar beet (*Beta vulgaris* L.). Plant Physiol. 94, 607-613.

Morales F, Cerovic Z G and Moya I 1994 Characteristics of blue-green fluorescence in the mesophyll of sugar beet (*Beta vulgaris* L.) leaves affected by iron deficiency. Plant Physiol. 106, 127-133.

Morales F, Grasa R, Abadía A and Abadía J 1998 Iron chlorosis paradox in fruit trees. J. Plant Nutr. 21, 815-825.

Morales F, Grasa R, Gogorcena Y, Abadía A and Abadía J 2000a Where is iron located in iron-chlorotic peach leaves? *In* 10th International Symposium on Iron Nutrition and Interactions in Plants, pp 99, Houston, Texas USA.

Morales F, Belkhodja R, Abadía A and Abadía J 2000b Photosystem II efficiency and mechanisms of energy dissipation in iron-deficient, field-grown pear trees (*Pyrus communis* L.). Photosynth. Res. 63, 9-21.

Morales F, Moise N, Quílez R, Abadía A, Abadía J and Moya I 2001 Iron deficiency interrupts energy transfer from a disconnected part of the antenna to the rest of photosystem II. Photosynth. Res. 70, 207-220.

Mori S 1998 Iron transport in graminaceous plants. *In* Metal ions in biological systems, Eds A Siegel and H Sigel, pp 215-238, Basel, Switzerland.

Mori S 1999 Iron acquisition by plants. Curr. Opin. Plant Biol. 2, 250-253.

Moseley J L, Allinger T, Herzog S, Hoerth P, Wehinger E, Merchant S and Hippler M 2002 Adaptation to Fe-deficiency requires remodeling of the photosynthetic apparatus. Embo J. 21, 6709-6720.

Münch E 1930 Die Stoffwebegungen in der Pflanze. G. Fisher, Jena, Germany.

Murgia I, Delledonne M and Soave C 2002 Nitric oxide mediates iron-induced ferritin accumulation in *Arabidopsis*. Plant J. 30, 521-528.

Nakamura S, Hayashi H, Mori S and Chino M 1995 Detection and characterization of protein kinases in rice phloem sap. Plant Cell Physiol. 36, 19-27.

Nakanishi H, Okumura N, Umehara Y, Nishizawa N K, Chino M and Mori S 1993 Expression of a gene specific for iron deficiency (*Ids3*) in the roots of *Hordeum vulgare*. Plant Cell Physiol. 34, 401-410.

Negishi T, Nakanishi H, Yazaki J, Kishimoto N, Fujii F, Shimbo K, Yamamoto K, Sakata K, Sasaki T, Kikuchi S, Mori S and Nishizawa N K 2002 cDNA microarray analysis of gene expression during Fe-deficiency stress in barley suggests that polar transport of vesicles is implicated in phytosiderophore secretion in Fe-deficient barley roots. Plant J. 30, 83-94.

Ngo T T and enhoff H M 1980 A sensitive and versatile chromogenic assay for peroxidase and peroxidase-coupled reactions. Anal. iochem. 105, 389-397.

Nhiri M, akrim N, akrim N, El Hachimi-Messouak , Echevarria C and idal J 2000 Post-translational regulation of phosphoenolpyruvate carboxylase during germination of *Sorghum* seeds: influence of NaCl and L-malate. Plant Sci. 151, 29-37.

Nishio J N, Abadía J and Terry N 1985 Chlorophyll-proteins and electron transport during iron nutrition-mediated chloroplast development. Plant Physiol. 78, 296-299.

Okumura N, Nishizawa N K, Umehara Y, Ohata T, Nakanishi H, Yamaguchi T, Chino M and Mori S 1994 A dioxygenase gene (*Ids2*) expressed under iron deficiency conditions in the roots of *Hordeum vulgare*. Plant Mol. Biol. 25, 705-719.

Olsen R A, Bennett J H, Blume D and Brown J C 1981 Chemical aspects of the Fe stress response mechanism in tomatoes. J. Plant Nutr. 3, 905-921.

Oparka K J and Santa Cruz S 2000 The great escape: Phloem transport and unloading of macromolecules. Annu. Rev. Plant Physiol. Plant Mol. Biol. 51, 323-347.

Osuna L, González M C, Cejudo F J, Vidal J and Echevarría C 1996 *In vivo* and *in vitro* phosphorylation of the phosphoenolpyruvate carboxylase from wheat seeds during germination. Plant Physiol. 111, 551-558.

Osuna L, Pierre J N, González M C, Álvarez R, Cejudo F J, Echevarría C and Vidal J 1999 Evidence for a slow-turnover form of the Ca^{2+}-independent phosphoenolpyruvate carboxylase kinase in the aleurone-endosperm tissue of germinating barley seeds. Plant Physiol. 119, 511-520.

Pacquit V, Giglioli N, Crétin C, Pierre J N, Vidal J and Echevarría C 1995 Regulatory phosphorylation of C_4 phosphoenolpyruvate carboxylase from *Sorghum*: An immunological study using specific anti-phophorylation site-antibodies. Photosynth. Res. 43, 283-288.

Pakrasi H B, Riethman H C and Sherman L A 1985 Organization of pigment proteins in the photosystem II complex of the cyanobacterium *Anacystis nidulans* R2. P. Natl. Acad. Sci. USA 82, 6903-6907.

Palauqui J C, Elmayan T, De Borne F D, Crete P, Charles C and Vaucheret H 1996 Frequencies, timing and spatial patterns of co-suppression of nitrate reductase and nitrite reductase in transgenic tobacco plants. Plant Physiol. 112, 1447-1456.

Palmgren M G 2001 Plant plasma membrane H^+-ATPases: powerhouses for nutrient uptake. Annu. Rev. Plant Physiol. Plant Mol. Biol. 52, 817-845.

Paulsen H, Finkenzeller B and Kuhlein N 1993 Pigments induce folding of light-harvesting chlorophyll a/b-binding protein. Eur. J. Biochem. 215, 809-816.

Peltier J B, Emanuelsson O, Kalume D E, Ytterberg J, Friso G, Rudella A, Liberles D A, Soderberg L, Roepstorff P, von Heijne G and van Wijk K J 2002 Central functions of the lumenal and peripheral thylakoid proteome of *Arabidopsis* determined by experimentation and genome-wide prediction. Plant Cell 14, 211-236.

Peltier J B, Friso G, Kalume D E, Roepstorff P, Nilsson F, Adamska I and van Wijk K J 2000 Proteomics of the chloroplast: systematic identification and targeting analysis of lumenal and peripheral thylakoid proteins. Plant Cell 12, 319-341.

Pérez-Bueno M L, Rahoutei J, Sajnani C, García-Luque I and Barón M 2004 Proteomic análisis of the oxygen-evolving complex of photosystem II under biotec stress: Studies on *Nicotiana benthamiana* infected with tobamoviruses. Proteomics 4, 418-425.

Petit J M, van Wuytswinkel O, Briat J F and Lobreaux S 2001 Characterization of an iron-dependent regulatory sequence involved in the transcriptional control of *AtFer1* and *ZmFer1* plant ferritin genes by iron. J. Biol. Chem. 276, 5584-5590.

Pich A, Scholz G and Stephan U W 1994 Iron-dependent changes of heavy metals, nicotianamine, and citrate in different plant organs and in the xylem exudate of two tomato genotypes. Nicotianamine as a possible copper translocator. Plant Soil 165, 189-196.

Pich A, Manteuffel R, Hillmer S, Scholz G and Schmidt W 2001 Fe homeostasis in plant cells: does nicotianamine play multiple roles in the regulation of cytoplasmic Fe concentration? Planta 213, 967-976.

Pinton R, Cesco S, de Nobili M, Santi S and Varanini Z 1998 Water and pyrophosphate extractable humic substances fractions as a source of iron for Fe-deficient cucumber plants. Biol. Fert. Soils 26, 23-27.

Platt-Aloia K A, Thomson W W and Terry N 1983 Changes in plastid ultrastructure during iron nutrition-mediated chloroplast development. Plant Physiol. 78, 269-299.

Pontiggia A, De Nisi P and Zocchi G 2003 Effect of iron deficiency on RNA and protein synthesis in cucumber roots. J Plant Nutr 26, 2177-2186.

Pushnik J C, Miller G W and Manwaring J H 1984 The role of iron in higher-plant chlorophyll biosynthesis, maintenance and chloroplast biogenesis. J. Plant Nutr. 7, 733-758.

Quílez R, Abadía A and Abadía J 1992 Characteristics of thylakoids and photosystem II membrane preparations from iron deficient and iron sufficient sugar beet (*Beta vulgaris* L.). J. Plant Nutr. 15, 1809-1819.

Rabotti G, De Nisi P and Zocchi G 1995 Metabolic implications in the biochemical responses to iron deficiency in cucumber (*Cucumis sativus* L.) roots. Plant Physiol. 107, 1195-1199.

Rexroth S, Meyer zu Tittingdorf J M, Krause F, Dencher N A and Seelert H 2003 Thylakoid membrane at altered metabolic state: challenging the forgotten realms of the proteome. Electrophoresis 24, 2814-2823.

Riethman H C and Sherman L A 1988 Purification and characterization of an iron stress-induced chlorophyll-protein from the cyanobacterium *Anacystis nidulans* R2. Biochim. Biophys. Acta 935, 141-151.

Robinson N, Procter C, Connolly E and Guerinot M 1999 A ferric-chelate reductase for iron uptake from soils. Nature 397, 694-697.

Rogers E E and Guerinot M L 2002 FRD3, a member of the multidrug and toxin efflux family, controls iron deficiency responses in *Arabidopsis*. Plant Cell 14, 1787-1799.

Rogers E E, Eide D J and Guerinot M L 2000 Altered selectivity in an Arabidopsis metal transporter. P. Natl. Acad. Sci. USA 97, 12356-12360.

Rombolà A D 1998 Aspetti fisiologici e biochimici della nutrizione ferrica in actinidia (*A. deliciosa*). PhD Thesis *In* Dipartimento di Colture Arboree. Universitá degli Studi di Bologna, Bologna.

Rombolà A D, Gogorcena Y, Larbi A, Morales F, Baldi E, Marangoni B, Tagliavini M and Abadía J 2005 Iron deficiency-induced changes in carbon fixation and leaf elemental composition of sugar beet (*Beta vulgaris*) plants. Plant Soil 271, 39-45.

Romera F J and de la Guardia M D 1991 La nutrición férrica de las plantas. Grupo Gestión Editorial, Córdoba. ISBN 84-7801-135-8.

Romera F J, Alcántara E and de la Guardia M D 1992 Role of roots and shoots in the regulation of the Fe efficiency responses in sunflower and cucumber. Physiol. Plant. 85, 141-146.

Romera F J, Welch R M, Norwell W A, Schaefer S C and Kochian L V 1996a Ethylene involvement in the over-expression of Fe(III)-chelate reductase by roots of *E107* pea [*Pisum sativum* L. (*brz, brz*)] and *chloronerva* tomato (*Licopersicon esculentum* L.) mutant genotypes. Biometals 9, 38-44.

Romera F J, Welch R M, Norwell W A and Schaefer S C 1996b Iron requirement for and effects of promoters and inhibitors of ethylene action on stimulation of Fe(III)-chelate reductase in roots of strategy I species. Biometals 9, 45-50.

Römheld V 1997 The chlorosis paradox: Fe inactivation in leaves as a secondary event in Fe deficiency chlorosis. *In* Ninth International Symposium on Iron Nutrition and Interactions in Plants, Stuttgart, 1997. pp. 10.

Römheld V and Marschner H 1981 Iron deficiency stress induced morphological and physiological changes in root tips of sunflower. Physiol. Plant. 53, 354-360.

Römheld V and Marschner H 1983 Mechanism of iron uptake by peanut plants. I. Fe(III) reduction, chelate splitting, and release of phenolics. Plant Physiol. 71, 949-954.

Römheld V, Müller C and Marschner H 1984 Localization and capacity of proton pumps in roots of intact sunflower plants. Plant Physiol. 76, 603-606.

Rosenfield C L, Reed D W and Kent M W 1991 Dependency of iron reduction on developement of a unique root morphology in *Ficus benjamina* L. Plant Physiol. 95, 1120-1124.

Ruiz-Medrano R, Xoconostle-Cazares B and Lucas W J 2001 The phloem as a conduit for inter-organ communication. Curr. Opin. Plant Biol. 4, 202-209.

Sakaguchi T, Nishizawa N K, Nakanishi H, Yoshimura E and Mori S 1999 The role of potassium in the secretion of mugineic acids family phytosiderophores from iron-deficient barley roots. Plant Soil 215, 221-227.

Sakuth T, Schobert C, Pecsvaradi A, Eichholz A, Komor E and Orlich G 1993 Specific proteins in the sieve-tube exudate of *Ricinus communis* L. seedling conteins ubiquitin and chaperones. Planta 191, 207-213.

Santi S, Schmidt W, Varanini Z and Pinton R 2004 Water soluble humic substances and Fe-deficiency induce three *AHA* genes in *Arabidopsis*. *In* XII International symposium on iron nutrition and interactions in plants, pp 202, Tokio, Japan.

Santi S, Cesco S, Varanini Z and Pinton R 2005 Two plasma membrane H^+-ATPase genes are differentially expressed in iron-deficient cucumber plants. Plant Physiol. Bioch. 43, 287-292.

Santoni V, Molloy M and Rabilloud T 2000 Membrane proteins and proteomics: Un amour impossible? Electrophoresis 21, 1054-1070.

Sanz M, Cavero J and Abadía J 1992 Iron chlorosis in the Ebro river basin, Spain. J. Plant Nutr. 15, 1971-1981.

Schaaf G, Schikora A, Häberle J, Vert G, Ludewig U, Briat J F, Curie C and von Wirén G 2005 A putative function for the *Arabidopsis* Fe-phytosiderophore transporter homolog AtYSL2 in Fe and Zn homeostasis. Plant Cell Physiol. 46, 762-774.

Schägger H and von Jagow G 1991 Blue native electrophoresis for isolation of membrane protein complexes in enzymatically active form. Anal. Biochem. 199, 223-231.

Schägger H, Cramer W A and von Jagow G 1994 Analysis of molecular masses and oligomeric states of protein complexes by blue native electrophoresis and isolation of membrane protein complexes by two-dimensional native electrophoresis. Anal. Biochem. 217, 220-230.

Schevchenko A, Wilm M, Vorm O, Mann M 1996 Mass spectrometric sequencing of proteins from silver stained polyacrylamide gels. Anal. Chem. 68, 850-858.

Schikora A and Schmidt W 2001 Iron stress-induced changes in root epidermal cell fate are regulated independently from physiological responses to low iron availability. Plant Physiol 125, 1679-1687.

Schmidt W 1993 Iron stress-induced redox reactions in bean roots. Physiol. Plant. 89, 448-452.

Schmidt W 1999 Mechanisms and regulation of reduction-based iron uptake in plants. New Phytol. 141, 1-26.

Schmidt W 2003 Iron solutions: acquisition strategies and signaling pathways in plants. Trends Plant Sci. 8, 188-193.

Schmidt W and Janiesch P 1991 Ferric reduction by *Geum urbanum*: a kinetic study. J. Plant Nutr. 14, 1023-1034.

Schmidt W and Bartels M 1996 Formation of root epidermal transfer cells in *Plantago*. Plant Physiol. 110, 217-225.

Schmidt W and Schuck C 1996 Pyridine nucleotide pool size changes in iron-deficient *Plantago lanceolata* roots during reduction of external oxidants. Physiol. Plant. 98, 215-221.

Schmidt W and Buckhout T J 1997 The response of tomato roots (*Lycopersicon esculentum* Mill.) to iron deficiency stress: alterations in the pattern of protein synthesis. J. Exp. Bot. 48, 1909-1918.

Schmidt W, Boomgaarden B and Ahrens V 1996 Reduction of root iron in *Plantago lanceolata* during recovery from Fe deficiency. Physiol. Plant. 98, 587-593.

Schmidt W, Michalke W and Schikora A 2003 Proton pumping by tomato roots. Effect of Fe deficiency and hormones on the activity and distribution of plasma membrane H^+-ATPase in rhizodermal cells. Plant Cell and Environ. 26, 361-370.

Schobert C, Großmann P, Gottschalk M, Komor E, Pecsvaradi A and Nieden U Z 1995 Sieve-tube exudate from *Ricinus communis* L. seedling contains ubiquitin and chaperones. Planta 196, 205-210.

Schobert C, Baker L, Szederkényi J, Großmann P, Komor E, Hayashi H, Chino M and Lucas W J 1998 Identification of immunologically related proteins in sieve-tube exudate collected from monocotyledonous and dicotyledonous plants. Planta 206, 245.252.

Scholz G, Becker R, Pich A and Stephan U W 1992 Nicotianamine- a common constituent of Strategies I and II of iron acquisition in plants. A review. J. Plant Nutr. 15, 1649-1665.

Schuller K A and Werner D 1993 Phosphorylation of soybean (*Glycine max* L.) nodule phosphoenolpyruvate carboxylase *in vitro* decreases sensitivity to inhibition by L-malate. Plant Physiol. 101, 1267-1273.

Schuller K A, Plaxton W C and Turpin D H 1990a Regulation of phosphoenolpyruvate carboxylase from the green alga *Selenastrum minutum*: properties associated with replenishment of tricarboxylic acid cycle intermediates during ammonium assimilation. Plant Physiol. 93, 1303-1311.

Schuller K A, Turpin D H and Plaxton W C 1990b Metabolite regulation of partially purified soybean nodule phosphoenolpyruvate carboxylase. Plant Physiol. 94, 1429-1435.

Shingles R, North M and McCarty R E 2002 Ferrous ion transport across chloroplast inner envelope membranes. Plant Physiol. 128, 1022-1030.

Shinmachi F, Hasegawa I and Yazaki J 1992 Analysis of iron-deficiency response systems on the plant root using the hairy root. J. Soil Sci. Plant Nutr. 63, 202-209.

Shinmachi F, Hasegawa I and Yazaki J 1994 The relation between riboflavin secretion as a result of iron deficiency and ferric reduction system on the plant Japanese. J. Soil Sci. Plant Nutr. 65, 413-418.

Shinmachi F, Hasegawa I and Yazaki J 1995 Difference in riboflavin secretion phenomenon as a result of iron-deficiency among plant species. J. Soil Sci. Plant Nutr. 66, 337-341.

Sijmons P C and Bienfait H F 1983 Source of electrons for extracellular Fe(III) reduction in iron-deficient bean roots. Physiol. Plant. 59, 409-415.

Sijmons P C, Van der Briel W and Bienfait H F 1984 Cytosolic NADPH is the electron donor for extracellular Fe(III) reduction in iron deficient bean roots. Plant Physiol. 75, 219-221.

Sijmons P C, Kolattukudi P E and Bienfait 1985 Iron deficiency decreased suberinization in bean roots through a decrease in suberin – specific peroxidase activity. Plant Physiol. 78, 115-120.

Snowden R E D and Wheeler B D 1993 Iron toxicity to fen species. J. Ecol. 81, 35-46.

Spiller S and Terry N 1980 Limiting factors in photosynthesis. II. Iron stress diminishes photochemical capacity by reducing the number of photosynthetic units. Plant Physiol. 65, 121-125.

Stephan U W and Scholz G 1990 Nicotianamine concentrations in iron sufficient and iron deficient sunflower and barley roots. J. Plant Physiol. 136, 631-634.

Stephan U W and Scholz G 1993 Nicotianamine: mediator of transport of iron and heavy metals in the phloem? Physiol. Plant. 88, 522-529.

Stephan U W, Schmidke I and Pich A 1994 Phloem translocation of Fe, Cu, Mn and Zn in *Ricinus* seedlings in relation to the concentrations of nicotianamine, an endogenous chelator of divalent metal-ions, in different seedling parts. Plant Soil 165, 181-188.

Stephan U W, Schmidke I, Stephan V W and Scholz G 1996 The nicotianamine molecule is made-to-measure for complexation of metal micronutrients in plants. Biometals 9, 84-90.

Suckau D, Resemann A, Schuerenberg M, Hufnagel P, Franzen J and Holle A 2003 A novel MALDI LIFT-TOF/TOF mass spectrometer for proteomics. Anal. Bioanal. Chem. 376, 952-965.

Sueyoshi K, Hirata O and Oji Y 1997 Characterization of plasma membrane-bound Fe^{3+}-chelate reductase form Fe-deficient and Fe-sufficient cucumber roots. Soil Sci. Plant Nutr. 43, 149-156.

Suorsa M, Regel R E, Paakkarinen V, Battchikova N, Herrmann R G and Aro E M 2004 Protein assembly of photosystem II and accumulation of subcomplexes in the absence of low molecular mass subunits PsbL and PsbJ. Eur. J. Biochem. 271, 96-107.

Susín S 1994 Respuestas inducidas por la deficiencia de hierro en el sistema radicular de *Beta vulgaris* L. PhD Tesis. Bioquímica y Biología Molecular y Celular. Universidad de Zaragoza, Zaragoza.

Susín S, Abián J, Sánchez-Baeza F, Peleato M L, Abadía A, Gelpí E and Abadía J 1993 Riboflavin 3'- and 5'-sulfate, two novel flavins accumulating in the roots of iron-deficient Sugar Beet (*Beta vulgaris*). J. Biol. Chem. 268, 20958-20956.

Susín S, Abián J, Peleato M L, Sánchez-Baeza J, Abadía A, Gelpí E and Abadía J 1994 Flavin excretion from iron deficient sugar beet (*Beta vulgaris* L.). Planta 193, 514-519.

Susín S, Abadía A, González-Reyes J A, Lucena J J and Abadía J 1996 The pH requeriment for in vivo activity of the iron-deficiency-induced "turbo" ferric chelate reductase. A comparison of the iron-deficiency-induced iron reductase activities of intact plants and isolated plasma membrane fractions in sugar beet. Plant Physiol. 110, 111-123.

Sussman M R 1994 Molecular analysis of proteins in the plant plasma membrane. Annu. Rev. Plant Physiol. Plant Mol. Biol. 45, 211-234.

Süss K H, Arkona G, Manteuffel R and Adler K 1993 Calvin cycle multienzyme complexes are bound to chlorplast thylakoid membranes of higher plants *in situ*. P. Natl. Acad. Sci. 90, 5514-5518.

Süss K H, Prokhorenko I and Adler K 1995 *In situ* association of Calvin cycle enzymes, ribulose-1,5-bisphosphate carboxylase/oxigenase activase, ferredoxin-$NADP^+$ reductase, and nitrile reductase with thylakoid and pyrenoid membranes of *Chlamydomonas reinhardtii* chloroplasts as revealed by immunoelectron microscopy. Plant Physiol. 107, 1387-1397.

Tagliavini M, Abadía J, Rombolà A D, Abadía A, Tsipouridis C and Marangoni B 2000 Agronomic means for the control of iron chlorosis in deciduous fruit trees. J. Plant Nutr. 23, 2007-2022.

Takagi S 1976 Naturally occurring iron-chelating compounds in oat- and rice-root washings. Soil Sci. Plant Nutr. 22, 423-433.

Takahashi M, Yamaguchi H, Nakanishi H, Shioiri T, Nishizawa N K and Mori S 1999 Cloning two genes for nicotianamine aminotransferase, a critical enzyme in iron acquisition (Strategy II) in graminaceous plants. Plant Physiol. 121, 947-956.

Taylor S E, Terry N and Huston R P 1982 Limiting factors in photosynthesis. III. Effects of iron nutrition on the activities of three regulatory encimes of photosynthetic carbon metabolism. Plant Physiol. 70, 1541-1543.

Terry N 1979 The use of mineral nutrient stress in the study of limiting factors in photosynthesis. *In* Photosynthesis and Plant Development, Eds R Marcelle, H Clijsters and M Van Poucke. pp 151-160. Dr W. Junk Publishers, The Hague.

Terry N 1980 Limiting factors in photosynthesis. I. Use of iron stress to control photochemical capacity *in vivo*. Plant Physiol. 65, 114-120.

Terry N and Abadía J 1986 Function of iron in chloroplasts. J. Plant Nutr. 9, 609-646.

Thidholm E, Lindstrom V, Tissier C, Robinson C, Schroder W P and Funk C 2002 Novel approach reveals localisation and assembly pathway of the PsbS and PsbW proteins into the photosystem II dimer. FEBS Lett. 513, 217-222.

Thimm O, Essigmann B, Kloska S, Altmann T and Buckhout T J 2001 Response of *Arabidopsis* to iron deficiency stress as revealed by microarray analysis. Plant Physiol. 127, 1030-1043.

Thoiron S and Briat J F 1999 Differential expression of maize sugar responsive genes in response to iron deficiency. Plant Physiol. Bioch. 37, 759-766.

Thomine S, Wang R, Ward J M, Crawford N M and Schroeder J I 2000 Cadmium and iron transport by members of a plant metal transporter family in *Arabidopsis* with homology to *Nramp* genes. P. Natl. Acad. Sci. USA 97, 4991-4996.

Thompson G A and Schulz A 1999 Macromolecular trafficking in the phloem. Trends Plant Sci. 4, 354-360.

Tiffin L O 1966 Iron translocation. II Citrate/iron ratios in plant stem exudates. Plant Physiol. 41, 515-518.

Toyoshima C, Nakasako M, Nomura H and Ogawa H 2000 Crystal structure of the calcium pump of sarcoplasmic reticulum at 2.6 Å resolution. Nature 405, 647-655.

Tyler G and Falkengren-Grerup U 1998 Soil chemistry and plant performance ecological considerations. Progr. Bot. 59, 634-658.

van Bel A J E 2003 The phloem, a miracle of ingenuity. Plant Cell Environ. 26, 125-149.

van Goor B J and Wiersma D 1976 Chemical forms of manganese and zinc in phloem exudates. Physiol. Plant. 36, 213-216.

Vance C P, Stade S and Maxwell C A 1983 Alfalfa root nodule carbon dioxide fixation. I. Association with nitrogen fixation and incorporation into aminoacids. Plant Physiol. 72, 469-473.

Varin L, Barron D and Ibrahim R K 1987 Enzymatic assay for flavonoid sulfotransferase. Anal. Biochem. 161, 176-180.

Vert G, Grotz N, Dedaldechamp F, Gaymard F, Guerinot M L, Briat J F and Curie C 2002 IRT1, an *Arabidopsis* transporter essential for iron uptake from the soil and for plant growth. Plant Cell 14, 1223-1233.

Vert G A, Briat J F and Curie C 2003 Dual regulation of the *Arabidopsis* high-affinity root iron uptake system by local and long-distance signals. Plant Physiol. 132, 796-804.

Vidal J and Chollet R 1997 Regulatory phosphorylation of C_4 PEP carboxylase. Trends Plant Sci. 2, 230-237.

Von Wirén N, Mori S, Marschner H and Romheld V 1994 Iron inefficiency in maize mutant *ys1* (*Zea mays* L. cv Yellow-Stripe) is caused by a defect in uptake of iron phytosiderophores. Plant Physiol. 106, 71-77.

Von Wirén N, Klair S, Bansal S, Briat J F, Khodr H, Shioiri T, Leigh R A and Hider R C 1999 Nicotianamine chelates both Fe(III) and Fe(II). Implications for metal transport in plants. Plant Physiol. 119, 1107-1114.

Vose P B 1982 Iron nutrition in plants. J. Plant Nutr. 5, 233-249.

Walz C, Juenger M, Schad M and Kehr J 2002 Evidence for the presence and activity of a complete antioxidant defence system in mature sieve tubes. Plant J. 31, 189-197.

Wang Y H and Chollet R 1993 In vitro phosphorylation of purified tobacco-leaf phosphoenolpyruvate carboxylase. FEBS Lett. 328, 215-218.

Wang Y H, Garvin D F and Kochian L V 2002 Rapid induction of regulatory and transporter genes in response to phosphorus, potassium, and iron deficiencies in tomato roots. Evidence for cross talk and root/rhizosphere-mediated signals. Plant Physiol. 130, 1361-1370.

Waters B M, Blevins D G and Eide D J 2002 Characterization of FRO1, a pea ferric-chelate reductase involved in root iron acquisition. Plant Physiol. 129, 85-94.

Watson B S, Asirvatham V S, Wang L and Summer L W 2003 Mapping the proteome of barrel medic (*Medicago truncatula)*. Plant Physiol. 131, 1104-1123.

Wei L, Loeppert R and Ocumpaugh W 1997 Fe-deficiency stress response in Fe-deficiency resistant and susceptible subterranean clover - importance of induced H^+ release. J. Exp. Bot. 48, 239-246.

Welkie G W 1996 Iron-deficiency stress responses of a chlorosis-susceptible and a chlorosis-resistant cultivar of muskmelon as related to root riboflavin excretion. J. Plant Nutr. 19, 1157-1169.

Welkie G W and Miller G W 1960 Iron nutrition of *Nicotiana tabaccum* L. in relation to riboflavin, riboflavin-5'-phosphate, and flavin adenine dinucleotide content. Plant Physiol. 35, 516-520.

Welkie G W and Miller G W 1988 Riboflavin excretion from roots of iron-stressed and reciprocally grafted tobacco and tomato plants. J. Plant Nutr. 11, 691-700.

Welkie G W and Miller G W 1992 Iron stress and salt stress responses of lettuce (*Lactuca sativa* L.). J. Plant Nutr. 15, 1757-1764.

Welkie G W and Miller G W 1993 Plant iron uptake physiology by nonsiderophore systems. *In* Iron Chelation in Plants and Soil microorganisms, Eds L Barton and B Hemming. pp 345-369. Academic Press, San Diego, USA.

White M C, Decker A M and Chaney R L 1981a Metal complexation in xylem fluid. I. Chemical composition of tomato and soybean stem exudate. Plant Physiol. 67, 292-300.

White M C, Baker F D, Chaney R L and Decker A M 1981b Metal complexation in xylem fluid. II. Theoretical equilibrium model and computational computer program. Plant Physiol. 67, 301-310.

Whitelegge J P, Gomez S M and Faull K F 2003 Proteomics of membrane proteins. Adv. Protein Chem. 65, 271-307.

Winder T L and Nishio J N 1995 Early iron deficiency stress response in leaves of sugar beet. Plant Physiol. 108, 1487-1494.

Wintz H, Fox T, Wu Y Y, Feng V, Chen W, Chang H S, Zhu T and Vulpe C 2003 Expression profiles of *Arabidopsis thaliana* in mineral deficiencies reveal novel transporters involved in metal homeostasis. J. Biol. Chem. 278, 47644-47653.

Xoconostle-Cazares B, Ruiz-Medrano R and Lucas W J 2000 Proteolytic processing of CmPP36, a protein from the cytochrome b_5 reductase family, is required for entry into the phloem translocation pathway. Plant J. 24, 735-747.

Yamaguchi M, Sasaki T, Sivaguru M, Yamamoto Y, Osawa H, Ahn S J and Matsumoto H 2005 Evidence for the plasma membrane localization of Al-activated malate trasporter (ALMT1). Plant Cell Physiol. 46, 812-816.

Yamaguchi-Iwai Y, Dancis A and Klausner R D 1995 AFT1: a mediator of iron regulated transcriptional control in *Saccharomyces cerevisiae*. Embo J. 14, 1231-1239.

Yen M R, Tseng Y H and Saier M H 2001 Maize *Yellow Stripe1*, an iron-phytosiderophore uptake transporter, is a member of the oligopeptide transporter (OPT) family. Microbiology 147, 2881-2883.

Yi Y and Guerinot M L 1996 Genetic evidence that induction of root Fe(III) chelate reductase activity is necessary for iron uptake under iron deficiency. Plant J. 10, 835-844.

Young T F and Terry N 1982 Transport of iron into leaves following iron resupply to iron stressed sugar beet plants. J. Plant Nutr. 5, 1273-1283.

Zhang X Q, Li B and Chollet R 1995 *In vivo* regulatory phosphorylation of soybean nodule phosphoenolpyruvate carboxylase. Plant Physiol. 108, 1561-1568.

Zouari M 1996 Reponses radiculaires face a la deficience en fer chez differents genotypes de tomate et de betterave. Master Thesis Instituto Agrónomico Mediterraneo (CIHEAM), Zaragoza.

Zouari M, Abadía A and Abadía J 2001 Iron is required for the induction of root ferric chelate reductase activity in iron-deficient tomato. J. Plant Nutr. 24, 383-396.

Capítulo 12

ANEXOS

1. PUBLICACIONES

- López-Millán AF, Morales F, Andaluz S, Gogorcena Y, Abadía A, De Las Rivas J, Abadía J 2000 Responses of sugar beet roots to iron deficiency: changes in carbon assimilation and oxygen use. Plant Physiol. 124, 885-897.

- Andaluz S, López-Millán AF, Peleato ML, Abadía J, Abadía A 2002 Increases in phosphoenol pyruvate carboxylase activity in iron deficient sugar beet roots: Analysis of spatial localization and post-translational modification. Plant Soil 241, 75-86.

- Andaluz S, López-Millán AF, De Las Rivas J, Aro EM, Abadía J, Abadía A 2005 Proteomic profiles of thylakoid membrane proteins and changes in response to iron deficiency. Proteomics, en 2ª revisión.

- Andaluz S, Abadía A, Abadía J, López-Millán AF 2005 Effects of iron deficiency on activity and expression of several key enzymes in *Medicago truncatula* roots. Próximo envío a Plant Cell Physiology.

- Andaluz S, Abadía A, Abadía J, López-Millán AF 2005 Regulation of phosphoenol pyruvate carboxylase activity in iron deficient sugar beet roots. En preparación.

- Andaluz S, Abadía A, Abadía J, López-Millán AF 2005 Proteomic analysis of *Lupinus texensis* phloem:study of iron and zinc transporter. En preparación.

- Andaluz S, López-Millán AF, Abadía J, Abadía A 2005 Proteomic profiles of root tips proteins from *Beta vulgaris* and changes induced in response to iron deficiency. En preparación.

2. PRESENTACIONES A CONGRESOS

- XV International Plant Nutrition Colloquium. Beijing, China, 14-19 de Septiembre de 2005. Comunicación poster.

-Andaluz S, Abadía A, Abadía J, López-Millán A F. PEPC induction in roots of iron-deficient *Medicago truncatula.*

- 1st Scientific Workshop COST 859. Pisa, Italia, 14-16 de Junio de 2005. Comunicación poster.

-Andaluz S, López-Millán AF, Abadía J, Abadía A. Proteomic analysis of Lupinus texensis phloem.

- I Congress of the Spanish Proteomics Society. Córdoba, 14-17 de Febrero de 2005. Comunicación oral en inglés y comunicación poster.

-Andaluz S, López-Millán A F, De las Rivas J, Abadía J, Abadía A. Proteomic analysis of sugar beet thylakoids in response to iron deficiency. Comunicación oral en inglés.

-Andaluz S, López-Millán A F, De las Rivas J, Abadía J, Abadía A. Changes induced by iron deficiency in roots. Comunicación poster.

- COST action 859 "Phytotechnologies to promote sustainable land use and improve food safety". Kick-off meeting Working. Parma, Italia, 4-6 de Noviembre de 2004. Comunicación.

-Andaluz S, Solanas M, Álvarez-Fernández A, López-Millán AF, Abadía A, Abadía J. Metal-related metabolomics and proteomics in plants.

- XII International Symposium on Iron Nutrition and Interactions in Plants. Tokio, Japón, 11-15 de Abril de 2004. Comunicación poster.

-Andaluz S, Solanas M, Abadía J, Aro EM, Abadía A. Changes induced by iron deficiency in the thylakoid proteome of sugar beet.

- Jornadas sobre proteómica UCO 2003. Universidad de Córdoba, 5-7 de Febrero de 2003. Comunicación poster.

-Andaluz S, Abadía J, Abadía A. Plant thylakoid proteome separation by 2-D IEF-PAGE.

- IX Simposio Ibérico sobre nutrición mineral de las plantas. Zaragoza, 10-13 Septiembre de 2002. Tres comunicaciones poster.

-Andaluz S, Abadía J, Abadía A. Separación mediante electroforesis en 2-D de membranas tilacoidales y membranas enriquecidas en PSII.

-Larbi A, Andaluz S, Morales F, Abadía J, Abadía A. Efecto del aporte de Fe sobre la composición en ácidos orgánicos en xilema y apoplasto de plantas de remolacha deficientes en Fe.

-Larbi A, Andaluz S, Morales F, Abadía J, Abadía A. Cambios producidos por el tratamiento de Fe sobre la composición en ácidos orgánicos en xilema de melocotonero.

- COST action 837 "Phytoremediation of trace elements in contaminated soils and waters (with special emphasis on Zn, Cd, Pb and As". Madrid, 5-7 de Abril de 2001. Comunicación poster.

-Gogorcena Y, Larbi A, Andaluz S, Abadía J, Abadía A. Physiological and morphological responses of cork oak to cadmium.

- 10^{th} International Symposium on Iron Nutrition and Interactions in Plants. Houston, Texas, USA, 14-19 de Mayo de 2000. Comunicación poster.

-Andaluz S, López-Millán AF, Peleato ML, Abadía J, Abadía A. Phosphoenol pyruvate carboxylase: a key enzyme in iron deficient sugar beet roots.

Plant and Soil **241:** 43–48, 2002.

Increases in phospho*enol*pyruvate carboxylase activity in iron-deficient sugar beet roots: Analysis of spatial localization and post-translational modification

Sofía Andaluz[1], Ana-Flor López-Millán[1], María Luisa Peleato[2], Javier Abadía[1] & Anunciación Abadía[1,3]

[1]*Departamento de Nutrición Vegetal, Estación Experimental de Aula Dei, CSIC, Apartado 202, 50080 Zaragoza, Spain.* [2]*Departamento de Bioquímica y Biología Molecular y Celular, Facultad de Ciencias, Universidad de Zaragoza, 50009 Zaragoza, Spain.* [3]*Corresponding author**

Key words: iron deficiency, malate, phospho*enol*pyruvate carboxylase, root tips, sugar beet

Abstract

Root tips of Fe-deficient and Fe-sufficient sugar beet plants grown in hydroponics have been used to study the changes in the amount and activity of the cytosolic enzyme phospho*enol*pyruvate carboxylase (PEPC, EC 4.1.1.31). Phospho*enol*pyruvate carboxylase activity in extracts of the yellow Fe-deficient root tips was, at pH 7.3, 30-fold higher (when expressed on a FW basis) and 7.1-fold higher (when expressed on a protein basis) than that found in the extracts of Fe-sufficient root tips. The amount of phospho*enol*pyruvate carboxylase protein determined by immuno-blotting was, on a protein basis, 35-fold larger in the yellow zone of Fe-deficient root tips than in the Fe-sufficient root tips. The inhibition of the phospho*enol*pyruvate carboxylase activity by 500 μm malate was 41 and 58% in the extracts Fe-deficient and Fe-sufficient roots. The possibility that post-translational regulation of phospho*enol*pyruvate carboxylase may occur mediated through phosphorylation, was studied by immunological detection of phosphoserine residues in root tip extracts.

Abbreviations: BCIP – 5-bromo-4-chloro-3-indolyl phosphate; BSA – bovine serum albumin; CS – citrate synthase; DMF – N,N-dimethylformamide; FC-R – ferric chelate reductase; Fru6P – fructose-6-phosphate; Glc6P – glucose-6-phosphate; G3PDH – glyceraldehyde-3-phosphate dehydrogenase; IgG – immunoglobulin G; MDH – malate dehydrogenase; NBT – nitrotetrazolium blue; NMR – nuclear magnetic resonance; PAGE – polyacrylamide gel electrophoresis; PAR – photosynthetic active radiation; PEP – phospho*enol*pyruvate; PEPC – phospho*enol*pyruvate carboxylase; PFK – phosphofructokinase; PK – pyruvate kinase; PPFD – absorbed photosynthetic photon flux density; PVP – polyvinylpirrolydone; UDP-Glc – uridine diphosphate glucose; SDS – sodium dodecyl sulfate; TCA – trichloroacetic acid

Introduction

Iron deficiency is a widespread agricultural problem in many crops, especially in calcareous soils. In these soils, total Fe is high but occurs in chemical forms not available to plant roots (Lindsay and Schwab, 1982). The adaptive response of the so-called Strategy I plants, which include dicotyledonous and non-graminaceous monocotyledonous plant species, involves root morphological and physiological changes (Marschner et al., 1986). Among the morphological changes there is an increased formation of lateral roots, root hairs and transfer cells. All these changes increase the root surface available for Fe uptake (Landsberg, 1982). The physiological responses of Strategy I plants include higher rates of proton extrusion, which decreases the pH of the rhizosphere, a release of reducing and/or chelating substances such as phenolics and flavins and a two step mechanism for Fe uptake, in which Fe(III) is first reduced by a plasma membrane-bound ferric-chelate reductase (FC-R) and

* FAX No: +976-716-145. E-mail: mabadia@eead.csic.es

subsequently absorbed as Fe(II) (for reviews see Moog and Brüggemann, 1994; Welkie and Miller, 1993).

The metabolism of roots is highly affected by Fe deficiency. Several changes at the metabolic level have been reported to occur in Fe-deficient roots, including an accumulation of organic acids, mainly malate and citrate (reviewed in Abadía et al., 2000), shifts in the redox state of the cytoplasm (López-Millán et al., 2000a; Schmidt, 1999) and an increase in the activities of PEPC and several enzymes of the Krebs cycle (Landsberg, 1986; López-Millán et al., 2000a; Rabotti et al., 1995) and of the glycolytic pathway (Espen et al., 2000; Rabotti et al., 1995).

The role of the organic acids in the Fe deficiency responses in not well established (Abadía et al., 2000; López-Millán et al., 2000a; Schmidt, 1999), although is commonly accepted that citrate could play an important role in Fe transport via xylem to the shoot (Tiffin, 1966). Two hypotheses have been put forward so far to explain the accumulation of organic acids in Fe-deficient roots. Landsberg (1986) reported that the organic acid increase coincided with the enhanced proton extrusion found in Fe-deficient roots. This may occur through cytosolic alkalinisation associated to proton efflux, which could activate phospho*enol*pyruvate carboxylase (PEPC) activity (Espen et al., 2000; Rabotti et al., 1995). The second hypothesis (De Vos et al., 1986) suggested that Fe deficiency may cause an alteration in the glycolytic pathway, as reported in fungi. Under Fe deficiency, phosphofructokinase would lose its regulation by citrate and pyruvate kinase would be inhibited by citrate, causing an accumulation of PEP, that in turn, via PEPC activity, would cause root organic acid concentrations to increase. In any case, Fe deficiency could cause an increase in root PEPC activity leading to organic acid accumulation. This increase in PEPC activity has been described previously in root extracts of Fe-deficient plants (Huffaker et al., 1959; Landsberg, 1986; López-Millán et al., 2000a; Rabotti et al., 1995; Rombolà, 1998).

The aim of this work was to determine whether PEPC activity was enhanced in root tips of Fe-deficient sugar beet plants. The amount of PEPC in Fe-deficient and Fe-sufficient root tip extracts was determined by immuno-blotting and PEPC phosphorylation was investigated by immunochemical detection of phospho-serine residues. Inhibition of PEPC by malate was studied to assess the regulation of the enzyme activity under Fe deficiency conditions.

Materials and methods

Plant material

Sugar beet (*Beta vulgaris* L. Monohil hybrid from Hilleshög, Landskröna, Sweden) was grown in a growth chamber with a PPFD of 350 μmol m^{-2} s^{-1} PAR at a temperature of 25 °C, 80% humidity and a photoperiod of 16 h light/8 h dark. Seeds were germinated and grown in vermiculite for 2 weeks. Seedlings were grown for 2 more weeks in half-strength Hoagland nutrient solution with 45 μM Fe(III)-EDTA and then transplanted to 20 L plastic buckets (four plants per bucket) containing half-strength Hoagland nutrient solution with either 0 or 45 μM Fe(III)-EDTA. The pH of the Fe-free nutrient solutions was buffered at approximately 7.7 by adding 1 mM NaOH and 1 g L^{-1} of $CaCO_3$. Root tips from plants grown for 10 days in the presence or absence of Fe(III)-EDTA were used in all experiments.

Root sections were taken approximately 0–5 and 5–10 mm from the root apex with a surgical blade (López-Millán et al., 2000a). The 0–5 mm section (YZ) from the zero-Fe treatment had root hairs and was yellow due to the presence of flavins, whereas the 5–10 mm section (WZ) in the zero-Fe treatment and both the 0–5 mm and 5-10 mm sections in the control treatments had practically no root hairs and were white.

Protein quantification

Extracts for protein quantification were made according to Granier (1988) with the solubilisation buffer of Herbik et al. (1996). Samples were washed twice with TCA to avoid interferences by SDS and 2-mercaptoethanol. Aliquots of the extracts were incubated with 12% TCA (1 h at 4 °C) and centrifuged for 15 min at 10 000 *g* at 4 °C. In the second washing step the pellet was resuspended with 6% TCA, centrifuged at 10 000 *g* for 15 min at 4 °C and solubilised with ultrapure water. Proteins were quantified with the Bio-Rad DC Protein System Assay using BSA as standard.

Enzyme assays

Extracts for measuring enzyme activity were made by grinding 100 mg FW of root material in a mortar with 1 mL of extraction buffer containing 30 mM sorbitol, 1% BSA and 1% PVP in 100 mM HEPES-KOH, pH 8.0. The slurry was centrifuged for 15 min

at 10 000 *g* and 4 °C, the supernatant collected and enzyme activity measured immediately. *In vitro* phospho*enol*pyruvate carboxylase (PEPC: EC 4.1.1.31) activity was measured in a coupled enzymatic assay with malate dehydrogenase, according to Vance et al. (1983), with 75 μL of extract in 1 mL of 2 mM PEP, 1 mM $NaHCO_3$, 5 mM $MgCl_2$, 0.16 mM NADH, 50 mM HEPES, pH 7.3. The endogenous root malate concentration (approximately 5.95 and 0.37 μmol g^{-1} FW in –Fe and control roots, respectively; see López-Millán et al., 2000a), will give (with a ratio 100 mg/mL extract and then 75 μL extract/mL of assay) final malate concentrations in the assay medium of approximately 45 and 3 μm for Fe-deficient and control roots, respectively. These concentrations are much lower than the inhibition assay carried out with 500 μm malate. The addition of the protease inhibitor chymostatin (10 μg mL^{-1}) did not increase PEPC activities.

Immunoblotting

Extracts for immunobloting were made according to Granier (1988) with the solubilization buffer of Herbik et al. (1996). Root soluble protein was boiled for 5 min at 95 °C. Electrophoresis was carried out with a discontinuous system (Laemmli, 1970). The resolving gel contained 8% acrylamide and the stacking gel 7.2% acrylamide in a Tris-glycine buffer. Proteins were electrophoresed for 2 h at 20 mA constant current and 25 °C in a discontinuous PAGE system. Semi-dry electroblotting onto nitrocellulose membranes was carried out at 50 mA for 2 h, using a Semiphor TE70 apparatus according to the manufacturer's instructions. Blots were blocked for 45 min with 20 mM Tris, 0.9% NaCl and 5% BSA and then washed with 20 mM Tris, 0.9% NaCl and 0.1% BSA. For the identification of PEPC, blots were incubated for 2 h with a 1:1000 dilution of rabbit IgG against the phosphorylation site of PEPC and washed as above. The PEPC antibody was a polyclonal antibody obtained against a synthetic peptide of 23 amino-acids from the N-terminal sequence of sorghum PEPC (from Dr. J. Vidal, Orsay, France). A second incubation with a 1:2000 dilution of goat anti-rabbit IgG (H+L) horseradish peroxidase conjugate from Bio-Rad was performed for 45 min. After thorough washing with 20 mM Tris and 0.9% NaCl, PEPC was detected with 20 mM Tris, 0.9% NaCl, 9 mg ml^{-1} chloronaftol in ethanol and 17 μl H_2O_2. Quantification of PEPC was performed using a Molecular Imager FX apparatus (BioRad, San Francisco, USA).

Table 1. Phospho*enol*pyruvate carboxylase activity in root extracts from Fe-deficient and Fe-sufficient sugar beet. Enzyme assays were done at pH 7.3. Data are means ± SE of 10 replicates. Values in the same column followed by a different letter are statistically significant at $p \leq 0.05$ (*t* Student's test)

	μmol g^{-1} FW min^{-1}	μmol mg^{-1} protein min^{-1}
–Fe	5.04±0.42 a	1.77±0.42 a
+Fe	0.17±0.02 b	0.25±0.02 b
–Fe /+Fe	29.6	7.1

Phosphoserine residues were identified by incubating the blot for 3 h with a 1:50 dilution of rabbit IgG against phosphoserine residues from SIGMA, St. Louis, USA. After washing the blot a second incubation was carried out for 1 h using a 1:2500 dilution of anti-Rabbit IgG-phosphatase. After thorough washing with 20 mM Tris and 0.9% NaCl, phosphoserine residues were detected with 0.2 M Tris, pH 9.6, 1 mM $MgCl_2$, 4 mg mL^{-1}BCIP and 1 mg mL^{-1}NBT in DMF.

Results and discussion

The amount of soluble protein in root tips was 2.85 and 1.18 mg protein g^{-1} FW in the yellow tip and the white adjacent zone of Fe-deficient roots, respectively. These values were approximately 4.2- and 2.4-fold higher than that found in the Fe-sufficient root tips, that was approximately 0.68 mg protein g^{-1} FW.

The antibody against the phosphorylation site of PEPC immunodecorated a single 113-kDa polypeptide in sugar beet root tip extracts. The amount of PEPC was 34.7- and 6.5-fold higher in the yellow and white zones of Fe-deficient root tips, respectively, than in the Fe-sufficient root tips (Figure 1). The activity of PEPC in root extracts was much higher in the yellow zone of Fe-deficient root tips than in the control. These increases were 29.6-fold when expressed on a FW basis and 7.1-fold when expressed on a protein basis. An increase in PEPC activity in root extracts of Fe-deficient plants was first described by Huffaker et al. (1959). Later, increases in PEPC activity in root extracts under Fe deficiency of 1.85-, 2.3-, 4 to 6 and 7 to 14-fold were reported in pepper (Landsberg, 1986), kiwifruit (Rombolà, 1998), cucumber (De

46

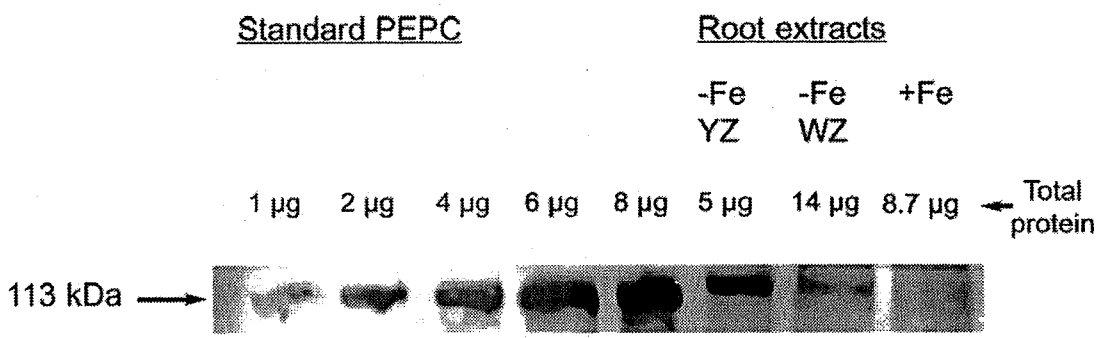

Figure 1. Protein immunoblot of partially purified PEPC (from SIGMA) and sugar beet root extracts. Extracts were made from the yellow (-Fe, YZ) and white parts (-Fe, WZ) of Fe-deficient root tips and from Fe-sufficient root tips (+Fe). PEPC was labelled using PEPC antibody.

Table 2. Inhibition of phospho*enol*pyruvate carboxylase activity in root extracts from Fe-deficient and Fe-sufficient sugar beet by 500 μm malate. Enzyme assays were done at pH 7.3. Data (in μmol g^{-1} FW min^{-1}) are means ± SE of 5 replicates. Values in the same column followed by a different letter are statistically significant at $p \leq 0.05$ (*t* Student's test)

	Activity		% Inhibition
	0 μM malate	500μM malate	
−Fe	4.57±0.56 a	2.72± 0.33 a	40.5 a
+Fe 0	0.21±0.03 b	0.09± 0.02 b	58.4 b

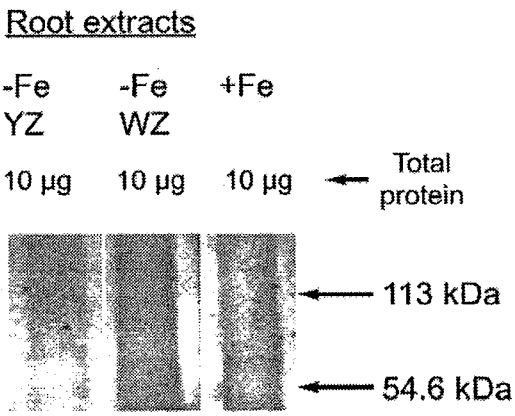

Figure 2. Protein immunoblot of root tip extracts. Extracts were made from the yellow (-Fe, YZ) and white parts (-Fe, WZ) of Fe-deficient root tips and from Fe-sufficient root tips (+Fe). Phosphoserine residues were labelled using phosphoserine antibody from Sigma.

Nisi and Zocchi, 2000; Rabotti et al., 1995) and sugar beet (López-Millán et al., 2000a), respectively. The increase in PEPC activity in Fe-deficient roots coincides spatially with areas having increased FC-R activity (López-Millán et al., 2000a). Similar data were reported for the swollen root tip area of Fe-deficient pepper plants (Landsberg, 1986). The white parts of Fe-deficient roots did not have major increases neither in the total amount of PEPC (Figure 1) nor in FC-R activity (López-Millán et al., 2000a).

Increases in PEPC activity could be also mediated by post-translational regulation through phosphorylation as it occurs in the leaves of C4 and CAM species (see Chollet et al., 1996, for a review) and in proteoid roots of P-stressed plants (Gilbert et al., 1998). The activity of PEPC in the presence of 500 μm malate decreased from 4.57 to 2.72 nmol g^{-1}FW min^{-1}in extracts of the yellow zone of Fe-deficient roots and from 0.21 to 0.09 nmol g^{-1}FW min^{-1}in extracts of Fe-sufficient roots (Table 2). Inhibition by malate was therefore 58% in Fe-sufficient roots and 41% in Fe-deficient yellow root tips (Table 2). The relatively small but significant difference in PEPC sensitivity to malate could be explained by the presence of some endogenous malate in the assay medium of the Fe-deficient roots (approximately 45 μm). This could make the PEPC activity in Fe-deficient root extracts apparently less sensitive to malate. Post-translational regulation of PEPC through phosphorylation was also studied by immunological detection of phosphorylated residues of serine in the 113-kDa band, previously identified as PEPC. Phosphoserine residues were not detected in the PEPC region in any of the root extracts analysed (Figure 2). These data suggest that post-translational regulation by phosphorylation may not occur in Fe-deficient roots. However, this does not necessarily exclude phosphorylation because the steric conformation of the target protein may hinder

the interaction of the antibody with the phosphoserine residues. Therefore, a more detailed analysis should be carried out with additional experiments, including ^{32}P labelling of PEPC protein, studies with inhibitors of protein kinases and phosphatases and PEPC-kinase tests.

Other factors could further enhance PEPC activity in root cells. For instance, a cytoplasmic pH increase could boost PEPC activity, since the optimum pH for the enzyme is quite high. Espen et al. (2000) have recently shown with ^{31}P-NMR techniques, however, that in Fe-deficient cucumber roots cytosolic pH may increase only by approximately 0.02–0.06 units with respect to the controls, whereas the vacuolar pH increased by 0.03–0.20 units. This may be the consequence of a very efficient PEPC-mediated cytosolic pH regulation. The PEPC increase in Fe-deficient sugar beet root tips does not appear to depend on bicarbonate since root tips of plants grown without Fe in the absence of $CaCO_3$ also had PEPC activities 40-fold higher (on a FW basis and at pH 8.5) than the controls (not shown in the present work; López-Millán et al., 2000a).

The possible functions of the increase in PEPC with Fe deficiency are still unclear. A metabolic model for C assimilation has been proposed recently to be triggered by Fe deficiency in sugar beet roots (López-Millán et al., 2000a). In this model, PEPC catalyzes the carboxylation of PEP to oxalacetate, which could be then reduced to malate via cytosolic MDH. Malate could be transported to the mitochondria via the malate-oxalacetate shuttle and converted to citrate by CS. Part of this C could be used, through an increase in mitochondrial activity in transfer cells, to increase the capacity to produce reducing power (Bienfait et al., 1996), whereas another part would be exported to the shoot via xylem (Bialzyck and Lechowski, 1992; López-Millán et al., 2000b). A possible function of the export of organic acids to the leaves is the use of these C compounds for the maintenance of basic processes such as respiration. PEP needed to maintain PEPC activity could possibly come via glycolysis from compounds previously synthesized and/or stored within the plant. Both phloem (De Vos et al., 1986; Maas et al., 1988), and root sugar concentrations (Thoiron and Briat, 1999) have been reported to increase with Fe-deficiency. The activities of some enzymes involved in the glycolytic pathway have also been shown to increase in Fe-deficient roots (Espen et al., 2000; see Abadía et al., 2000, for a review).

Also, increased biosynthesis of carboxylates (particularly of citrate) and of phenolics (derived from organic acid metabolism) under Fe deficiency may be important for increased root exudation of these compounds, mediating Fe(III) mobilization in the rizhosphere, its transfer to the root surface and the subsequent reduction to Fe(II) and uptake. Exudation is further promoted by proton extrusion (Römheld and Marschner, 1983), and protons may be provided by enhanced biosynthesis of organic acids. Increased PEPC activity may be related to Fe-deficiency inhibition of NO_3 uptake, resulting in excess uptake of cations over anions which could be balanced by proton extrusion (Cakmak and Marschner, 1990).

In summary, PEPC is a key enzyme in root responses to Fe deficiency that could enhance C fixation in roots and contribute to organic acid export from the roots to the leaves via xylem. The increase in PEPC activity measured in yellow root tip extracts appears to be mainly due to an increase in the amount of the enzyme induced by Fe deficiency. Other factors like post-translational regulation by phosphorylation do not seem to control PEPC activity.

Acknowledgements

Authors gratefully acknowledge the skilful technical assistence of Aurora Poc in growing the plants. This work was supported by grants AGR97-1177 from the Comisión Interministerial de Ciencia y Tecnología to A.A., and PB97-1176 from the Dirección General de Investigación Científica y Técnica and AIR3-CT94-1973 from the Commission of European Communities to J.A.

References

Abadía J, López-Millán A F, Rombolà A and Abadía A 2000 Organic acids and Fe deficiency: A review. These Proceedings.

Bialzyk J and Lechowski L 1992 Absorption of HCO_3^- by roots and its effect on carbon metabolism of tomato. J. Plant Nutr. 15, 293–312.

Bienfait H F 1996 Is there a metabolic link between H^+ excretion and ferric reduction by roots of iron-deficient plants: A viewpoint. J. Plant Nutr. 19, 1211–1222.

Cakmak I and Marschner H 1990 Decrease in nitrate uptake and increase in proton release in zinc deficient cotton, sunflower and buckwheat plants. Plant Soil 129, 261–268.

Chollet R, Vidal J and O'Leary M H 1996 Phosphoenolpyruvate carboxylase: A ubiquitous, highly regulated enzyme in plants. Annu. Rev. Plant Physiol. Plant Mol. Biol. 47, 273–298.

48

De Nisi P and Zocchi G 2000 Phospho*enol*pyruvate carboxylase in cucumber (*Cucumis sativus* L.) roots under iron deficiency: Activity and kinetic characterization. J. Exp. Bot. 51, 1903–1909.

De Vos C R, Lubberding H J and Bienfait H F 1986 Rhizosphere acidification as a response to iron deficiency in bean plants. Plant Physiol. 81, 842–846.

Espen L, Dell'Orto M, De Nisi P and Zocchi G 2000 Metabolic responses in cucumber (*Cucumis sativus* L.) roots under Fe-deficiency: A ^{31}P-nuclear magnetic resonance *in-vivo* study. Planta 210, 985–992.

Gilbert G A, Vance C P and Allan D L 1998 Regulation of white lupin root metabolism by phosphorus availability. *In* Phosphorus in Plant Biology: Regulatory Roles in Molecular, Cellular, Organismic, and Ecosystem Processes. Eds. JP Lynch and J Deikman. American Society of Plant Physiologysts. 157–167.

Granier F 1988 Extraction of plant proteins for two dimensional electrophoresis. Electrophoresis 9, 712–718.

Herbik A, Giritch A, Horstmann C, Becker R, Balzer H J, Bäumlein H and Stephan U W 1996 Iron and copper nutrition-dependent changes in protein expression in a tomato wild type and the nicotianamine-free mutant chloronerva. Plant Physiol. 111, 533–540.

Huffaker R C, Hall D O, Shannon L M, Wallace A and Rhoads W A 1959 Effects of iron and chelating agents on dark carboxylation reactions in plant homogenates. Plant Physiol. 34, 446–449.

Laemmli U K 1970 Cleavage of structural proteins during the assembly of the head of bacteriophage T4. Nature 227, 680–685.

Landsberg E C 1982 Transfer cell formation in the root epidermis: A prerequisite for Fe-efficiency? J. Plant Nutr. 5, 415–432.

Landsberg E C 1986 Function of rhizodermal transfer cells in the Fe stress response mechanisms of *Capsicum annuum* L. Plant Physiol. 82, 511–517.

Lindsay W L and Schwab A P 1982 The chemistry of iron soils and its availability to plants. J. Plant Nutr. 5, 821–840.

López-Millán A F, Morales F, Andaluz S, Gogorcena Y, Abadía A, De las Rivas J and Abadía J 2000a Protective mechanisms in roots of iron deficient sugar beet: changes in carbon assimilation and oxygen use. Plant Physiol. 124, 885–897.

López-Millán A F, Morales F, Abadía A and Abadía J 2000b Effects of iron deficiency on the composition of the leaf apoplastic fluid and xylem sap in sugar beet. Implications for iron and carbon transport. Plant Physiol. 124, 873–884.

Maas F M, Van der Wetering D A M, Van Beusichem M L and Bienfait H F 1988 Characterization of phloem iron and its possible role in the regulation of the Fe-efficiency reactions. Plant Physiol. 87, 167–171.

Marschner H, Römheld V and Kissel M 1986 Different strategies in higher plants in mobilization and uptake of iron. J. Plant Nutr. 9, 695–713.

Moog P R and Brüggemann W 1994 Iron reductase systems on the plant plasma membrane – A review. Plant Soil 165, 241–260.

Rabotti G, De Nisi P and Zocchi G 1995 Metabolic implications in the biochemical responses to iron deficiency in cucumber (*Cucumis sativus* L.) roots. Plant Physiol. 107, 1195–1199.

Rombolà 1998 Aspetti fisiologici e biochimici della nutrizione ferrica in actinidia (*A. deliciosa*). PhD Thesis. Dipartimento di Colture Arboree. Universitá degli Studi di Bologna.

Römheld V and Marschner H 1983 Mechanism of iron uptake by peanut plants.I- Fe(III) reduction chelate splitting, and release of phenolics. Plant Physiol. 71, 949–954.

Schmidt W 1999 Mechanisms and regulation of reduction-based iron uptake in plants. New Phytol. 141, 1–26.

Thoiron S and Briat J F 1999 Differential expression of maize sugar responsive genes in response to iron deficiency. Plant Physiol. Biochem. 37, 759–766.

Tiffin L O 1966 Iron translocation II Citrate/iron ratios in plant stem exudates. Plant Physiol. 41, 515–518.

Vance C P, Stade S and Maxwell C A 1983 Alfalfa root nodule carbon dioxide fixation. I. Association with nitrogen fixation and incorporation into amino acids. Plant Physiol. 72, 469–473.

Welkie G W and Miller G W 1993 Plant iron uptake physiology by nonsiderophore systems. *In* Iron Chelation in Plants and Soil Microorganisms. Eds. LL Barton and BC Hemming. pp 345–369. Academic Press, San Diego, USA.

Estación Experimental de Aula Dei

Consejo Superior de Investigaciones Científicas (CSIC)
Departamento de Nutrición Vegetal

Universidad de Zaragoza

Departamento de Bioquímica y Biología Molecular y Celular

Bi